

Imperial College London



Mechanical Engineering

**Failure Characteristics of All Polyethylene Cemented Glenoid
Implants in Total Shoulder Arthroplasty**

PhD Thesis

Sarah Junaid

2010

Abstract

Total shoulder arthroplasty (TSA) still suffers today from mid-term and long-term complications such as glenoid implant loosening, wear, humeral head subluxation/dislocation and implant fracture. Unlike the hip and knee joint replacements, the artificial shoulder joint has yet to offer a long-term satisfactory solution to shoulder replacement. With loosening being the number one reason for TSA revision, investigating methods of monitoring the glenoid implant loosening and investigate the effects of various design parameters on the loosening behaviour of the glenoid fixation is necessary to explore the problem. Several studies were carried out using in-vitro cyclic testing and FEA to; investigate failure progression and its correlation to quantitative measures in a 2D study (n = 60), investigating key glenoid design features in a 2D (n = 60) and 3D study (n = 20), investigating the validity of using bone substitute foam for studying glenoid fixation in a cadaveric study and investigating any correlation between failure and CT or in-vitro quantitative measures (n = 10). Visible failure was observed, for the first time, correlating to inferior rim displacement and vertical head displacement measures. CT failure was detected in 70% of specimens before visible failure was observed. Out of the design pairs tested; smooth-back/rough-back (range of roughnesses), peg/keel, curved-back/flat-back and conforming/non-conforming, roughening the back-surface to 3.4 μm or more improved fixation performance ($p < 0.05$). Roughening the back-surface changed the mode of failure from implant/cement failure inferiorly due to tensile/shear stresses, to cement/bone failure superiorly due to compressive/shear loading. Differences in the other design pairs were marked showing peg to perform better than keel, conforming over non-conforming and no difference in curved-back over flat-back, although these differences are marginal. Improvements in the standard testing method have also been suggested.

Acknowledgements

First and foremost I praise and thank God. May He accept it from me and may this work be a benefit to others.

There are many people who deserve my thanks, firstly to my parents for their unending support, love and inspiration, without them, writing this thesis would not have been possible. To my brother for sharing the highs and the lows with me throughout my PhD. To Ulrich, my supervisor, for his guidance and patience. My thanks and appreciation go to the Arthritic Research Campaigns (ARC) who funded my research.

To all my sisters in the PR, you were my family away from home, thank you for all the good times that I will never forget. To Prof Amis, my colleagues and friends in the Biomechanics Group.

To Thomas Gregory, Sanjay Sanghavi, Sanjay Gupta and Min Zhang for their help and support in my work. To Philip Wilson and Stephen Johnson for help and advice in manufacturing. To Shirley Fetherston for the super early CT sessions! My thanks go to Tornier Inc. for their collaboration and support in this work.

Finally, to all those people, past and present, who have indirectly inspired and taught me through actions and words. God bless you.

Contents

<u>Abstract.....</u>	<u>2</u>
<u>Acknowledgements</u>	<u>3</u>
<u>Contents</u>	<u>4</u>
<u>List of Figures.....</u>	<u>11</u>
<u>List of Tables</u>	<u>19</u>
<u>Nomenclature</u>	<u>20</u>
<u>Chapter 1: Introduction</u>	<u>21</u>
1.1 Introduction	21
1.2 Anatomical Planes & Movement	21
1.3 Shoulder Joint Anatomy	22
1.4 Glenohumeral Joint.....	23
1.5 Shoulder Joint Cartilage & Ligaments	24
<i>1.5.1 Cartilage Structure & Mechanics</i>	<i>25</i>
<i>1.5.2 Muscles of the Shoulder (Thompson & Floyd 2001)</i>	<i>26</i>
<i>1.5.3 Joint Stabilising Mechanisms</i>	<i>28</i>
1.6 Shoulder Joint Forces	31
1.7 Common problems in the Shoulder Joint	32
1.8 Total Shoulder Arthroplasty	33
<i>1.8.1 History.....</i>	<i>33</i>
<i>1.8.2 Surgical Approach.....</i>	<i>37</i>
<i>1.8.3 Surgical Outcome</i>	<i>37</i>
1.9 Fixation Problem in TSA.....	38

1.10 References	40
<u>Chapter 2: Literature Review of the Problems in Glenoid Implant Loosening.....</u>	44
2.1 Glenoid Implant Loosening	44
2.2 Causes of Loosening	45
2.2.1 <i>Area of Failure</i>	45
2.2.2 <i>Interfacial Strength & Material Strength</i>	46
2.2.3 <i>Osteolysis</i>	47
2.3 Failure Progression	48
2.4 Current Methods of Monitoring Glenoid Failure	48
2.5 Design Parameters.....	51
2.5.1 <i>Radial Mismatch</i>	53
2.5.2 <i>Peg Versus Keel</i>	53
2.5.3 <i>Curved-back Versus Flat-back</i>	53
2.5.4 <i>Implant Roughness</i>	54
2.5.5 <i>Cemented Versus Cementless</i>	54
2.6 Conclusion.....	55
2.7 PhD Aims	55
2.8 PhD Objectives	55
2.9 References	57
<u>Chapter 3: Failure Mechanism in 2D All-Polyethylene Glenoid Implant Designs.....</u>	61
3.1 Contributors	61
3.2 Abstract.....	61
3.3 Introduction	62
3.4 Materials and Method.....	63
3.4.1 <i>Mechanical Test</i>	63
3.4.2 <i>FE Analysis</i>	66
3.5 Results	68
3.5.1 <i>Cyclic Testing</i>	68

3.5.2 <i>FE Results</i>	70
3.6 Discussion.....	71
3.6.1 <i>Location of Failure</i>	72
3.6.2 <i>The Weakest Link of the Fixation</i>	72
3.7 Conclusions	74
3.8 References	76
<u>Chapter 4: A 2D Comparison of Glenoid Design Parameters in TSA</u>	79
4.1 Abstract.....	79
4.2 Introduction	80
4.3 Conformity	80
4.3.1 <i>Arguments For High Radial Mismatch</i>	80
4.3.2 <i>Arguments Against High Radial Mismatch</i>	80
4.4 Keel Versus Peg	81
4.5 Flat-back Versus Curved-back	82
4.6 Back-Surface Roughness	82
4.7 Materials and Method.....	85
4.7.1 <i>Mechanical Test</i>	85
4.7.2 <i>FE Analysis</i>	87
4.8 Results	88
4.8.1 <i>Mechanical Test</i>	88
4.8.2 <i>Rim Displacement Versus Head Displacement</i>	90
4.8.3 <i>FE Validation</i>	92
4.8.4 <i>FE Analysis</i>	92
4.9 Discussion.....	94
4.9.1 <i>Roughness</i>	94
4.9.2 <i>Peg Versus Keel</i>	95
4.9.3 <i>Flat-back Versus Curved-back</i>	95
4.9.4 <i>Conformity</i>	96
4.9.5 <i>FE Predictions</i>	98

4.9.6 <i>Rim Displacement Measure</i>	99
4.9.7 <i>Water Bath</i>	99
4.10 Conclusion	100
4.11 References	101
<u>Chapter 5: Failure Mechanism in All-Polyethylene Cemented Glenoid Implants:.....</u>	104
5.1 Abstract	104
5.2 Introduction	105
5.3 Materials & Methods	106
5.3.1 <i>Specimen Preparation</i>	106
5.3.2 <i>Mechanical Test</i>	107
5.3.3 <i>CT Scans</i>	108
5.3.4 <i>Post-Testing Observations</i>	109
5.3.5 <i>Finite Element Modelling</i>	109
5.4 Results	110
5.4.1 <i>Cyclic Results</i>	110
5.4.2 <i>Microscopic Results</i>	112
5.4.3 <i>Finite Element Results</i>	113
5.4.4 <i>Rim Displacement & Vertical Head Displacement</i>	117
5.5 Discussion	119
5.6 Conclusion	122
5.7 References	124
<u>Chapter 6: Comparison of Design Parameters in.....</u>	126
6.1 Abstract	126
6.2 Introduction	128
6.3 Materials & Methods	128
6.3.1 <i>Specimen Preparation</i>	128
6.3.2 <i>Mechanical Test</i>	130
6.3.3 <i>Finite Element Modelling</i>	132

6.4 Results	132
6.4.1 Mechanical Test.....	132
6.4.2 Peg Versus Keel	133
6.4.3 Surface Roughness	133
6.5 Radial Mismatch	134
6.5.1 Rim Displacement & Vertical Head Displacement	134
6.5.2 FE Validation.....	135
6.5.3 FE Analysis.....	136
6.6 Discussion.....	142
6.6.1 Peg Versus Keel	142
6.6.2 Surface Roughness & Macro-Features	144
6.6.3 Radial Mismatch.....	144
6.6.4 Rim Displacement Versus Head Displacement	145
6.6.5 Cadaveric Versus Bone Substitute	146
6.6.6 In-Vitro Test.....	146
6.7 Conclusion.....	147
6.8 References	149
<u>Chapter 7: In-Vitro Measurements and their Correlation to Failure</u>	<u>151</u>
7.1 Abstract.....	151
7.2 Introduction	152
7.3 Materials & Methods	153
7.3.1 Subluxation Curves	153
7.3.2 Mechanical Test.....	153
7.3.3 CT Scans	155
7.4 Results	155
7.4.1 Cyclic Results	155
7.4.2 Rim & Vertical Displacements	156
7.4.3 CT Results.....	158
7.5 Discussion.....	159
7.5.1 Superior Rim Displacement & Failure	160

7.5.2 <i>Inferior Rim Displacement & Failure</i>	161
7.5.3 <i>2D Versus 3D</i>	161
7.5.4 <i>Cadaver Versus Bone substitute</i>	161
7.5.5 <i>Vertical Head Displacement & Failure</i>	162
7.6 Conclusion	163
7.7 References	165
<u>Chapter 8: Discussion</u>	167
8.1 Glenoid Implant Mechanical Failure	167
8.2 Clinical Findings & Biological Factors	168
8.3 Design Recommendations	170
8.4 Indirect Measures of Failure	172
8.4.1 <i>Rim Displacement Versus Vertical Displacement Measure</i>	173
8.5 Human Bone & Bone Substitute	173
8.6 Testing Recommendations	174
8.7 References	176
<u>Chapter 9: Future Work</u>	178
9.1 Future Work	178
9.1.1 <i>Improvements in In-Vitro Fatigue Test</i>	178
9.1.2 <i>New Glenoid Implant Design Project Proposal</i>	178
9.2 References	182
<u>Appendix A: Table Summary of TSA Clinical Studies</u>	184
<u>Appendix B: Comparison of Radiographic and Clinical Results in TSA Studies</u>	187
<u>Appendix C: 3D Versus 2D Contact Pressure Calculations</u>	191
<u>Appendix D: FE predicted interfacial and material stress plots of each 2D design</u>	196
<u>Appendix E: Cross-sectional photos of the cadaveric specimens after fatigue testing</u> ..	200

Appendix F: Failure graphs of each specimen plotting visual & CT failure with vertical head & inferior rim displacement203

Appendix G: Comparison of implant/cement shear and normal contact stresses in the 2D and 3D cases.....207

Appendix H: Table of Displacements for Each Specimen in 2D, Cadaver and 3D Study & Summary Table.....208

List of Figures

- Figure 1.1: Medical anatomical directions (Thompson & Floyd, Manual of Structural Kinesiology, 14th Ed., 2000, McGraw-Hill. Reproduced with permission from The McGraw-Hill Companies) and planes.21**
- Figure 1.2: Shoulder joint movements (Thompson & Floyd, Manual of Structural Kinesiology, 14th Ed., 2000, McGraw-Hill. Reproduced with permission from The McGraw-Hill Companies).....22**
- Figure 1.3: Anterior view of the three articulating bones of the shoulder joint; (the humerus, scapula and clavicle (left) and posterior view of the scapula and lateral part of the clavicle (right) Thompson & Floyd, Manual of Structural Kinesiology, 14th Ed., 2000, McGraw-Hill. Reproduced with permission from The McGraw-Hill Companies).....23**
- Figure 1.4: Posterior view of the shoulder girdle (red) and thorax (Grays 1918). Figure reprinted and modified with permission from Gray, Henry. *Anatomy of the Human Body*. Philadelphia: Lea & Febiger, 1918; Bartleby.com, 2000. www.bartleby.com/107/. [2009].23**
- Figure 1.5: CT of transverse section of glenoid and cartilage tissue (top) and schematic of the glenoid cross-section (bottom) demonstrating the conforming cartilage structures.....24**
- Figure 1.6: Lateral view of the glenoid showing ligaments of the scapula (Gray 1918). Note: glenoid ligament is more commonly known as the labrum. Figure reprinted with permission from Gray, Henry. *Anatomy of the Human Body*. Philadelphia: Lea & Febiger, 1918; Bartleby.com, 2000. www.bartleby.com/107/. [2009].25**
- Figure 1.7: Glenohumeral ligament (inferior, middle & superior bands), which are continuous with the capsule (blue). Figure reprinted with permission from Basic Human Anatomy, O’Rahilly et al., (1983), published online <http://www.dartmouth.edu/~humananatomy>.25**

Figure 1.8: Muscles of the shoulder joint (Dutton 2004). Figures reprinted from Orthopaedic Examination, Evaluation and Intervention, (2004), Dutton, M, with permission from McGraw-Hill Companies.....28

Figure 1.9: Subluxation and dislocation definitions where arrows denote resultant joint force.....29

Figure 1.10: Glenoid depth and perpendicular compressive force (F_y) are both proportional to the transverse force (F_x). Note: forces generated by surrounding muscles.....29

Figure 1.11: Rotator cuff muscles, superior view (Thompson & Lloyd, Manual of Structural Kinesiology, 14th Ed., 2000, McGraw-Hill. Reproduced with permission from The McGraw-Hill Companies).....30

Figure 1.12: Adhesion-Cohesion mechanism (Barnett et al. 1961).31

Figure 1.13: Suction mechanism in the natural glenohumeral joint.....31

Figure 1.14: Resultant forces of neutral (N), external rotation (X) and internal rotation (I) vectors (Poppen & Walker 1978). Figure reprinted with permission by Wolters Kluwer Health from Poppen, N K & Walker, P S, Forces at the Glenohumeral Joint in Abduction, Clinical Orthopaedics and Related Research, 1978, 135, 165-170.....32

Figure 1.15: Neer Hemiarthroplasty (left) and non-constrained total shoulder arthroplasty (right). Figures reprinted with permission from Journal of Bone and Joint Surgery American, 1974, 56A, 1, Replacement Arthroplasty for Glenohumeral Osteoarthritis, Neer, 1-13.....34

Figure 1.16: The Michael Reese shoulder (left) and Neer Mark III reverse shoulder (right), two examples of a fixed-fulcrum TSA design (Williams et al. 2004; Zadeh & Calvert 1998). Figure reprinted with permission from Surgical Disorders of the Shoulder, Watson, M (Ed), Michael Reese shoulder implant, p 132, Copyright (1990).....35

Figure 1.17: Glenoid designs showing non-constrained PE (two left), non-constrained metal-back (middle), and two semi-constrained metal-back glenoids (two right). Note: semi-constrained implants were designed to prevent upward head migration (Neer et al. 1982). Note: figure reprinted with permission from Journal of Bone and Joint Surgery American, 1982, 64A, 3, Recent experience in total shoulder replacement, Neer, 319-337.....35

Figure 1.18: (Left to right) Metal-back Cofield, Neer and Tornier implants that are no longer in use (Katz et al. 2009). Images used with permission from Tornier, Inc., and Smith & Nephew, Inc., February 2010.....36

Figure 1.19: Eccentric loading of glenoid implant, leading to “rocking horse” mechanical loosening (Matsen III & Lippitt 2004). Image reprinted with permission from University of Washington website, <http://www.orthop.washington.edu>.....39

Figure 2.1: Before implantation (left) & retrieved threaded implant (right) showing partially intact cement at the pegs (Yian et al. 2005). Figure reprinted with permission from Journal of Bone and Joint Surgery American, 2005, 87A, 9, Radiographic and Computed Tomography Analysis of Cemented Pegged Polyethylene Glenoid Components in Total Shoulder Replacement, Yian, 1928-1936.46

Figure 2.2: Revision surgery showing cement intact with the glenoid bone (left) & retrieved glenoid showing failure occurring at the implant/cement interface (right) (Nyffeler et al. 2003). Figure reprinted with permission from Journal of Bone & Joint Surgery-British, 2003, 85B, 5, Influence of peg design and cement mantle thickness on pull-out strength of glenoid component pegs, 748-752.....46

Figure 2.3: Mechanical fatigue testing of glenoid fixation (Reprinted and annotated from Journal of Shoulder and Elbow Surgery, 9 /2, Anglin, C. et al., Prosthesis Subluxation: Theory and Experiment, 104-114, Copyright (2000), with permission from Elsevier and C. Anglin).....51

Figure 2.4: Main glenoid design parameters; keel/peg, curved/flat-back, conforming/less conforming.53

Figure 3.1: Four glenoid designs with two radius of curvatures, making a total of 8 designs.....63

Figure 3.2: cemented 2D-specimen in bone substitute; flat-back peg (left) and curved-back keel (right).64

Figure 3.3: The ASTM F2028-02 biaxial testing rig, modified according to the 2D configuration of this study.64

Figure 3.4: Subluxation curve of three conforming specimens with loading point derived at the linear section of the curve (dotted) using an average offset of 0.25 mm. Note: displacement range (shaded) at point of subluxation.....66

Figure 3.5: definition of failure where red represents failure at the implant/cement interface, where the literature mentions failure, this refers to 3/4 failure. Note: diagonal red lines in the pegged glenoid indicate failure in the bone substitute.68

Figure 3.6: In all cases failure was observed in the implant/cement interface and initiated in the inferior part of the fixation (arrows).69

Figure 3.7: Failure pathway in keeled (left) and pegged glenoids (right). A similar failure path was observed for all design configurations.69

Figure 3.8: Plot of the predicted stresses in the fixation of the curved-back keel specimen. The plotted stresses are at: the two interfaces, in the bulk PMMA bone cement and in PU bone substitute. The strengths of the two interfaces, of the cement and of the PU bone substitute are also shown. The implant/cement interface strength is only known within a range and this range is indicated by the hatched area. Only a minimum value of the cement/bone-substitute strength is known (2.32 MPa) and the arrows indicate that the strength is likely to be higher than 2.32 MPa.71

Figure 4.1: FE predictions showing a correlation between vertical head and inferior rim displacements with failure progression at the implant/cement interface.....84

Figure 4.2: Schematic of the LVDTs fixed to the bone substitute (above) and location of reference pins at the superior and inferior rim (below).....86

Figure 4.3: Specimens tested in a $37 \pm 2^{\circ}\text{C}$ water bath (left) and horizontal rim measurements were taken using LVDTs every 2000 cycles (right).....86

Figure 4.4: Subluxation curve of 8 designs ($n = 2$), a significant difference in subluxation loads was found between the two conformities ($p = 0.04$)......87

Figure 4.5: 2D (left) and 3D (right) non-conforming 29 mm flat-back keel FE models..88

Figure 4.6: Average number of cycles in roughened specimens at failure for each design.89

Figure 4.7: Comparable results between less (29 mm) & more (25 mm) conforming, keel & peg and flat & curved-back.....89

Figure 4.8: Increase in number of cycles to failure and surface roughness was proportional.90

Figure 4.9: A significant difference was found between roughnesses $0\text{-}3.4 \mu\text{m}$ and $> 3.4 \mu\text{m}$ ($p < 0.0001$).90

Figure 4.10: A positive correlation was found with number of cycles in both vertical head and inferior rim displacement.....91

Figure 4.11: Bar chart showing a positive correlation between average vertical head displacement, average inferior rim displacement and progressive failure.91

Figure 4.12: Conforming FE & average in-vitro subluxation curves for each design. ...92

Figure 4.13: Less conforming FE & average in-vitro subluxation curves for each design.92

Figure 4.14: Colour plot of the predicted stresses in the fixation of the conforming curved-back keel model. Note: plot is the same as Fig. 3.8.....93

Figure 4.15: The moment generated by loading the glenoid is defined as the product of the compressive load (1800 N) and vertical head displacement (moment arm).97

Figure 5.1: Aequalis Tornier curved-back cemented glenoid implant (left). NB2 specimen cemented and potted for testing (right).107

Figure 5.2: Rods were prepared for measuring horizontal rim displacement using LVDTs, attached directly to the specimens.....107

Figure 5.3: Mechanical cadaveric test.....108

Figure 5.4: Number of cycles to failure. Red solid and dotted lines represent average and upper/lower standard deviations respectively.111

Figure 5.5: CT slices of the transverse plane showing an example of superior (left) and inferior (right) failure at the implant/cement interface in the specimen NB1.112

Figure 5.6: Cross-sectional slice of NB1 after failure. Note: inferior failure of the implant/cement (circle) and superior bone crushing (square).113

Figure 5.7: One implant detached completely at the implant/cement interface (NB12), the pegs show the cement still intact in the peg grooves.113

Figure 5.8: Normal contact stress plot of NB1 at the implant/cement interface.....114

Figure 5.9: Tensile normal contact stress plot of NB1 at the implant/cement interface. Note: peak stresses at the inferior edge and pegs.114

Figure 5.10: contact stress plot of NB1 at the cement/bone interface.115

Figure 5.11: Tensile normal contact stresses at the cement/bone interface. Note: peak stresses at the inferior edge and pegs.....115

Figure 5.12: Colour plot slices through the pegs of the cement mantle showing principal stress maximum. Note: Dark grey denotes compressive stresses and light grey areas have exceeded 5 MPa.....116

Figure 5.13: Colour plot of the cadaveric bone showing minimum principal stress (compressive stresses) and maximum principal stress (tensile stresses), both compressive and tensile stresses peak around the neck of the glenoid (left). Colour plot of principal stress minimum showing dark grey areas exceeding 4.6 MPa, the predicted compressive strength of lowest cancellous bone (right)......117

Figure 5.14: Comparison of vertical head displacement and inferior rim displacement with progressive failure..... 118

Figure 5.15: Positive correlation between vertical head displacement ($p = 0.04$) and inferior rim displacement ($p = 0.005$) before, at initial failure and at failure.....118

Figure 5.16: A specimen plot of visual and CT failure with inferior rim and vertical head displacement, showing correlation between CT and visual failure and correlation in displacements with CT and visual failure. Note: see Appendix F for failure key.....119

Figure 5.17: Retrieved smooth pegged cemented implant showing clear failure at the implant/cement interface (Nyffeler et al. 2003). Figure reprinted with permission from Journal of Bone & Joint Surgery-British, 2003, 85B, 5, Influence of peg design and cement mantle thickness on pull-out strength of glenoid component pegs, 748-752.120

Figure 6.1: TOPEL smooth pegged design with macrostructures.129

Figure 6.2: TOKL smooth keeled design with macrostructures. Note: Only large sized implants were tested.129

Figure 6.3: n-S/n-R rough pegged design.129

Figure 6.4: Glenoid fixation fatigue testing in bone substitute foam. Reference pins for rim displacement measure indicated by arrows.131

Figure 6.5: Subluxation curve of 3 designs ($n = 2$), a significant difference in subluxation loads was found between the smooth peg (TOPEL) and both the smooth keel and rough peg (TOKL and n-R respectively) ($p = 0.005$). Note: TOPEL and TOKL are identical except for the anchorage with peg and keel components used respectively.131

Figure 6.6: Average number of cycles at initial failure, showing a marked difference between the smooth keel specimens to all three peg groups.133

Figure 6.7: Design comparison shows marked differences between the keel & peg, the smooth, 8.5 mm mismatch & rough, 4 mm mismatch.....134

Figure 6.8: An increase in both vertical and inferior rim displacement with progressive failure in the smooth keel (TOKL) group. Note: the remaining groups did not reach complete failure.....135

Figure 6.9: FE & in-vitro subluxation curves of the three implant designs. Loads at 90% subluxation showed good correlation in all implants (5.7-12.3% difference).....136

Figure 6.10: FE contact stresses in the superior/inferior direction at the implant/cement interface for TOPEL, TOKL and n-S/n-R implants respectively.137

Figure 6.11: Tensile normal contact stress plot at the implant/cement interface for TOPEL (left), TOKL (middle) and n-S/n-R (right) implants. Note: Dark grey denotes compressive stresses.....138

Figure 6.12: FE contact stresses in the superior/inferior direction at the cement/bone interface for TOPEL, TOKL and n-S/n-R implants respectively.139

Figure 6.13: Tensile normal contact stress colour plot at the cement/bone interface for TOPEL (left), TOKL (middle) and n-S/n-R (right). Note: Dark grey denotes compressive stresses.140

Figure 6.14: Colour plot slices of the cement mantle for TOPEL (left), TOKL (middle) and n-S/n-R (right)implants showing principal stress maximum (tensile stresses). Note: Dark grey denotes compressive stresses and light grey areas have exceeded 5 MPa.141

Figure 6.15: Colour plot of bone substitute for TOPEL (left), TOKL (middle) and n-S/n-R (right) implants showing principal stress minimum (negative or compressive stresses). Note: Light grey denotes tensile stresses.142

Figure 7.1: superiorly and inferiorly aligned LVDTs for rim displacement measures in 2D (left), cadaveric (middle) and 3D (right) studies. Note: figures are the same as Fig. 4.3, 5.2 and 6.4 respectively.154

Figure 7.2: Superior rim (top), inferior rim (middle) and vertical head (bottom) displacements against failure progression in the 3 studies. Note: significant differences were found between before failure and after failure in all 3 measures and studies ($p < 0.01$).....157

Figure 7.3: Superior, inferior and vertical displacements before, during and after testing in the implants that did not fail in the 3D study ($n = 7$), compared to the implants that failed ($n = 5$). Note: no significance was found before and after testing

**in the non-failed implants, whereas significance was found in the failed ($p < 0.05$).
.....158**

**Figure 7.4: Plot showing vertical head and inferior rim displacements correlating to
both CT and visual failure. Note: same figure as Fig. 5.16.....159**

**Figure 9.1: Poor quality scapula bone. Note: excessive posterior wear of the glenoid
surface (right).....179**

**Figure 9.2: Sclerotic, poor quality bone. Note: poor implant seating and excessive
posterior wear (middle) and failure at the implant/cement and cement/bone
interface (right).180**

List of Tables

Table 1.1: Shoulder joint muscles, primary function and movement.	27
Table 2.1: Design comparison of all major glenoid implants on the market. Permission granted to print images from respective implant companies.	52
Table 3.1: Material properties used in the FE model.	67
Table 3.2: Results showing average, and in brackets the standard deviation, number of cycles to failure for different implant designs. Number of samples is ‘n’.	69
Table 4.1: Three treatments to achieve variable implant back roughness.	85
Table 5.1: Results of the cyclic test; number of cycles to failure, nature of failure and confirmation of failure on final CT scans. Note: NB3 and 7 were not tested.....	111
Table 6.1: Description of glenoid implants tested. Note: Implant C and D are identical except in roughness.....	130
Table 6.2: Comparison of superior and inferior rim displacements before and after testing or after failure with published data, showing comparable data between studies.	145
Table 7.1: Summary of results for the 3 fatigue studies, showing cycles to failure and displacements at failure. See Appendix H for displacement raw data and chapters 4, 5 and 6 for cyclic data.....	155
Table 7.2: Superior and inferior rim displacements before and after failure compared with published data. Note: this is the same table as table 6.2 in chapter 6.	160
Table 7.3: Superior and inferior rim displacements in cadaveric study before and after failure compared to published data.	162

Nomenclature

TSA	Total shoulder arthroplasty
Hemi	Hemiarthroplasty
UHMWPE	Ultra high molecular weight polyethylene
HDPE	High density polyethylene
PE	Polyethylene
PU	Polyurethane
PMMA	Polymethylmethacrylate
Co-Cr	Cobalt-chromium alloy
R. lines	Radiolucent lines
A/P	Anterior/Posterior direction
S/I	Superior/Inferior direction
GH	Glenohumeral
FE	Finite element
FEA	Finite element analysis
CT	Computed tomography
RSA	Radiostereometric analysis
SD	Standard deviation
Ra	Average measure of surface roughness (root mean square)

Chapter 1: Introduction

1.1 Introduction

Total shoulder arthroplasty (TSA) still suffers today from mid-term and long-term complications such as glenoid implant loosening, wear, humeral head subluxation/dislocation and implant fracture to mention a few (Wirth & Rockwood Jr. 1996). Unlike the hip and knee joint replacements, the artificial shoulder joint has yet to offer a long-term satisfactory solution to shoulder replacement. TSA is commonly used for severe and advanced forms of arthritis, osteoarthritis and traumatic comminuted fractures of the shoulder. TSA aims, primarily, to alleviate pain and secondly, to restore some function to the shoulder (Neer et al. 1974). In order to understand the design aims of shoulder implants, a brief insight into shoulder anatomy, mechanical structure, tissue formation, shoulder pathology and treatment is due.

1.2 Anatomical Planes & Movement

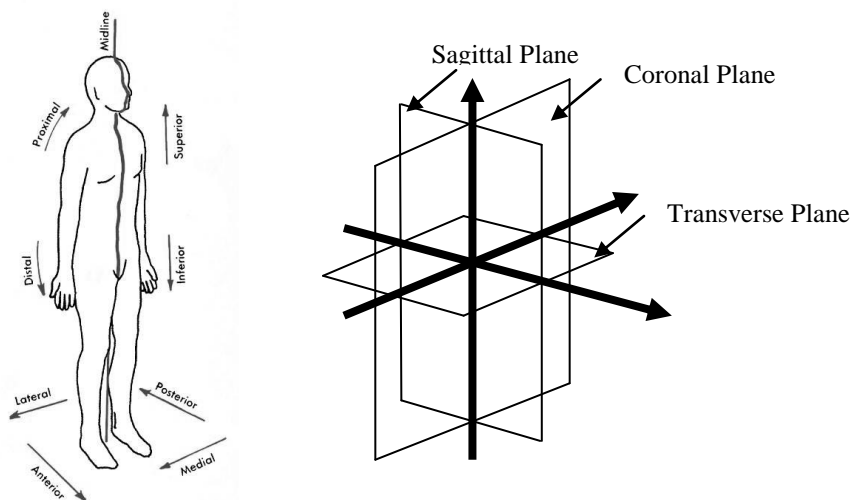


Figure 1.1: Medical anatomical directions (Thompson & Floyd, Manual of Structural Kinesiology, 14th Ed., 2000, McGraw-Hill. Reproduced with permission from The McGraw-Hill Companies) and planes.

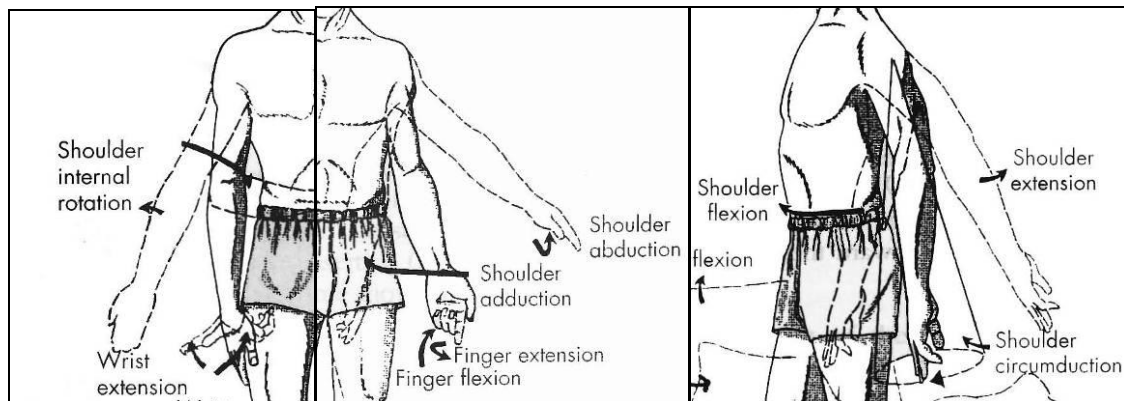


Figure 1.2: Shoulder joint movements (Thompson & Floyd, Manual of Structural Kinesiology, 14th Ed., 2000, McGraw-Hill. Reproduced with permission from The McGraw-Hill Companies).

1.3 Shoulder Joint Anatomy

The shoulder consists of the three articulating bones; the humerus, scapula and clavicle. The humerus, a long shaft bone, articulates proximally with the scapula bone at the glenoid fossa (Fig. 1.3). The scapula, a triangular flat bone, articulates with the humerus, clavicle and thorax and primarily acts as a mobile mast for muscular attachments to achieve upper arm to above shoulder level movement. The clavicle is an S-shaped bone that articulates with the scapula distally and the sternum and opposite clavicle proximally. The left and right scapulas and clavicles anatomically form a broken articulating ring, referred to as the shoulder girdle (Fig. 1.4).

Thus the upper arm movement; arm elevation, extension, abduction, adduction, external and internal rotation, are achieved via three articulations; the glenohumeral (GH) joint, the scapulothoracic joint and the acromioclavicular joint. However, the shoulder joint generally refers to the glenohumeral joint, although it is important to note that the scapulothoracic joint allows the arm to be lifted above the shoulder, which is not achievable by the GH joint alone.

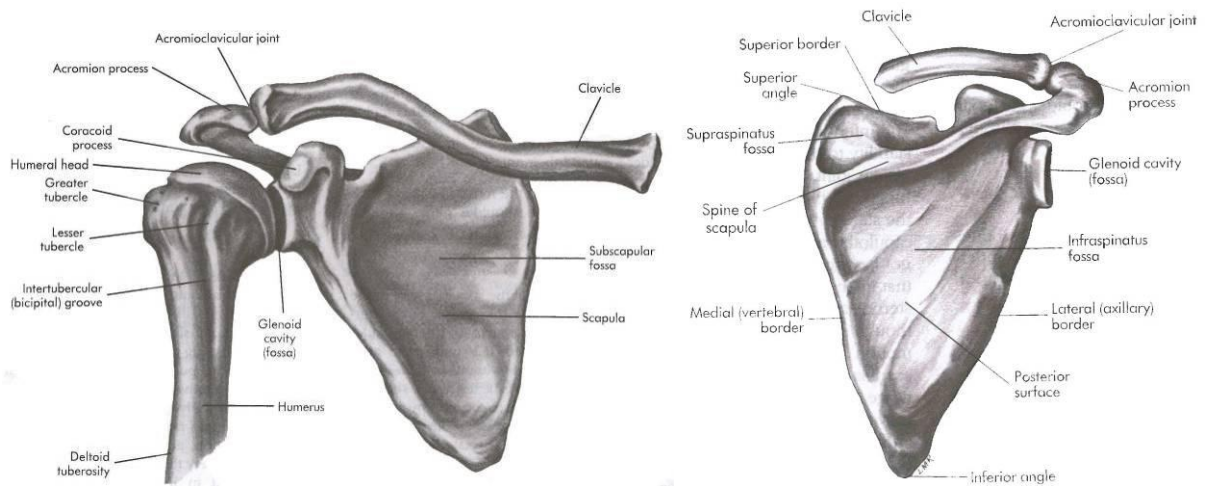


Figure 1.3: Anterior view of the three articulating bones of the shoulder joint; (the humerus, scapula and clavicle (left) and posterior view of the scapula and lateral part of the clavicle (right) Thompson & Floyd, Manual of Structural Kinesiology, 14th Ed., 2000, McGraw-Hill. Reproduced with permission from The McGraw-Hill Companies).

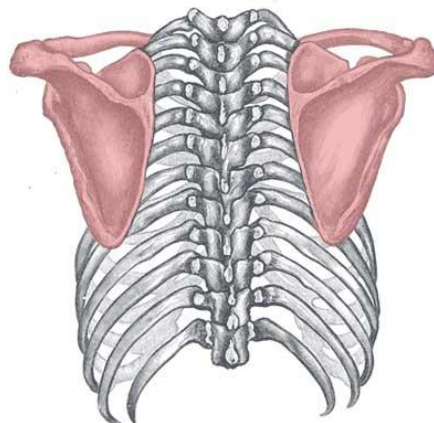


Figure 1.4: Posterior view of the shoulder girdle (red) and thorax (Grays 1918). Figure reprinted and modified with permission from Gray, Henry. *Anatomy of the Human Body*. Philadelphia: Lea & Febiger, 1918; Bartleby.com, 2000. www.bartleby.com/107/. [2009].

1.4 Glenohumeral Joint

The glenohumeral joint is an enarthrodial synovial ball and socket joint. The curvature of the glenoid and humerus do not perfectly match and are usually found with a radial difference of 2-3 mm. The shallow glenoid fossa allows for large ranges of motion. The anterior-posterior

and superior-inferior depths of the glenoid are not equal, varying the level of constraint with the humeral head (Matsen III & Lippitt 2004).

1.5 Shoulder Joint Cartilage & Ligaments

Both articulating surfaces are lined with a layer of cartilage, where the humeral cartilage thickens in the middle of the humeral head surface, and conversely, the glenoid cartilage layer thickens at the rim, thereby increasing conformity (Fig. 1.5).

The labrum is the fibrous cartilage ring of triangular cross-section found to be continuous with the articulating cartilage of the glenoid. The labrum allows the glenoid to form a deeper, more conforming socket for the head (Fig. 1.5 & 1.6). The inner surface of the ring contacts the humeral head and the outer surface serves as attachment sites for ligaments, thus providing the perfect fit between the humeral head and glenoid fossa.

The joint is supported by the joint capsule and the glenohumeral (GH) ligament, which runs continuous with the capsule. The GH ligament is subdivided into 3 bands; the inferior, middle and superior ligament bands (Fig. 1.7), acting as a passive support for the GH joint.

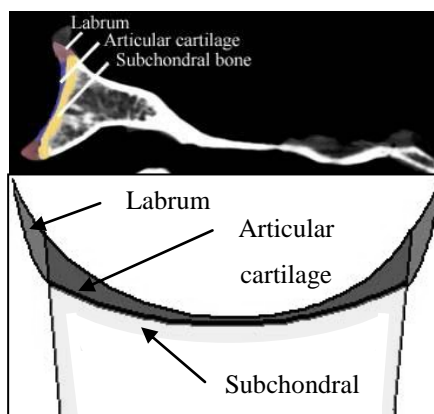


Figure 1.5: CT of transverse section of glenoid and cartilage tissue (top) and schematic of the glenoid cross-section (bottom) demonstrating the conforming cartilage structures.

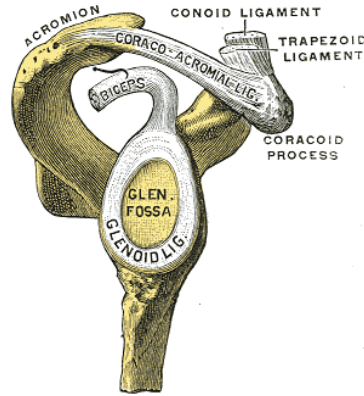


Figure 1.6: Lateral view of the glenoid showing ligaments of the scapula (Gray 1918). Note: glenoid ligament is more commonly known as the labrum. Figure reprinted with permission from Gray, Henry. *Anatomy of the Human Body*. Philadelphia: Lea & Febiger, 1918; Bartleby.com, 2000. www.bartleby.com/107/. [2009].

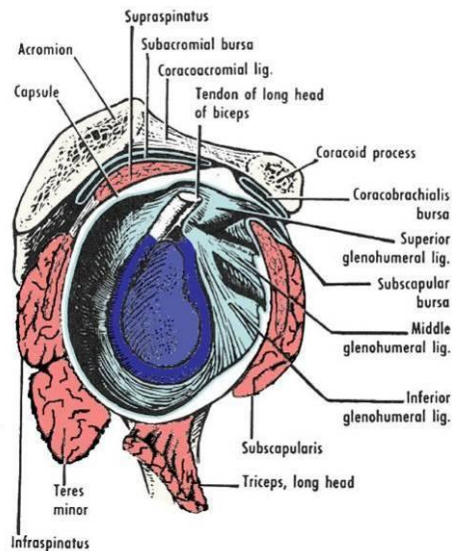


Figure 1.7: Glenohumeral ligament (inferior, middle & superior bands), which are continuous with the capsule (blue). Figure reprinted with permission from Basic Human Anatomy, O'Rahilly et al., (1983), published online <http://www.dartmouth.edu/~humananatomy>.

1.5.1 Cartilage Structure & Mechanics

The hyaline cartilage lining of the GH joint can vary from a thickness of 1-2 mm in smaller joints and in the aging population, to 4-7 mm in younger people and has been found to

thicken with long and short-term exercise. The thickness, compressibility and the transparency of the joint cartilage has been found to decrease with age (Barnett et al. 1961).

Cartilage consists predominantly of extracellular matrix, produced by chondrocyte cells that are sparsely distributed homogeneously throughout the matrix. The matrix consists of interwoven collagenous fibrils and ground substance, forming the glue to the fibrous network. Understandably there are no nerves within the cartilage and no vascular supply except at the bone/cartilage interface where the cartilage is calcified and interface bonding is strong. Although the matrix consists of 70% water in weight, the characteristics of the bearing material is attributed to the mucopolysaccharides.

1.5.2 Muscles of the Shoulder (Thompson & Floyd 2001)

The major muscles responsible for glenohumeral joint movement are the deltoids (anterior, middle & posterior) located superiorly, the coracobrachialis and pectoralis major located anteriorly, the teres major and latissimus dorsi located posteriorly, and the rotator cuff muscles (supraspinatus, infraspinatus, subscapularis & teres minor) surrounding the joint (Fig. 1.8 & Table 1.1). The long head tendon of the biceps and triceps are also found to assist joint movement. The major muscles responsible for scapulothoracic joint movement are the three anterior muscles: the pectoralis minor, serratus anterior, subclavius and the three posterior muscles: trapezius, rhomboid and levator scapula (Fig 1.8 & Table 1.1).

Table 1.1: Shoulder joint muscles, primary function and movement.

Glenohumeral joint muscles	Primary function	Movement
Deltoid	Lifting the humerus & above shoulder movement	Abduction, adduction Flexion, extension External & internal rotation
Rotator cuff	Stabilising the GH joint Aid joint movement	Abduction, adduction Extension External & internal rotation
Coracobrachialis	Assists flexion & adduction	Adduction Flexion
Pectoralis major	Moves scapula forward via flexion of the humerus	Adduction Internal rotation
Latissimus dorsi	Adductor and extends humerus	Adduction Extension Internal rotation
Teres major	Assists latissimus dorsi	Adduction Extension Internal rotation
Biceps (long head)	Depresses the humeral head in glenoid fossa (Rockwood et al. 2009)	
Triceps (long head)	Extends GH joint	Extension
Scapulothoracic joint muscles		
Serratus anterior	Moving scapula forward (abduction) e.g. throwing	Upward rotation Abduction
Pectoralis minor	Aids serratus anterior move scapula forward	Scapula depression Abduction Downward rotation
Subclavius	Stabilises sternoclavicular joint	Depression
Trapezius	Raising arms above head, stabilising scapula & preventing glenoid from dropping during lifting	Elevation, depression Upward rotation
Rhomboid	Stabilises scapula in adduction e.g. while extending or adducting arm	Elevation Downward rotation Adduction
Levator scapula	Elevates scapula	Elevation

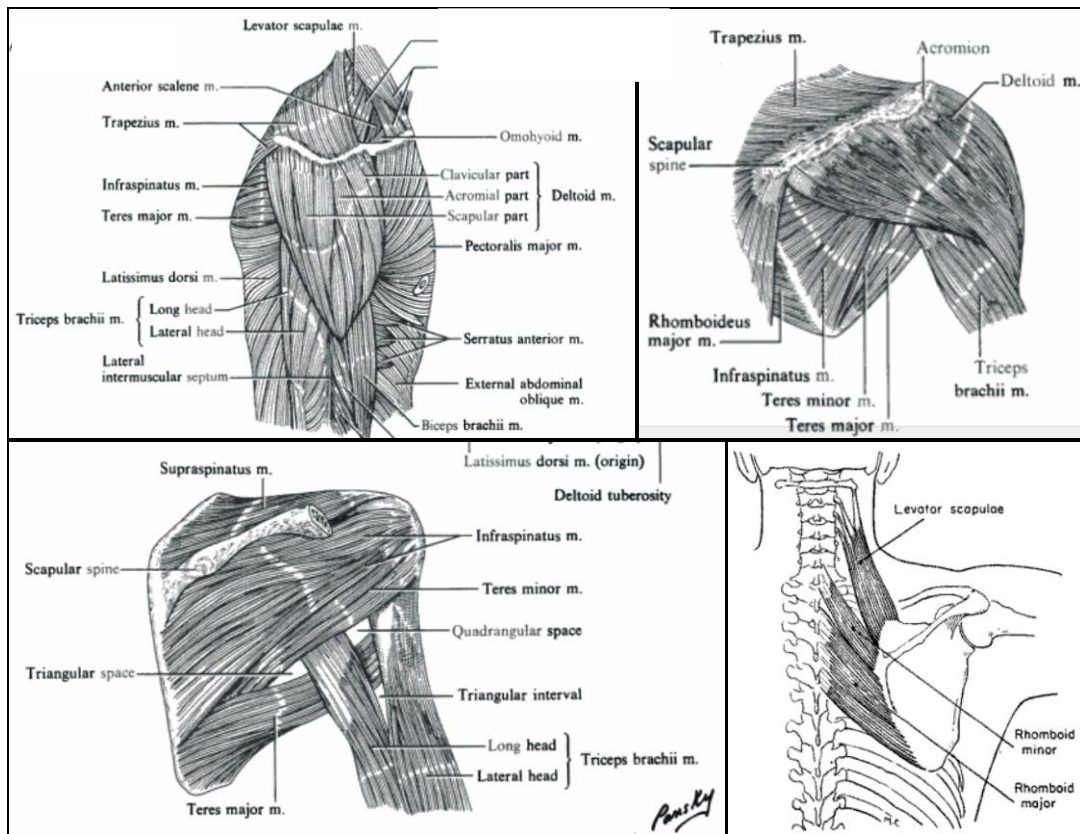


Figure 1.8: Muscles of the shoulder joint (Dutton 2004). Figures reprinted from Orthopaedic Examination, Evaluation and Intervention, (2004), Dutton, M, with permission from McGraw-Hill Companies.

1.5.3 Joint Stabilising Mechanisms

Several mechanisms that help stabilise the joint are categorised as static, dynamic, passive and active stabilisers (Matsen III et al. 2006). The mechanisms of stabilisation in the shoulder joint are the glenoid conformity/concavity, muscular compression, capsuloligamentous restraints, adhesion-cohesion of the articulation surfaces and suction. Instability is defined as the point when the resultant joint force falls beyond the joint rim edge and the point of instability is defined as the subluxation point. Dislocation is defined as the point when rim edge aligns with the head centre (Fig. 1.9).

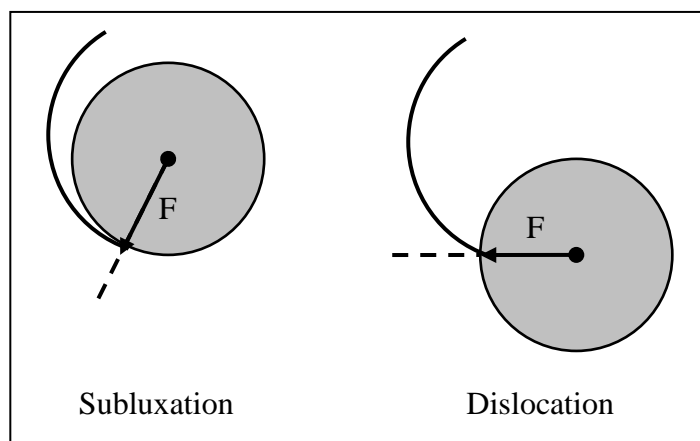


Figure 1.9: Subluxation and dislocation definitions where arrows denote resultant joint force.

The glenoid concavity works by creating a conforming surface in order to centre the humeral head (Fig. 1.5). Joint stability is affected by the level of concavity and conformity in two ways; increasing either the glenoid conformity or depth will increase the transverse force required to subluxate or dislocate the joint (Fig. 1.10). Similarly, increasing the compressive perpendicular force from surrounding muscular tissues increases the transverse force needed to destabilise the joint. The flexibility of the labrum allows for small head movement in the ball and socket joint without compromising the stability (Matsen III et al. 2006).

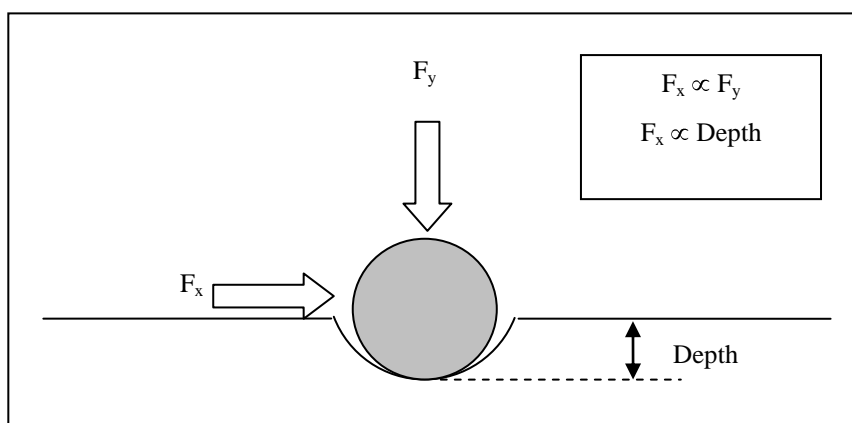


Figure 1.10: Glenoid depth and perpendicular compressive force (F_y) are both proportional to the transverse force (F_x). Note: forces generated by surrounding muscles.

The joint compression (F_y) is provided primarily by the four rotator cuff muscles, each providing compression and stability around the joint both passively and actively (Fig. 1.11). The subscapularis is the primary stabiliser for anterior aspect of the joint. The supraspinatus is mainly the superior stabiliser and the infraspinatus and teres minor, provide the main posterior support. Other shoulder and scapula muscles help provide compression, however,

their support are more effective at various positions during shoulder movement. It is the rotator cuff providing the mid-range stability of the joint and throughout all movements of the shoulder. The second purpose of the rotator cuff is to act as agonists and antagonists in shoulder motion (Chadwick et al. 2004).

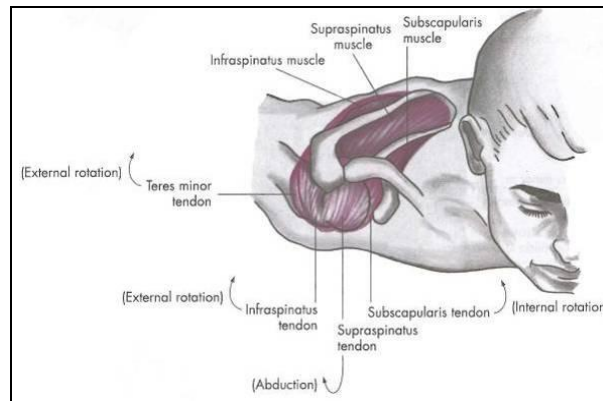


Figure 1.11: Rotator cuff muscles, superior view (Thompson & Lloyd, Manual of Structural Kinesiology, 14th Ed., 2000, McGraw-Hill. Reproduced with permission from The McGraw-Hill Companies).

The joint capsule and ligaments serve as restraints to restrict the range of motion of the humeral head, and by doing so, prevent damage to the tissues. Therefore the ligaments stay lax and unloaded during mid-range movement where the muscular forces dominate (Labriola et al. 2005; Matsen III et al. 2006; Schiffen et al. 2002). As the shoulder reaches its limit, the forces exerted by the muscles decrease and are no longer sufficient to provide stability, the ligaments and capsule become effective and stretch in tension, creating a reactionary force applied to the head, preventing further movement. This capsuloligamentous mechanism is passive and does not require energy like muscles do.

The adhesion-cohesion and suction mechanisms are also passive and work on the physical properties of water and tissues. The adhesion-cohesion is the smooth sliding of the glenohumeral joint due to the thin film of synovial fluid between the articulating tissues which allow sliding and resist separation as a drop of water does between two glass sheets (Fig. 1.12). The suction is created between the head and glenoid socket as a result of the concavity and conformity (radial match) provided by the labrum, generating low pressure in the joint, which maintains the glenohumeral contact (Fig. 1.13).

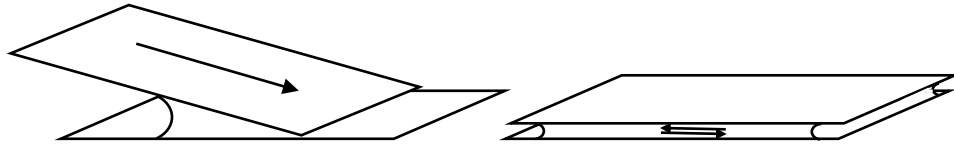


Figure 1.12: Adhesion-Cohesion mechanism (Barnett et al. 1961).

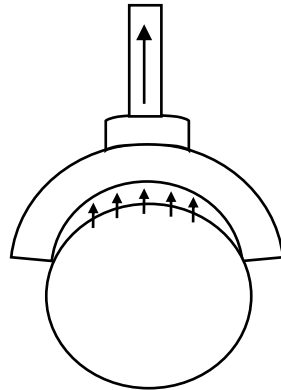


Figure 1.13: Suction mechanism in the natural glenohumeral joint.

1.6 Shoulder Joint Forces

The shoulder muscles generating a force vector through the GH joint has been shown to be maximum at 90° abduction, where the resultant force lies superiorly in the glenoid (Fig. 1.14).

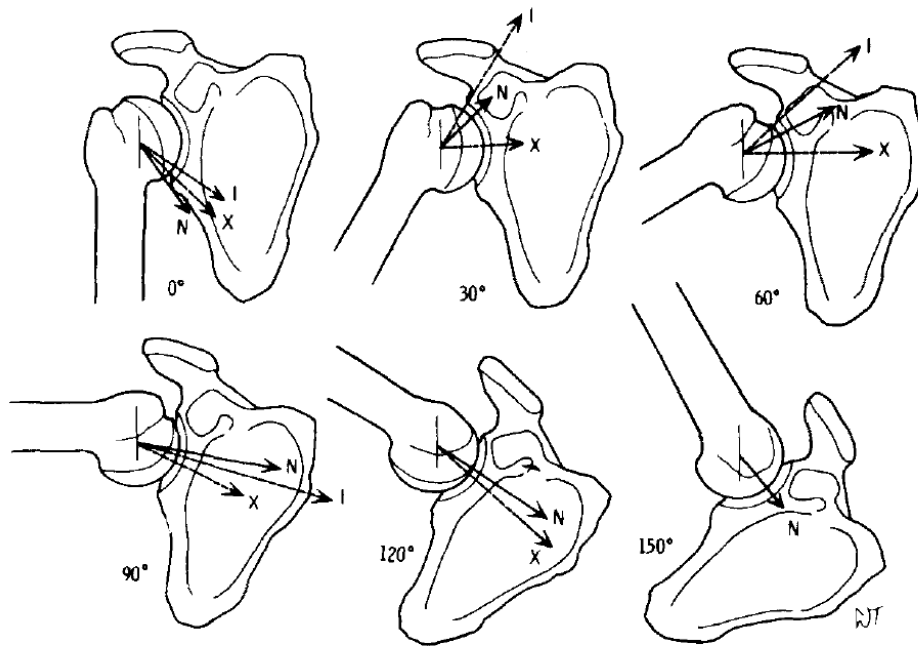


Figure 1.14: Resultant forces of neutral (N), external rotation (X) and internal rotation (I) vectors (Poppen & Walker 1978). Figure reprinted with permission by Wolters Kluwer Health from Poppen, N K & Walker, P S, Forces at the Glenohumeral Joint in Abduction, Clinical Orthopaedics and Related Research, 1978, 135, 165-170.

1.7 Common problems in the Shoulder Joint

The most common shoulder pathologies that can sometimes lead to TSA surgery include osteoarthritis, rheumatoid arthritis and comminuted fractures of the shoulder joint. Other less common pathologies that often require TSA include avascular necrosis, traumatic arthrosis, psoriatic arthritis, atraumatic instability, rotator cuff tear arthropathy and capsulorrhaphy arthropathy. Osteoarthritis is an age-related disease where an articular joint surface is worn away to the bone, and in the case of the shoulder joint, usually leads to posterior humeral head translation, causing asymmetric posterior wear. Rheumatoid arthritis of the shoulder, a multi-joint inflammatory disease, causes destruction of the glenoid surface and poor bone quality, often accompanied by rotator cuff tears. In severe cases where pain and lack of joint movement affects quality of life and in trauma cases, TSA is performed, aimed at alleviating pain first, and then improving joint movement (Neer et al. 1974).

1.8 Total Shoulder Arthroplasty

1.8.1 History

The first documented total shoulder replacement in 1893 was carried out by the French surgeon Jules E. Pèan (Lugli 1978), using a platinum stem and rubber head. However, the first ever TSA may have been a few years earlier by the surgeon Themistocles Gluck in Germany (Bankes & Emery 1995), using ivory and cadaveric bone. Attempts at treating the shoulder joint in the 1930's were unsuccessful, including arthrodesis and autologous fibula transplants (Wilson & Lance 1965). So too were the use of acrylic and cobalt-chrome implants in the 1940's and 1950's to replace the humeral head (Fealy et al. 2008; Post et al. 1979). The first satisfactory TSA surgery was by Krueger in 1950 who aimed at replicating the anatomical shape of the humeral head by making acrylic models of cadaveric bones and manufacturing vitallium implants. The authors reported a "well-functioning, painless shoulder" in a patient suffering osteonecrosis. However it was Neer et al. (1955) who pioneered shoulder replacement surgery, showing satisfactory results of a vitallium humeral implant, Neer I, used in hemiarthroplasty procedures for cases of humeral fracture dislocations.

In 1974, a total non-constrained design, Neer II, was used, resurfacing the glenoid with a cemented high density polyethylene (HDPE) implant in osteoarthritic cases (Neer et al. 1974) (Fig. 1.15). However, TSA was hampered by stability problems, particularly in cases of rotator cuff damage. To address this problem, a wave of fixed fulcrum and 'constrained' designs were introduced in the 1970's and 1980's (Fig. 1.16), with largely unsatisfactory results (Cofield & Stauffer 1977; Gregory et al. 2007; Post et al. 1979). Some of the TSA designs used in the 1970s and 1980s include the metal-on-metal Stanmore shoulder, the reverse Liverpool shoulder, the non-constrained and semi-constrained DANA shoulder, the Bickel prosthesis and St Georg shoulder. The use of non-cemented metal-backed PE glenoids was also commonly used in the 1980s and 1990s, in an attempt to provide a more stable fixation and promote bone in-growth (Boileau et al. 2002; Martin et al. 2005; Sperling et al. 2000; Tammachote et al. 2009; Taunton et al. 2008; Wallace et al. 1999) (Fig 1.17 & 1.18). However, problems with PE wear, PE liner dissociation, loosening, osteolysis and screw

breakages and now clinical studies suggest avoiding its use (Boileau et al. 2002; Taunton et al. 2008). Currently the non-constrained glenoid design, first introduced by Neer et al. (1974), is most commonly used in TSA surgery, although the design has not fundamentally changed, there have been features introduced to improve implant outcomes (Table 2.1).

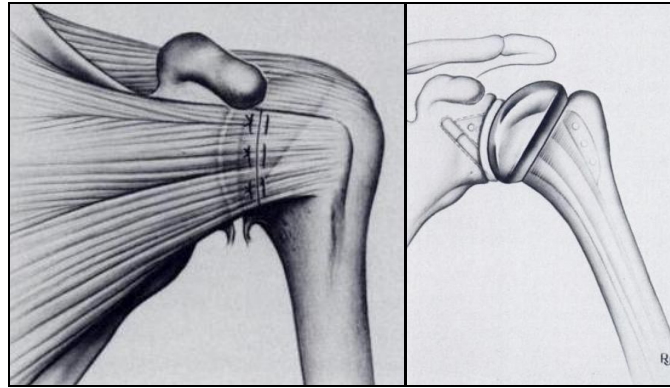


Figure 1.15: Neer Hemiarthroplasty (left) and non-constrained total shoulder arthroplasty (right). Figures reprinted with permission from Journal of Bone and Joint Surgery American, 1974, 56A, 1, Replacement Arthroplasty for Glenohumeral Osteoarthritis, Neer, 1-13.

After the first generation of Neer II implants came the 2nd generation of modular implants, aimed at customising the implants by enabling the surgeon to vary the stem and humeral head component sizes. The three main advantages of a modular implant are firstly to make implantation easier. Secondly, a variety of stem sizes avoids the need to ream the humeral intramedullary canal, avoiding unnecessary trauma. Thirdly, selecting the best humeral head to achieve the correct tension of the joint capsule and surrounding muscles (Mileti et al. 2005). The 3rd generation of TSA implants introduced offset humeral heads in the medial and posterior directions in order to produce a more anatomically aligned humeral component. Companies still offer the 1st generation “monoblock”, 2nd generation “modular” and 3rd generation “anatomical” humeral stems. The reverse shoulder, first used in the 1980’s, are now used mostly in shoulders where the rotator cuff function is almost nonexistent (often RA shoulders). The reverse shoulder has recently gained wider use since its FDA approval in 2004. Some of the complications that are found in reverse shoulder implants include scapula notching, loosening and screw fracture, which also need to be addressed.

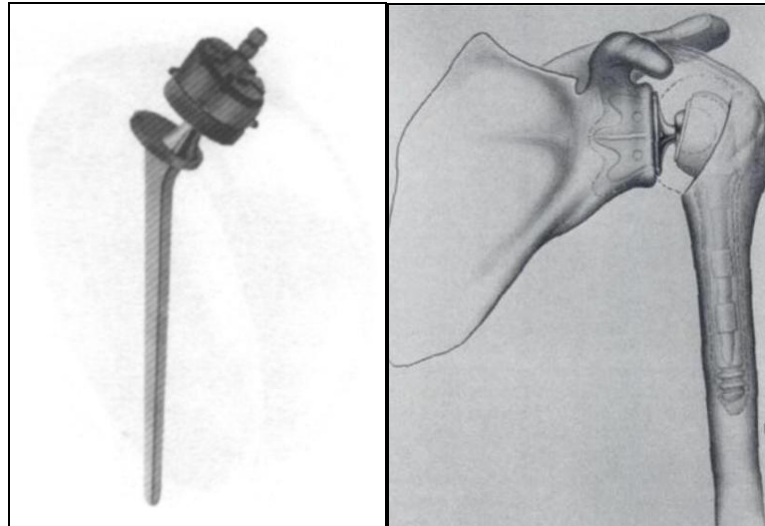


Figure 1.16: The Michael Reese shoulder (left) and Neer Mark III reverse shoulder (right), two examples of a fixed-fulcrum TSA design (Williams et al. 2004; Zadeh & Calvert 1998). Figure reprinted with permission from Surgical Disorders of the Shoulder, Watson, M (Ed), Michael Reese shoulder implant, p 132, Copyright (1990).

Other current TSA designs include the bi-polar design, using a standard humeral ball and stem and attaching the required head size for the glenoid articulation. Modular bio-material stems offer the choice of a metallic or ceramic head. Humeral surface replacements such as the Copeland design are also marketed to minimise the removal of bone stock and preserve the anatomical neck in order to maintain the geometry of the humeral head. New glenoid designs are attempting to marry the cemented and cementless fixation by featuring a centralised peg encased in a metal mesh to promote osseointegration (Table 2.1).

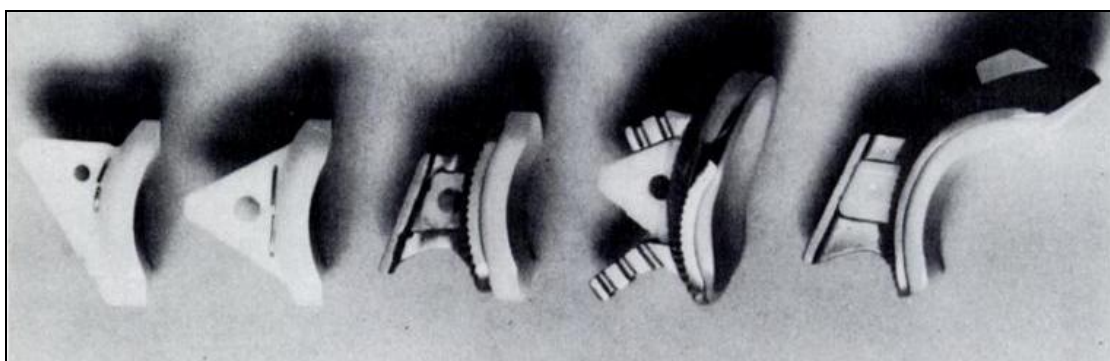


Figure 1.17: Glenoid designs showing non-constrained PE (two left), non-constrained metal-back (middle), and two semi-constrained metal-back glenoids (two right). Note: semi-constrained implants were designed to prevent upward head migration (Neer et al. 1982). Note: figure reprinted with permission from Journal of Bone and Joint Surgery American, 1982, 64A, 3, Recent experience in total shoulder replacement, Neer, 319-337.



Figure 1.18: (Left to right) Metal-back Cofield, Neer and Tornier implants that are no longer in use (Katz et al. 2009). Images used with permission from Tornier, Inc., and Smith & Nephew, Inc., February 2010.

The debate between choosing hemi and total shoulder arthroplasty is still on-going, indeed the choice of using a hemi seems to also be driven by the lack of reliable long-term success rates of TSA. According to the Norwegian Joint Registry (2007), 59 TSAs and 213 hemis were carried out, likewise, in Scotland, a 5 year period showed only 54 TSA compared to 397 hemis (Sharma & Dreghorn 2006). In Sweden, 312 hemis were performed compared to 47 TSAs in 1999 alone. It is well documented that TSA performs better in function and pain relief compared to a hemi (Bryant et al. 2005; Gartsman et al. 2000; Orfaly et al. 2003; Sperling et al. 2004). However, due to the issues with long-term glenoid fixation, TSA is often avoided or delayed by performing a hemi (Rahme et al. 2001). This is not to say that a hemi has better long term outcomes, in fact failed hemis have been shown to have worse function than failed TSAs (Hasan et al. 2002), it is also reported that the rate of revision in hemis is higher at 10 years compared to TSA (Sperling et al. 2004) and converting a hemi to a TSA can result in poorer functional and pain outcomes compared to the case if a TSA was performed in the first place (Carroll et al. 2004). Finally, the main causes of revision for hemis are glenoid erosion and wear (Sperling & Cofield 1998). Thus the much larger number of hemi operations compared to TSA procedures seems to stem partly from avoiding the problems associated with TSAs, partly from limited surgical view or grossly deformed glenoid, and thirdly, the option of converting a hemi to a TSA can be an attractive one. Although short term functional outcomes between hemi and TSA are comparable, the problem of glenoid arthrosis is a concern and in the long-term hemis may reveal poorer outcomes to TSA. Thus, investigating glenoid fixation is relevant for both TSA and hemi cases. Currently, there are several varied glenoid implant designs on the market aimed to improve the glenoid fixation (Table 2.1), namely flat-back and curved-back designs, metal-

back and all-polyethylene implants, cementless and cemented fixations and keel versus pegged anchorage.

1.8.2 Surgical Approach

The most common surgical approach in TSA is the deltopectoral approach anteriorly. The surgery consists of detaching the subscapularis from the lesser tuberosity on the humerus, removing the humeral articulating surface from the anatomical neck line and reaming the intramedullary canal. Depending on the surgeon's preference, the humeral stem is either cemented or press fitted. The glenoid is exposed and reamed to remove the cartilage layer and create a conforming surface for the glenoid implant, taking care to maintain the subchondral cortical bone layer on the glenoid surface as this is thought to improve implant seating. The peg or keel holes are drilled and the glenoid implant cemented, usually without accurate guides to locate scapula orientation or visual cues such as fluoroscopy.

Passive movement is applied immediately postoperatively, keeping the arm in a sling for the first few weeks, and then dynamic shoulder exercises are introduced. Patients are assessed on pain relief, ranges of motion, satisfaction and radiographic observations. In cases of unsatisfactory outcomes and particularly severe pain, revision surgery is carried out. Due to complications of poor bone stock and quality in revision surgery, revision is usually avoided as much as possible.

1.8.3 Surgical Outcome

Clinical outcome scores and assessments carried out by the surgeons and clinicians assess the patient in pain, range of motion (ROM), ability to carry out daily activities and strength (Smith, 2006). There are several different outcome scores that are widely used such as the Constant and Murley Score, the American Surgeons Elbow and Shoulder score (ASES), the University of California score (UCLA), the Oxford Test and finally using the clinician's own assessment or department protocol, each assessment having its own scoring system. Subjective assessments also vary from the Simple Shoulder score, the Western Ontario Osteoarthritis of the Shoulder index (WOOS) to the Short Form Health Survey (SF-36 test), each with its own scoring system. The radiographic views are more standardised using anteroposterior views, anteroposterior 40 degree oblique views and axillary views. Self

assessment questionnaires use similar criteria as the clinical examination to assess the patient. In addition to this, quality of life and general patient satisfaction assessments are used which are a somewhat hard to define and analyse. Having said that Smith et al. (2006) compared a self-filled assessment by a patient and a clinical assessment carried out by the surgeon found an 87% agreement between the doctor and patient assessment. However the questionnaire did not include quality of life, general state of satisfaction/happiness, et cetera.

1.9 Fixation Problem in TSA

If any of the four stability mechanisms are compromised, the shoulder experiences corresponding instability, in other words, the inability for the GH joint to correctly align the resultant joint reaction force of the humeral head to the glenoid surface (Fig. 1.9). The head centring can also be compromised due to the loss or reduction in concavity, since the labrum and cartilage have been removed. Clinically, the loss of concavity can be felt by a lack of resistance to head displacement where the head should be resisted by the lip of the glenoid.

Secondary effects of surgery can also impact on the joint fixation. Damage, tear, dysfunction, paralysis and detachment of any of the four rotator cuff muscles results in a lack of compressive stability in the corresponding area and hence can cause excessive head displacement. A lack of ligament or capsule support will result in the humeral head over rotating, reducing the effect of muscles to compress the joint, and leading to patients feeling a weakness of the arm under certain shoulder movements (Matsen III et al. 2006).

The adhesion-cohesion and suction mechanisms can be compromised as a result of a lack of concavity. This can often be described by the patients as a feeling of the shoulder being “out of place” (Matsen III et al. 2006) and humeral head feels less secure as is often the case in shoulder replacement surgery. On the other hand, excessive liquid (effusion) or bleeding at the joint can also be a cause of loss of suction or adhesion.

All the above problems result in excessive head translation, giving a “rocking horse affect” on the joint (Matsen III & Lippitt 2004) (Fig. 1.19), resulting in eventual loosening of the

fixation and often instability at mid-term results of approximately 2-5 years. This loosening problem has hampered TSA surgery for decades, thus investigating the various aspects of TSA to improve clinical outcomes is an important area of medical research. Currently the vision in shoulder joint replacement is to maintain a long term (over 10 years) pain-free, functioning TSA shoulder, free from loosening complications.

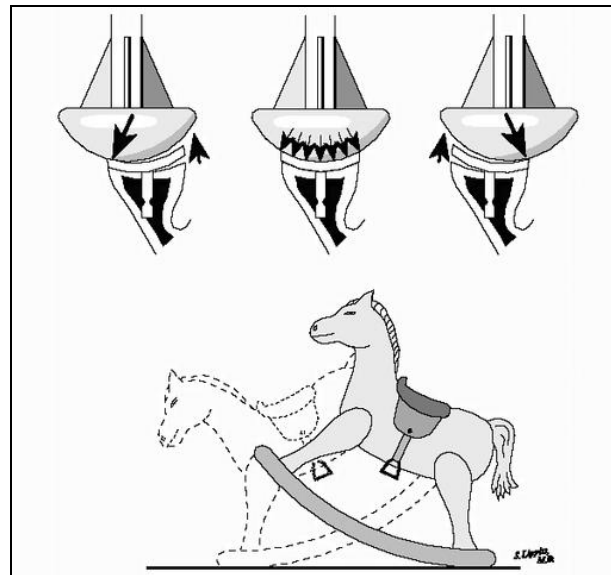


Figure 1.19: Eccentric loading of glenoid implant, leading to “rocking horse” mechanical loosening (Matsen III & Lippitt 2004). Image reprinted with permission from University of Washington website, <http://www.orthop.washington.edu>.

1.10 References

- Bankes, M J K & Emery, R J H (1995). Pioneers of Shoulder Replacement: Themistocles Gluck and Jules Emile Pèan, *Journal of Shoulder and Elbow Surgery*, 4, (4): 259-262.
- Barnett, C H, et al. (1961). *Synovial Joints: Their Structure and Mechanics*, Longmans, London.
- Boileau et al. (2002). Cemented Polyethylene Versus Uncemented Metal-backed Glenoid Components in Total Shoulder Arthroplasty: A Prospective, Double-blind, Randomized Study, *Journal of Shoulder and Elbow Surgery*, 11, (4): 351-359.
- Bryant, D, et al. (2005). A Comparison of Pain, Strength, Range of Motion, and Functional Outcomes After Hemiarthroplasty and Total Shoulder Arthroplasty in Patients with Osteoarthritis of the Shoulder. A Systematic Review and Meta-Analysis, *Journal of Bone and Joint Surgery, American Volume*, 87A, (9): 1947-1956.
- Carroll, R M, et al. (2004). Conversion of Painful Hemiarthroplasty to Total Shoulder Arthroplasty: Long-Term Results, *Journal of Shoulder and Elbow Surgery*, 13, (6): 599-603.
- Chadwick, E K J, et al. (2004). Biomechanical Analysis of Scapular Neck Malunion-A Simulation Study, *Clinical Biomechanics*, 19: 906-912.
- Cofield, R H & Stauffer, R N (1977). The Bickel Glenohumeral Arthroplasty, Conference on Joint Replacement in the Upper Limb, Institution of Mechanical Engineers, London, 21-25.
- Dutton, M (2004). *Orthopaedic Examination, Evaluation and Intervention*. McGraw-Hill, New York. [Http://books.google.co.uk](http://books.google.co.uk), 418-419.
- Fealy, S, et al. (2008), *Shoulder Arthroplasty: Complex Issues in the Primary and Revision Setting*, Thieme Publishing Group, New York.
- Gartsman, G M, et al. (2000). Shoulder Arthroplasty with or without Resurfacing of the Glenoid in Patients Who Have Osteoarthritis, *Journal of Bone and Joint Surgery, American Volume*, 82A, (1): 26-34.
- Gregory, T et al. (2007). Developments in Shoulder Arthroplasty, *Proceedings of the Institution of Mechanical Engineers*, 221, Part H: Journal Engineering in Medicine, 87-96.

- Gray, H, *Anatomy of the Human Body*. Philadelphia, Lea & Febiger, 1918; Bartleby.com, 2000.
- Hasan, S S, et al. (2002). Characteristics of Unsatisfactory Shoulder Arthroplasties, *Journal of Shoulder and Elbow Surgery*, 11, (5): 431-441.
- Katz, D, et al. (2009). Plaidoyer en Faveur du Concept D'embase Glénoïdienne Métallique Dans Les Prothèses Totales Anatomiques D'Épaule, www.maitrise-orthop.com, September 2009.
- Labriola, J E, et al. (2005). Stability and Instability of the Glenohumeral Joint: The Role of Shoulder Muscles, *Journal of Shoulder and Elbow Surgery*, 14, (1S): 32S-38S.
- Lugli, T (1978). Artificial Shoulder Joint by Pèan (1893). *Clinical Orthopaedics and Related Research*, 133: 215-218.
- Martin, S D et al. (2005). Uncemented Glenoid Component in Total Shoulder Arthroplasty. Survivorship and Outcomes, *Journal of Bone and Joint Surgery, American Volume*, 87A, (6): 1284-1292.
- Matsen III, F A, & Lippitt, S B (2004). *Shoulder Surgery: Principles and Procedures*. Saunders, Philadelphia. Principles of glenoid arthroplasty.
- Matsen III, F A, et al. (2006). Principles for the Evaluation and Management of Shoulder Instability, *Journal of Bone and Joint Surgery, American Volume*, 88A, (3): 647-659.
- Mileti, J, et al. (2005). Monoblock and Modular Total Shoulder Arthroplasty for Osteoarthritis, *Journal of Bone and Joint Surgery, British Volume*, 87B, (4): 496-500.
- Neer II, C S, et al. (1955). Articular Replacement for the Humeral Head, *Journal of Bone and Joint Surgery, American Volume*, 37A, (2): 215-228.
- Neer II, C S, et al. (1974). Replacement Arthroplasty for Glenohumeral Osteoarthritis, *Journal of Bone and Joint Surgery, American Volume*, 56A, (1): 1-13.
- Neer II, C S, et al. (1982). Recent Experience in Total Shoulder Replacement, *Journal of Bone and Joint Surgery, American Volume*, 64A, (3): 319-337.
- O'Rahilly, R, et al. (1983). *Basic Human Anatomy*, <http://www.dartmouth.edu>, figure 8-6, 2009.
- Orfaly, R M, et al. (2003). A Prospective Functional Outcome Study of Shoulder Arthroplasty For Osteoarthritis With An Intact Rotator Cuff, *Journal of Shoulder and Elbow Surgery*, 12, (3): 214-221.

- Poppen, N K & Walker, P S (1978). Forces at the Glenohumeral Joint at Abduction, *Clinical Orthopaedics and Related Research*, 135: 165-170.
- Post, M, et al. (1979). Constrained Total Shoulder Joint Replacement: A Critical Review, *Clinical Orthopaedics and Related Research*, 144: 135-150.
- Rahme, H, et al. (2001). The Swedish Elbow Arthroplasty Register and The Swedish Shoulder Arthroplasty Register, *Acta Orthopaedica Scandinavica*, 72, (2): 107-112.
- Rockwood Jr., C A, et al. (2009). *The Shoulder*, 4th edition, Saunders Elsevier, Philadelphia.
- Schiffert, S C, et al. (2002). Anteroposterior Centering of the Humeral Head on the Glenoid In Vivo, *The American Journal of Sports Medicine*, 30, (3); 382-387.
- Sharma, S & Dreghorn, C R (2006). Registry of Shoulder Arthroplasty – The Scottish Experience, *Annals of The Royal College of Surgeons of England*, 88: 122-126.
- Smith, A M, et al. (2006). Patient and Physician-Assessed Shoulder Function After Arthroplasty, *Journal of Bone and Joint Surgery, American Volume*, 88A, (3): 508-513.
- Sperling, J W & Cofield, R H (1998). Revision Total Shoulder Arthroplasty for the Treatment of Glenoid Arthrosis, *Journal of Bone and Joint Surgery, American Volume*, 80A, (6): 860-867.
- Sperling, J W, et al. (2000). Radiographic Assessment of Ingrowth Total Shoulder Arthroplasty, *Journal of Shoulder and Elbow Surgery*, 9, (6): 507-513.
- Sperling, J W, et al. (2004). Minimum Fifteen-year Follow-up of Neer Hemiarthroplasty and Total Shoulder Arthroplasty in Patients Aged Fifty Years or Younger, *Journal of Shoulder and Elbow Surgery*, 13, (6): 604-613.
- Tammachote, N, et al. (2009). Long-Term Results of Cemented Metal-Backed Glenoid Components for Osteoarthritis of the Shoulder, *Journal of Bone and Joint Surgery, American Volume*, 91A, (1): 160-166.
- Taunton, M J, et al. (2008). Total Shoulder Arthroplasty with a Metal-Backed, Bone-Ingrowth Glenoid Component, *Journal of Bone and Joint Surgery, American Volume*, 90A, (10): 2180-2188.
- Thompson, C W & Floyd, R T, *Manual of Structural Kinesiology*, McGraw-Hill Higher Education, 14th edition, 2000.

- Wallace, A L, et al. (1999). Resurfacing of the Glenoid in Total Shoulder Arthroplasty - A Comparison, At a Mean of Five Years, of Prostheses Inserted With and Without Cement, *Journal of Bone and Joint Surgery, American Volume*, 81A: 510-518.
- Williams, G R, et al. (2004). *Shoulder and Elbow Arthroplasty*, Lippincott Williams & Wilkins, Philadelphia, p 6.
- Wilson, P D & Lance, E M (1965). Surgical Reconstruction of the Skeleton Following Segmental Resection for Bone Tumours, *Journal of Bone and Joint Surgery, American Volume*, 47A, (8): 1629-1656.
- Wirth, M A & Rockwood Jr, C A, (1996). Current Concepts Review - Complications of Total Shoulder-Replacement Arthroplasty, *Journal of Bone and Joint Surgery, American Volume*, 78A, (4): 603-616.
- Zadeh, H G & Calvert, P T (1998). Recent Advances in Shoulder Arthroplasty, *Current Orthopaedics*, 12: 122-134.

Chapter 2: Literature Review of the Problems in Glenoid Implant Loosening

2.1 Glenoid Implant Loosening

The short term to mid-term outcomes (postoperative to 5 years) of TSA have shown excellent to good clinical results as shown by Neer and Morrison (1988) where out of 19 patients 89% showed excellent to good results. Similarly Gill et al. (1999) found 88% of patients (15 out of 17) had excellent or better pain relief. Collins et al. (2004) found in 25 TSA shoulders, all subjects experience better pain relief and function. Cofield (1984) publicised a mid-term study (2-6 years) of 73 shoulders showing 92% of patients found an improvement to pain, Torchia et al. (1997) showed 81% of the 89 patients had improved with regards to pain after 5-17 years follow-up. It is clear that the short-term outcomes of TSA are very good (Appendix A & B).

However more mid-term results reveal some of the problems in TSA as shown by Hill and Norris (2001) who investigated the follow up of 14 patients after an average of 5.8 years showing 9 patients (64%) with good to satisfactory outcome whereas 5 (36%) were unsatisfactory with 2 (21%) failing due to glenoid loosening, requiring re-surgery. Instability and loosening accounted for the majority of the complications. Martin et al. (2005) show TSA failure occurred in 16 out of 140 shoulders (11%) from which 5 were due to loosening of the glenoid implant. Comparatively in a paper by Wallace et al. (1999), out of 86 shoulders, 14 showed complications (16%) with 8 (9%) requiring revision, however loosening was not a cause for re-surgery. A retrieval study by Scarlat and Matsen (2001) investigated 37 retrieved implants. The authors found the cause for re-surgery for 95% (18/19) of the glenoids were due to instability and loosening.

2.2 Causes of Loosening

2.2.1 Area of Failure

Information on loosened glenoids and retrieved glenoids are few. However some papers have touched on this, such as Wirth et al. (1999) who investigated the wear particles of UHMWPE in three cases of retrieved glenoids 10 to 16 years postoperatively due to aseptic loosening. The conditions of the loosened keel glenoids (the fixation site) were described as “the cement was mainly attached to the keel of the glenoid component although some cement was recovered from the glenoid trough”. This indicates the glenoid fixation detached mainly from the cement/bone interface at the keel but also partially from the implant/cement interface. However it is still not clear which of the two interfaces are more resistant to failure and which interface fails first in-vivo. Similarly, photos of a retrieved glenoid in a paper by Yian et al. (2005) indicate the cement partially covering the glenoid back and pegs (Fig. 2.1). However, Nyffeler et al. (2003) demonstrated failure completely at the implant/cement interface from one retrieval case (Fig. 2.2). With the few retrieval studies published, most have focused on the surface wear and PE cold flow.

PMMA bone cement failure is believed by some authors to contribute to fixation failure (Lacroix & Prendergast 1997). The material properties of bone cement have also been shown to be weak under tension, particularly under fatigue loading (Wixson et al. 1987). Many of these studies are FE based, however, clinically there is no mention of such failure. The variability of the cement mantle thickness is notoriously varied and cement cracks from the retrieval photos (Fig. 2.1) are evident. However, this may be a result of another failure elsewhere in the fixation. Thus some comments on the nature of fixation failure have not been conclusive and warrant further study.

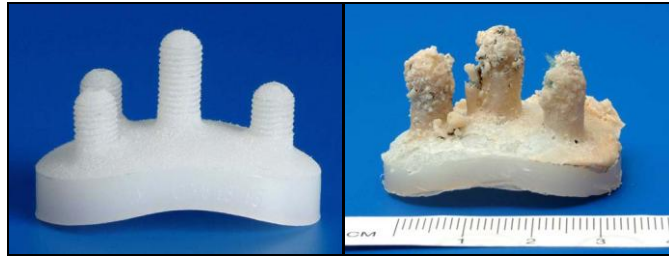


Figure 2.1: Before implantation (left) & retrieved threaded implant (right) showing partially intact cement at the pegs (Yian et al. 2005). Figure reprinted with permission from Journal of Bone and Joint Surgery American, 2005, 87A, 9, Radiographic and Computed Tomography Analysis of Cemented Pegged Polyethylene Glenoid Components in Total Shoulder Replacement, Yian, 1928-1936.

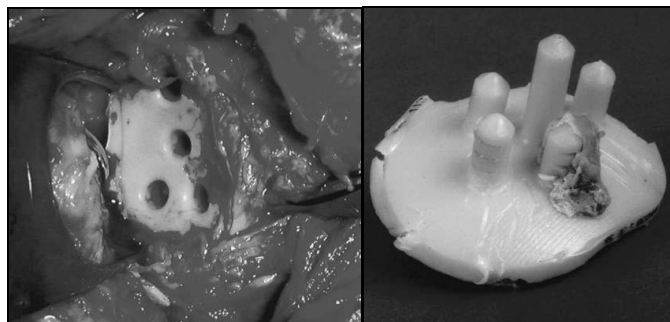


Figure 2.2: Revision surgery showing cement intact with the glenoid bone (left) & retrieved glenoid showing failure occurring at the implant/cement interface (right) (Nyffeler et al. 2003). Figure reprinted with permission from Journal of Bone & Joint Surgery-British, 2003, 85B, 5, Influence of peg design and cement mantle thickness on pull-out strength of glenoid component pegs, 748-752.

Clinical studies, using radiolucent lines (r. lines) have associated the appearance of r. lines as a loss of fixation, either by a physical interfacial gap or by the formation of fibrocartilage tissue, indicating glenoid loosening as a cement/bone interface problem (Bohsali et al. 2006; Matsen III et al. 2008). Despite the correlation between a complete lucent line around the glenoid implant and loosening of the glenoid (Torchia et al. 1997), the emergence of r. lines is yet to be fully understood.

2.2.2 Interfacial Strength & Material Strength

Mann et al. (1999) tested the cement/bone interface in tension and shear in tibia bone and found the interface is weak under tensile loads (1.35 MPa and 2.25 MPa respectively). Mixed-mode failure of the cement/bone interface under tensile and shear loads showed an increase in strength compared to pure tensile loads (Mann et al. 2001). Perhaps this raises questions as to what the predominating loads are at the interfaces during loading.

However, there are no published studies on the cement/bone strength in glenoid bone and the implant/cement interface strength. A study at the Biomechanics group (Sanghavi et al. 2007) has shown the interface strength between PE of roughnesses varying from 0 μm to $5.55 \pm 0.37 \mu\text{m}$ and cement to be 0 to 3.2 MPa respectively. The interface strength \pm SD between cadaveric glenoid bone and cement was found to be 3 ± 1.4 MPa compared to the interface between cement and bone substitute of minimum 2.32 ± 0.54 MPa.

Many studies on the tensile, compressive and fatigue properties of PMMA and other commercially available bone cements have been published (Krause & Hoffman 1989; Lewis 1997; Linden et al. 1989; Wixson et al. 1987). The considerably lower tensile fatigue strength of cement compared to the material's quasi-static tensile strength has led some to believe cement as one of the problems in fixation failure. Fatigue tests to 100,000 cycles, or the equivalent of 20 arm abductions a day for 13.5 years have shown the fatigue strength to be as low as 6 MPa compared to 27.1 MPa (Krause & Mathis 1988; Krause & Hoffman 1989), a problem that is predicted to arise at long-term results. However, it is still clear glenoid fixations are being lost at mid-term outcomes, indicating to a much earlier problem than cement fatigue. Therefore the awareness of interfacial strengths under static and fatigue loads is important when investigating fixation performance.

2.2.3 Osteolysis

Osteolysis, defined as an immune response to foreign particles, such as polymer or metallic particulates, present at the bone/cement or bone/implant interface, resulting in resorption of bone round the implant. This leads to loss of the implant fixation and eventual loosening. This phenomenon was particularly prevalent in early hip replacements where high PE wear of the acetabular cup caused PE particulate build up at the joint, particularly at the cement/bone interface, leading to osteolysis and loosening.

Although osteolysis is a concern across all implanted PE bearing surfaces, the short term complications in TSA indicate wear is not the primary problem. Furthermore, due to lower bearing loads at the shoulder, it is rather joint stability and loosening, which are the most common complications.

2.3 Failure Progression

Only clinical studies have been able to show failure progression, based on the questionable r. lines. Studies have shown r. lines appearing at the peg/keel, at the superior rim and inferior rim (Nagel et al. 2002; Kelly et al. 1986; Klepps et al. 2005, Lazarus et al. 2002, Rahme et al. 2004). Most studies observed r. Lines were more prevalent inferiorly, where the lines often ‘grow’ around the implant (Nagel et al. 2002; Klepps et al. 2005, Rahme et al. 2004). However, Stewart & Kelly (1997) have shown the appearance of r. lines does not necessarily suggest loosening, unless the r. lines are progressive and ‘grow’ over time. Likewise, it is only if a 1.5 mm thick r. line is found completely around the implant or the implant visibly shifts or rotates, that it is deemed ‘definitely loose’ (Torchia et al. 1997). The lack of in-vitro failure progression studies highlights an important need for further research using standardised lab testing techniques.

2.4 Current Methods of Monitoring Glenoid Failure

Clinical studies consist of a medical examination, radiographs and often patient evaluation. Apart from the indications of implant success through assessing range of motion, level of function and pain relief, the only method of ‘seeing’ the implant is through radiographs. The appearance of r. lines have interested clinicians for years particularly the appearance of lines immediately postoperatively. Although it often requires an experienced eye, it is observed as a low density area or band observed between the implant/bone interface, the cement/bone interface or the implant/cement interface. This band has been attributed to loss of fixation or a detachment between the two interfaces which often ‘grows’ in thickness along the interface path with time.

To define the different levels of r. lines, Wallace et al. (1999) defined a stable glenoid implant as having no r. lines or incomplete r. lines of less than 1.5 mm thickness. A complete

r. line, which surrounds the whole interface, is considered possibly loose. A complete r. line greater than 1.5 mm (often defined as 2 mm in other studies) is considered radiographically loose, and implants with visible tilt or implant migration is considered definitely loose (both clinically and radiographically). The relationship between radiolucent lines and loosening is not a clear one; however a correlation has been shown between the emergence of r. lines and increase in pain (Hertel & Ballmer 2003). Other studies such as Brostrom et al. (1992) and Torchia et al. (1997) have concluded that r. lines adversely affect functional outcome and is linked to aseptic loosening.

As an assessment or predictor tool there are a few problems with using radiographs, firstly the use of standardised views and protocols are important in order to achieve reproducible results as shown by Havig et al. (1997). Secondly, the radiographic image conveys a 2D image from a 3D subject. Thirdly, density changes in the images are not clearly defined boundaries and it can therefore be difficult to assess and it is still not clear what exactly occurs at these sites. Finally, often patients are clinically satisfied with the outcome when in fact the radiographic assessment concludes radiographically loose implants.

Some retrieval studies have been useful in analysing the failed implants as mentioned earlier (Hertel & Ballmer 2003; Nyffeler et al. 2003; Yian et al. 2005). Some of the retrieval photos indicate the cement on the pegs were partially intact. It is therefore not so clear where the failure occurs, at the implant/cement interface, within the cement or at the cement/bone interface. Perhaps there are weaknesses in all three interfaces and failure is a combination of minor defects and areas of interface weakness which collectively cause macroscopic failure. Retrieval studies also do not indicate the cause of failure, it may be that failure may begin in one interface and progress to another. Additionally, interface strengths require investigation and, in particular, the behaviour of these interfaces during repetitive compressive and tensile stresses.

Early in-vitro studies of the glenoid implant investigated conformity tests and surface changes of ex-vivo implants (Harryman et al. 1995; Braman et al. 2006; Collins et al. 1992). The first published in-vitro test using rim displacement as a quantitative measure of seating of the glenoid was by Collins et al. (1992). Later Anglin (1999) developed an experimental protocol for fatigue testing the fixation of glenoid implants in-vitro in bone substitute and

using the superior and inferior rim displacement measures as a quantitative measure of fixation performance (Fig. 2.3). As a result, the ASTM F2028-02 test was developed as a standard for comparative studies of glenoid fixations, both cemented and cementless.

Despite this standard, no published fatigue studies have observed implant failure (Anglin et al. 2000; Oosterom et al. 2004). Therefore the comparative results must be showing the fatigue and viscoelastic processes of the test. A study on the correlation between rim displacement and failure progression, as well as investigating other measurements is warranted. Due to the visual limitation in commercial designs, designing 2D custom-made specimens using the cross-sectional geometry of a commercial implant may allow direct observation of failure. Other measures of failure that can be investigated include increase in horizontal and vertical head displacement as the implant progressively fails and measuring the strains on the keel or pegs, for example, via the use of strain gauges or optical strain measures of the entire cross-section using digital image correlation (DIC).

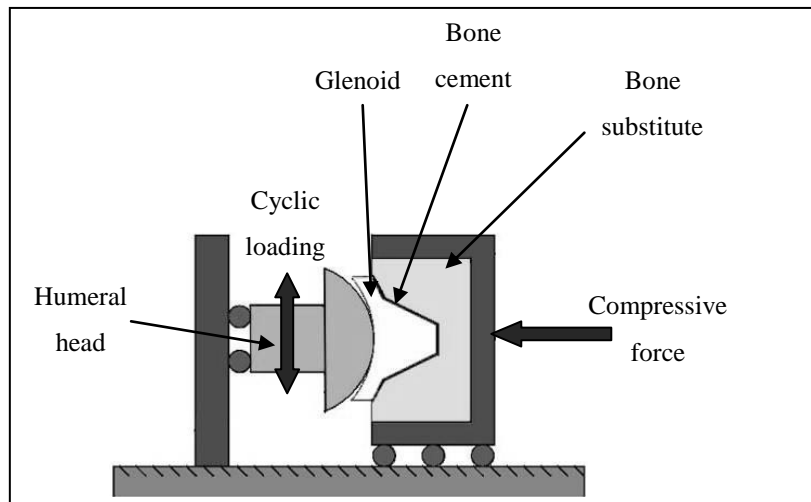


Figure 2.3: Mechanical fatigue testing of glenoid fixation (Reprinted and annotated from Journal of Shoulder and Elbow Surgery, 9 /2, Anglin, C. et al., Prosthesis Subluxation: Theory and Experiment, 104-114, Copyright (2000), with permission from Elsevier and C. Anglin).

2.5 Design Parameters

Current cemented all-PE glenoid implant designs primarily vary with respect to the anchorage of the implant, namely; curved-back versus flat-back, keeled versus pegged (Table 2.1) and roughening or macrostructures on the implant back for cement interlocking. Surgeons additionally have the option to choose the level of radial mismatch between the humeral head implant and the glenoid surface radius. These major design variations and their affect on implant fixation are still discussed and not clearly known.

Table 2.1: Design comparison of all major glenoid implants on the market. Permission granted to print images from respective implant companies.

Company & Implant	Pegged Glenoid	Keeled Glenoid
<p>Tornier Aequalis® peg & keel Images used with permission from Tornier, Inc., Feb 2010.</p>		
<p>Zimmer Anatomical Shoulder™ peg & Zimmer Bigliani/Flatow® The Complete Shoulder System Images © Zimmer Inc. Used by permission only</p>		
<p>Depuy Global® APG Anchor Peg Glenoid & Keel</p>		
<p>Exactech Equinox® peg & keel Images used with permission from Exactech Ltd..</p>		
<p>Biomet Integrated™ peg & keel Images used with permission from Biomet, Inc..</p>		
<p>Stryker Solar™ peg</p>		
<p>Biomet Modular Hybrid Glenoid Post Regenerex™ & Polyethylene (Semi-cemented) Images used with permission from Biomet, Inc..</p>		
<p>Zimmer Trabecular Metal™ peg (Semi-cemented) Images © Zimmer Inc. Used by permission only</p>		

2.5.1 Radial Mismatch

Studies have shown having a radial mismatch between the glenoid and the humeral head, allows translation of the head across the articular surface, which is similarly found in the natural joint (Harryman et al. 1995; Karduna et al. 1997; Walch et al. 2002). However, a lower radial mismatch and more conforming joint would result in less eccentric loading of the glenoid rim and have lower articulating pressure, leading to less wear (Lacroix & Prendergast 1997; Oosterom et al. 2004; Swieszkowski et al. 2003).

2.5.2 Peg Versus Keel

FE, clinical and in-vitro studies have shown various results on the comparison of pegged versus keeled implants (Anglin et al. 2001; Lacroix and Prendergast 1997; Mansat et al. 2007; Nuttall et al. 2007), which will be discussed further in chapter 4.

2.5.3 Curved-back Versus Flat-back

A radiographic study comparing curved-back and flat-back glenoids by Szabo et al. (2005) showed mixed results, with flat-back glenoids showing more r. lines immediately postoperatively, whereas after 24 months, both designs demonstrated similar r. lines. Other studies have used in-vitro rim displacements, showing a curved-back design, which is more compliant to the bone, will delay loosening compared to the flat-back design (Anglin et al. 2001; Collin et al. 1992).

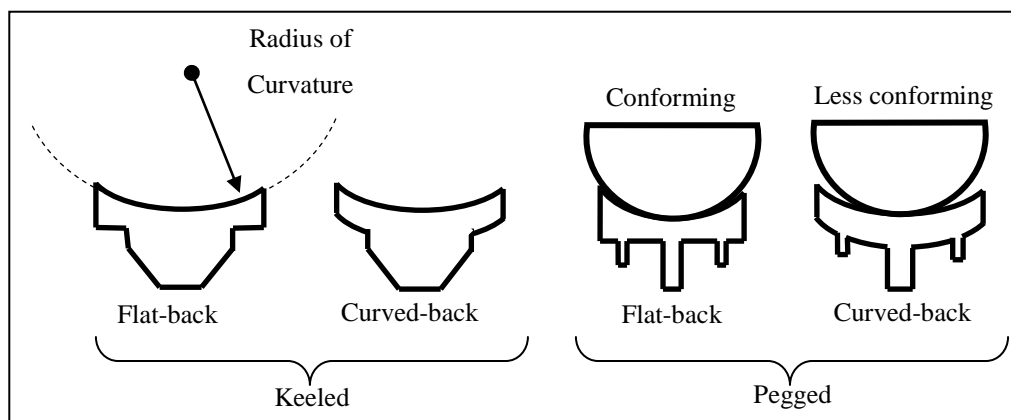


Figure 2.4: Main glenoid design parameters; keel/peg, curved/flat-back, conforming/less conforming.

2.5.4 Implant Roughness

Roughening the back of implants to improve interfacial strength between the implant and cement has also been debatable. Since clinically the consensus is that loosening of the cement/bone interface is the primary cause of loosening, improving the implant/cement interface would naturally be overlooked. However, Anglin et al. (2001) and Nyffeler et al. (2006) have shown the affect of roughening and the use of micro-features for cement interlocking improves the implant's resistance to mechanical failure at the implant/cement interface. However, it is not clear what exactly the correlation between level of roughness and failure is.

2.5.5 Cemented Versus Cementless

Cementless versus cemented studies have generally shown cementless designs to be less successful than the cemented designs. Complications in cementless cases are usually more serious (Boileau et al. 2002), a direct correlation between radiolucent lines and a decrease in function and increase in pain has been found (Martin et al. 2005) and problems with PE lining detachment has meant that cemented designs are preferred. However, PE wear and osteolysis in cementless cases (Boileau et al. 2002; Taunton et al. 2008) may have a compounding effect and may impact on the outcome of the implant. Out of the 8 requiring re-surgery in the study by Wallace et al. (1999), 5 of the glenoids were cementless, despite this, the authors also found the clinical intermediate outcome of cementless versus cemented were not significantly different.

Although beyond the scope of this PhD, cemented versus cementless also opens the discussion in cemented designs to the heating effect during cement polymerisation on the surrounding bone cells, the quality and condition of the bone at implantation, the affect of 'wetness' of the bone on the cement/bone interface and the bone modelling process in both types of designs, and are all factors requiring further investigation.

2.6 Conclusion

It would be useful to study the source of failure and the effect of all the major design parameters on fatigue failure. However, no failure has yet to be directly observed in-vitro. Testing these parameters in a model that will allow failure observation directly, such as a two-dimensional model is where the study should begin.

2.7 PhD Aims

This PhD thesis has several aims:

1. Using the ASTM F2028-02 test to identify the failure mechanism in the glenoid fixation due to fatigue loading in-vitro
2. identify the correlation between fatigue failure and rim displacement measurements in-vitro
3. identify alternative measures to monitor fatigue failure in-vitro
4. analyse the cause of failure by investigating the material and contact behaviours in FE
5. analyse the affect of the major design features; pegged versus keeled, flat-back versus curve-back, conforming versus non-conforming and smooth versus rough, on the fixation performance
6. identify the importance of bone variation in the mechanical outcome of the fixation

2.8 PhD Objectives

The aims will be achieved in three stages:

1. By testing custom-made 2D implants to reflect the plane strain situation, aims 1-5 can be investigated.
2. Testing one commercial implant in normal cadaveric bone to validate and verify stages 1 and 2, to investigate aim 6, and validate the use of PU bone substitute foam in implant fatigue studies.

3. Testing commercial 3D implants to investigate aims 1-5 and verify and validate the 2D investigation.

2.9 References

- Anglin, C, (1999). *Shoulder Prosthesis Testing*, PhD Thesis, Mechanical Engineering, Queen's University, Canada.
- Anglin, C. et al. (2000), Prosthesis Subluxation: Theory and Experiment, *Journal of Shoulder and Elbow Surgery*, 9, (2): 104-114.
- Anglin, C, et al. (2001). Loosening Performance of Cemented Glenoid Prosthesis Design Pairs, *Clinical Biomechanics*, 16: 144-150.
- ASTM F 2028-02, 2004. Standard Test Methods for the Dynamic Evaluation of Glenoid Loosening or Disassociation. Book of ASTM Standards: 1083-88.
- Bohsali et al. (2006). Complications of Total Shoulder Arthroplasty, *Journal of Bone and Joint Surgery. American Volume*, 88A: 2279-2292.
- Boileau, P, et al. (2002). Cemented Polyethylene Versus Uncemented Metal-backed Glenoid Components in Total Shoulder Arthroplasty: A Prospective, Double-blind, Randomized Study, *Journal of Shoulder Elbow Surgery*, 11, (4): 351-359.
- Braman, J P, et al. (2006). Alterations in surface geometry in retrieved polyethylene glenoid component, *Journal of Orthopaedic Research*, 24 (6): 1249-1260.
- Brostrom, L A, et al. (1992). Should the Glenoid be Replaced in Shoulder Arthroplasty with an Unconstrained Dana or St-George Prosthesis, *Annales Chirurgiae et Gynaecologiae*, 81: 54-57.
- Cofield, R H (1984). Total Shoulder Arthroplasty with the Neer Prosthesis, *Journal of Bone and Joint Surgery, American Volume*, 66A: 899-906.
- Collins, D N, et al. (1992). Edge Displacement and Deformation of Glenoid Components in Response to Eccentric Loading The Effect of Preparation of the Glenoid Bone, *Journal of Bone and Joint Surgery, American Volume*, 74A, (4): 501-507.
- Collins, D N, et al. (2004). Shoulder Arthroplasty for the Treatment of Inflammatory Arthritis, *Journal of Bone and Joint Surgery, American Volume*, 86A (11): 2489-2496.
- Gill, D R J, et al. (1999). Ipsilateral Total Shoulder and Elbow Arthroplasties in Patients Who Have Rheumatoid Arthritis, *Journal of Bone and Joint Surgery, American Volume*, 81A: 1128-1137.

- Harryman, D T, et al. (1995). The Effect of Articular Conformity and the Size of the Humeral Head Component on Laxity and Motion After Glenohumeral Arthroplasty - A Study in Cadavera, *Journal of Bone and Joint Surgery, American Volume*, 77A, (4): 555-563.
- Havig, M T, et al. (1997). Assessment of Radiolucent Lines about the Glenoid: An In Vitro Radiographic Study, *Journal of Bone and Joint Surgery, American Volume*, 79A: 428-432.
- Hertel, R, and Ballmer, F T (2003). Observations on Retrieved Glenoid Components, *The Journal of Arthroplasty*, 18: 361-366.
- Hill, J M & Norris, T R (2001). Long-Term Results of Total Shoulder Arthroplasty Following Bone-Grafting of the Glenoid, *Journal of Bone and Joint Surgery, American Volume*, 83A: 877-883.
- Karduna, A R, et al. (1997). Joint Stability After Total Shoulder Arthroplasty in a Cadaver Model, *Journal of Shoulder and Elbow Surgery*, 6, (6): 506-511.
- Kelly, I G, et al. (1986), Neer Total Shoulder Replacement in Rheumatoid Arthritis, *Journal of Bone and Joint Surgery, British Volume*, 69B, (5): 723-726.
- Klepps, S., et al. (2005). Incidence of Early Radiolucent Glenoid Lines in Patients Having Total Shoulder Replacements, *Clinical Orthopaedics and Related Research*, (435): 118-125.
- Krause, W and Mathis, R S (1988). Fatigue Properties of Acrylic Bone Cement: Review of the Literature, *Journal Biomedical Materials Research: Applied Biomaterials*, 22, (A1): 37-53.
- Krause, W and Hoffman, A (1989). Antibiotic Impregnated Acrylic Bone Cements: A Comparative Study of the Mechanical Properties, *Journal of Bioactive and Compatible Polymers*, 4: 345-361.
- Lacroix, D & Prendergast, P J (1997). Stress Analysis of Glenoid Component Designs for Shoulder Arthroplasty, *Proceedings of the Institute of Mechanical Engineers*, 211, Part H: Journal Engineering in Medicine, 467-474.
- Lazarus, M D, et al. (2002). The Radiographic Evaluation of Keeled and Pegged Glenoid Component, *Journal of Bone and Joint Surgery, American Volume*, 84A, (7): 1174-1182.
- Lewis, G (1997). *Properties of Acrylic Bone Cement: State of the Art Review*, *Journal of Biomedical Materials Research Part B: Applied Biomaterials*. 14: 155-182.

- Linden, U (1989). Fatigue Properties of Bone Cement: Comparison of Mixing Techniques, *Acta Orthopaedica*, 60, (4): 431-433.
- Mann, K A, et al. (1999). Mechanical Strength of the Cement-Bone Interface is Greater in Shear Than in Tension, *Journal of Biomechanics*, 32: 1251-1254.
- Mann, K A, et al. (2001). Mixed-Mode Failure Response of the Cement-Bone Interface, *Journal of Orthopaedic Research*, 19: 1153-1 161.
- Mansat, P, et al. (2007). Evaluation of the Glenoid Implant Survival Using a Biomechanical Finite Element Analysis: Influence of the Implant Design, Bone Properties, and Loading Location, *Journal of Shoulder and Elbow Surgery*, 16, (3S): 79S-83S.
- Martin, S D, et al. (2005). Uncemented Glenoid Component in Total Shoulder Arthroplasty - Survivorship and Outcomes. *Journal of Bone and Joint Surgery, American Volume*, 87A: 1284-1292.
- Matsen III, F A, et al. (2008). Glenoid Component Failure in Total Shoulder Arthroplasty, *Journal of Bone and Joint Surgery, American Volume*, 90A: 885-896.
- Nagels, J, et al. (2002). Patterns of Loosening of the Glenoid Component. *Journal of Bone and Joint Surgery, British Volume*, 84B, (1): 83-87.
- Neer, C S & Morrison, D S (1988). Glenoid Bone Grafting in Total Shoulder Arthroplasty, *The Journal of Bone and Joint Surgery, American Volume*, 70A: 1154-1162.
- Nuttall, D, et al. (2007). A Study of the Micromovement of Pegged and Keeled Glenoid Components Compared Using Radiostereometric Analysis, *Journal of Shoulder and Elbow Surgery*, 16, (3): 65S-70S.
- Nyffeler, R W, et al. (2003). Influence of Peg Design and Cement Mantle Thickness on Pull-out Strength of Glenoid Component Pegs, *Journal of Bone and Joint Surgery, British Volume*, 85B (5), 748-752.
- Nyffeler, R W, et al. (2006). The Effect of Cementing Technique on Structural Fixation of Pegged Glenoid Components in Total Shoulder Arthroplasty, *Journal of Shoulder and Elbow Surgery*, 15, (1): 106-111.
- Oosterom, R, et al. (2004). Effect of Glenoid Component Inclination on its Fixation and Humeral Head Subluxation in Total Shoulder Arthroplasty, *Clinical Biomechanics*, 19: 1000-1008.
- Rahme, H, et al. (2004). Stability of Cemented All-Polyethylene Keeled Glenoid Components, *Journal of Bone and Joint Surgery, British Volume*, 86B, (6): 856-860.

- Sanghavi, S, et al. (2007). Glenoid Bone-PMMA Interface Tensile Strength, Pending submission.
- Scarlat, M M & Matsen III, F A (2001). Observations of Retrieved Polyethylene Glenoid Components, *The Journal of Arthroplasty*, 16, (6): 795-801.
- Stewart, M P M & Kelly, I G (1997), Total Shoulder Replacement in Rheumatoid Disease, *Journal of Bone and Joint Surgery, British Volume*, 79B, (1): 68-72.
- Swieszkowski, W W, et al. (2003). Contact Stresses in the Glenoid Component in Total Shoulder Arthroplasty, *Proceedings of the Institution of Mechanical Engineers*, 217, Part H: Journal Engineering in Medicine, 49-57.
- Szabo, I, et al. (2005). Radiographic Comparison of Flat-back and Convex-back Glenoid Components in Total Shoulder Arthroplasty, *Journal of Shoulder and Elbow Surgery*, 14, (6): 636-642.
- Taunton, M J, et al. (2008), Total Shoulder Arthroplasty with a Metal-Backed, Bone-Ingrowth Glenoid Component. Medium to Long-Term Results, *Journal of Bone and Joint Surgery, American Volume*, 90A, (10): 2179-2188.
- Torchia, M E, et al. (1997). Total Shoulder Arthroplasty With the Neer Prosthesis: Long-Term Results, *Journal of Shoulder and Elbow Surgery*, 6: 495-505.
- Walch, G, et al. (2002). The Influence of Glenohumeral Prosthetic Mismatch on Glenoid Radiolucent Lines - Results of a Multicenter Study, *Journal of Bone and Joint Surgery, American Volume*, 84A, (12): 2186-2191.
- Wallace, A L, et al. (1999). Resurfacing of the Glenoid in Total Shoulder Arthroplasty - A Comparison, At a Mean of Five Years, of Prostheses Inserted With and Without Cement, *Journal of Bone and Joint Surgery, American Volume*, 81A, (4): 510-518.
- Wirth, M A (1999). Isolation and Characterization of Polyethylene Wear Debris Associated with Osteolysis Following Total Shoulder Arthroplasty, *Journal of Bone and Joint Surgery, American Volume*, 81A, (1): 29-37.
- Wixson, R L, et al. (1987). Vacuum Mixing of Acrylic Bone Cement, *The Journal of Arthroplasty*, 2, (2): 141-149.
- Yian, E H, et al. (2005). Radiographic and Computed Tomography Analysis of Cemented Pegged Polyethylene Glenoid Components in Total Shoulder Replacement, *Journal of Bone and Joint Surgery, American Volume*, 87A, (9): 1928-1936.

Chapter 3: Failure Mechanism in 2D All-Polyethylene Glenoid Implant Designs

3.1 Contributors

The design, manufacture and testing of many of the samples were carried out in collaboration with Dr S. Gupta.

3.2 Abstract

Fixation failure of glenoid components is the main cause of unsuccessful total shoulder arthroplasties. The characteristics of these failures are still not well understood, hence, attempts at improving the implant fixation are somewhat blind and the failure rate remains high. This lack of understanding is largely due to the fundamental problem that direct observations of failure are impossible as the fixation is inherently embedded within the bone. Twenty custom made implants, reflecting various common fixation designs, and a specimen set-up was prepared to enable direct observation of failure when the specimens were exposed to cyclic superior loads during laboratory experiments. Finite element analyses of the laboratory tests were also carried out to explain the observed failure scenarios. All implants, irrespective of the particular fixation design, failed at the implant-cement interface and failure initiated at the inferior part of the component fixation. Finite element analyses indicated that this failure scenario was caused by weak implant-cement interface strength and tensile stresses in the inferior region possibly worsened by a stress raiser effect at the inferior rim. The results of this study indicate that glenoid failure can be delayed or prevented by improving the implant/cement interface strength. Also any design features that reduce the geometrical stress raiser and the inferior tensile stresses in general should delay implant loosening.

3.3 Introduction

Glenoid loosening constitutes 32% of all total shoulder arthroplasty (TSA) complications and has a revision rate of 7% (Bohsali et al. 2006). To overcome this, curved-back designs, variations in pegged or keeled designs and other macro-features have been used. Despite many efforts, the optimal design parameters are still not established. This difficulty is probably caused by the fact that, fundamentally, the characteristics of failure are not yet clear.

Previous studies have indicated failure to occur; around the keel/pegs (Kleppe et al. 2005; Trail and Nuttall 2002); in the superior region (Nagels et al. 2002) or in the inferior region (Nagels et al. 2002). Most clinical studies report failure to occur in the cement/bone interface (Yian et al. 2005). However, most of these studies base their findings on the presence of radiolucent lines, which, apart from being difficult to quantify and understand the significance of, are also unlikely to capture narrow de-bonds at the implant/cement interface or thin cracks in the bulk cement. Therefore, the findings from these radiographic studies are questionable and there are retrieval studies that show results indicating failure to occur wholly (Nyffeler et al. 2003) or partly (Yian et al. 2005) in the implant/cement interface. Finally, some studies describe failure of the bulk cement (Terrier et al. 2005). In summary, the location of failure along and within the fixation is not well established.

It is the purpose of this study is to determine characteristics such as: (1) does the failure initiate inferiorly, superiorly or at the keel/pegs? (2) What is the weakest link in the fixation; the cement, the bone or at the interfaces? Knowing which of the constituents that is the weakest link will determine if, for example, stronger cement would be beneficial or if more optimal surface preparation techniques are required to improve glenoid fixation.

Based on the concept of the “rocking horse effect” (Matsen et al. 1994) and the work by Anglin, 1999, the American Society for Testing and Materials (ASTM) adopted a standard for testing of glenoid implant loosening (ASTM F2028-02 2004). This method uses a measure of changing implant rim displacement with number of load cycles as an indicator of loosening. However, the measure of rim displacement is only an indirect measure of fixation failure and it has not, in fact, been shown that an increase in rim displacement correlates with initial or progressive loosening.

The reason for using these questionable, indirect measures is that the fixation is inherently embedded in the bone and impossible to observe directly. To overcome this problem, custom made implants allowing direct observation of the fixation and the progressive failure were used in this study. However, mere observation of failure may not explain the reason for that failure, hence, a parallel finite element analysis predicting the stresses in the fixation was also carried out.

3.4 Materials and Method

3.4.1 Mechanical Test

Modified glenoid specimens were manufactured and will be referred to as two-dimensional or 2D specimens in this study. The cross-sectional dimensions in the coronal plane of commercially available keeled and pegged glenoids were extruded by 40 mm normal to the coronal plane to create 2D implants (Fig. 3.2). A testing rig in compliance with the ASTM standard (ASTM F2028-02, 2004) was used to carry out the cyclic testing (Fig. 3.3). The glenoid specimens articulated against a humeral head. The humeral head was a stainless steel semi-circular cylinder, 24 mm radius by 40 mm long, corresponding to the 2D geometry of the glenoid components (Fig. 3.3). The glenoid implants were CNC machined from ultra high molecular weight polyethylene or UHMWPE (RS 2004). In total, twenty implants of different design parameters were manufactured to make a total of 8 specimen groups (Fig. 3.1); peg versus keel, flat-back versus curve-back, conforming (25 mm glenoid radius) versus less conforming (29 mm glenoid radius).

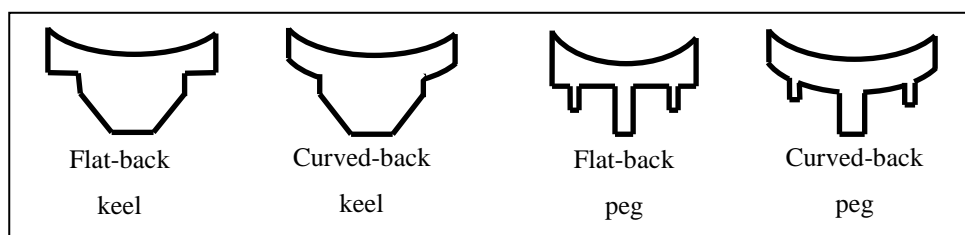


Figure 3.1: Four glenoid designs with two radius of curvatures, making a total of 8 designs.

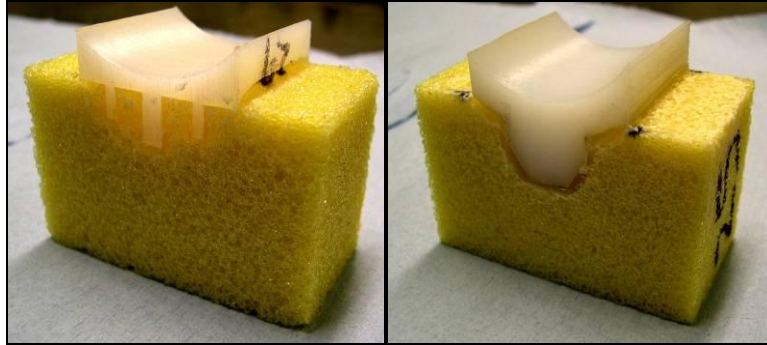


Figure 3.2: cemented 2D-specimen in bone substitute; flat-back peg (left) and curved-back keel (right).

The implants were cemented into porous polyurethane (PU) bone substitute (Sawbones Europe, Malmö, Sweden), which has mechanical properties ($\rho = 0.2$ g/cc, cell size = 0.5-1.5 mm, $E = 47.5$ MPa, compressive strength = 3.9 MPa) representative of the rheumatoid bone (Yang et al. 1997) present in many TSA cases. The PU parts were also CNC machined and designed to accommodate a uniform 2 mm thick cement mantle. Stryker Simplex[®] polymethylmethacrylate (PMMA) bone cement was used and the implantation carried out by an experienced shoulder surgeon (S.M.S.).

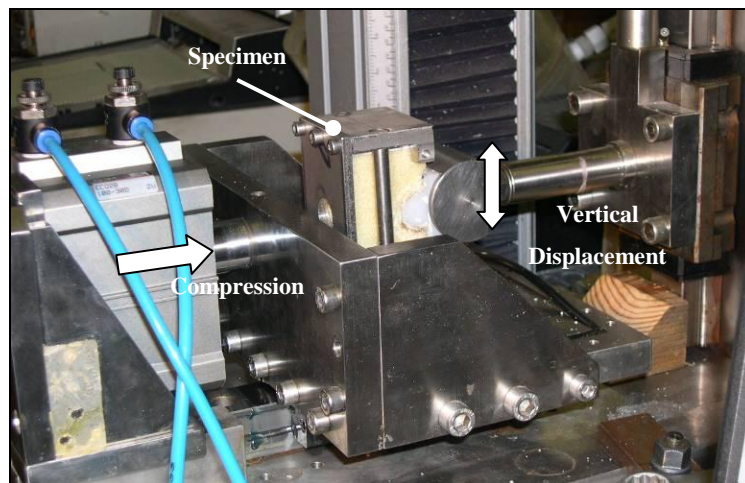


Figure 3.3: The ASTM F2028-02 biaxial testing rig, modified according to the 2D configuration of this study.

The humeral head was compressed into the glenoid using a horizontal load of 1800 N applied by a pneumatic cylinder. This load is higher than the compressive load specified in the ASTM standard but is not physiologically unreasonable (Anglin et al. 2000). The 2D implants were bulkier and stiffer structures than real implants, so higher loads were applied in order to generate stresses in the 2D fixation that were similar to those in-vivo.

In addition to the constant horizontal load applied through the glenoid, the specimens were loaded by displacing the humeral head vertically at 0.5 Hz in sets of 4000 cycles via displacement control. The humeral head was displaced superiorly from the centre of the glenoid and back to the centre. This imposed compressive stresses mostly onto the superior part of the fixation and tensile stresses mostly on the inferior part of the glenoid fixation, thereby making it easier to understand the type of failure observed. This loading regime does not seem unreasonable as, clinically, superior migration and loads are more common (Bergmann et al. 2007; Trail and Nuttall 2002).

Prior to fixation failure testing, two specimens of each design were tested quasi-statically to determine the load and displacement to subluxation. The ASTM standard specifies that 90% of the subluxation displacement must be determined and used as the vertical displacement during the cyclic test. However, it was not easy to determine the 90% subluxation displacement. This was due to: 1) the force-displacement response being very flat near the subluxation point (Fig. 3.4) making it difficult to accurately determine the subluxation displacement; 2) great inter-specimen variability of the non-linear behaviour in the near-subluxation region (Fig. 3.4), resulting in significant scatter of the 90% subluxation displacement between specimens. Instead, the load and displacement at the end of the initial linear region of the curve, where there was much less variability between specimens, were used (Fig. 3.4). This corresponded to 2.25 mm for the conforming designs and 3.25 mm for the less conforming designs or 1200 N and 1100 N respectively. That is, approximately 83% of the subluxation load. Although these loads were slightly lower than would have been the result of strictly applying the 90% ASTM recommendation, they were still near-subluxation loads, which is the principal recommendation of the ASTM standard.

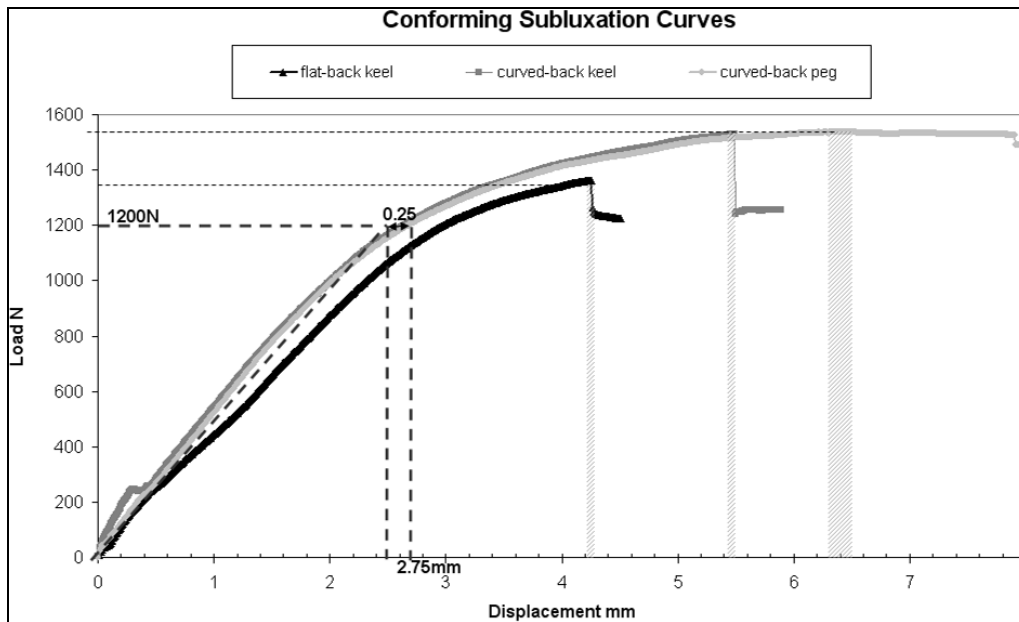


Figure 3.4: Subluxation curve of three conforming specimens with loading point derived at the linear section of the curve (dotted) using an average offset of 0.25 mm. Note: displacement range (shaded) at point of subluxation.

3.4.2 FE Analysis

To represent each of the implant configurations, eight 2D models were built using 8,800 to 14,400 quadrilateral elements in each model. The materials were modelled as linear elastic and the relevant properties are shown in Table 3.1. The FE analysis was carried out in Marc/Mentat 2005 and modelled as a plane strain problem. The humeral head was assumed rigid with a friction coefficient of 0.07 between the humeral head and glenoid implant (Anglin et al., 2000). The interfaces between the UHMWPE and PMMA and the between PMMA and bone substitute, were modelled as fully-bonded. The loading and boundary conditions mimicked the laboratory test set-up. Mesh convergence was verified.

Table 3.1: Material properties used in the FE model.

Material	Young's Modulus, GPa	Poisson's Ratio
UHMWPE implant*	0.6	0.4
PMMA bone cement†	2.2	0.3
PU bone substitute‡	0.0475	0.3

* **White polyethylene rod from manufacturer's data sheet (RS, 2004).**

† **(Lewis et al., 1997)**

‡ **Cellular rigid polyurethane foam 12.5 pcf (Sawbones, 2009)**

Predicted stresses, normal and tangential to the interfaces, were used to evaluate the risk of failure of the implant/cement and cement/bone interfaces. The maximum principal stress was used to evaluate the risk of failure of the cement mantle. The minimum principal stresses were used to predict bone crushing.

To predict failure the stresses were compared to relevant strength values. Unpublished work in the Group's laboratory has found the cement/bone-substitute interface tensile strength to be *greater* than 2.32 ± 0.54 MPa. The strength of the polyethylene-implant/PMMA bone cement interface depends on the roughness (Ra) of the polyethylene surface. The interface study has also found the tensile strength of this interface to range between virtually zero and 3.2 MPa for realistic implant surface roughness's (that is, roughness ranging from "smooth" to 5.5 μm). The roughness (Ra) of the backside of the polyethylene glenoids in this study was to 3-6 μm and it was assumed that the implant/cement interface strength for this study was in the range of 1 MPa to 3.2 MPa. The tensile strength of PMMA bone cement is 27.1 MPa (Krause and Hofmann 1989) and the compressive strength of the bone substitute is 3.9 MPa (Sawbones 2009).

3.5 Results

Failure was defined by the following criteria:

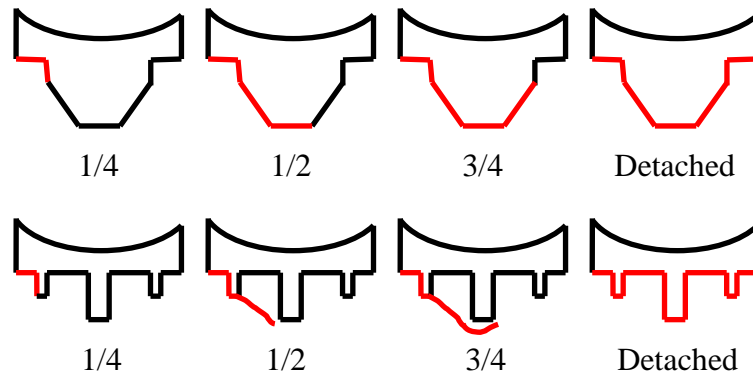


Figure 3.5: definition of failure where red represents failure at the implant/cement interface, where the literature mentions failure, this refers to 3/4 failure. Note: diagonal red lines in the pegged glenoid indicate failure in the bone substitute.

3.5.1 Cyclic Testing

In all twenty specimens, irrespective of design type, failure was observed at the implant/cement interface (Fig. 3.6). Initial failure occurred at the inferior edge of the glenoid component and propagated superiorly across the back of the glenoid until it met a fixation feature. The crack propagated around the periphery of the fixation keels. However, for pegged designs, the crack propagated as far as the tip of the inferior peg and then ‘jumped’ across the bone to the tip of the next peg where failure progressed at the cement/bone interface. (Fig. 3.6 & 3.7). Progressive superior bone crushing was also observed. Cycles to failure varied between 8000-14,905 cycles (Table 3.2), failure being defined as the crack having reached the centre line of the implant (Fig. 3.7).

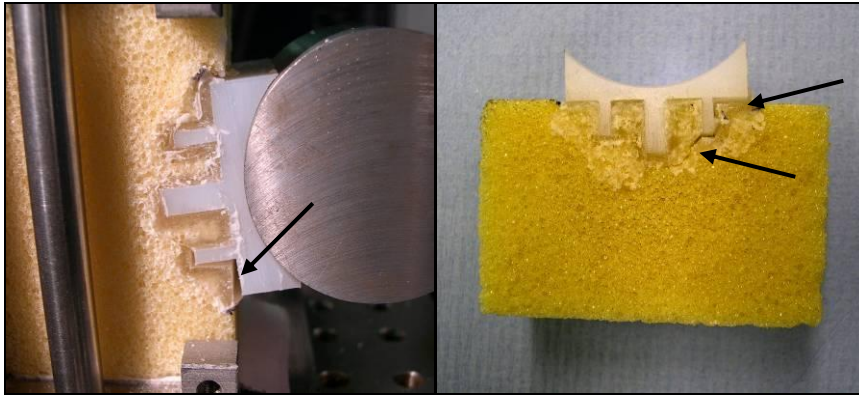


Figure 3.6: In all cases failure was observed in the implant/cement interface and initiated in the inferior part of the fixation (arrows).

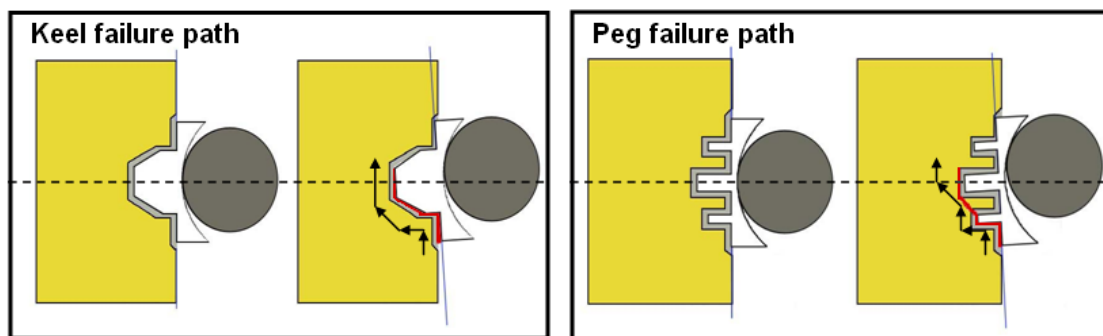






Figure 3.7: Failure pathway in keeled (left) and pegged glenoids (right). A similar failure path was observed for all design configurations.

Table 3.2: Results showing average, and in brackets the standard deviation, number of cycles to failure for different implant designs. Number of samples is 'n'.

	 Flat-back peg	 Flat-back keel	 Curve-back keel	 Curve-back peg
Less conforming (5 mm radial mismatch)	8275 (706) n = 4	9764 (525) n = 4	10519 (858) n = 4	13150 (763) n = 4
Conforming (1 mm radial mismatch)	13969 n = 1	12297 n = 1	14905 n = 1	12100 n = 1

3.5.2 FE Results

Figure 3.8 shows the predicted stresses in the fixation of the curved-back, keeled implant. While there were differences in stresses between the different implant designs, this figure demonstrates the characteristic features of the stress distributions for all the implants and is used to demonstrate the FE results. The figure also includes the strength values, mentioned earlier, of the various components of the fixation.

The normal stress along the implant/cement interface was predominantly compressive superiorly and tensile inferiorly. The average tensile stress in the inferior region was 0.83 MPa and increased to 3.35 MPa towards the edge and was within the range of the implant/cement interface strength of 1-3.2 MPa, indicating that failure of this interface is likely. In contrast, the maximum principal stresses in the cement were much lower than the tensile strength of the PMMA bone cement (27.1 MPa). The stresses in the cement/bone interface were also tensile in the inferior zone and reached the cement/bone interface strength, conservatively estimated to be 2.32 MPa, only in the small region very close to the edge.

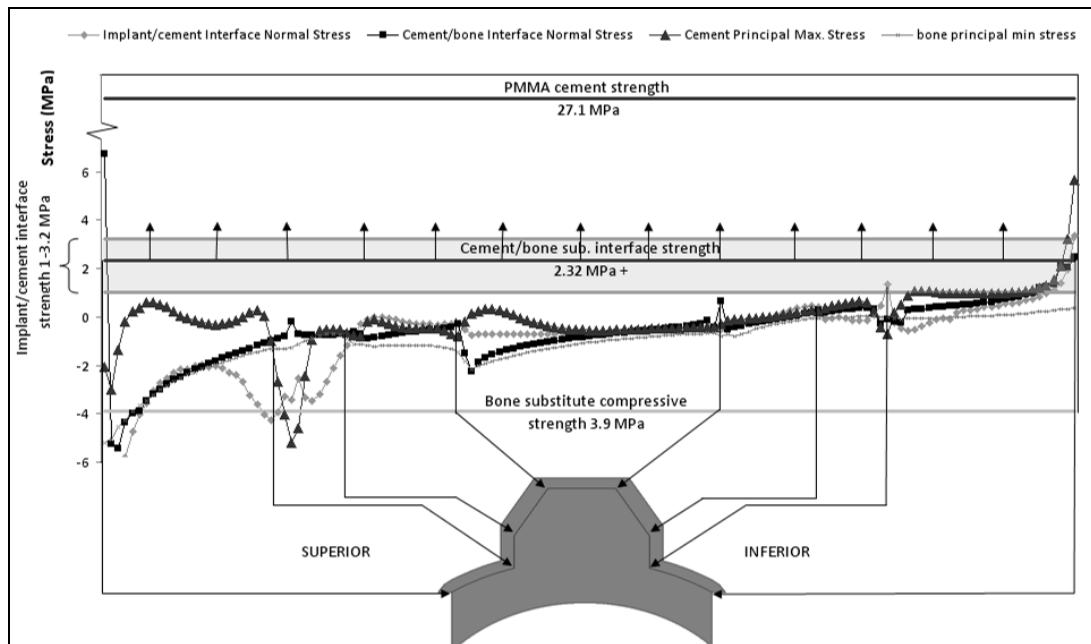


Figure 3.8: Plot of the predicted stresses in the fixation of the curved-back keel specimen. The plotted stresses are at: the two interfaces, in the bulk PMMA bone cement and in PU bone substitute. The strengths of the two interfaces, of the cement and of the PU bone substitute are also shown. The implant/cement interface strength is only known within a range and this range is indicated by the hatched area. Only a minimum value of the cement/bone-substitute strength is known (2.32 MPa) and the arrows indicate that the strength is likely to be higher than 2.32 MPa.

The minimum principal (compressive) stresses in the underlying bone substitute in the superior part of the fixation are predicted to reach -5.2 MPa, exceeding the 3.9 MPa compressive strength of the PU bone substitute. This predicted bone substitute crushing in the superior region was also observed during the experiments (Fig. 3.6).

3.6 Discussion

All implants, irrespective of the particular fixation design, failed at the implant-cement interface and failure initiated at the inferior edge part of the component fixation. Finite element analyses indicated that this failure scenario was caused by weak implant/cement interface strength and relatively high tensile stresses in the inferior region, possibly worsened by a stress concentration at the inferior edge, where tensile stresses are highest. Crushing of the bone substitute in the superior region was also apparent.

3.6.1 Location of Failure

Clinical radiographic studies have found radiolucent lines around the peg/keel which have been interpreted as a loss of fixation (Barrett et al. 1987; Hertel and Ballmer 2003). Other studies (Nagels et al. 2002; Nuttall et al. 2007; Yian et al. 2005) have reported radiolucent lines inferiorly. In particular, Nagels et al. (2002) found that radiolucent lines grew over time inferiorly, while radiolucent lines existed in the superior part of the fixation immediately following the surgery (Nagels et al. 2002), possibly indicating the critical nature of inferior radiolucent lines.

Failure of the fixation in the inferior region was the obvious failure mode in all specimens, which is consistent with the clinical studies mentioned earlier. The finite element analysis showed that this region is exposed to tensile stresses and interfaces are typically weak in tension. The tensile stresses increased rapidly towards the inferior edge (Fig. 3.8), due to the geometry of the edge of the component. Although the edge of the 2D set-up may not have represented the real implant features accurately, the analysis does demonstrate that implant failure may be sensitive to subtle details of the edge geometry, which could probably be modified to lower the risk of failure.

3.6.2 The Weakest Link of the Fixation

PMMA bone cement has been a cause for concern in implant loosening because it is known to be weak in tensile fatigue (Saha and Pal 1984). It is often presumed that the cement is the weakest link in the fixation (Hopkins et al. 2004; Lacroix and Prendergast 1997). However, in this study there were no indication that cement was fracturing and the cement stresses were predicted to be very much lower than both the tensile strength of cement of 27.1 MPa and the fatigue strength of 10 MPa (Murphy and Prendergast 2000). Thus, the bulk cement is unlikely to be the weakest part of the fixation.

In this study, the bone substitute was crushed superiorly and finite element predictions also found stresses indicative of compressive failure. This may explain the radiolucent lines observed in clinical studies. However, this interpretation has to be viewed in the context that this study used bone substitute material which may have a lower compressive strength (3.9

MPa) than real glenoid bone (10.3 MPa, Anglin et al. 1999). However, rheumatoid bone strength is likely to be much lower (Yang et al., 1997) and possibly reasonably represented by the bone substitute strength. Also the compressive stresses in the superior region of the 2D set-up are possibly larger than in the physiological (3-dimensional) implant fixation.

An important limitation of this study is the use of the possibly non-physiological 2D set-up. The simple justification for the 2D set-up is that, whatever its shortcomings, it is the only way to be able to observe failure directly. A recent study that was in many ways similar to the present study but using real (3D) implants, also found that failure took place at the implant/cement interface (Gregory et al. 2009). It would therefore seem that the 2D set-up is reasonably representative of physiological conditions.

The stresses predicted for the implant/cement interface were of similar magnitude to those at the bone-substitute/cement interface. Possibly it could be argued that the strength of the bone-substitute/cement interface (*greater* than 2.32MPa) is higher than the implant/cement interface strength (1 MPa to 3.2 MPa) and that this would explain why it was consistently the implant/cement interface that was observed to fracture. However, the fracture of the implant/cement interface appeared to show minimal resistance (there was no cement attached to the fracture surface of the polyethylene and no polyethylene attached to the fracture surface of the cement). It may be that the implant/cement interface has a less resistive fracture path than the cement inter-digitised bone-substitute/cement interface. Perhaps to fully explain the observed failure scenario a fracture mechanics approach is necessary.

Although using bone substitute material instead of real glenoid is a limitation of the study, unpublished work in the Group laboratory has shown that the glenoid-bone/cement interface strength is higher than the bone-substitute/cement interface strength. It would therefore seem unlikely that using the stronger glenoid bone would have changed the finding that the implant/cement interface is the weakest link. On the other hand, poor cementing or bone preparation techniques and the presence of interstitial fluids may lead to very much lower cement/bone interface strengths than used here and could change the conclusion. However, the scope of this study was not to investigate the effects of imperfect surgical techniques.

The results of this study contrast with the apparent consensus from clinical studies (primarily radiographic) that loosening is at the cement/bone interface (Bohsali et al. 2006; Matsen et al. 2008). However, radiolucent lines have been attributed to a formation of fibrous connective tissue (Wirth et al. 2001). It is unlikely that there would be any soft tissue at a de-bonded implant/cement interface. One possible reason that the clinical studies do not report implant/cement interface failures may be that such failures are not captured on radiographs, even when present. There are also retrieval studies that show clinical failure to take place wholly (Nyffeler et al. 2003) or partly (Yian et al. 2005) at the implant/cement interface. It may also be that the failure scenario cannot be explained completely as taking place at just one interface. The results shown for the pegged implant in figures 3.5 and 3.6 show such a mixed failure scenario where fixation fracture initiates in the implant/cement interface but later propagates through the cement and into the bone and bone-cement interface.

Some authors have suggested that glenoid failure is due to a biological reaction caused by polyethylene wear particles (Wirth et al. 1999). Such biological reactions at the cement-bone interface cannot be accounted for in our in-vitro study and could also explain why cement/bone interface failure is not observed in this study. Even if this is the case, the results of this study may still be clinically relevant in a similar manner to the clinical relevance of in-vitro studies of, for example, poor cementing or bone preparation techniques. Such factors may be most directly relevant to early loosening or to early stages of clinical (gross) loosening. Early stages of fixation failure are difficult to observe in clinic and may differ from the later stage failures that can be observed clinically. However, any such factor that may influence early fixation failure may in turn have an effect on long-term failures that may or may not be influenced by biological reactions.

3.7 Conclusions

A 2D laboratory set-up enabled, for the first time, direct observations of glenoid fixation failure, which was shown to initiate in the inferior part of the fixation, the implant/cement interface being the weakest part of the fixation. The results indicated that efforts to

strengthen PMMA bone cement are unlikely to have any effect on glenoid loosening because the cement is not the weakest link.

The results indicated that strengthening the polyethylene implant/cement interface, for example by roughening the polyethylene surface, will improve the fixation strength of glenoid implants. Also, design features that lead to overall lower tensile stresses inferiorly and in particular features that reduce the stress raiser at the edges of the fixation are likely to improve implant loosening performance.

3.8 References

- Anglin, C, (1999). *Shoulder Prosthesis Testing*, PhD Thesis, Mechanical Engineering, Queen's University, Canada.
- Anglin, C, et al. 2000, Shoulder Prosthesis Subluxation: Theory and Experiment. *Journal of Shoulder and Elbow Surgery*, 9, (2): 104-114.
- ASTM F 2028-02, 2004. Standard Test Methods for the Dynamic Evaluation of Glenoid Loosening or Disassociation. Book of ASTM Standards: 1083-88.
- Barrett, W P, et al. (1987). Total Shoulder Arthroplasty, *Journal of Bone and Joint Surgery, American Volume*, 69A, (6): 865-872.
- Bergmann, G, et al. (2007). In Vivo Glenohumeral Contact Forces-Measurements in the First Patient 7 Months Postoperatively, *Journal of Biomechanics*, 40: 2139-2149.
- Bohsali, K I, et al.(2006). Complications of Total Shoulder Arthroplasty, *Journal of Bone and Joint Surgery, American Volume*, 88A, (10): 2279-2292.
- Gregory, T, et al. (2009). Glenoid Loosening After Total Shoulder Arthroplasty: and In-Vitro CT-scan Study, *Journal of Orthopaedic Research* (accepted).
- Hertel, R and Ballmer, F T (2003). Observations On Retrieved Glenoid Components, *The Journal of arthroplasty*, 18, (3): 361-366.
- Hopkins, A R, et al. (2004). The Effects Of Glenoid Component Alignment Variations On Cement Mantle Stresses In Total Shoulder Arthroplasty, *Journal of Shoulder and Elbow Surgery*, 13 (6): 668-675.
- Klepps, S, et al. (2005). Incidence of Early Radiolucent Glenoid Lines In Patients Having Total Shoulder Replacements, *Clinical Orthopaedics and Related Research*, (435): 118-125.
- Krause, W and Hofmann, A (1989). Antibiotic Impregnated Acrylic Bone Cements: A Comparative Study of the Mechanical Properties, *Journal of Bioactive and Compatible Polymers*, 4: 345-361.
- Lacroix, D & Prendergast, P J (1997). Stress Analysis of Glenoid Component Designs for Shoulder Arthroplasty, *Proceedings of the Institute of Mechanical Engineers*, 211, Part H: Journal Engineering in Medicine, 467-474.
- Lewis, G, et al. (1997). Effect of Mixing Method on Selected Properties of Acrylic Bone Cement, *Journal of Biomedical Materials Research*, 38, (3): 221-228.

- Matsen, F A, Lippitt, S B, Sidles, J A and Harryman, D T, (1994), Practical Evaluation and Management of the Shoulder, Saunders, Philadelphia.
- Matsen, F A, et al. (2008). Glenoid Component Failure in Total Shoulder Arthroplasty, *Journal of Bone and Joint Surgery, American Volume*, 90A, (4): 885-896.
- Murphy, B P and Prendergast, P J (2000). On The Magnitude and Variability of the Fatigue Strength of Acrylic Bone Cement, *International Journal of Fatigue*, 22, (10): 855-864.
- Nagels, J, et al. (2002). Patterns of Loosening of the Glenoid Component, *Journal of Bone and Joint Surgery, British Volume*, 84B (1): 83-87.
- Nuttall, D, et al. (2007). A Study of the Micromovement of Pegged and Keeled Glenoid Components Compared Using Radiostereometric Analysis, *Journal of Shoulder and Elbow Surgery*, 16, (3): 65S-70S.
- Nyffeler, R W, et al. (2003). Influence of Peg Design and Cement Mantle Thickness on Pull-out Strength of Glenoid Component Pegs, *Journal of Bone and Joint Surgery, British Volume*, 85B, (5): 748-752.
- RS catalogue, (2004). White polyethylene rod datasheet, RS Components Ltd, <http://uk.rs-online.com>.
- Saha, S and Pal, S, (1984). Mechanical Properties of Bone-Cement-A Review, *Journal of Biomedical Materials Research*, 18, (4): 435-462.
- Sawbones product catalogue (2009). Sawbones Europe AB, Division of Pacific Research Laboratories, Inc., Malmö, Sweden.
- Terrier, A, et al. (2005). Bone-Cement Interface of the Glenoid Component: Stress Analysis for Varying Cement Thickness, *Clinical Biomechanics*, 20, (7): 710-717.
- Trail, I A and Nuttall, D (2002). The Results of Shoulder Arthroplasty in Patients with Rheumatoid Arthritis, *Journal of Bone and Joint Surgery, British Volume*, 84B, (8): 1121-1125.
- Wirth, M A, et al. (1999). Isolation and Characterization of Polyethylene Wear Debris Associated With Osteolysis Following Total Shoulder Arthroplasty, *Journal of Bone and Joint Surgery, American Volume*, 81A, (1): 29-37.
- Wirth, M A, et al. (2001). Radiologic, Mechanical, and Histologic Evaluation of 2 Glenoid Prosthesis Designs in a Canine Model, *Journal of Shoulder and Elbow Surgery*, 10, (2): 140-148.

- Yang, J P, et al. (1997). Stiffness of Trabecular Bone of the Tibial Plateau in Patients With Rheumatoid Arthritis of the Knee, *The Journal of Arthroplasty*, 12, (7): 798-803.
- Yian, E H, et al. (2005). Radiographic and Computed Tomography Analysis of Cemented Pegged Polyethylene Glenoid Components in Total Shoulder Replacement, *Journal of Bone and Joint Surgery, American Volume*, 87A, (9): 1928-1936.

Chapter 4: A 2D Comparison of Glenoid Design Parameters in TSA

4.1 Abstract

Many commercial glenoid designs claim superior bone-cement-implant fixation and improved joint mechanics for longer lasting implants in total shoulder replacement. However, studies have shown conflicting results and it is still unclear whether these design variations significantly improve the mechanics of the joint and hence improve the loosening rate of glenoid implants. Cyclic tests were carried out on 60 custom made glenoids implanted into a bone substitute. Specimen design parameters that were investigated included variable back-surface roughness, flat-back versus curved-back, keel versus peg and more versus less conforming, repeating each design three times. Rim and vertical head displacements were monitored throughout testing. All implants failed inferiorly, 57 at the implant/cement interface. A positive correlation was found between inferior rim displacement and failure progression and between vertical head translation and failure progression. Roughening the implant back by 3.4 μm or more significantly improved resistance to failure by almost 4 times ($p < 0.0001$). All other design parameters were not significant in the failure of the glenoid fixation. The results also suggest the use of vertical head displacement as a more cost effective and time efficient method of monitoring failure. The use of a water bath did not affect the outcome of the cyclic test compared to implants tested in dry conditions. Finally the improvement in implant/cement interface strength by roughening should be considered in glenoid implants. Since macro-features of the pegs and keel are already featured in all implants on the market, investigating surface roughness and macro-features at the implant back may significantly improve the resistance to interface failure or failure progression.

4.2 Introduction

Current glenoid implant designs primarily vary with respect to the anchorage of the implant, namely; curved-backs versus flat-backs, keel versus peg and roughening or macrostructures of the implant back or peg/keel for cement interlocking. Surgeons additionally have the option to choose the level of conformity by varying the radial mismatch between the humeral head implant and the glenoid implant surface radius. These key design variations and their effect on implant fixation are still debated and not clearly known.

4.3 Conformity

4.3.1 Arguments For High Radial Mismatch

Implant companies tend recommend a radial mismatch of between 3-5 mm. Harryman et al. (1995) tested the range of motion of eight cadaveric shoulders and found a radial mismatch of 4 mm produced joint translations more comparable to the natural joint than 0-3 mm radial mismatch. This is also supported by Walch et al. (2002) who conclude that a radial mismatch of 5-7 mm should be used and Karduna et al. (1997), in an in-vitro study, found that a conforming design produced 20-50% higher strains on the keel than 1-5 mm mismatch designs during eccentric loads. Friedman et al. (1992) supported using a less conforming design, although the authors also argue that a high radial mismatch should be avoided due to high stress concentrations. A radial mismatch allows some joint translation and therefore reduces rim loading.

4.3.2 Arguments Against High Radial Mismatch

However, Oosterom et al. 2004 cyclically tested commercial glenoid implants cemented in bone substitute and measured the superior and inferior rim displacements in-vitro, and concluded a more conforming design reduces rim displacement and would therefore be better in-vivo. Similarly Lacroix & Prendergast (1997) suggest that conforming designs may lower cement stresses, and therefore, susceptibility to loosening. Likewise, Karduna et al. (1997) found radial mismatch increases compressive strains at the keel during concentric loads. In a

FE study by Swieszkowski et al. (2003), it was found that a mismatch of 5 mm generates surface loads above UHMWPE yield of 19 MPa and therefore might lead to surface wear. Therefore minimal radial mismatch reduces the rocking effect and distributes the load across the implant surface and fixation, reducing likelihood of fixation failure and implant surface wear.

4.4 Keel Versus Peg

Following the success of the non-constrained cemented keeled Neer II design, keeled glenoids were commonly used for TSA cases in the 1970s and 1980s (Barrett et al. 1987; Cofield 1984; Neer et al. 1974). The mid to long-term loosening and stability problems lead to fixed fulcrum designs and cemented pegged designs to emerge. With comparable pain and functional outcomes to keeled implants, the pegged design gained popularity. Peg and keel have now become the two main anchorage designs in cemented glenoids. Thus the choice between peg and keel implants is debatable. Lacroix and Prendergast (1997) suggest the use of peg in normal bone in an FE study, whereas the use of keel in rheumatic bone is better for cement survivability. However, the authors found no difference in the bone stresses. Another FE study by Mansat et al. (2007) found no significant difference in the cement stresses between peg and keel, although the assumption that failure primarily occurs in the cement is debatable in itself. Anglin et al. (2001) fatigue tested commercial implants in bone substitute and assessed implant performance using rim displacement measures, and found the peg implants produced less rim displacements than the keel. A clinical RSA study by Nuttall et al. (2007) on twenty patients, ten implanted with peg and ten with keel, found no significant difference in implant migration between the two implant groups except in the superior-inferior axis. There were also significant differences in rotations between the peg and keel group, indicating better stability in the peg group.

4.5 Flat-back Versus Curved-back

A curved-back design provides a more conforming implant to the underlying bone structure, however, curved-back and flat-back glenoid implants have been shown, via the appearance of radiolucent lines, not to be significantly different short term, with flat-back and curved-back showing 83% and 90% partial radiolucent lines respectively (Szabo et al., 2005). However the same authors found a significant difference in the two implant groups immediately postoperatively at 63% and 29% for the flat-back and curved-back respectively. Although the latter can be attributed to poor cementing, the former indicates no obvious differences in mechanics, at least at 24 months. An FE study has shown the highest strain at the keel is found in the flat-back case, whereas the curved-back model predicts the highest strains at the implant back (Iannotti et al., 2005). This is interesting as failure is thought to initiate at the rim (Matsen III et al. 2008; Nagels et al. 2002), rather than starting at the keel/peg. However, the same authors predicted the flat-back produces higher rim displacements compared to the curved-back glenoid, when the implant surfaces were not bonded, indicating higher interfacial stresses in the flat-back case. Finally, both Collin et al. (1992) and Anglin et al. (2001) agree that curved-back designs are superior based on rim displacement measures during eccentric glenoid loading in-vitro. It is therefore unclear if using a curved-back design is an important factor in the mechanical survivability of the glenoid in TSA and would be useful to investigate.

4.6 Back-Surface Roughness

Implant roughening has been adopted by one company, after a study on the loosening performance of glenoid implants in-vitro demonstrated resistance to mechanical loosening of up to 250,000 cycles in two implants by sandblasting the back of glenoid implants. In comparison, leaving the implant smooth caused almost immediate failure in two other implants (Anglin et al. 2001). However, all major commercial designs incorporate macro-features either on the back surface or on the anchorage. These features must improve interfacial strength as immediate and complete failures of implants are not observed clinically, though this does not eliminate its possibility. This is further confirmed by Nyffeler

at al. (2003), where pull-out strengths of polyethylene pegs in cement, showed an improvement of pull-out force by using a thread and roughening at 425 ± 7 N and 259 ± 42 N respectively, compared to 26 ± 11 N of smooth pegs. Although a simple roughness study comparing two 'smooth' back designs to a roughened design (Anglin 1999) has shown strong indications on the affects of implant roughening, what relation does roughness have with loosening performance?

Conformity recommendations confusingly vary from 3 mm to 10 mm, the trade-off between allowing natural movement to lower rim loading and preventing surface wear from high contact stress, has resulted in mixed responses to the ideal conformity. Clinically, peg and keel implants do not appear to be significantly different, as is the same with curved-back and flat-back implants, despite the differing conclusions from FE studies indicate. Finally, the study of roughness has been largely overlooked, despite the potential affect it can have on the mechanical outcome of the implant. Therefore, the aim of this study is to test the mentioned parameters in-vitro and via FE modelling to consolidate the various conclusions in the literature.

As rim displacement has not shown correlation to failure, but rather correlation to fatigue (Anglin et al. 2001; Oosterom et al. 2004), the 2D work showing progressive failure during fatigue loading in chapter 3 will allow important monitoring of failure progression in this study. Based on FE predictions of the test, rim displacement is predicted to show correlation to failure (Fig. 4.1), however, vertical head displacement also shows a positive correlation, which may be superior to rim displacement. Therefore, both measures will be monitored throughout the test as a quantitative measure to failure. As such, a water bath will also be used to comply with the testing standard and to test the validity of the use of a water bath.

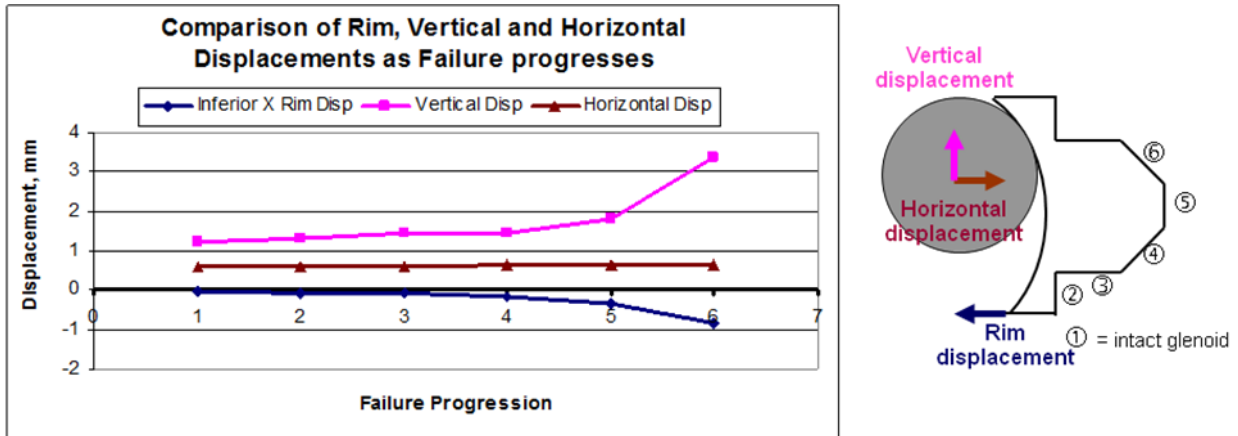


Figure 4.1: FE predictions showing a correlation between vertical head and inferior rim displacements with failure progression at the implant/cement interface.

Finally, deriving the testing parameters from subluxation curves is still open to debate, should the test be displacement controlled or load controlled? One study uses 90% of the subluxation distance (Anglin et al. 2001) and one uses 90% of the subluxation load (Oosterom et al. 2004). The method used in chapter 3 uses the linearity of the subluxation curves, which can be difficult to analyse and somewhat subjective. Therefore the choice between displacement and load must be addressed. Clinically, highly constrained (fixed fulcrum), conforming glenoids loosen very quickly due to high loading stresses, whereas less constrained, less conforming joints have shown higher incidence of instability and wear (Wirth & Rockwood 1996). Thus the rationale is, less conforming joints suffer from excessive displacement and lower rim loads, whereas conforming joints form high rim loads and lower displacements. Thus the testing parameters should reflect this. However clinically, the deciding factor is the conditions of the surrounding soft tissues, therefore, whether the test should be displacement or force controlled is unclear without in-vivo data, which is just beginning to emerge (Bergmann et al. 2007).

Specimens from each design will be tested non-destructively to the subluxation limit. Due to the difficulty in reading the subluxation displacement, it would be easier to determine 90% of the subluxation load accurately. Secondly, due to the range of displacement magnitudes (4.25-6.40 mm, chapter 3) compared to the magnitudes of the loads (1350-1550N), 90% of the average subluxation displacement will still be testing some of the specimens at the subluxation region, whereas there would be no such problem with using 90% of the

subluxation load. Thus, deriving the loading regime using 90% of the subluxation load will be adopted in the proceeding tests.

4.7 Materials and Method

4.7.1 Mechanical Test

Sixty 2D specimens of 8 designs were manufactured as described in chapter 3. The implants were divided into 3 groups, 24 implants were left smooth (S), 12 were roughened (table 4.1) to a roughness of 3-5 μm (R) and 24 were roughened with the aim of reaching a roughness of 5+ μm (VR). A sandblaster was used to roughen the back of the implants and a Talysurf surface profiler (Taylor-Hobson, AMETEK Inc., Pennsylvania, USA) was used to measure the surface roughness of the specimen at specific points across the surfaces, which were then averaged for each implant. A total of 20 groups were tested ($n = 3$). The 29 mm non-conforming implants of medium roughness (R) were not included in this test as the results of the specimens tested in chapter 3 will be used.

Table 4.1: Three treatments to achieve variable implant back roughness.

Roughness	Method
< 1 μm	No treatment
3-5 μm	Sandblast using 30-40 Ali-Oxide grit size Distance from nozzle: 20 cm Duration: 30 seconds
5-8 μm	Sandblast using 30-40 Ali-Oxide grit size Distance from nozzle: 5 cm Duration: 30 seconds

As described in chapter 3, the implants were cemented and tested using the same testing rig. All specimens were tested in a water bath at $37 \pm 2^\circ\text{C}$ (Fig. 4.3). The specimens were removed from the water bath every 2000 cycles and two linear variable displacement transducers (LVDTs) (Solatron Metrology, Bognor Regis, UK) were attached directly to the Failure Characteristics of All Polyethylene Cemented Glenoid Implants in TSA

bone substitute and horizontally aligned to measure horizontal rim displacement at the superior and inferior rim via reference pins inserted at the implant rim edge, as specified by the standard (F2028-02) (Fig. 4.2). The LVDTs measured a range of 2 mm with a resolution of < 0.0001 mm. Every 4000 cycles the vertical head displacement was readjusted to maintain the testing loads.

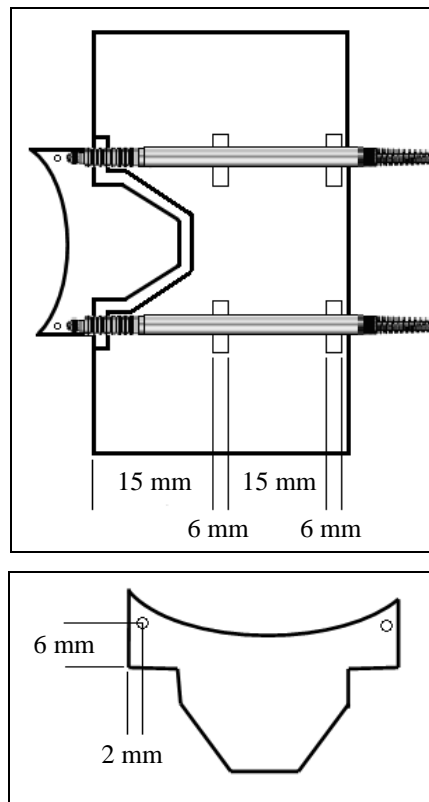


Figure 4.2: Schematic of the LVDTs fixed to the bone substitute (above) and location of reference pins at the superior and inferior rim (below).

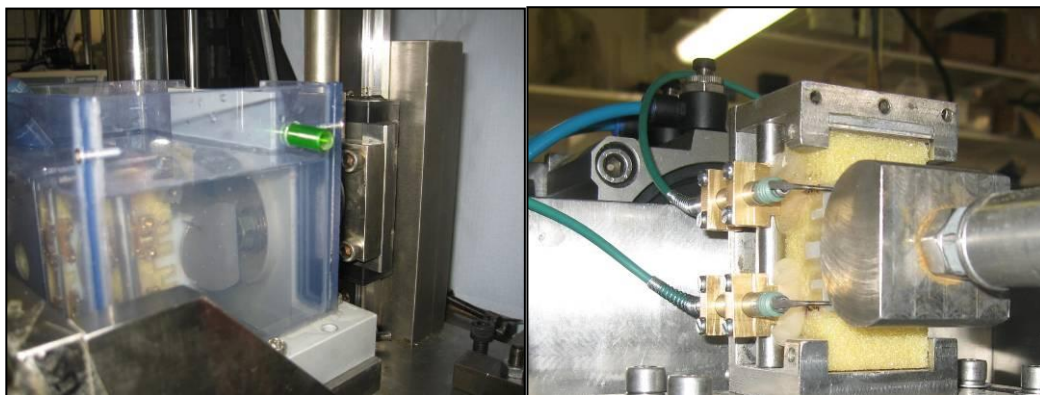


Figure 4.3: Specimens tested in a $37 \pm 2^\circ\text{C}$ water bath (left) and horizontal rim measurements were taken using LVDTs every 2000 cycles (right).

Prior to cyclic testing, two specimens of each design were tested quasi-statically to determine the load and displacement to subluxation. The test was non-destructive, thus the specimens were stopped once subluxation was reached or until the load/displacement curve began to plateau in order to protect the specimen from failure. Ninety percent of the corresponding load was defined as the testing load (Fig. 4.4).

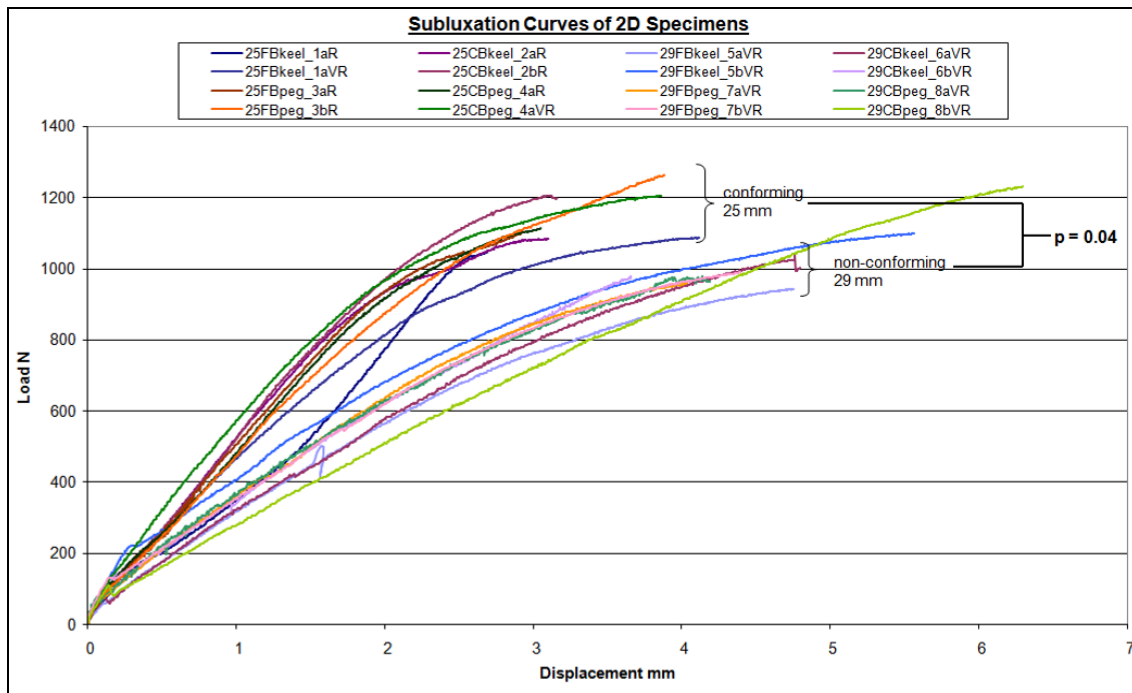


Figure 4.4: Subluxation curve of 8 designs (n = 2), a significant difference in subluxation loads was found between the two conformities (p = 0.04).

4.7.2 FE Analysis

As mentioned in chapter 3, 8 FE models that were built and run using Marc/Mentat 2005 were used to analyse the interfacial stresses, cement and bone material stresses.

A 3D FE model of a flat-back keel glenoid cemented in bone substitute was built in Marc/Mentat 2005 (Fig. 4.5), containing 27,423 elements, in order to compare the stress distributions between the 2D and 3D scenario. As with the 2D models, the same material properties were used and modelled as linear elastic. The model was tested to mesh convergence.

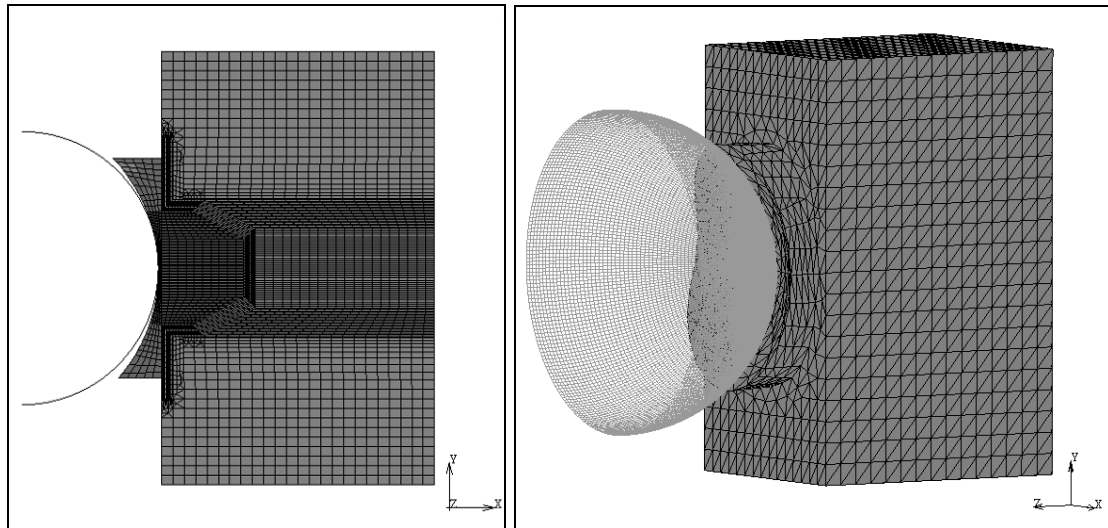


Figure 4.5: 2D (left) and 3D (right) non-conforming 29 mm flat-back keel FE models.

The stress distribution of the 2D and 3D 29 mm flat-back keel models were compared. The contact pressure at the humeral head/PE articulation was calculated analytically (Appendix C) for comparison and validation. These precautions were taken to compare the mechanical differences in the 2D and 3D scenario, since using a 2D method can be criticised for not being a realistic model to investigate failure behaviour.

4.8 Results

4.8.1 Mechanical Test

All 60 specimens, irrespective of design, failed inferiorly at the implant/cement interface, except for three roughened conforming flat-back keel specimens, two of which failed inferiorly in the bone and one at the cement/bone interface with an average of 3102-11,729 cycles to failure (Fig. 4.6). With respect to failure, there were comparable results between all design pairs (Fig. 4.7), although conformity seemed to show some effect, the only significant parameter was roughness (Fig. 4.8 & 4.9). There were no significant differences between roughnesses $< 1 \mu\text{m}$ and $1\text{-}2 \mu\text{m}$, however, there was a significant difference between the two smoother groups, $0\text{-}3.4 \mu\text{m}$ and $> 3.4 \mu\text{m}$ ($p < 0.0001$). The average cycles to failure for the rough group ($> 3.4 \mu\text{m}$) was nearly 4 times greater at 8712 ± 5584 compared to the $0\text{-}3.4$

μm group at 1080 ± 1197 cycles. A non-orthogonal array ANOVA statistical test was carried out on the data.

Although the study aimed to test the three roughnesses in table 4.1, the roughness measures showed a similar range of roughnesses in both sandblasted groups from 3.4 to 11.1 μm . The untreated group showed a roughness range of 0.61 to 2.0 μm , thus the results were divided into three roughness groups; $< 1 \mu\text{m}$, 1-2 μm and $< 3.4 \mu\text{m}$.

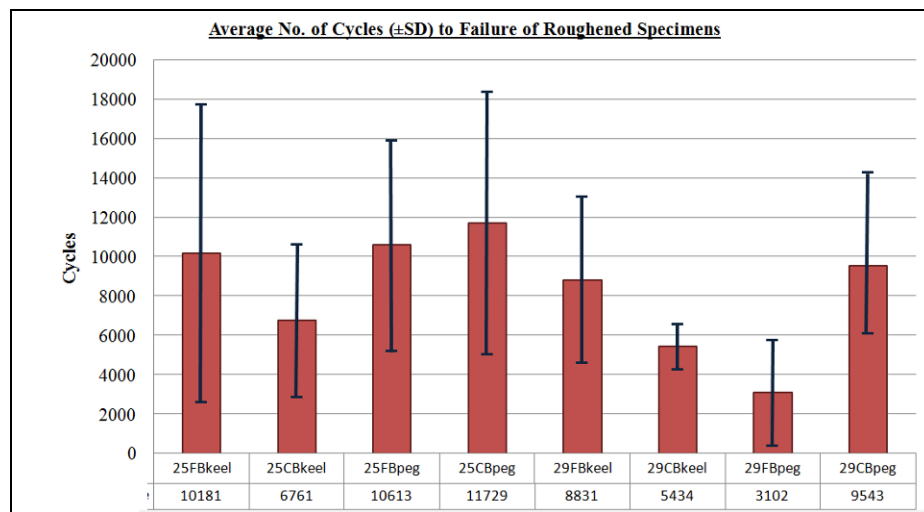


Figure 4.6: Average number of cycles in roughened specimens at failure for each design.

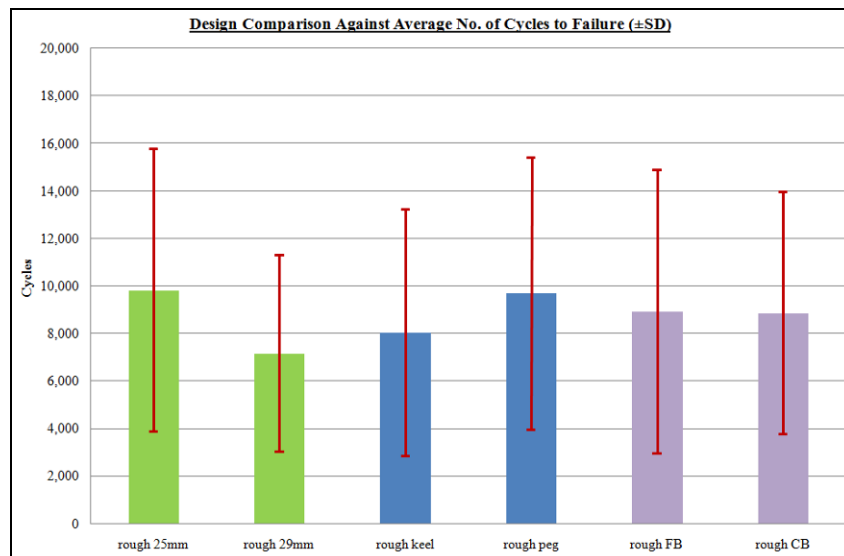


Figure 4.7: Comparable results between less (29 mm) & more (25 mm) conforming, keel & peg and flat & curved-back.

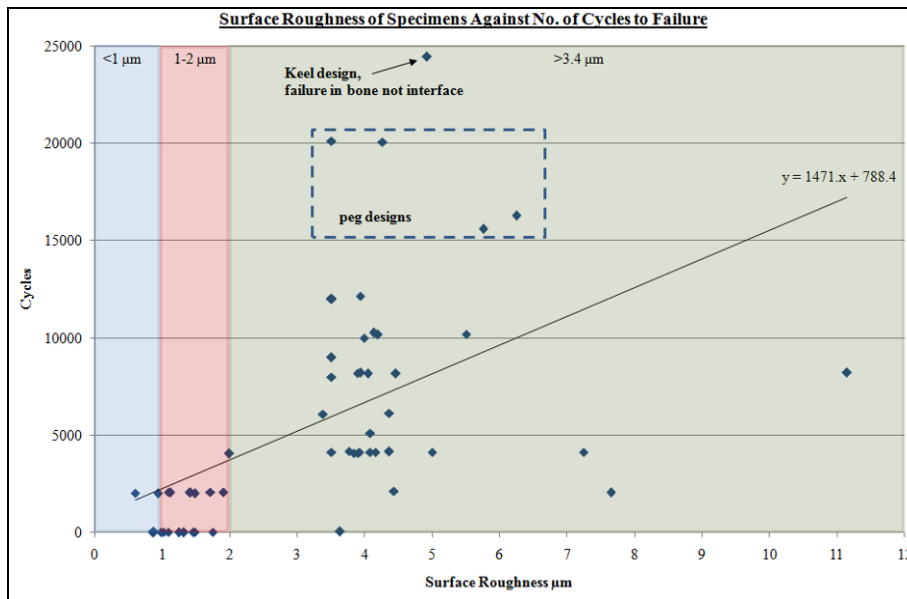


Figure 4.8: Increase in number of cycles to failure and surface roughness was proportional.

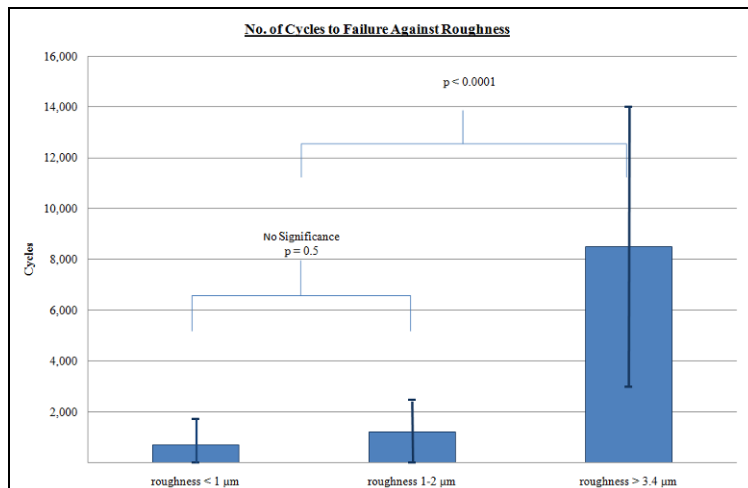


Figure 4.9: A significant difference was found between roughnesses 0-3.4 μm and > 3.4 μm ($p < 0.0001$).

4.8.2 Rim Displacement Versus Head Displacement

An increase in inferior rim displacement and vertical head displacement was observed with number of cycles (Fig. 4.10), this correlation is also found during failure progression (Fig. 4.11).

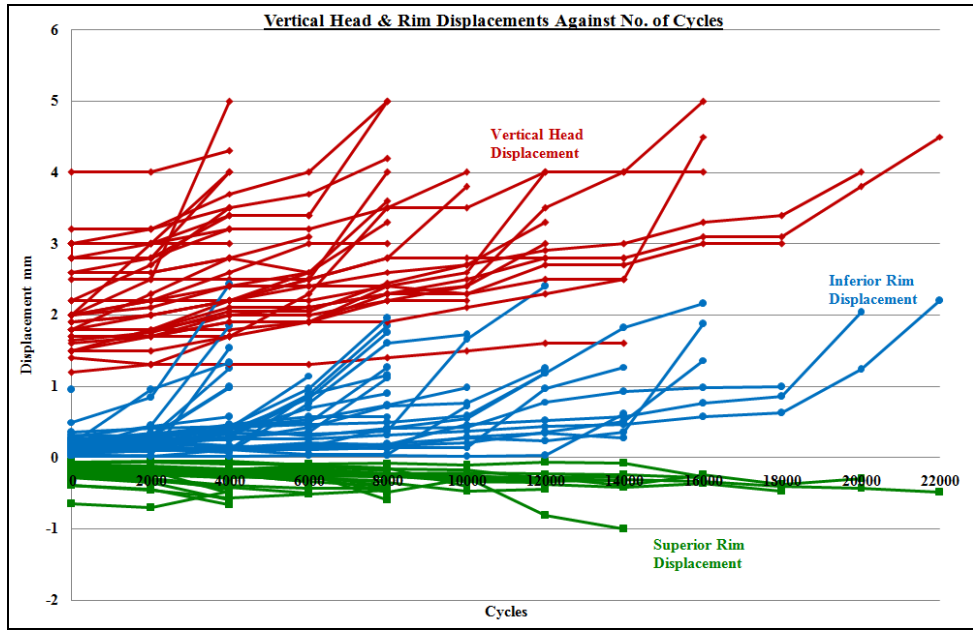


Figure 4.10: A positive correlation was found with number of cycles in both vertical head and inferior rim displacement.

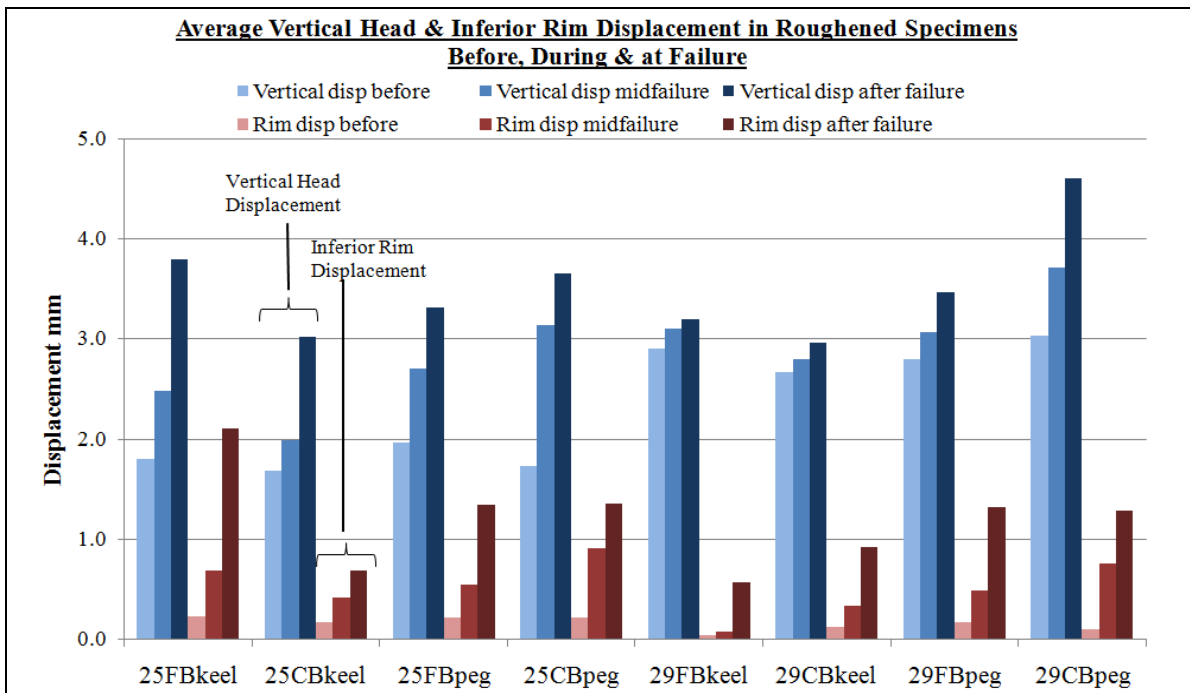


Figure 4.11: Bar chart showing a positive correlation between average vertical head displacement, average inferior rim displacement and progressive failure.

4.8.3 FE Validation

All FE models were tested to mesh convergence, using subluxation load and displacement. The load convergence between FE and in-vitro subluxation curves was between 87-99% and displacement convergence was between 74-99% (Fig. 4.12 & 4.13). The 2D and 3D models showed similar stress distributions and stress magnitudes, showing high compressive stresses superiorly and relatively lower tensile stresses inferiorly.

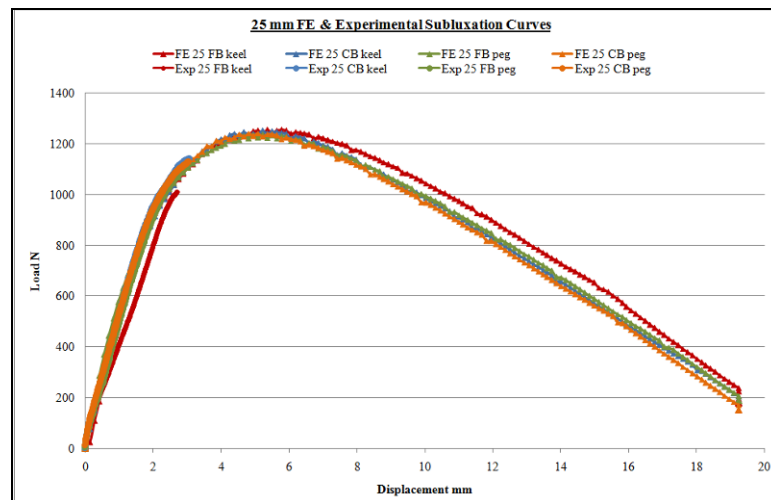


Figure 4.12: Conforming FE & average in-vitro subluxation curves for each design.

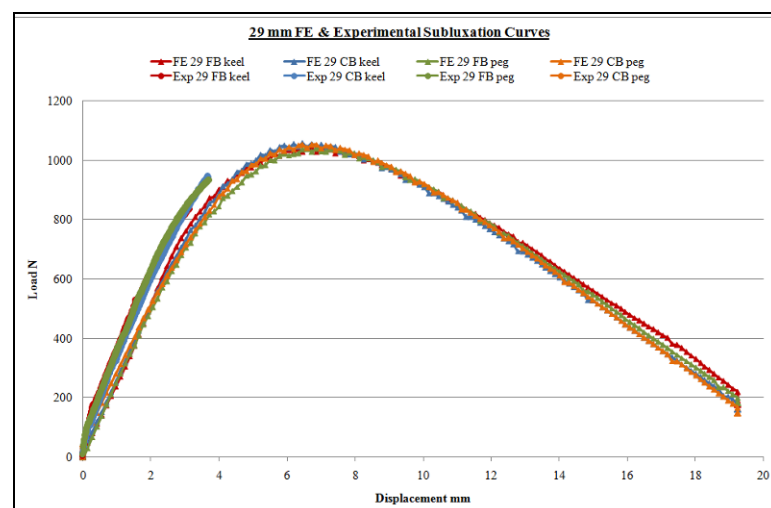


Figure 4.13: Less conforming FE & average in-vitro subluxation curves for each design.

4.8.4 FE Analysis

Predicted stress plots of interfacial stresses at the implant/cement and bone/cement interfaces, as well as stresses in the cement mantle and bone substitute were plotted for all implants.

Figure 4.14 of the 25 mm curved-back keel demonstrates tensile inferior peak stresses at the implant/cement and cement/bone interface. This was similarly found in all models. Thus it is unclear which interface is susceptible to detach first. However, interfacial strengths indicate the cement/bone stresses are predicted to be below or reach the minimum strength of 2.32 MPa, whereas the implant/cement stresses are predicted to be well within the interfacial strength range of 1-3.2 MPa. Thus based on experimental strength values from a previous study (Sanghavi et al. 2007), the FE models indicate susceptibility for the implant/cement interface to fail first. All stress plots indicate bone stresses in the superior part to be above the compressive strength of bone substitute. This is corroborated by visible bone crushing superiorly.

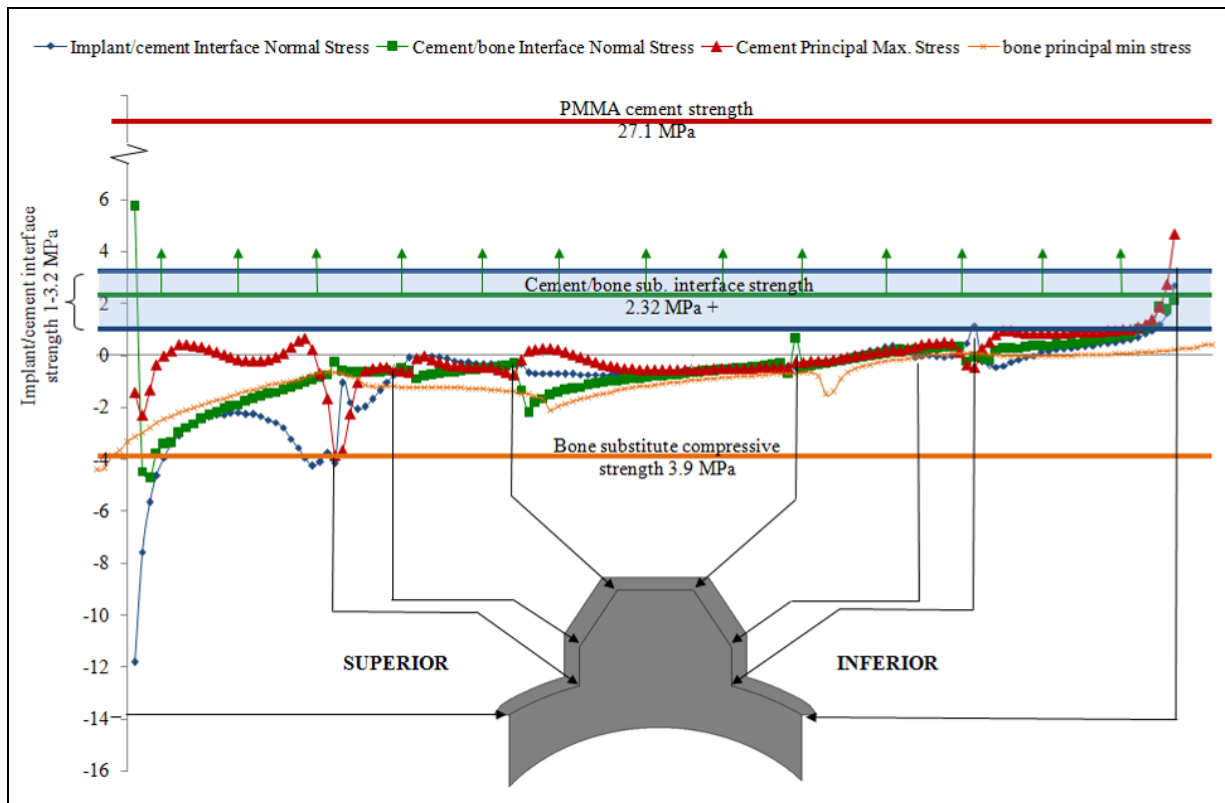


Figure 4.14: Colour plot of the predicted stresses in the fixation of the conforming curved-back keel model. Note: plot is the same as Fig. 3.8.

4.9 Discussion

With the exception of three flat-back keel specimens, all designs failed inferiorly at the implant/cement interface, indicating that this is the weakest part of the fixation as also found in chapter 3. Stress plots from FE results and interfacial strength data indicates interfacial weakness at the implant/cement rim edge under tensile stresses. Failure progression was visible and correlated to vertical head displacement and inferior rim displacement, verifying the validity of the use of rim displacement as an indication of fixation performance, which until now has been unproven. None of the design parameters significantly affected the failure outcome, except for roughness ($p < 0.0001$).

4.9.1 Roughness

Increasing roughness was shown to have a significant effect on the fixation performance, more so than all other design parameters. Where Anglin et al. (2001) demonstrated the importance of roughening based on the immediate failure of two smooth implants, this study provides a comprehensive study of the effect of increasing roughness on the implant fixation. The roughnesses were grouped into three ($< 1 \mu\text{m}$, $1-2 \mu\text{m}$ and $> 3.4 \mu\text{m}$). The first and second roughness groups performed equally poorly, but a significant improvement was found in implants with roughness of $3.4 \mu\text{m}$ or more ($p < 0.0001$). However, there was some improvement in the peg implants compared to the keeled in the non-conforming cases, although this was not significant. This may be due to the peg structures, resisting crack propagation better than the keeled structure, though this improvement was not seen in the conforming implants. Most commercial implants focus on the design of macro-features at the peg or keel such as fins, grooves and threads to improve the interface strength via mechanical interlocking, since cement does not chemically bond to the implant surface or bone. The effects of these features are not fully known and possible variations of manufacturer designs are endless. However, simply roughening the polyethylene above $3.4 \mu\text{m}$ will improve the implant rim's resistance to failure. Since implants already feature various macro-features on the peg or keel, it may also be useful to investigate the affects of macro-features and surface texture on the implant rim.

4.9.2 Peg Versus Keel

Although no significant difference was found between peg and keel, the roughened group showed a non-significant improvement in the curved-back peg implant compared to the curved-back keel, regardless of conformity. Nuttall et al. (2007) found keel implants migrated in the superior/inferior axis significantly more than peg implants and rotate significantly more in two axes compared to the peg implants. Interestingly, the postoperative outcomes using the Constant-Murley Score of the keel implants were slightly better than the peg, although these results are based on a study of only 10 peg and 10 keel implants. The anchorage design may have an effect on the mechanics of the implant, the results from the study suggests roughening the implant will improve implant outcome regardless of the anchorage, however, within the roughness groups, there are some noticeable differences in number of cycles to failure between the peg and keel, however, the stress plots demonstrate similar inferior stresses at the interfaces (Appendix D).

Although the 2D set up will not allow comments on the rotational stability of the implant, it may be the pegs improve the implant/cement fixation due to a more interlocking design compared to the single keel. The choice of peg over keel may also be technical as Lazarus et al. (2002) showed a higher reliability of reading radiographs in the pegged implants compared to the keel. In some practices, keeled implants are only used in cases where the glenoid view is compromised and the bone condition is not ideal, thus introducing bias which may affect the outcome of TSA joints (Lazarus et al. 2002).

4.9.3 Flat-back Versus Curved-back

No significance was found between flat-back and curved-back implants, however, it is important to note that, in theory, implanting the curved-back implant will preserve the subchondral layer as the glenoid surface is uniformly reamed using a spherical reamer. Whereas the flat-back implant will require more resection of the glenoid bone, particularly on the edges of the glenoid. This difference cannot be modelled in bone substitute, which may also impact on the outcome of the two designs in-vitro. The FE stress plots predict lower contact stresses in the curved-back case and although no differences were found in the number of cycles to failure compared to the flat-back specimens, less bone crushing was observed superiorly, which was also predicted in the FE models, showing lower bone

stresses. The idea behind curved-back designs is to conform to the natural curvature of the glenoid surface and thus improve the mechanics of the joint by lowering the shear loading and generating a more perpendicular load to the surface. However, the results indicate shear loading is not necessarily the cause of the failure, in fact it is the nature of the implant/cement interface that is fundamentally affecting the outcome of the implant.

The study by Szabo et al. (2005) indicates no significant difference in the appearance radiolucent lines between the curved and flat-back glenoid implants, however, with the uncertainty of radiographs and lack of patient outcome data, it is hard to tell if this is truly the case. Some of the in-vitro work, thus far have indicated curved-back implants to be superior to flat-back implants (Anglin et al. 2001; Collin et al. 1992). FE studies have shown varied results with one study finding higher stresses at the implant back in curved-back designs, whereas higher stresses were found at the keel in flat-back designs. The same study found, non-bonded models predicted higher rim displacement in the flat-back models (Iannotti et al. 2005). Whereas Mansat et al. (2007) predicted similar stresses using peg and keel implants in an osteoarthritic model of the joint replacement. The stress plots from this study indicate a lower, more uniform and less variable stress distribution throughout the interfaces in the curved-back models compared to the flat-back. The stresses at the inferior region of all models were also lower in all interfaces and cement stresses in the curved-back case. However, inferior edge stress peaks were still comparable (Appendix D).

4.9.4 Conformity

Despite the conformity showing no significant difference on fixation failure, the differences were still noticeable ($p = 0.12$). The small sample size and large scatter may be the cause of the large p-value. Additionally, the subluxation curves showed a significant difference in subluxation loads between the conforming and less conforming specimens ($p = 0.04$). The results indicate a higher conformity is mechanically more resistant to fatigue failure compared to the less-conforming design, as supported by Oosterom et al. (2004) and Lacroix & Prendergast (1997). However, other studies suggest the opposite (Anglin et al. 2001; Orr et al. 1988). Clinically pain, mobility and functional outcomes of TSA using various conformities of an anatomical (non-constrained) designs have not shown any significant difference, however, there has been shown a higher prevalence of r. lines with higher conformities (Walch et al. 2002).

What comes to question is the mechanics of the implanted joint; if loaded the same, perhaps the less conforming designs will fail first, whereas testing the same displacement is prone to cause early failure of the conforming joint. A look into the loading regime adopted shows that using the principle of taking 90% of the subluxation load, glenoids of varied conformities are tested at various displacements and loads, although the extent of loading, in relative terms, is the same throughout. Testing all implants using a constant displacement or constant load varies the level of loading between implants, with some being tested close to their subluxation limits and others well within their limits. One hypothesis proposed, is that TSA patients would not allow the joint to subluxate, since they can sense a feeling of the joint wanting to ‘give way’. With this reasoning, each implant should be tested within its subluxation limits as these limits will not be transgressed by the patient.

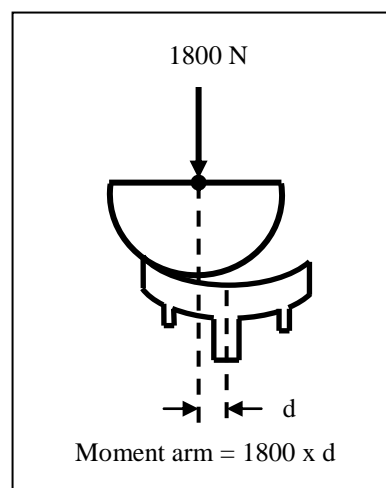


Figure 4.15: The moment generated by loading the glenoid is defined as the product of the compressive load (1800 N) and vertical head displacement (moment arm).

Subsequently, the conforming 25 mm and less-conforming 29 mm implants require a vertical loading regime of 1000 N and 900 N respectively or an average displacement of 2.3 mm and 3.5 mm respectively. With a compressive force of 1800 N, the resultant force generated by the 25 mm implants is 2059 N, with an average moment of 4.3 Nm (moment defined in Fig. 4.15). Comparatively, the 29 mm implant has a lower resultant force of 1849 N and a higher moment of 6.1 Nm. Based on these observations, it is unclear which of the two implants are mechanically susceptible to loosening. The 25 mm implants experience higher rim loads whereas the 29 mm implants experience higher moments. As these observations are isolated to the superior region, it is unclear which of these are more effective in the inferior region.

From the fatigue test results of 60 2D implants, failure has been predominantly observed inferiorly at the implant/cement interface. The in-vitro results indicate the higher moment arm in the less-conforming 29 mm specimens makes the less-conforming designs more susceptible to failure. Arguably the loads between the two conformities are comparable with only 11% difference, whereas the differences in moment arms are 42%. Thus, with this in mind, the relatively small differences in the resultant force have had little effect and the more prominent changes in moments have had some affect on the loosening rate of the glenoid fixation.

Clinical outcomes of unsuccessful fully constrained joints has led many surgeons to use a less conforming design to better match the anatomical mechanics of the natural glenoid joint. However, the results from this study suggests a radial mismatch of 5 mm may lead to earlier loosening due to a dramatic increase in the moment arm of the joint, although the results does not show this to be significant ($p = 0.16$). Harryman et al. (1995) in a cadaveric study have also shown ROM and laxity of the implanted GH joint is not significantly different between a 0 mm radial mismatch and a mismatch of 4 mm. Thus it is unclear, based on fatigue testing and joint mechanics, what the ideal conformity should be. Indeed it is also well known clinically that humeral head translations and mechanics of the joint are dependent on the surrounding soft tissue and less on the geometries of the joint.

Arguably the loads between the two conformities from the above cyclic tests are not considerably different to the difference in moments with 11% and 42% respectively. As such it may be that a more extreme and equal difference, albeit unrealistic, in the loads may result in different conclusions. Additionally, the affect of loading differences and moments to the surrounding fixation interfaces and in particular bone, is not clearly known. However, in-vitro fatigue tests and FE results in 2D suggest the differences between conformities are not significant, at least with a radial mismatch of 1-5mm.

4.9.5 FE Predictions

The FE models were unable to predict order of failure using both inferior tensile and shear stresses. However, the failure of the rough 25 mm flat-back keels all failed at the cement/bone interface or in the bone inferiorly was interesting. The FEA reveals a tensile

average stress inferiorly of only 0.14 MPa, compared to all the other models which predicted stresses of 0.47-1.06 MPa. Based on the interface strength of 1-2.32 MPa for roughnesses of 3.5 μm or more, it appears that the conforming flat-back keel creates lower tensile stresses inferiorly compared to the other designs and thus only reached the lower range of the interface strength (appendix D). However, the cement/bone normal stresses were close to the cement/bone interface strength, perhaps explaining why failure occurred at the cement/bone interface and within the bone substitute rather than at the implant/cement interface. In-vitro, this design combination on average was the second best implant at resisting failure (12,255 cycles), after the conforming curved-back peg (14,022 cycles), although these differences are not significant.

4.9.6 Rim Displacement Measure

An increase in rim displacement and vertical head displacement was observed with progressive failure in all implant designs. Although studies have used rim displacement as an indirect measure of instability and fixation weakness (Anglin et al. 2001; Collins et al. 1992; Oosterom et al. 2004), it is clear from this study that off-loaded rim displacement can be a measurement for glenoid loosening and can monitor loosening progression.

By re-adjusting the vertical displacement to the testing load every 4000 cycles, the vertical displacement similarly increased with progressive failure. Re-designing the rig parts, purchasing expensive LVDTs and the difficulty of removing the water bath and re-attaching LVDTs throughout the test, makes the use of vertical displacement a more cost effective, time efficient and convenient method of analysing and measuring the failure of the implant fixation.

4.9.7 Water Bath

A water bath was used in the study as described by the Standard. The outcome was very similar to the initial study in dry conditions (chapter 3) as both studies showed failure occurring at the implant/cement interface inferiorly and bone crushing superiorly. However, due to the small sample sizes in chapter 3, testing for significance between the number of cycles to failure is not possible, although the range of cycles are comparable with chapter 3 averages ranging from 9764 to 13,969 cycles compared to 3102-11,729 cycles in this study.

This raises the question whether it is necessary to test the fixation in a water bath. Anglin (1999) fatigue tested two glenoids in a water bath at 37 °C and two in the air, finding a 5% decrease in subluxation loads using the water bath. The mechanical properties of polymers can be altered with temperature change, however, this has not been shown to affect the outcome of the cyclic test. In fact, if the subluxation loads are lower in a 37 °C water bath, the implants should be expected to take longer to fail, however, the range of cycles in chapter 3 and 4 shows contrary to this. By testing under dry conditions and at room temperature there is also the advantage of monitoring rim displacement throughout the test. Thus for the proceeding tests, there seems to be no clear advantage to test in a water bath.

4.10 Conclusion

The importance of implant surface roughness is evident by the clear difference in cycles to failure with a significant improvement in resistance to failure with a roughness of 3.4 µm or more. A difference in flat-back versus curved-back was not significant. Similarly peg and keel overall did not show any differences, however, under certain design conditions, a noticeable improvement was observed in peg specimens. Studies from the literature suggest the importance on bone stock and its role in implant fixation outcome. Likewise, the difference in roughness of the peg and keel group was shown to be different, thus the implant/cement strength may well have been the main factor for the differences. Finally conformity, a hotly debated topic, has been shown to noticeably improve the fixation outcome, although this difference is not significant. Thus the importance of roughening the back of the implant or investigating the affect of macro-features on the implant/cement strength should be considered to improve the short-term effects of loosening, which can improve the long-term mechanical survivability of the implant.

This study also confirms the use of rim displacement as a measure of failure and suggests an easier way of measuring failure using vertical head displacement. The results will allow a more confident investigation into the affects of design parameters on the outcome of commercial 3D implants using the mechanical test, which will be investigated in the following chapters.

4.11 References

- Anglin, C, (1999). *Shoulder Prosthesis Testing*, PhD Thesis, Mechanical Engineering, Queen's University, Canada.
- Anglin, C, et al. (2001). Loosening Performance of Cemented Glenoid Prosthesis Design Pairs, *Clinical Biomechanics*, 16: 144-150.
- ASTM F 2028-02, 2004. Standard Test Methods for the Dynamic Evaluation of Glenoid Loosening or Disassociation. Book of ASTM Standards: 1083-88.
- Barrett, W P, et al. (1987). Total Shoulder Arthroplasty, *Journal of Bone and Joint Surgery, American Volume*, 69A, (6): 865-872.
- Bergmann, G, et al. (2007). In Vivo Glenohumeral Contact Forces-Measurements in the First Patient 7 Months Postoperatively, *Journal of Biomechanics*, 40: 2139-2149.
- Cofield, R H (1984). Total Shoulder Arthroplasty With the Neer Prosthesis, *Journal of Bone and Joint Surgery, American Volume*, 66A, (6): 899-906.
- Collins, D, et al. (1992). Edge Displacement and Deformation of Glenoid Components in Response to Eccentric Loading. The Effect of Preparation of the Glenoid Bone. *Journal of Bone and Joint Surgery, American Volume*, 74A, (4): 501-507.
- Friedman, R, et al. (1992). The Use of Computerized-Tomography in the Measurement of Glenoid Version. *Journal of Bone and Joint Surgery, American Volume*, 74A, (7), 1032-1037.
- Harryman, D T, et al. (1995). The Effect of Articular Conformity and the Size of the Humeral Head Component on Laxity and Motion After Glenohumeral Arthroplasty. A study in Cadavera, *Journal of Bone and Joint Surgery, American Volume*, 77A, (4): 555-563.
- Iannotti, J P, et al. (2005). Prosthetic Positioning in Total Shoulder Arthroplasty, *Journal of Shoulder and Elbow Surgery*, 14, (1S): 111S-121S.
- Karduna, A R, et al. (1997). Joint Stability After Total Shoulder Arthroplasty in a Cadaver Model, *Journal of Shoulder and Elbow Surgery*, 6, (6): 506-511.
- Lacroix, D & Prendergast, P J (1997). Stress Analysis of Glenoid Component Designs for Shoulder Arthroplasty, *Proceedings of the Institute of Mechanical Engineers*, 211, Part H: Journal Engineering in Medicine, 467-474.

- Lazarus, M D, et al. (2002). The Radiographic Evaluation of Keeled and Pegged Glenoid Component Insertion, *Journal of Bone and Joint Surgery, American Volume*, 84A, (7): 1174-1182.
- Mansat, P, et al. (2007). Evaluation of the Glenoid Implant Survival Using a Biomechanical Finite Element Analysis: Influence of the Implant Design, Bone Properties, and Loading Location, *Journal of Shoulder and Elbow Surgery*, 16, (3S): 79S-83S.
- Matsen III, F A, et al. (2008). Glenoid Component Failure in Total Shoulder Arthroplasty, *Journal of Bone and Joint Surgery, American Volume*, 90, (4): 885-896.
- Neer II, C S, et al. (1974). Replacement Arthroplasty for Glenohumeral Osteoarthritis, *Journal of Bone and Joint Surgery, American Volume*, 56A, (1): 1-13.
- Nagels, J, et al. (2002). Patterns of Loosening of the Glenoid Component, *Journal of Bone and Joint Surgery, British Volume*, 84B, (1): 83-87.
- Nuttall, D, et al. (2007). A Study of the Micromovement of Pegged and Keeled Glenoid Components Compared Using Radiostereometric Analysis, *Journal of Shoulder and Elbow Surgery*, 16, (3S): 65S-70S.
- Nyffeler, R W, et al. (2003). Influence of Peg Design and Cement Mantle Thickness on Pull-Out Strength of Glenoid Component Pegs, *Journal of Bone and Joint Surgery, British Volume* 85B, (5): 748-752.
- Oosterom, R, et al. (2004). Effect of Glenoid Component Inclination on Its Fixation and Humeral Head Subluxation in Total Shoulder Arthroplasty, *Clinical Biomechanics*, 19: 1000-1008.
- Orr, T E, et al. (1988). Stress Analyses of Glenoid Component Designs, *Clinical Orthopaedics and Related Research*, 232: 217-224.
- Sanghavi, S, et al. (2007). Glenoid Bone-PMMA Interface Tensile Strength. Pending submission.
- Swieszkowski, W W, et al. (2003). Contact Stresses in the Glenoid Component in Total Shoulder Arthroplasty, *Proceedings of the Institution of Mechanical Engineers*, 217, Part H: Journal Engineering in Medicine, 49-57.
- Szabo, I, et al. (2005). Radiographic Comparison of Flat-back and Convex-back Glenoid Components in Total Shoulder Arthroplasty, *Journal of Shoulder and Elbow Surgery*, 14, (6): 636-642.

- Walch, G, et al. (2002). The Influence of Glenohumeral Prosthetic Mismatch on Glenoid Radiolucent Lines - Results of a Multicenter Study, *Journal of Bone and Joint Surgery, American Volume*, 84A, (12): 2186-2191.
- Wirth, M A, & Rockwood, Jr, C A, (1996). Current Concepts Review-Complications of Total Shoulder-Replacement Arthroplasty, *Journal of Bone and Joint Surgery, American Volume*, 78A, (4): 603-616.

Chapter 5: Failure Mechanism in All-Polyethylene Cemented Glenoid Implants:

A Cadaveric Study

5.1 Abstract

Data on the fatigue behaviour of the glenoid fixation using human bone has been minimal. It is important to address how realistic the use of a generic bone substitute is for investigating glenoid fixation in TSA. Ten cadaveric scapulae were implanted with a curved-back, smooth, pegged glenoid and cyclically tested to failure. The scapulae were CT scanned every 20,000 cycles and at failure to monitor progressive radiolucent lines with visible failure. The superior and inferior rim displacements were monitored, as well as the vertical head displacement, which was readjusted to maintain the testing load. All 10 implants failed inferiorly at the implant/cement interface, of these, 2 also failed at the cement/bone interface inferiorly. Superior bone crushing was observed clearly in 3 cases. Failure occurred at $80,966 \pm 53,729$ cycles, corresponding to time scale, 20% of TSAs would fail long-term (> 10 years), 50% would fail mid to long-term (5-10 years) and 30% short to mid-term (< 5 years). Despite the difficulty in measuring rim displacements, a positive correlation was found between increasing inferior rim displacement and failure of the glenoid implant ($p < 0.005$). A positive correlation was also found with increase in vertical head displacement and failure. CT scans confirmed failure of the glenoid fixation, although in 3 cases (30%) it was not clear which interface had failed, highlighting the problem with the ambiguity of reading radiographic images. The study shows promising results, which support some of the 2D findings and will be an important validation step when using bone substitute. The study also highlights the need to address short to mid-term problems of the fixation, namely the implant/cement interface and the need to address the biological problem, which manifests in mid to long-term TSA cases.

5.2 Introduction

Speculation as to whether bone substitute tests are relevant and realistic is a valid one. Until more recently, there was a lack of published work on the mechanical properties of scapula bone (Frich et al. 1997; Lim et al. 2006; Mimar et al. 2008), in fact, most studies on human bone properties are exclusively derived from the tibial or femoral bone, where cancellous bone is relatively abundant and easy to extract (Carter & Hayes 1977; Turner et al. 1999). Therefore generic bone substitute foam, such as polyurethane used in previous chapters, may not necessarily represent the specific bone properties of the scapula. Secondly, studies of bone properties largely focus on the bulk properties of bone and this does not necessarily indicate the material's ability to bond to cement. Thirdly the scapula consists of thin cortical structures and sheets and a relatively small volume of cancellous bone. The importance of maintaining the cortical subchondral layer on the glenoid surface is also known and commonly practiced during TSA surgery (Lazarus et al. 2002). Therefore, whether these structural considerations and large distribution of mechanical properties will make the cancellous bone substitute an unrealistic model of the scapula bone warrants investigation and will be an important validation step in this PhD study.

No comparison was made with the results in chapter 4 between clinical outcomes and rim displacement studies of commercial implants due to the 2D modelling of the shoulder replacement. In cadaveric and clinical studies, the absence of visual observation requires investigators to depend on radiographs and outcomes from clinical examination. A study investigating TSA complications found loosening to be the most common complication after stiffness (Hasan et al. 2002). This has been confirmed by other studies (Wirth & Rockwood 1996). However, radiographs have been used to investigate the locality and source of the loosening problem. Clinical observations have found the majority of r. lines in the inferior region of the implant, possibly indicating glenoid loosening and a mechanical disadvantage inferiorly (Klepps et al. 2005; Nagels et al. 2002; Yian et al. 2005).

Only one study (Anglin 1999) successfully tested one cadaveric scapula to compare the rim displacement to two bone substitute tests. Only one sample investigating only one questionable measure of loosening (rim displacement) is clearly not sufficient to confirm the

use of PU bone substitute in glenoid loosening studies. Thus the purpose of this study is to test the validity of using PU bone substitute by mechanically testing a significant number (10) of implanted cadaveric scapulae and FE modelling the test in-vitro, investigating the importance of bone variation to the failure mechanism. This study will also use CT scans to compare visible r. lines to measured rim displacements, as visible loosening may be difficult to observe.

5.3 Materials & Methods

Eleven fresh-frozen cadaveric scapulas were used for the study, however, one was excluded due to very poor sclerotic bone. Another was also defined as partially sclerotic, however, this was included in the study, and a total of 10 normal scapulae were implanted and tested.

5.3.1 Specimen Preparation

The 10 scapulae were implanted with a Tornier Aequalis all-polyethylene curved-back pegged glenoid (Fig. 5.1). Three small, six medium and one large glenoid with radial curvatures of 27.5 mm, 30 mm and 32.5 mm respectively were implanted by an experienced shoulder surgeon (T.G.). The soft tissue and labrum were excised, the glenoid surface was reamed, removing the cartilage layer, and care was taken to maintain the subchondral layer. The glenoid implants were cemented using Simplex[®] bone cement (Stryker Europe, Montreux, Switzerland). The scapulae were cut to size using an Exakt 310 CP diamond-tipped high precision saw (Exakt Technologies Inc., Oklahoma City, USA) and cemented using Simplex[®] bone cement into the specimen holder. Care was taken to ensure the glenoid surface was correctly aligned with no implant tilt (Fig. 5.1). Two holes were drilled into each glenoid implant to accommodate a 2 mm diameter rod at the superior and inferior edge of the glenoid, 2.5 mm from the corresponding rim. Two rods were prepared as reference points to measure the corresponding rim displacements via the LVDTs (Fig. 5.2).



Figure 5.1: Aequalis Tornier curved-back cemented glenoid implant (left). NB2 specimen cemented and potted for testing (right).

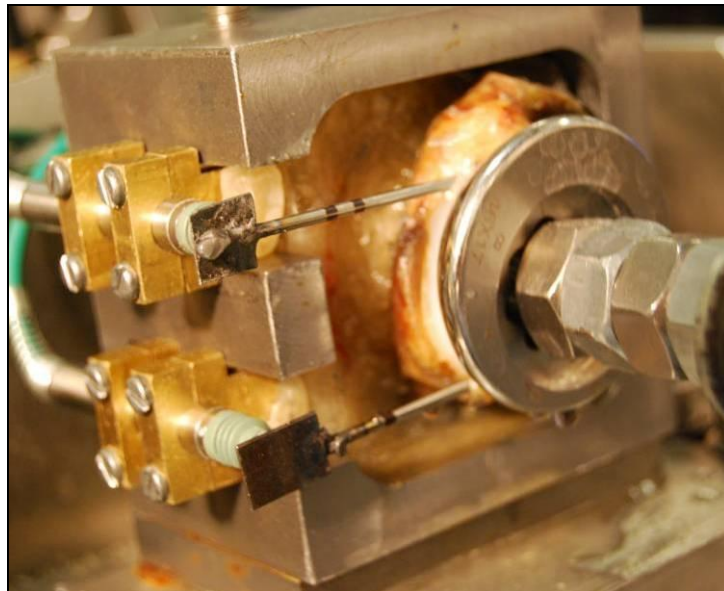


Figure 5.2: Rods were prepared for measuring horizontal rim displacement using LVDTs, attached directly to the specimens.

5.3.2 Mechanical Test

The 10 scapulae were cemented into the specimen holder and tested using the same testing rig as chapter 3 and as described by the standard, a compressive load of 750 N was applied. A 24 mm humeral head manufactured by Tornier was used to test all specimens, thus making a radial mismatch of 3.5, 6 and 8.5 mm corresponding to the three glenoid sizes; small, medium and large respectively. Following the conclusions from chapter 4, the specimens were tested without a water bath, however, the exposed scapulae and joint were kept wet via

a water spray. LVDTs were attached directly to the specimen and horizontally aligned to measure horizontal rim displacement at the superior and inferior rim via reference pins inserted at the implant rim edge as specified by the standard (F2028-02) (Fig. 5.2 & 5.3). The LVDTs were fixed throughout the test and rim displacement measures were recorded every 2000 cycles. Every 4000 cycles the vertical head displacement was readjusted to maintain the testing loads.

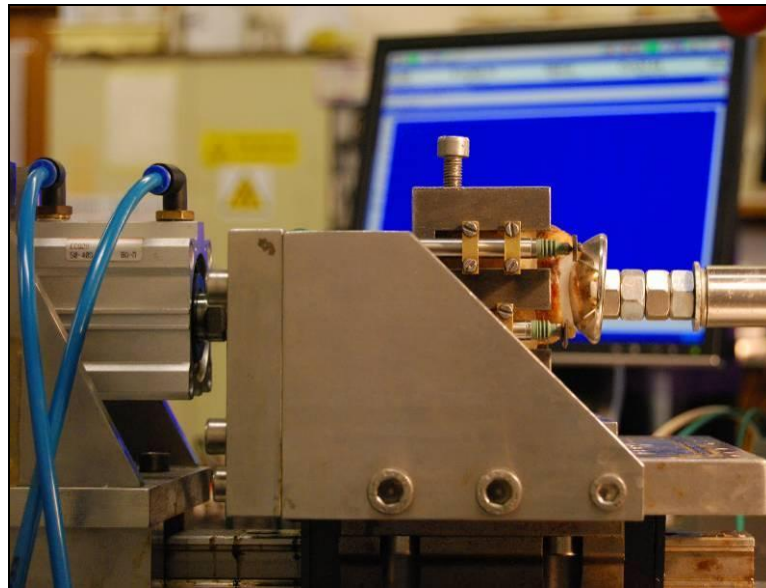


Figure 5.3: Mechanical cadaveric test.

The loading regime was derived from the subluxation curves derived from 2 medium glenoids implanted in bone substitute. The vertical load was chosen to be 400 N by deriving 90% of the subluxation load as described in chapter 4 and comparing the values to subluxation curves in chapter 6. A common load was used throughout, despite 3 different implant sizes being tested. The subluxation load differences between large and medium glenoids were comparable at 500 N and 465 N respectively. Thus 400 N was used for all specimens.

5.3.3 CT Scans

CT scans were taken of all the scapulae before implantation, after implantation, at 20,000, 40,000, 60,000 cycles and after failure.

During testing, failure visually was defined in two stages, initial failure is indicated by visible distraction of the inferior glenoid rim from the cement or bone substitute block. Half failure was defined as the point when the inferior pegs are visible during inferior rim distraction, where the test was stopped. Half failure is referred in following text as failure. Superior bone crushing is defined by visible embedding of the superior implant rim and superior failure was defined as visible distraction of the superior rim.

5.3.4 Post-Testing Observations

After testing to failure or at 200,000 cycles, the specimens were sliced through the superior/inferior centreline using an Exakt 310 CP diamond-tipped saw (Exakt Technologies Inc., Oklahoma City, USA) and the fixation and bone conditions were observed under a Nikon SMZ 800 microscope (Nikon Instruments Inc., New York, USA) with a magnification of 20.

5.3.5 Finite Element Modelling

The CT scan for one scapula (NB1) was used to construct the 3D FE model of the shoulder. Amira[®] (Visage Imaging, California, USA) was used to construct the tetrahedral mesh and insert the glenoid implant. Marc/Mentat 2001 (MSc Software Corporation, California, USA) was used to perform the FE analysis. The glenoid implant model was built using CAD files obtained from the orthopaedic manufacturer. The material properties of the bone were assigned by using BIOMESH, a program developed by Andrew Hopkins in the Biomechanics Group. The program assigns the Young's modulus, apparent density and Poisson's ratio from the CT number to the tetrahedral mesh. The Carter & Hayes relation describing the material properties of bone from the CT number was used:

$$E = 2875\rho_{app}^3$$

Where E is Young's Modulus, ρ_{app} is apparent density Carter & Hayes (1977). CT numbers 30 and 2000 correspond to ρ_{app} of 0.3 to 1.8 g/cm³

The contact surfaces were matched to ensure node-to-node contact. The contact surfaces were glued and the humeral head was modelled as a rigid semi-sphere. The scapula was cut to size, as carried out in the in-vitro test. The surface nodes of the scapula beyond the scapula neck

were constrained in all 3 axes. The frictional coefficient between the humeral head and glenoid was 0.07 (Anglin et al. 2000). A compressive load of 750 N was applied to the humeral head and a vertical load was applied via head displacement of 11 mm, to generate a load/displacement subluxation curve beyond subluxation. The FE model was tested to mesh convergence.

5.4 Results

5.4.1 Cyclic Results

All implants visibly failed except one (NB5), which only partially failed and the test was stopped after 200,000 cycles. Six (60%) failed exclusively at the implant/cement interface, 2 (20%) failed both at the implant/cement and cement/bone interface and 2 (20%) failed superiorly due to cortical bone failure (table 5.1). Implant failure occurred between 16,300 and 122,500 cycles, with an average (\pm SD) of $80,966 \pm 53,729$ cycles (Fig. 5.4). The earliest specimen to fail was NB10 at 16,300 cycles, which was previously identified as partially sclerotic. NB5 was stopped at 200,000 cycles due to no failure, although some superior and inferior implant/cement distraction was observed and CT scans revealed initial good implant seating. All final CT scans confirmed failure, which were observed visually (Fig. 5.5), however, in 3 specimens (30%) it was difficult to identify which interface loosening was apparent. No significant difference was found between the 3 radial mismatches ($p = 0.05$).

Specimen	Implant size	Cycles to failure	Cause of Failure	CT confirms failure
NB1	Medium	64450	I/C interface inferiorly	✓
NB2	Medium	52220	I/C interface inferiorly	✓
NB4	Small	122500	Superior bone failure	✓ Though failure appears in C/B
NB5	Medium	200075	Some I/C interface inferiorly, no gross failure, test stopped	✓ Though failure appears in C/B
NB6	Large	90770	Superior bone failure	✓ Superior failure not clear
NB8	Small	77890	I/C interface inferiorly	✓
NB9	Small	60050	I/C interface inferiorly	✓ Failure not clear at I/C interface
NB10	Medium	16300	I/C & C/B interface inferiorly	✓
NB11	Medium	105000	I/C interface inferiorly	✓ Superior failure not clear
NB12	Medium	20405	I/C & C/B interface inferiorly	✓

Table 5.1: Results of the cyclic test; number of cycles to failure, nature of failure and confirmation of failure on final CT scans. Note: NB3 and 7 were not tested.

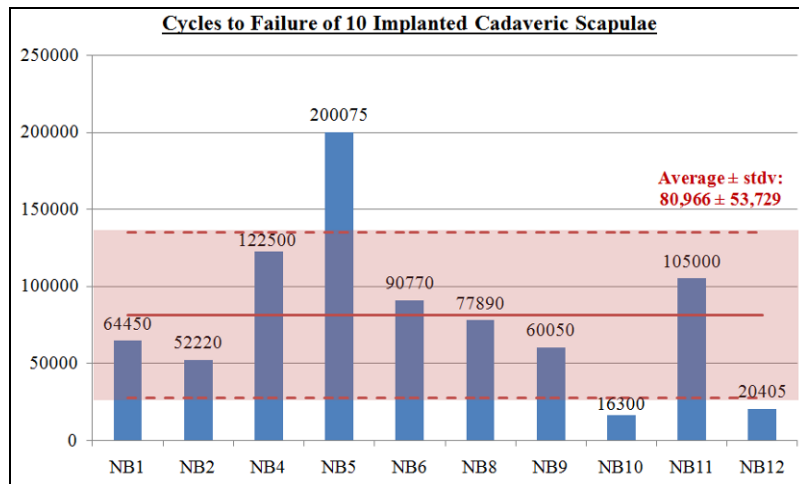


Figure 5.4: Number of cycles to failure. Red solid and dotted lines represent average and upper/lower standard deviations respectively.

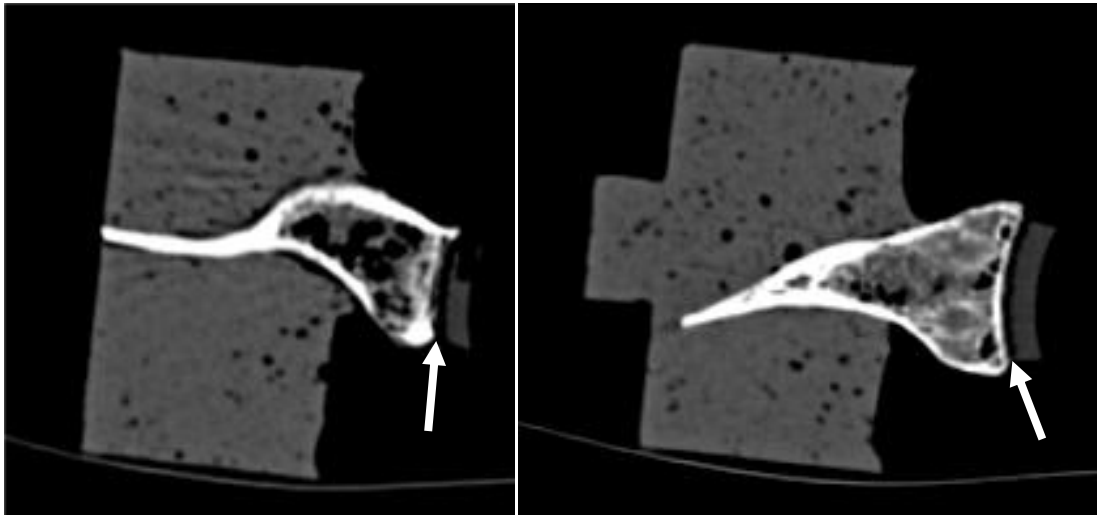


Figure 5.5: CT slices of the transverse plane showing an example of superior (left) and inferior (right) failure at the implant/cement interface in the specimen NB1.

5.4.2 Microscopic Results

The cross-sectional examination of the specimens confirmed clear failure at the implant/cement interface and superior bone crushing, as was observed from gross inspection of unsectioned specimens (Fig. 5.6). The microscopic study revealed the cement thickness varied from 0.5-1.5 mm and was cracked in three specimens at one of the peg junctions where bending stresses are experienced. There were no other apparent cement fractures anywhere else. In one case, the implant completely detached at the implant/cement interface, the cement embedded in the peg grooves were still intact (Fig. 5.7).

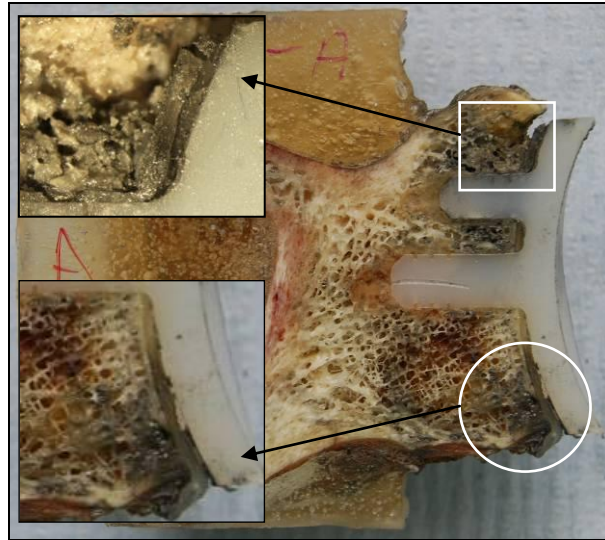


Figure 5.6: Cross-sectional slice of NB1 after failure. Note: inferior failure of the implant/cement (circle) and superior bone crushing (square).

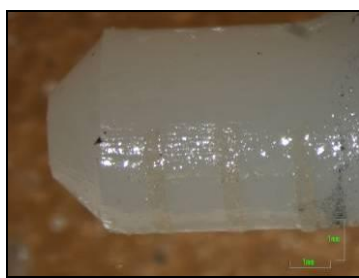


Figure 5.7: One implant detached completely at the implant/cement interface (NB12), the pegs show the cement still intact in the peg grooves.

5.4.3 Finite Element Results

The implant/cement interface normal stress from the predicted FE model showed superior compressive stresses and inferior tensile stresses. Tensile peak stresses were found at the base of the pegs and the tensile stresses peaked at the inferior edge of the implant, within the interface strength of 0-1MPa, predicting inferior failure (Fig. 5.8). The peg interlocking grooves vary the stresses at the interface (Fig. 5.8). High tensile contact stresses are also predicted at the inferior pegs (Fig. 5.9).

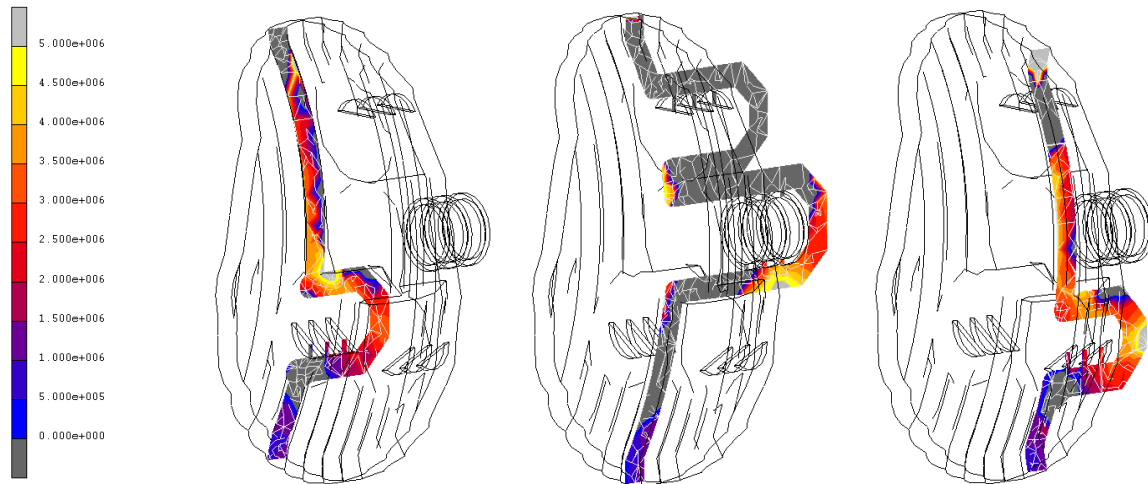


Figure 5.12: Colour plot slices through the pegs of the cement mantle showing principal stress maximum. Note: Dark grey denotes compressive stresses and light grey areas have exceeded 5 MPa.

The cadaveric bone experiences superior compressive and inferior tensile stresses, high stresses are predicted at the scapula neck (Fig. 5.13). The compressive strength of the bone was calculated as 4.6 MPa using the Carter & Hayes formula:

$$S = 51.58\rho^2$$

Where S is the compressive strength in MPa and ρ is the apparent density in g/cm^3 (Carter & Hayes 1977), 0.3 g/cm^3 was used as the lowest apparent density of the cancellous bone found at the first peg (Fig. 5.13).

The 4.6 MPa compressive strength value was calculated using the lowest apparent density of scapula bone in the FE model. Although this does not represent the compressive strength of all the cancellous bone, it is used as a worst-case value. The FE model predicts some cancellous bone at the superior peg insertion exceeds the calculated strength of 4.6 MPa (Fig. 5.13), which was also observed in-vitro (Fig. 5.6).

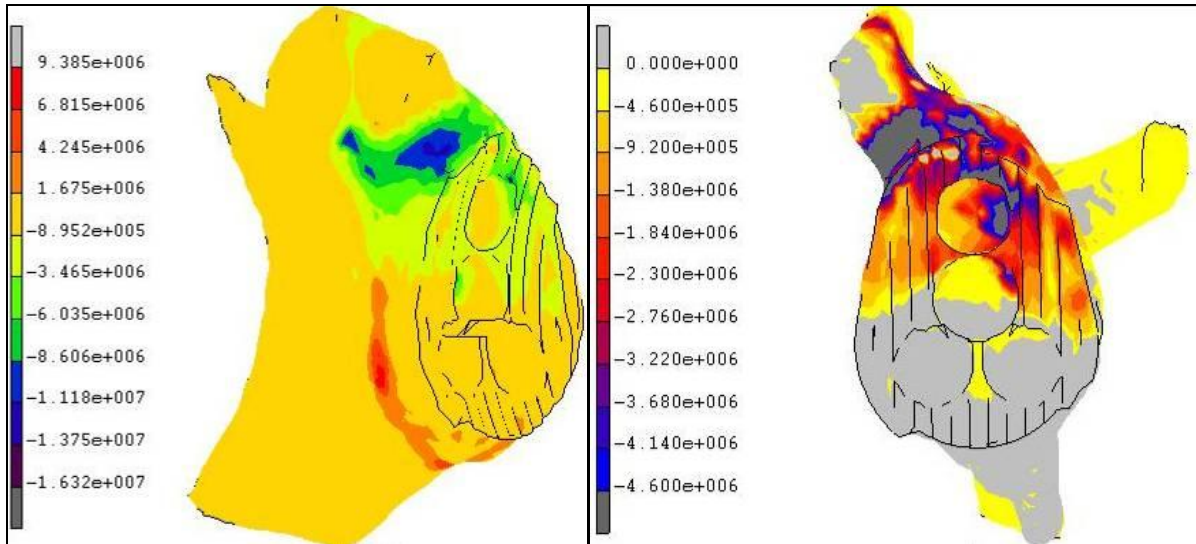


Figure 5.13: Colour plot of the cadaveric bone showing minimum principal stress (compressive stresses) and maximum principal stress (tensile stresses), both compressive and tensile stresses peak around the neck of the glenoid (left). Colour plot of principal stress minimum showing dark grey areas exceeding 4.6 MPa, the predicted compressive strength of lowest cancellous bone (right).

5.4.4 Rim Displacement & Vertical Head Displacement

Due to the relatively thin implant rim (4.7 mm) the reference pin holes in the superior and inferior rim were drilled to a 7-10 mm depth to avoid drilling through to the articulating surface. Due to the compliancy of the polymer implant and the relatively shallow hole, the pins were unable to measure the full range of rim displacements in some of the specimens. However, based on the sinusoidal changes in rim displacements, it was possible to extrapolate some of the measured rim displacement results. A positive correlation was found between vertical head displacement and failure progression (Fig. 5.14). This correlation was significant when comparing displacement at the start of the test and at failure ($p = 0.04$) (Fig. 5.15). A positive correlation was also found between inferior rim displacement and failure progression in 6 specimens, however, in 3 specimens this pattern was not observed and in one case (NB6), rim displacement data at failure was unobtainable. However, the correlation to failure using rim displacement was also significant at the start of the test and at failure ($p = 0.005$) (Fig. 5.15).

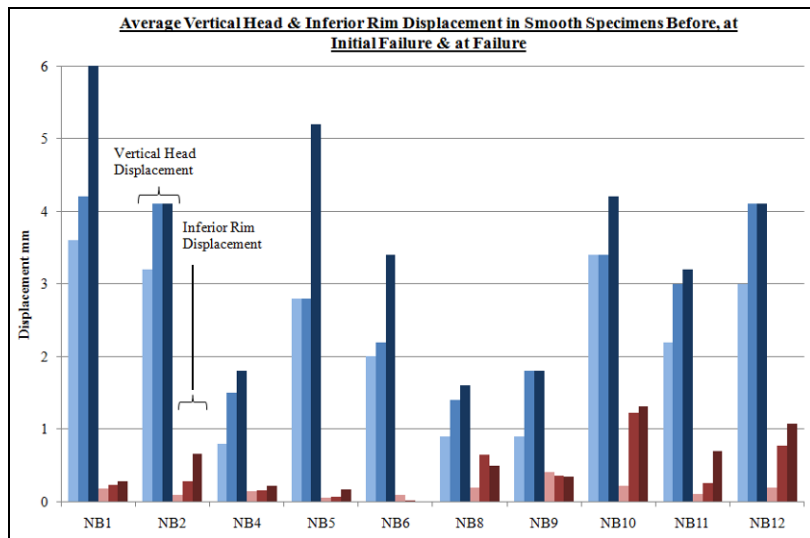


Figure 5.14: Comparison of vertical head displacement and inferior rim displacement with progressive failure.

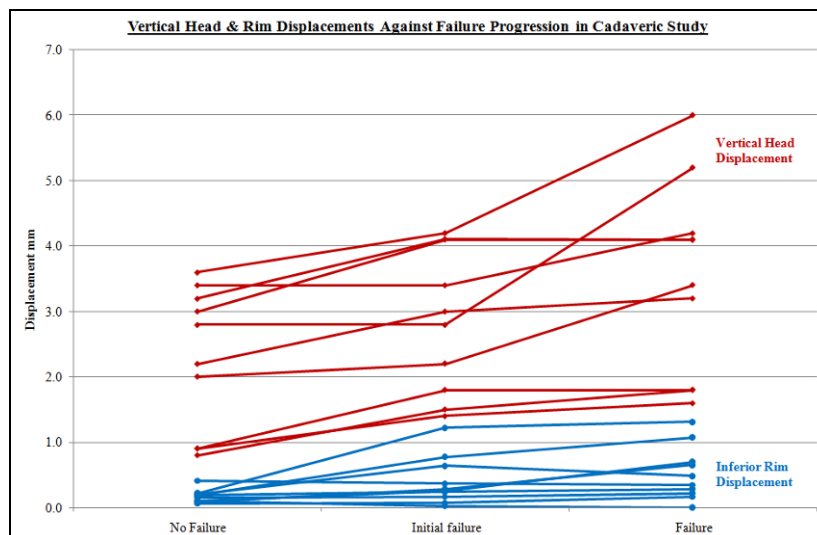


Figure 5.15: Positive correlation between vertical head displacement ($p = 0.04$) and inferior rim displacement ($p = 0.005$) before, at initial failure and at failure.

The initial failure in the CT scans was noticed before visual failure in eight shoulders. In the remaining two, one shows CT and visual failure together and one show visual failure before CT (Appendix F).

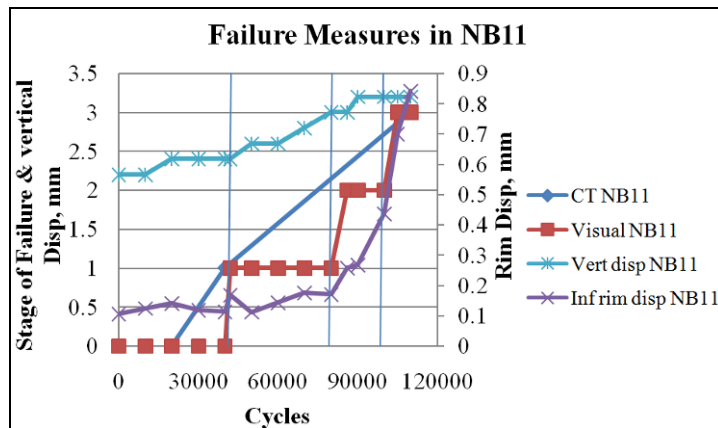


Figure 5.16: A specimen plot of visual and CT failure with inferior rim and vertical head displacement, showing correlation between CT and visual failure and correlation in displacements with CT and visual failure. Note: see Appendix F for failure key.

The vertical head displacement increases with visual failure and CT failure in all 10 specimens. However, inferior rim displacement only correlated in 7 specimens. The inferior rim displacement shows fluctuations throughout testing compared to vertical head displacement, which progressively increases (Appendix F).

5.5 Discussion

This study aimed to test and validate the use of bone substitute foam as an adequate substitute for human scapulae, when testing the mechanical outcome of glenoid implant fixations. Eight out of the 10 (80%) cadaveric scapulae failed inferiorly at the implant/cement interface, of these 8, 2 also failed at the cement/bone. No specimen failed at the cement/bone interface in isolation, however superior bone crushing was observed clearly in 3 specimens. The CT scans indicated failure at the observed interface in 70% of cases and was able to detect failure before or with visual failure in 8 specimens.

Clinical results have indicated predominantly cement/bone failure via radiographic examination. This study has investigated this phenomenon using a standardised in-vitro cyclic test, post-testing microscopic evaluation, FE modelling and monitoring failure both visually and quantitatively. The question of where the fixation is weakest is not a simple one, considering implant roughness, cement interdigitation, cement thickness, wetness of the bone

and bone quality all contributing to the interfacial conditions. Using a smooth implant in this case has demonstrated the fixation is weakest at the implant/cement interface. The FE model indicates stresses exceeding the strength of a smooth PE/PMMA interface.

Clinical studies have similarly shown loosening at the inferior part of the fixation (Klepps et al. 2005; Nagels et al. 2002; Yian et al. 2005). One study by Nyffeler et al. 2003, found a retrieved loosened glenoid had clearly failed at the implant/cement interface (Fig. 5.17), however, most studies (with few retrieved glenoids) indicate failure at the cement/bone interface. The question is why isn't the implant/cement interface observed as loosening clinically?

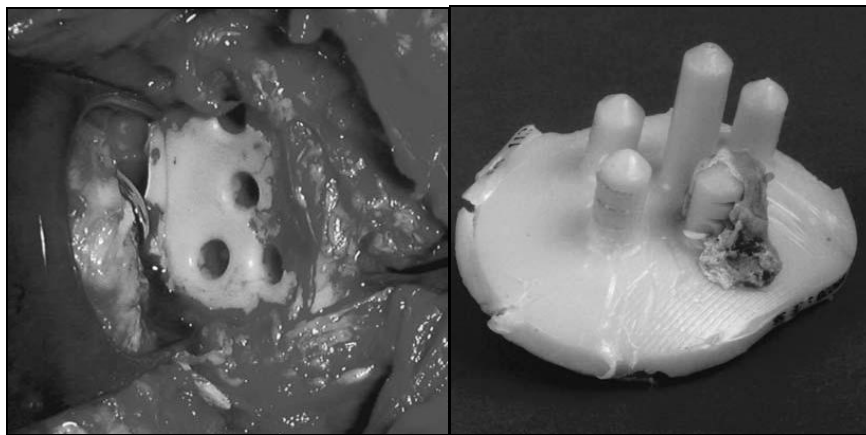


Figure 5.17: Retrieved smooth pegged cemented implant showing clear failure at the implant/cement interface (Nyffeler et al. 2003). Figure reprinted with permission from Journal of Bone & Joint Surgery-British, 2003, 85B, 5, Influence of peg design and cement mantle thickness on pull-out strength of glenoid component pegs, 748-752.

Most clinical studies use radiographs, a common practice to assess the extent of loosening. However, CT has been shown to be better at predicting loosening. Aliabadi et al. (1988) found no correlation between r. lines around the glenoid in radiographs and pain, function and range of motion. Similarly Yian et al. (2005) found no correlation between r. lines observed on plane radiographs and pain, however, a correlation was found between r. lines observed in CT and pain. Likewise, Nagels et al. (2002) found using RSA techniques to monitor glenoid motion and loosening found RSA was better at detecting glenoid loosening compared to radiographs. Thus, although radiographs have been useful to analyse grossly loose implants, monitoring early signs of failure is hit and miss.

Although the causes of failure were primarily found at the implant/cement interface inferiorly, the problem of bone crushing, found in a third of the specimens in this study, will also have a long-term biological impact. One of the drawbacks in this testing method is that the biological element is completely eliminated from the fatigue test. Improving the mechanical fixation of the glenoid implant at the implant/cement surfaces will improve the short to mid-term outcomes of the implant. However, the biological effects will inevitably be one of the primary concerns in long-term outcomes of the fixation. It is at this point that cement/bone interface, initially an excellent mechanical interlocking mechanism, will biologically break down into a fibrocartilage/cement interface. This fibrocartilage layer maybe the cause of the progressive r. lines found in radiographs (Wirth et al. 2001). It is therefore understandable that early static images of the shoulder do not reveal gaps in the implant/cement interface, which would manifest under dynamic movement.

Partial implant embedding superiorly was observed in 6 cases, however, the cross-sections revealed not all embedded implants caused obvious bone crushing. Despite this, embedding affects the subluxation mechanics, possibly exaggerating further the ‘rocking horse affect’, thus by avoiding the implant from embedding the bone will improve the stability and improve the longevity of the fixation. It may simply be a question of implant seating and correct sizing of the implant to align the implant rim with the cortical glenoid rim as also suggested by Iannotti et al. (2005) (appendix E).

There are several drawbacks in this study, firstly, the rim displacements were often difficult to monitor, due to the compliancy of the implant polymer. In some specimens the rim displacements were extrapolated from the data. A positive correlation to failure was found using inferior rim displacement ($p = 0.005$) and vertical head displacement ($p = 0.04$). This further reinforces the use of vertical head displacement to monitor failure. Correlation to CT failure was also found in both measurements. The correlation to CT and visual failure shows a moderate improvement in monitoring failure using vertical head displacement compared to inferior rim displacement. Unfortunately due to the relatively few CT data points compared to the data points in displacements and visual measures, it was not possible to identify whether the larger changes in displacements were directly a result of or preceding failure. More CT scans would be necessary for this analysis. Vertical head displacement best matched visual failure, although this match was not as close as expected. Interestingly, the vertical head

displacement, in some cases, preceded visual failure. This supports the “rocking horse” effect explanation.

Secondly, only one implant design was tested, thus comments regarding design weaknesses and stress raisers are limited to the particular design. However, restricting the test to one design allowed observations on generic parameters to be made such as the apparent weakness of the implant/cement strength using a smooth implant. Although using a smooth implant inevitably weakened the interface, this worst-case scenario is useful to analyse and the most clinically relevant as all companies, with one exception, do not roughen the glenoid implant.

Thirdly, due to the protocol, the specimens were required to be tested and refrozen every 20,000 cycles. Two major concerns were that the long fatigue tests at room temperature and multiple freezing/thawing will cause the mechanical bone properties to deteriorate or change. The effect of freezing has shown to alter the mechanical properties of bone compared to testing fresh bone (Linde & Sørensen 1993). However, testing at room temperature up to 3.5 days has not shown any change in bone strength (Kääb et al. 1998) and multiple freezing of up to 5 times has shown small increases in the stiffness and viscoelasticity, however they were not found to be significant (Linde & Sørensen 1993). This study tested within both limits.

Finally, a cadaveric study of 10 scapulae is a small one. Variability in bone quality, properties and various implant sizes, resulting in variable radial mismatches, makes conclusive remarks more difficult to make. However, successfully testing the cadavers to failure in-vitro has allowed valuable insight into the mechanics of the cemented fixation and the various parameters that contribute to the failure of the fixation.

5.6 Conclusion

Fatigue failure at the implant/cement interface was observed in 6 cadaveric scapulae and 3 failed superiorly in the bone with an average of $80,966 \pm 53,729$ cycles. The variation in glenoid size, and consequently radial mismatch, did not affect the result, although the sample

size was too small to make this finding conclusive. The FE model of one scapula predicted tensile inferior interfacial stresses exceeding the smooth implant/cement interface strength and superior principal minimum stress exceeding the predicted strength of cancellous bone, as observed in-vitro in 3 scapulae, showing bone crushing.

Converting the results in this study from number of cycles to the equivalent in years (30 high loading arm movements/day), it is predicted that 20% of TSAs would fail long-term (> 10 years), 50% would fail mid to long-term (5-10 years) and 30% short to mid-term (< 5 years). The figures in some short to mid-term clinical studies of possible radiographic evidence of glenoid loosening tend to be lower, though figures vary between 15-44% (Aliabadi et al. 1988; Torchia et al. 1997). It is important to note that loosening can be underestimated clinically (Nagels et al. 2002) and most loosened implants are not removed, even with loss of function, unless pain is a serious problem.

Small and large steps currently need to be taken to address these problems. Improving interfacial strengths is an important and relatively time and cost-effective strategy to improve the current TSA outcomes. Addressing the long term biological cement/bone problem by exploring cementless solutions for both osteoarthritic and rheumatoid arthritic shoulders is an equally important step to improve TSA outcomes and to increase the use of TSA.

Inferior rim displacement and vertical head displacement have both shown to correlate to progressive failure. Monitoring rim displacement is technically more difficult to implement compared to the 2D study in chapter 4, highlighting the shortcomings of using this method.

A comparative study of various glenoid designs will require large sample size, which is unobtainable in a cadaveric study. Here the use of a bone substitute with reliable properties is desirable. This study will therefore be an important validation step for the next chapter, investigating design parameters in commercial implants using bone substitute foam as the substrate.

5.7 References

- Aliabadi, P, et al. (1988). Evaluation of a Nonconstrained Total Shoulder Prosthesis, *American Journal of Roentgenology*, 151: 1169-1172.
- Anglin, C, (1999). *Shoulder Prosthesis Testing*, PhD Thesis, Mechanical Engineering, Queen's University, Canada.
- Anglin, C, et al. (2000). Shoulder Prosthesis Subluxation: Theory and Experiment, *Journal of Shoulder and Elbow Surgery*, 9, (2): 104-114.
- ASTM F 2028-02, 2004. Standard Test Methods for the Dynamic Evaluation of Glenoid Loosening or Disassociation. Book of ASTM Standards: 1083-88.
- Carter, D R, & Hayes, W C (1977). The Compressive Behaviour of Bone as a Two-Phase Porous Structure, *Journal of Bone and Joint Surgery, American Volume, American Volume*, 59A, (7): 954-962.
- Frich, L H, et al. (1997). Bone strength and material properties of the glenoid. *Journal of Shoulder and Elbow Surgery*, 6: 97-104.
- Hasan, S S, et al. (2002). Characteristics of Unsatisfactory Shoulder Arthroplasties, *Journal of Shoulder and Elbow Surgery*, 11, (5): 431-441.
- Iannotti, J P, et al. (2005). Prosthetic Positioning in Total Shoulder Arthroplasty. *Journal of Shoulder and Elbow Surgery*, 14, (1S): 111S-121S.
- Kääb, M J, et al. (1998). Changes in Cadaveric Cancellous Vertebral Bone Strength in Relation to Time, *SPINE*, 23, (11): 1215-1219.
- Klepps, S, et al. (2005). Incidence of Early Radiolucent Glenoid Lines in Patients Having Total Shoulder Replacements. *Clinical Orthopaedics and Related Research*, (435), 118-125.
- Krause, W, and Hofmann, A, (1989). Antibiotic Impregnated Acrylic Bone Cements: A Comparative Study of the Mechanical Properties, *Journal of Bioactive and Compatible Polymers*, 4: 345-361.
- Lazarus, M D, et al. (2002). The Radiographic Evaluation of Keeled and Pegged Glenoid Component Insertion, *Journal of Bone and Joint Surgery, American Volume*, 84A, (7): 1174-1182.
- Lewis, G (1997). *Properties of Acrylic Bone Cement: State of the Art Review*, *Journal of Biomedical Materials Research Part B: Applied Biomaterials*. 14: 155–182.

- Lim, D, et al. (2006). The Effect of the Loading Condition Corresponding to Functional Shoulder Activities on Trabecular Architecture of Glenoid, *Journal of Biomechanical Engineering*, 128: 250-258.
- Linde, F, & Sørensen, H C F, (1993). The Effect of Different Storage Methods on the Mechanical Properties of Trabecular Bone, *Journal of Biomechanics*, 26, (10): 1249-1252.
- Mimar, R, et al. (2008). Evaluation of the Mechanical and Architectural Properties of Glenoid Bone, *Journal of Shoulder and Elbow Surgery*, 17, (2): 336-341.
- Nagels, J, et al. (2002). Patterns of Loosening of the Glenoid Component. *Journal of Bone and Joint Surgery, British Volume*, 84B, (1): 83-87.
- Nyffeler, R W, et al. (2003). Influence of Peg Design and Cement Mantle Thickness on Pull-out Strength of Glenoid Component Pegs, *Journal of Bone and Joint Surgery, British Volume*, 85B, (5): 748-752.
- Torchia, M E, et al. (1997). Total Shoulder Arthroplasty with the Neer Prosthesis: Long-Term Results. *Journal of Shoulder and Elbow Surgery*, 6: 495-505.
- Turner, C H, et al. (1999). The Elastic Properties of Trabecular and Cortical Bone Tissues are Similar: Results From Two Microscopic Measurement Techniques, *Journal of Biomechanics*, 32: 437-441.
- Wirth, M A, & Rockwood Jr, C A, (1996) Complications of Total Shoulder-Replacement Arthroplasty. *Journal of Bone and Joint Surgery, American Volume*, 78A, (4): 603-616.
- Wirth, M A, et al. (2001). Radiologic, Mechanical, and Histologic Evaluation of 2 Glenoid Prosthesis Designs in a Canine Model, *Journal of Shoulder and Elbow Surgery*, 10, (2): 140-148.
- Yian, E H, et al. (2005). Radiographic and Computed Tomography Analysis of Cemented Pegged Polyethylene Glenoid Components in Total Shoulder Replacement, *Journal of Bone and Joint Surgery, American Volume*, 87A, (9): 1928-1936.

Chapter 6: Comparison of Design Parameters in

All-Polyethylene Cemented Glenoid Implants

6.1 Abstract

The aims of this study are threefold; to investigate the use of rim displacements and vertical head displacement to monitor failure in commercial implants, to investigate the effects of anchorage design (pegged and keeled), back surface roughness and macro-features on the fatigue failure of glenoid implants and to test the validation of using bone substitute as an adequate model for the human scapula. The ASTM F2028-02 testing standard for glenoid implant cyclic test was used to test a total of 20 implants, testing 4 groups (n = 5); a smooth pegged implant (TOPEL), a smooth keel implant (TOKL), a rough pegged implant (n-S) and a very rough pegged implant (n-R) until failure or 50,000 cycles. All the keel implants failed inferiorly at the implant/cement interface ($33,053 \pm 15,969$ cycles). One smooth pegged implant partially failed at 42,054 cycles at the implant/cement interface, 2 specimens from the rough pegged group partially failed at $40,628 \pm 13,704$ and 5 from the very rough pegged $42,645 \pm 7840$. A change in mode of failure was found in both rough groups where failure occurred at the cement/bone interface superiorly. A positive correlation was found between roughness and number of cycles to initial failure. Bone crushing was clearly observed in 8 specimens. FE analysis predicts similar contact normal stress distribution between the implants and predicts the cement mantle is unlikely to fatigue fail. A positive correlation was found with inferior rim displacement before and after initial failure/failure, as also found with vertical head displacement and initial failure/failure. The pegged implants were better at resisting fatigue failure compared to the keel. The use of macro-features and particularly roughness is important to improve the implant/cement interface strength and fatigue failure. This study suggests a pegged design with macro-features and roughened glenoid back of 7-8 μm roughness would help to improve fatigue characteristics of the glenoid fixation. Both inferior rim displacement and vertical head displacement has proved a viable way of monitoring fatigue failure, however, due to the difficulty and costs of measuring rim displacement, the vertical head displacement should be preferred. The results in this study

shows comparable results to previous cadaveric work and validates the use of bone substitute as a model to test fixation failure of the glenoid implant.

6.2 Introduction

Monitoring failure has been first investigated using a two dimensional method in chapter 4, allowing clear observation and quantitative rim displacements to be measured and a comparison of design parameters. Comparatively, in-vitro design comparisons of commercial implants have so far been indirect. Anglin (1999) utilised the relative change in inferior rim displacement to compare glenoid fixations. Chapter 3 found curve-back produced less relative inferior rim displacements compared to flat-back, as did rough-backed compared to smooth and less conforming compared to conforming.

A natural step would be to use the method developed in chapter 4 to test commercial glenoid implants in bone substitute with the aim of:

- 1) Investigating the loosening behaviour of the glenoid fixation in commercial designs in light of the rim displacement and vertical displacement work in chapter 4.
- 2) Compare the outcomes to the cadaveric study in chapter 5 as an important validation step for using bone substitute.
- 3) Compare the design parameters; keel versus peg, smooth macro-features versus plain rough by comparing two implant designs from two companies.

6.3 Materials & Methods

6.3.1 Specimen Preparation

Twenty polyurethane bone substitute blocks (12.5 pcf) were prepared for implantation (Sawbones Europe, Malmö, Sweden). Four glenoid implant designs were used in the study (n = 5) (Fig. 6.1-6.3 & table 6.1) and were implanted by an experienced shoulder surgeon (T.G.) into the prepared bone substitute blocks. The specimens were cemented into the specimen holder to ensure an excellent fit and minimal specimen movement.

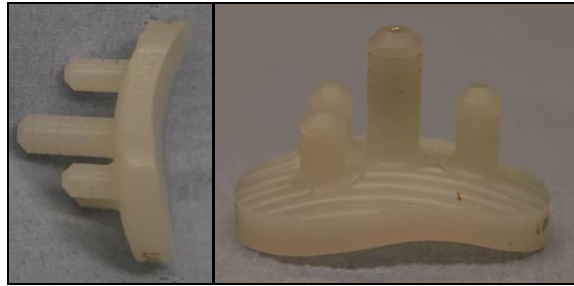


Figure 6.1: TOPEL smooth pegged design with macrostructures.



Figure 6.2: TOKL smooth keeled design with macrostructures. Note: Only large sized implants were tested.

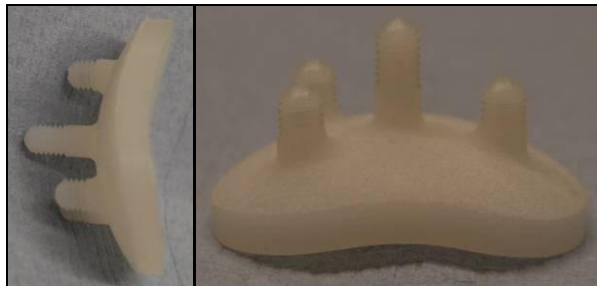


Figure 6.3: n-S/n-R rough pegged design.

Four implants were used for the study testing; three roughnesses, the use of implant grooves along the glenoid back, peg versus keel and two radial mismatches (table 6.1). The roughness was measured in all the specimens of implants C and D. Smooth implants A and B showed consistent roughness due to the manufacturing finish, thus only the roughness of three specimens were measured. The surface roughness was measured using a Talysurf surface profiler (Taylor-Hobson, AMETEK Inc., Pennsylvania, USA).

Table 6.1: Description of glenoid implants tested. Note: Implant C and D are identical except in roughness.

Implant n = 20	Size	Curvature & Radial Mismatch mm	Initial horizontal Moment, Nm (Fig. 4.15)	Design Features	Roughness, μm	Macro- features
A TOPEL1-5	L	32.5, 8.5	2.64	peg	smooth 1.58 ± 0.59	grooves
B TOKL1-5	L	32.5, 8.5	2.07	keel	smooth 1.29 ± 0.24	grooves
C F-S to J-S (s-R)	L	28, 4	2.61	peg	rough 4.43 ± 1.39	none
D A-R to E-R (n-R)	L	28, 4	2.78	peg	very rough 7.67 ± 1.14	none

The horizontal reference holes were drilled to accommodate the reference pins (Fig. 6.4) for the rim displacement measures. Care was taken to avoid penetrating the articulating surface. Some compliance was noted at the insertion sites of the pin, however, as this was consistent in all implants, this did not affect the relative changes in rim displacement.

6.3.2 Mechanical Test

The same standard test was used as described in chapter 4 and 5. A water bath was not used in order to monitor the specimen throughout the test by keeping the LVDTs attached to the specimen (chapter 4), but the articulating surface was kept wet (Fig. 6.4). The same humeral head used in chapter 5, with a radius of 24 mm, was used in all implants, giving a mismatch of 8.5 mm for implants A and B, and a mismatch of 4 mm for implants C and D. The rim displacements were measured every 2000 cycles and vertical head displacement was increased every 5000 when the load dropped below the testing load. Once the subluxation displacement was reached, the specimens were maintained at the same vertical displacement. All specimens were tested to 50,000 cycles or until failure was observed. The same definition of failure used in chapter 5 was used in this study. Initial failure is indicated by visible distraction of the inferior glenoid rim from the cement or bone substitute block. Half failure was defined as the point when the inferior pegs are visible during inferior rim distraction,

where the test was stopped. Half failure is referred in following text as failure or complete failure as the test was stopped.

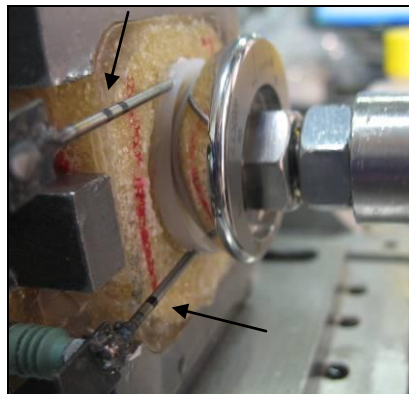


Figure 6.4: Glenoid fixation fatigue testing in bone substitute foam. Reference pins for rim displacement measure indicated by arrows.

Prior to testing, two tests for each type of design TOPEL, TOKL and n-R were tested to sublaxation to derive the 90% sublaxation load for testing (n-S was left out as the design is the same as the n-R implants).

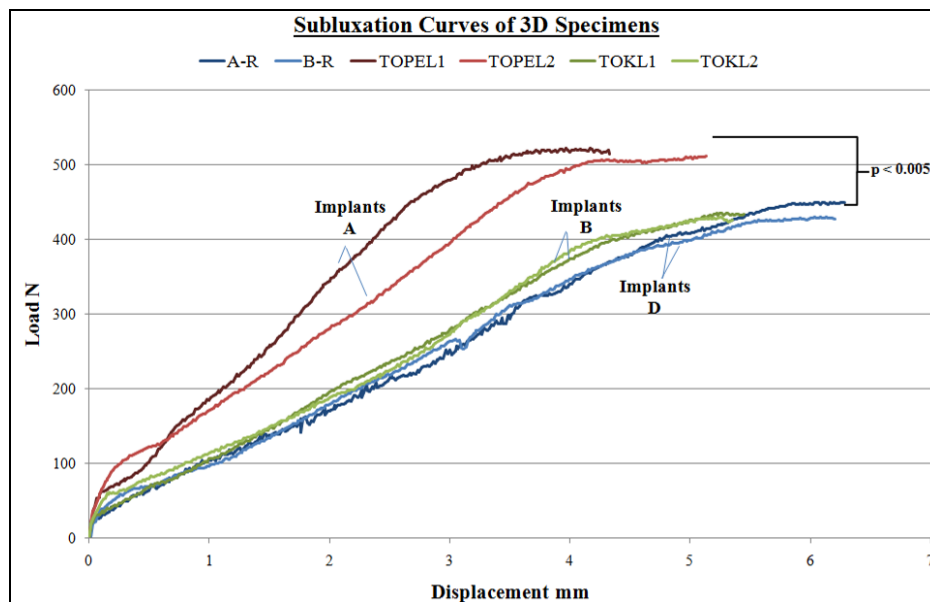


Figure 6.5: Subluxation curve of 3 designs (n = 2), a significant difference in sublaxation loads was found between the smooth peg (TOPEL) and both the smooth keel and rough peg (TOKL and n-R respectively) ($p = 0.005$). Note: TOPEL and TOKL are identical except for the anchorage with peg and keel components used respectively.

The average 90% subluxation load for each implant was 396 N, 390 N and 470 N for implants A-R/B-R, TOKL1/2 and TOPEL1/2 respectively. Despite the high load in the TOPEL implants, it was unclear why the subluxation curves for the identical peg and keel implants should be significantly different, therefore the testing load was chosen at 400 N for a consistent test for all implants. The maximum subluxation displacements for TOPEL, TOKL and n-S/n-R implants were 4.7 mm, 5.3 mm and 6.1 mm respectively. These corresponding displacements were not exceeded during testing to maintain realistic limits.

6.3.3 Finite Element Modelling

FE models were built using company CAD files. As the n-S and n-R implants only differed by surface roughness, three FE models were built, representing implants TOPEL, TOKL and n-S/n-R. The models were built in Marc/Mentat 2001 (MSc Software Corporation, California, USA) using 57,392-123,424 tetrahedral elements. A compressive load of 750 N was applied to the humeral head and a vertical load was applied via a vertical head displacement of 15 mm in order to derive a load/displacement subluxation curve beyond subluxation. The test was modelled as a static problem.

6.4 Results

6.4.1 Mechanical Test

All the smooth keel implant specimens (TOKL1-5) failed inferiorly at the implant/cement interface, with some failure superiorly due to bone crushing, failing at $33,053 \pm 15,969$ cycles. The remaining 3 design groups (15 specimens) did not fail by the end of the test. Failure was defined as the point where the inferior pegs or keel was visible during testing due to implant distraction and initial failure is defined when the implant rim had clearly detached from the cement or bone.

However, one smooth peg specimen began to fail inferiorly at 42,054 cycles (TOPEL5). Two rough peg specimens (G-S and I-S) and 5 very rough peg specimens (A to E-R) began to fail superiorly predominantly at the cement/bone interface at $42,069 \pm 8559$ cycles (Fig. 6.6).

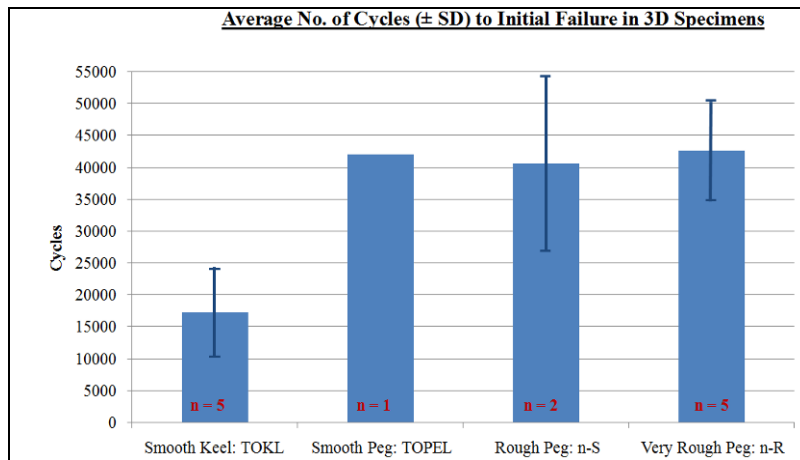


Figure 6.6: Average number of cycles at initial failure, showing a marked difference between the smooth keel specimens to all three peg groups.

6.4.2 Peg Versus Keel

All 5 keel specimens failed at the implant/cement interface inferiorly, with failure also observed superiorly due to bone crushing. None of the peg implants failed completely, regardless of roughness.

Initial failure was observed in 7 pegged implants; 6 of the rough and very rough implants showed initial failure superiorly at the cement/bone interface due to excessive rim movement and bone crushing and 1 of the smooth peg implants showed the start of failure inferiorly, at the implant/cement interface. Comparing initial failure between the four groups showed significant difference between the keel implants and all three peg implant groups ($p < 0.05$) (Fig. 6.6).

6.4.3 Surface Roughness

Only the ‘smooth’ keel (TOKL) and peg (TOPEL) implants with a roughness of $1.29 \pm 0.24 \mu\text{m}$ and $1.58 \pm 0.59 \mu\text{m}$ respectively showed failure occurring at the implant/cement interface inferiorly in 6 implants. None of the roughened implants, regardless of roughness, failed at the implant/cement interface inferiorly, however, a change in mode of failure was observed, with initial failure occurring superiorly at the cement/bone interface.

6.5 Radial Mismatch

The radial mismatch was a compounding variable with surface roughness, only the keeled implants with 8.5 mm mismatch failed completely (smooth) via interface failure, while the 4 mm (rough) implants did not fail at the interface. It is also not clear whether the difference in failure outcomes was also due to the keel design as 4 out of the 5 peg implants with 8.5 mm mismatch showed no sign of failure.

The change in vertical head displacements at the start of the test and at initial failure in the 8.5 mm group (0.84 mm & 0.08 mm) were significantly lower ($p < 0.05$) than the 4 mm group (2.52 mm & 1.46 mm) (Fig. 6.8). However, no significant difference was found in the inferior rim displacements between the two groups at the start of the test, although the displacements were significantly higher for the 8.5 mm mismatch at initial failure ($p < 0.05$). As the 4 mm group were also the roughened implants and the 8.5 mm group were only the smooth group, it is not clear whether it is mismatch or roughness that causes these displacement differences.

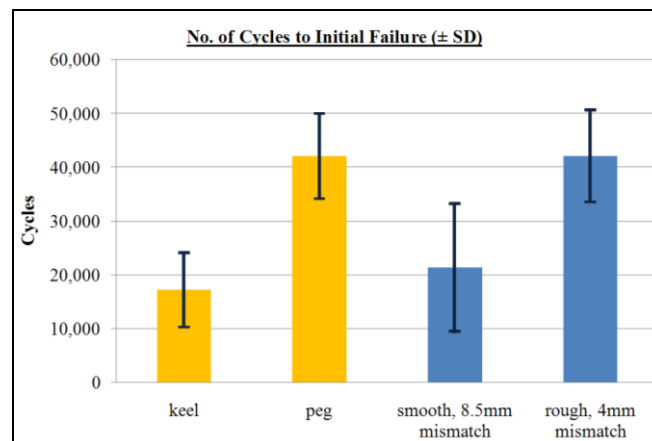


Figure 6.7: Design comparison shows marked differences between the keel & peg, the smooth, 8.5 mm mismatch & rough, 4 mm mismatch.

6.5.1 Rim Displacement & Vertical Head Displacement

An increase in vertical head displacement and inferior rim displacement was found with progressive failure in the smooth keel (TOKL) group. The peg groups did not reach the level Failure Characteristics of All Polyethylene Cemented Glenoid Implants in TSA

of failure to end the test, however a positive correlation was found before failure and at initial failure (Fig. 6.8). Changes in vertical head displacement and inferior rim displacement were not significantly different in the specimens where failure did not occur ($p = 0.05$) (Appendix G).

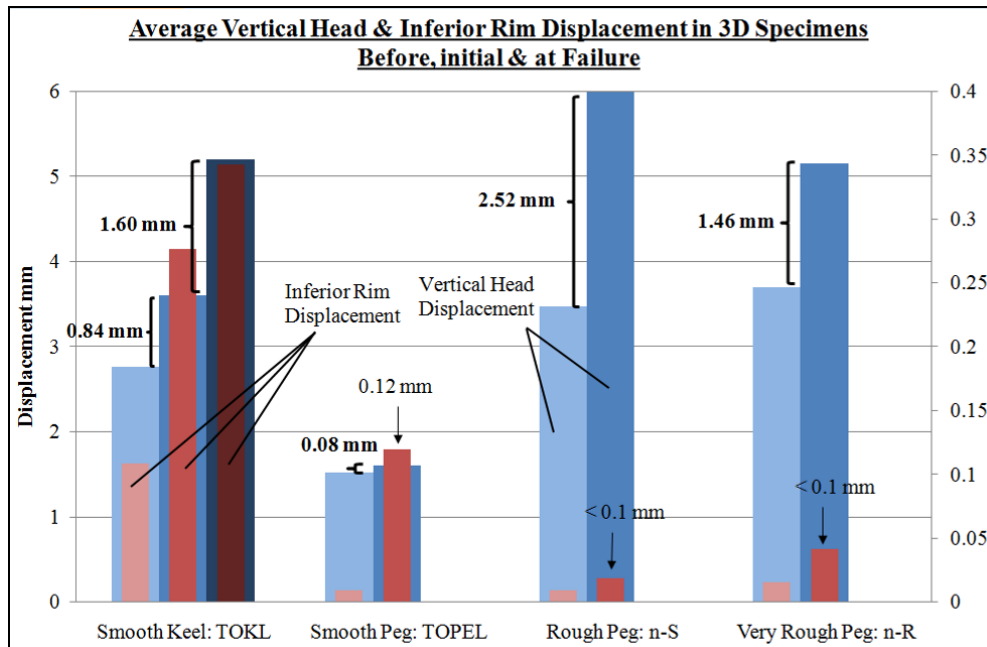


Figure 6.8: An increase in both vertical and inferior rim displacement with progressive failure in the smooth keel (TOKL) group. Note: the remaining groups did not reach complete failure.

6.5.2 FE Validation

The load comparison between FE and in-vitro subluxation curves were between 84-94% and the displacement comparison were between 77-90% (Fig. 6.9). Calculating 90% of the subluxation load, the FE and in-vitro results show load convergence between 88-94%.

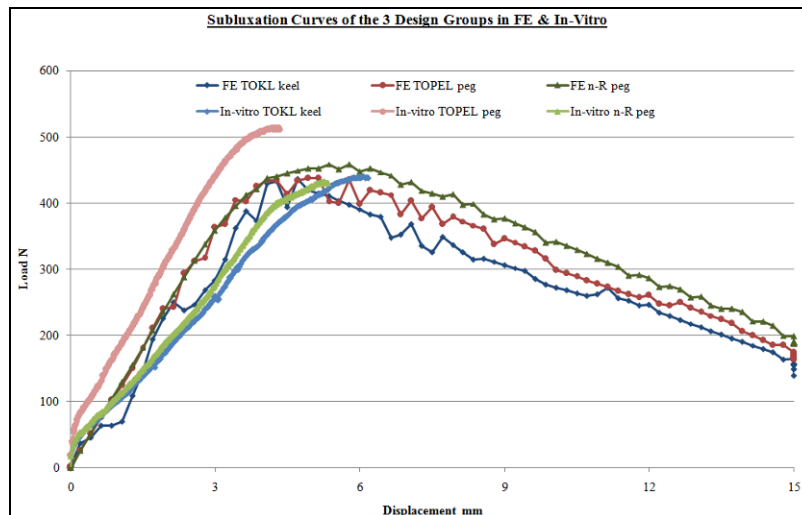


Figure 6.9: FE & in-vitro subluxation curves of the three implant designs. Loads at 90% subluxation showed good correlation in all implants (5.7-12.3% difference).

6.5.3 FE Analysis

The FE predicted stresses normal to the implant/cement were within the strength range of 0-1 MPa for ‘smooth’ PE ($< 1 \mu\text{m}$) (Sanghavi et al. 2007a) in the TOPEL and TOKL models, and predict stresses below the implant/cement strength of greater than 1 MPa in surface-roughened PE ($> 2 \mu\text{m}$) in the n-S/n-R FE model (Sanghavi et al. 2007a) (Fig. 6.10 & 6.11). The stresses normal to the cement/bone interface were below the cement/bone interface strength of 2.32 ± 0.54 MPa (Sanghavi et al. 2007b) in all three implants (Fig. 6.12 & 6.13). Despite the colour plots predicting higher implant/cement interface stresses inferiorly in the n-S/n-R model compared to the TOKL and TOPEL models, the increased strength of the implant/cement interface in roughened PE means that the FE models predict failure in the implant/cement interface in the TOKL and TOPEL implants.

The cement mantle demonstrates tensile stresses inferiorly and superiorly, and compressive stresses around the keel and peg areas (Fig. 6.14). The superior tensile stresses reaches above 5 MPa, the lowest published endurance limit (Lewis 1997) in all the implants. Thus predicting the problem of cement fatigue is not a concern in the short and mid-term outcome of the fixation.

The principal stress minimum plots of the bone substitute foam predict high compressive stresses superiorly. Implant n-S/n-R shows stresses close to the bone substitute compressive

strength of 3.9 MPa (Fig. 6.15). Bone crushing and excessive implant movement was observed in most of the n-S/n-R implants in-vitro. Although bone crushing was observed in the TOKL implants, the FE model predicts stresses lower than the compressive strength, however, the FE analysis models the initial testing conditions, where the interfaces are intact and the vertical head displacement have not been adjusted.

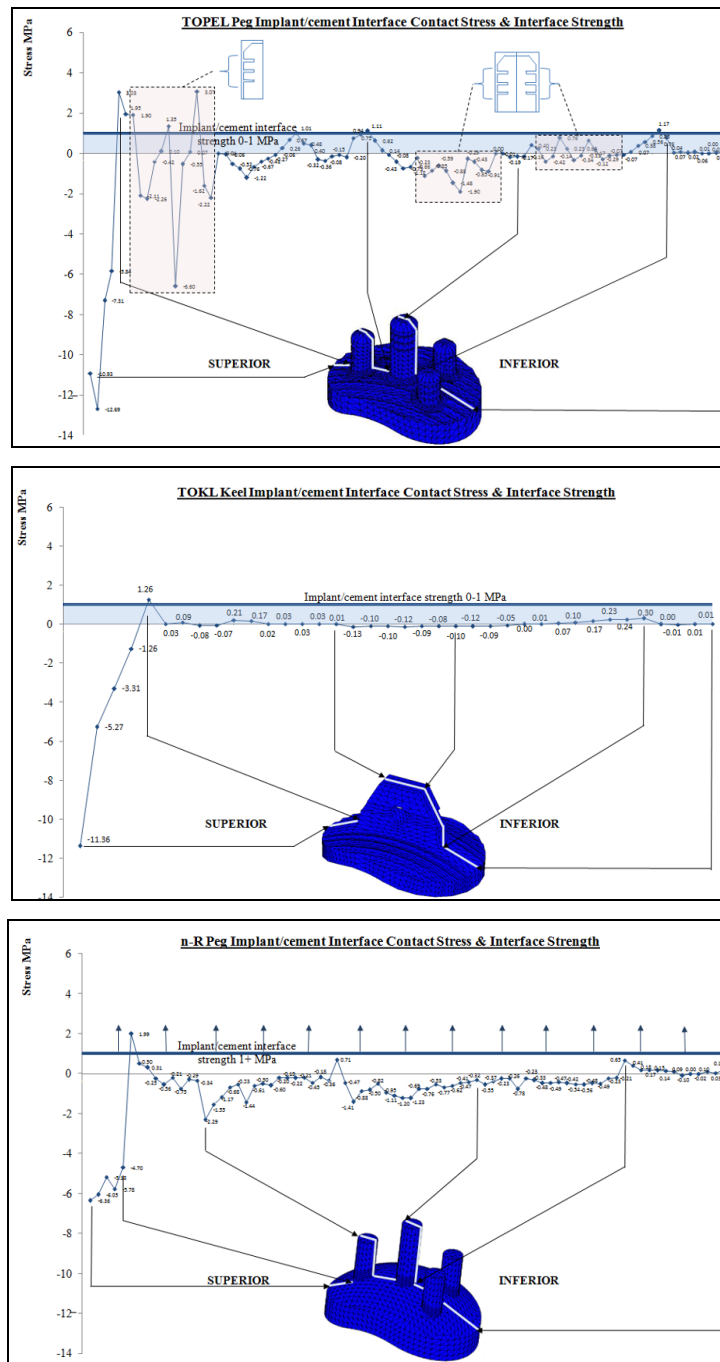


Figure 6.10: FE contact stresses in the superior/inferior direction at the implant/cement interface for TOPEL, TOKL and n-S/n-R implants respectively.

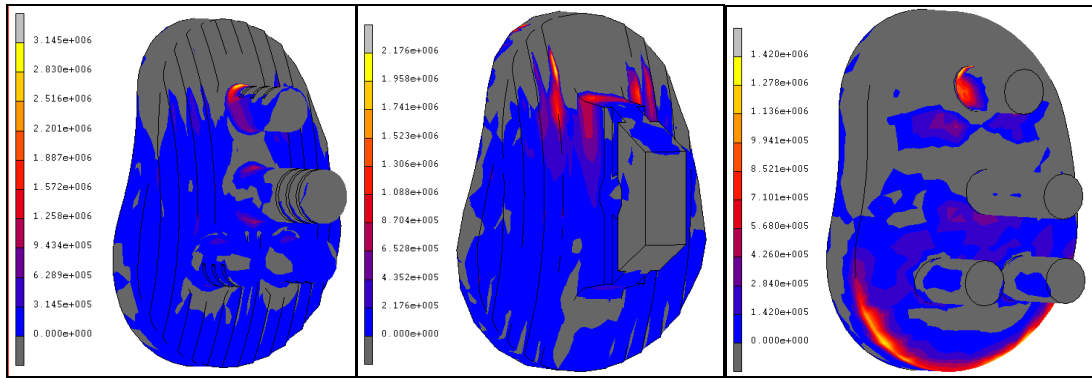


Figure 6.11: Tensile normal contact stress plot at the implant/cement interface for TOPEL (left), TOKL (middle) and n-S/n-R (right) implants. Note: Dark grey denotes compressive stresses.

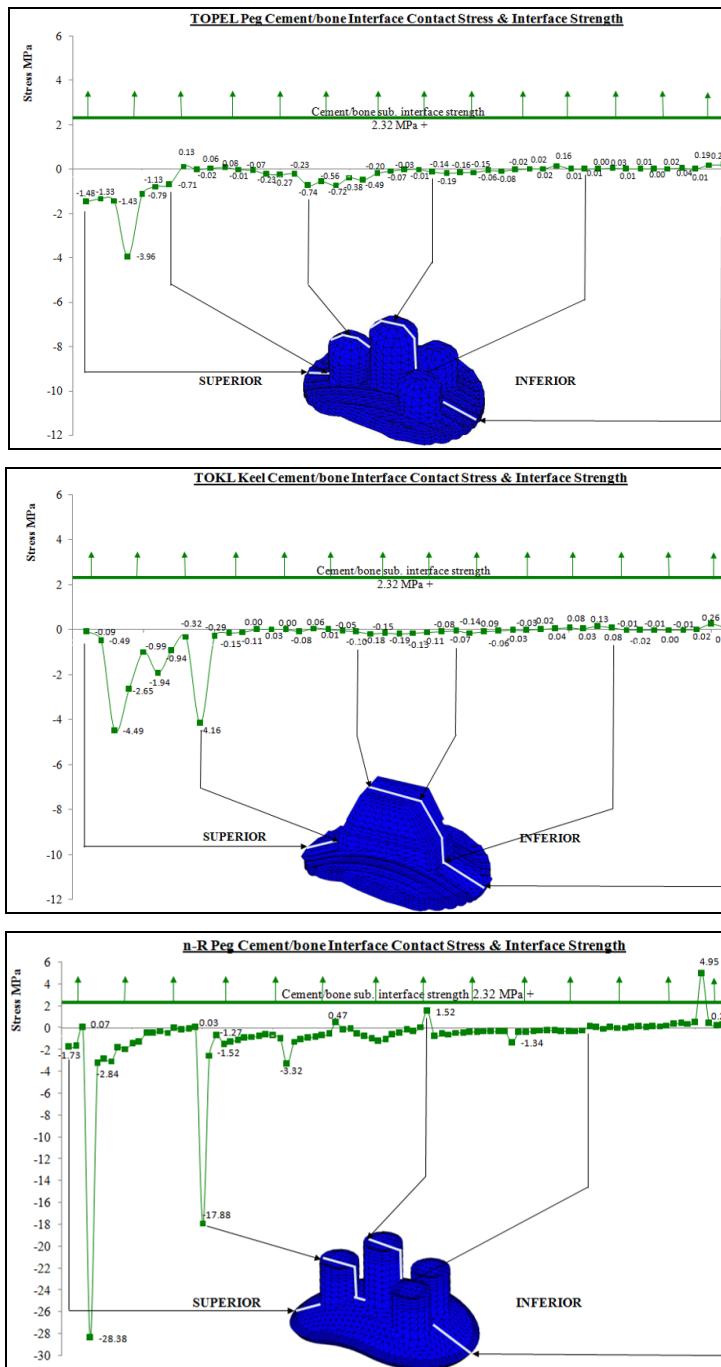


Figure 6.12: FE contact stresses in the superior/inferior direction at the cement/bone interface for TOPEL, TOKL and n-S/n-R implants respectively.

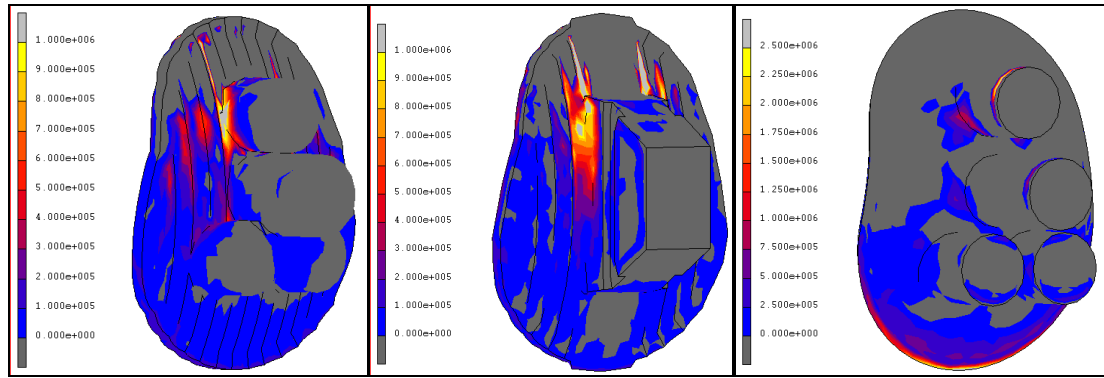


Figure 6.13: Tensile normal contact stress colour plot at the cement/bone interface for TOPEL (left), TOKL (middle) and n-S/n-R (right). Note: Dark grey denotes compressive stresses.

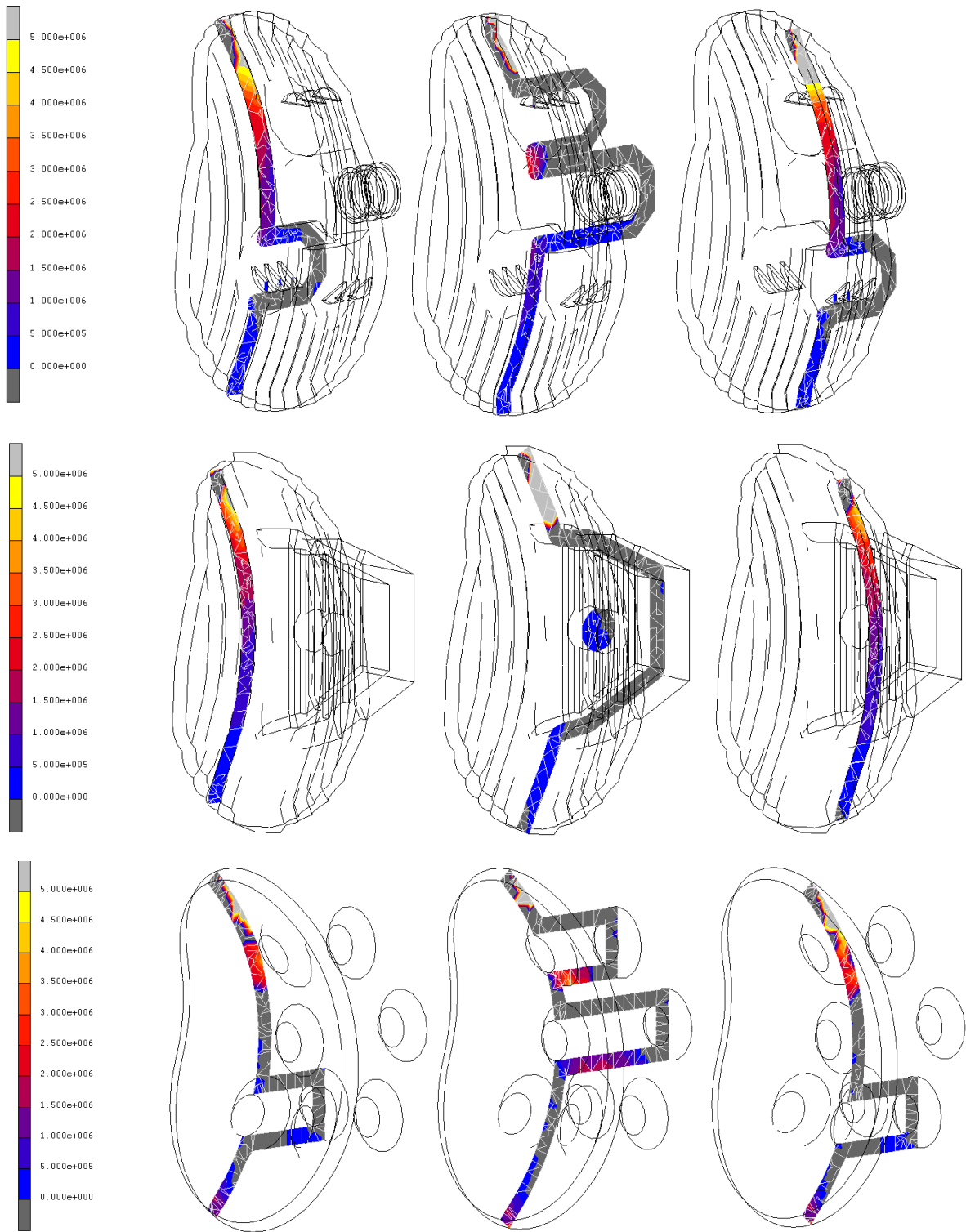


Figure 6.14: Colour plot slices of the cement mantle for TOPEL (left), TOKL (middle) and n-S/n-R (right) implants showing principal stress maximum (tensile stresses). Note: Dark grey denotes compressive stresses and light grey areas have exceeded 5 MPa.

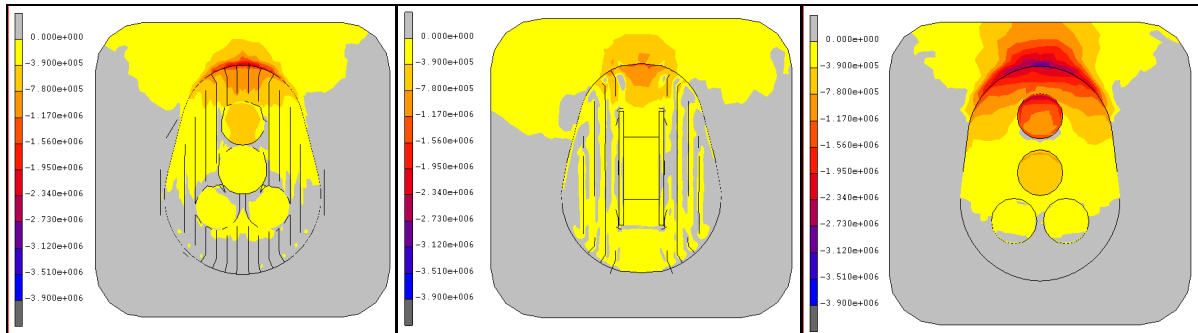


Figure 6.15: Colour plot of bone substitute for TOPEL (left), TOKL (middle) and n-S/n-R (right) implants showing principal stress minimum (negative or compressive stresses). Note: Light grey denotes tensile stresses.

6.6 Discussion

Thus far there are no published results on in-vitro simulated failure of glenoid implants. This study has tested three implant designs to 50,000 cycles, showing failure in 5 implants, initial failure in a further 6 implants and no failure in 9 implants, allowing some limited discussion on implant design parameters. CT scans of the specimens may reveal initial failure in the non-failed implants. The results from chapter 5 indicate that this is likely. This would help further in identifying failure differences (if any) of the 4 implant groups that have not been noticed visually.

6.6.1 Peg Versus Keel

The two identical implants except for the anchorage design in the TOPEL (peg) and TOKL (keel) cases showed the keel design to perform worse than the peg as all 5 keel implants failed compared to only one pegged implant, which partially failed. Despite this, the FE implant/cement interface plots Fig. 6.10 do not show any marked changes between the designs to indicate the keel design would perform poorly. However, there may be several reasons for this. Firstly there was a discrepancy in the in-vitro results from the subluxation tests between the TOPEL pegged implants, which demonstrated higher loads and displacements compared to the TOKL keel, despite having identical surface geometry (Fig. 6.9), indicating a stiffer implant. This discrepancy is not evident in the FE model where subluxation load and displacement were comparable to the TOKL design. Due to this

difference, the starting displacement for the TOPEL design was lower (1.52 ± 0.18 mm) compared to the other two designs (2.76 ± 0.93 mm & 3.59 ± 0.40 mm). This may be the reason why all the TOKL keel implants failed and only one TOPEL pegged implant began to fail by 50,000. It may also be that the keel design is insufficient as a structure to provide good mechanical interlocking with the bone cement. Only one notch either side of the keel is found to provide cement anchorage, the remaining keel is left smooth (roughness of 1.29 ± 0.24 μm). Comparatively, the TOPEL pegged design features three slots on each peg for cement interlocking, running circumferentially around the central peg and partially around the remaining three pegs (Fig. 6.1). This may have further improved the pegged implant's resistance to failure. However, all designs were tested to the same 400 N load, which reflects the idea that the muscular forces on the shoulder joint are the same, regardless of the implant.

The results in this study is confirmed by other studies as mentioned in previous chapters, Nuttall et al. (2007) found the pegged implants provided better stability. Anglin et al. (2001) found the pegged implants produced less inferior rim displacements compared to the keel, although no failure occurred in both designs. Finally, a clinical study found pegged implants produced less r. lines compared to keeled glenoids (Gartsman et al. 2005).

On the other hand, it is important to note other factors affecting the outcome and use of pegged versus keeled implants. For example, the choice of keel is often reserved for glenoids with poor bone stock or poor exposure during surgery (Lazarus et al. 2002), therefore introducing a bias towards pegged implants as they are usually implanted into relatively healthy bone. Lacroix et al. (2000) also highlight the importance of the bone quality, predicting the keel design to perform better in RA quality bone compared to a pegged implant. Lazarus et al. (2002) in a clinical study concluded pegged glenoids provided better stability and produced less r. lines compared to keeled, however the authors also commented on the pegged implants providing a thinner cement mantel and therefore may lower the level of bone necrosis due to cement heating as well as being a better implant to analyse on radiographs. Therefore the choice of peg can also be a technical one. In fact, the choice between using a pegged or keeled implant is often left to the preference of the surgeon.

6.6.2 Surface Roughness & Macro-Features

Anglin (1999) demonstrated almost immediate failure in two completely smooth implants with no macro-features, whereas implants that were smooth with macro-features or implants with a roughened surface withstood testing to 100,000 cycles without failure. Nyffeler et al. (2003) in pull-out peg tests using cadaveric bone found smooth peg had considerably lower pull-out strengths compared to roughened, notched or threaded pegs. This study confirms these findings and further investigates the relationship between roughness and failure. This further explains why almost immediate failure was found in the 2D smooth implants in chapter 4, which had no macro-features, compared to the smooth implants in this study, which had macro-features and therefore did not fail immediately.

The range of roughnesses used in this study has provided further information on the relationship between roughness and resistance to failure, showing a positive linear correlation. Out of the 10 smooth implants, 5 failed and 1 partially failed, compared to no failures of the 10 rough implants and 7 partial failures. The mode of failure also changed from failure at the implant/cement interface inferiorly in the smooth case due to tensile/shear failure, to cement/bone interface failure superiorly in the rough cases due to bone crushing and excessive superior head translation. The results from this study reinforces the argument that the back surface of the glenoid implant should be roughened, suggesting a surface roughness of 7-8 μm and the use of notches and macro-features to improve cement interlocking and the implant/cement interface strength.

6.6.3 Radial Mismatch

The change in radial mismatch was compounded by the roughness variable, where the 8.5 mm mismatch were the smooth TOKL and TOPEL designs and the 4 mm mismatch were the roughened n-S/n-R designs. The differences in fatigue performances in this study are possibly more influenced by roughness and not radial mismatch, since the 2D study has shown roughness to have the most significant affect on the fatigue performance. Furthermore, Terrier et al. (2006) found small changes in cement stresses and cement/bone shear stresses between mismatches 1-10 mm in an FE study of glenoid conformity. Walch et al. (2002) found a radial mismatch of more than 5.5 mm produced lower r. lines than implants with a mismatch of 5.5 mm or less, recommending a mismatch of 6-10 mm. A clinical study by

Yian et al. (2005) found the 2 out of 47 TSA shoulders where the loosened glenoid was revised had a radial mismatch of 0 mm. Thus there is a consensus that a small radial mismatch will adversely affect the glenoid fixation. The results in this study has shown the smooth implants with a higher mismatch (8.5 mm) fail before the more conforming, roughened designs (4 mm mismatch), perhaps further indicating the importance of surface roughness over conformity. Finally, the FE stress plots do not indicate major differences, although the n-S/n-R 4 mm mismatch shows higher superior bone stresses and higher inferior contact stresses at the implant/cement interface.

6.6.4 Rim Displacement Versus Head Displacement

An increase in superior and inferior rim displacement with number of cycles is confirmed by comparable data from Anglin (1999) and Oosterom et al. (2004) (table 6.2), particularly the rim displacements at the start of testing. At failure, TOKL shows inferior displacements, which are almost triple the displacements found in the literature with displacements (\pm SD) of 0.343 (\pm 0.0747), compared to 0.125 (\pm 0.125) and 0.05 (\pm 0.05) (table 6.2). Since failure was observed in the studies presented in this thesis, the rim displacements after testing are understandably more than other published work, where failure was not observed. The superior rim displacements also show comparable data with displacements before and after testing, although this study showed higher superior displacements at end of testing (table 6.2) due to the occurrence of visible failure and periodically increasing the head displacement to maintain testing loads, which was not done by previous published studies.

Table 6.2: Comparison of superior and inferior rim displacements before and after testing or after failure with published data, showing comparable data between studies.

Rim displacement mm (\pm SD)	Anglin (1999) Implant C, 33 mm CB keel, n = 3	Oosterom et al. (2004) 29 mm CB keel, n = 5	This study 32 mm CB keel, n = 5
Superior before testing	0.29 (\pm 0.317)	0.27 (\pm 0.07)	0.265 (\pm 0.154)
Superior after testing	0.383 (\pm 0.433)	0.37 (\pm 0.06)	0.498 (\pm 0.133)
Inferior before testing	0.107 (\pm 0.167)	0.01 (\pm 0.05)	0.108 (\pm 0.104)
Inferior after testing	0.125 (\pm 0.125)	0.05 (\pm 0.05)	0.343 (\pm 0.0747)

A positive correlation was found between number of cycles and vertical head displacement, as well as between number of cycles and inferior rim displacement. This correlation was significant between start of test and failure in the failed implants, as well as between the start of the test and initial failure in the partially failed implants. An important point to note is that for the implants that did not fail, no significance was found between changes in displacements between the start and end of the test, which further proves the usefulness of using rim or vertical displacements in monitoring fatigue failure.

6.6.5 Cadaveric Versus Bone Substitute

The cadaveric study in chapter 5 used the TOPEL smooth pegged design in all the specimens and found failure at the implant/cement interface, occurring in $80,966 \pm 53,729$ cycles. Only 2 specimens failed at less than 50,000 cycles, one of which was sclerotic. Comparing the cadaveric results to this study where only 1 TOPEL specimen partially failed at the cement interface, shows a very similar trend. The failed TOKL implants at the implant/cement interface in this study further reinforces the similarities in mode of failure between using scapula bone and bone substitute in testing the glenoid fixation. Although testing the implants in bone substitute to 100,000 cycles would give a more complete comparison, these early results strongly indicate the validity of using the Sawbones 12.5 pcf bone substitute.

6.6.6 In-Vitro Test

There are clearly several limitations with this study, firstly, the test was only carried out to 50,000 cycles due to time constraints, the equivalent of just less than 5 years of 27 high loading arm movements per day. Ideally the test should be carried out to 100,000 cycles, the equivalent of approximately 10 years. The result is not all the implants have failed with some showing no failure. However, this has helped to further study of the changes in rim and head displacements in implants that did not fail to failing implants and whether these changes are different between the two groups. This particular discussion is further explored in chapter 7.

Secondly, only two implant designs were tested; anchorage design and roughness/macro-features. Testing radial mismatch, various macro-features and flat-back/curved-back designs would be useful to expand this design study. Thirdly the radial mismatch in this study was a confounding variable with roughness, however, the study from chapter 4 indicates no

significant difference between 1 mm and 5 mm mismatch, in fact, other studies imply a less conforming design will improve resistance to loosening, thus indicating roughness to be the dominating factor. The smooth/rough parameter was also confounded by the peg/keel designs, making the roughness comparison more difficult. However, the interfacial failures in the smooth implants support the failure results in chapter 3, 4 and 5, and therefore shows roughness improves the implant/cement interface strength, which may possibly lead to a better performing implant.

The difficulty in locating screw holes and attaching the reference pins made measuring the rim displacement problematic. This further reinforces the argument that head displacement changes should be used to monitor the fixation in fatigue testing. However, this can only be adopted if the testing load is monitored and maintained, therefore requiring the head displacement to be changed.

Finally, the failure in the roughened implants suggests a different failure mode superiorly, perhaps highlighting another obvious problem in the fixation. This may be the case, although how the humeral head displacement changes with fatigue in-vivo is unknown. Although physiological in-vivo loads were used in this in-vitro test, increasing the humeral head displacement to maintain the testing load has allowed the glenoid implant to be tested beyond the displacement limit in-vivo where the head would be resisted by surrounding muscular tissue, ligaments and tendons and will restrict head movement. This was a limitation of the testing standard from the beginning and should not be forgotten. However, this test aims to test the implant in aggressive, yet physiologically viable conditions, which is why the head displacement in this study was not tested beyond the subluxation displacement limit.

6.7 Conclusion

Testing three implant designs (pegged, keeled and roughened) to 50,000 cycles found the pegged implants were better at resisting failure, with only the keel implants failing inferiorly at the implant/cement interface. Macro-features and roughness improves fatigue performance. A positive correlation was found between increase in roughness and number of cycles to

failure and roughnesses of more than 3 μm changes the mode of failure to superior cement/bone failure, recommending a roughness of 7-8 μm . Thus the data confirms the design conclusions from the 2D study in chapter 4 and FE models between the 2D and 3D cases show comparable implant/cement contact stresses (appendix G). Finally, the use of bone substitute shows comparable results to fatigue tests in cadaveric bone (chapter 5) and justifies the use of bone substitute in investigating glenoid implant fatigue failure, particularly where larger sample numbers are needed.

6.8 References

- Anglin, C, (1999). *Shoulder Prosthesis Testing*, PhD Thesis, Mechanical Engineering, Queen's University, Canada.
- Anglin, C, et al. (2001). Loosening performance of cemented glenoid prosthesis design pairs. *Clinical Biomechanics*, 16: 144-150.
- ASTM F 2028-02, (2004). Standard Test Methods for the Dynamic Evaluation of Glenoid Loosening or Disassociation. Book of ASTM Standards: 1083-88.
- Gartsman, G M, et al. (2005). Radiographic Comparison of Pegged and Keeled Glenoid Components. *Journal of Shoulder and Elbow Surgery*, 14, (3): 252-257.
- Lacroix, D, et al. (2000). Three-Dimensional Finite Element Analysis of Glenoid Replacement Prostheses: A Comparison of Keeled and Pegged Anchorage Systems. *Transactions of the ASME*, 122: 430-436.
- Lazarus, M D, et al. (2002). The Radiographic Evaluation of Keeled and Pegged Glenoid Component Insertion, *Journal of Bone and Joint Surgery, American Volume*, 84A, (7): 1174-1182.
- Lewis, G (1997). *Properties of Acrylic Bone Cement: State of the Art Review*, *Journal of Biomedical Materials Research Part B: Applied Biomaterials*. 14: 155–182.
- Nuttall, D, et al. (2007). A Study of the Micromovement of Pegged and Keeled Glenoid Components Compared Using Radiostereometric Analysis. *Journal of Shoulder and Elbow Surgery*, 16, (3): 65S-70S.
- Nyffeler, R W, et al. (2003). Influence of Peg Design and Cement Mantle Thickness on Pull-out Strength of Glenoid Component Pegs, *Journal of Bone and Joint Surgery, British Volume*, 85B, (5): 748-752.
- Oosterom, R, et al. (2004). Effect of Joint Conformity on Glenoid Component Fixation in Total Shoulder Arthroplasty. *Proceedings of the Institution of Mechanical Engineers*, 218, Part H: Journal Engineering in Medicine, 339-347.
- Sanghavi, S, et al. (2007a). Glenoid Bone-PMMA Interface Tensile Strength. Pending submission.
- Sanghavi, S, et al. (2007b). Glenoid Bone Substitute-PMMA Interface Tensile Strength. Pending submission.

- Terrier, A, et al. (2006). Influence of glenohumeral conformity on glenoid stresses after total shoulder arthroplasty. *Journal of Shoulder and Elbow Surgery*, 15, (4): 515-520.
- Walch, G, et al. (2002). The Influence of Glenohumeral Prosthetic Mismatch on Glenoid Radiolucent Lines - Results of a Multicenter Study. *Journal of Bone and Joint Surgery, American Volume*, 84A, (12): 2186-2191.
- Yian, E H, et al. (2005). Radiographic and Computed Tomography Analysis of Cemented Pegged Polyethylene Glenoid Components in Total Shoulder Replacement, *Journal of Bone and Joint Surgery, American Volume*, 87A, (9): 1928-1936.

Chapter 7: In-Vitro Measurements and their Correlation to Failure

7.1 Abstract

The glenoid fixation fatigue testing Standard specifies the use of rim displacements to monitor the behaviour of the fixation. Studies so far have not been able to observe or monitor glenoid implant failure. The aim of this study is to investigate fatigue failure in glenoid implants in-vitro as defined by the standard, investigate rim displacement measures and vertical head displacement and their relation to failure progression and to investigate the use of bone substitute as a viable substitute for scapula bone. The investigation was divided into three studies: studying the problem using custom-made 2D designs in bone substitute (n = 32), a cadaveric study (n = 10) and a 3D study using bone substitute and commercially available implants (n = 20). Each study used the ASTM 2028-02 testing standard to cyclically test specimens in the superior/inferior direction. Ninety per cent of the subluxation load was maintained by re-adjusting the vertical head displacement every 4000/5000 cycles. All three studies showed failure occurring at the implant/cement interface inferiorly, except in 7 roughened implants in the 3D study. A further 7 implants in the 3D study did not show signs of failure by the end of the test. The superior and inferior rim displacements increased linearly with failure progression in all failed implants. Vertical head displacement was also found to increase with failure progression. Changes in all three displacements at the start of the test and at failure were found to be significant ($p < 0.01$). The non-failed implants showed non-significant changes in all three displacements, validating the use of these measures in monitoring fatigue failure in the glenoid fixation. The study concludes rim displacements can monitor failure, however, recommends the vertical head displacement measure as a more robust, cost effective and time-efficient method. Finally, the use of bone substitute in glenoid fixation studies can be used as a replacement for scapula bone.

7.2 Introduction

Establishing a standard fatigue test to test implant designs and implant fixation has been useful in many ways; allowing implants to be tested in the development and prototyping stage to identify design flaws, in the final stages of development to meet ISO standards and finally, post-clinical use to compare and contrast other designs for further development. Fatigue testing is already used in many endoprosthetic applications; the most obvious are hip, knee, shoulder and elbow implants. The problem of using ambiguous radiographs in-vivo to monitor implant fixation is shared by all artificial joints, thus in-vitro tests, which use similar in-vivo loads and conditions have been used as an alternative and supportive study to quantitatively measure failure.

In the TSA implants, the glenoid implant test specifies the use of rim displacement changes to monitor changes in fixation (ASTM F2028-02). As mentioned in previous chapters, the studies using the fatigue testing standard have not reported failure of the implant fixation or the implant, except in two cases where a custom made implant with no macro-features and smooth back failed almost immediately (Anglin 1999) and in another case where distraction at the implant/cement interface was observed (Oosterom et al. 2004a). As loosening is currently one of the biggest concerns in TSA (Hasan et al. 2002; Matsen et al. 2005) it has been extensively studied in the past, particularly clinically, to determine the cause of failure, to test design features and to test methods of monitoring failure (Havig et al. 1997; Gregory et al. 2009; Nutall et al. 2007; Szoba et al, 2005).

The problem with the clinical and radiographic studies on glenoid designs is accurate monitoring of failure. Monitoring implant behaviour and fixation behaviour under in-vitro fatigue testing has been carried out using rim displacement measures (Anglin et al. 2001; Bicknell et al. 2003; Collins et al. 1992; Oosterom et al. 2004 a, b). The current standard has been useful at standardising this type of test and has allowed the results in this thesis to be compared directly. However, some improvements are warranted.

Since failure has not been observed, the primary aims of this study were to first investigate whether failure can be observed and monitored in-vitro. Secondly, whether rim displacement

is a sufficient and robust method to measure failure. Thirdly, to study whether progressive failure can be monitored. Fourthly, are there other ways, such as using the vertical head displacement, to monitor failure, which may be as good as or better than rim displacement measures?

The testing standard specifies fatigue testing can be carried out in the superior/inferior direction, the anterior/posterior direction or oblique directions. Although the anterior/posterior direction has the lowest constraint, the superior/inferior direction has been used previously, possibly due to the anterior/posterior direction being more susceptible to instability rather than loosening and failure. Implant migration has also been reported in the superior/inferior direction (Nuttall et al. 2007).

The aims have been addressed by subdividing the problem into three discrete studies, firstly testing the fixation in a 2D model (chapter 4) to clearly observe failure, secondly, testing in cadaveric scapulae to observe the affect of bone variability (chapter 5) and thirdly, testing in bone substitute using commercial implants to corroborate the patterns of progressive failure (more clearly seen in 2D) and compare four implant designs (chapter 6).

7.3 Materials & Methods

7.3.1 Subluxation Curves

The subluxation limit was derived for each study by non-destructively testing 2 implants from each design to subluxation and deriving the testing load as 90% of the subluxation load (Fig. 6.5). The testing standard specifies 90% of the subluxation displacement, however, both approaches uses the same principle of testing close to the subluxation limit.

7.3.2 Mechanical Test

The fatigue tests were carried out as described by the standard (F2028-02). However, 3 changes were made to the testing method. Firstly the testing load derived from the subluxation curves was maintained throughout the test by increasing the humeral head

displacement every 4000 cycles in the 2D study and every 5000 cycles in the cadaveric and 3D study. The second modification was the 37 ± 2 °C water bath, which was used in the 2D study in chapter 4 but not in the 3D and cadaveric study. The 2D study in chapter 3 tested under dry conditions using 16 specimens and 4 different designs ($n = 4$) found no change in mode of failure (chapter 3) compared to chapter 4, which was tested wet. Therefore the water bath was not used in the cadaveric and 3D studies, although the joint surfaces and bone were kept wet throughout testing. Thirdly, the superior glenoid rim was cyclically loaded only, rather than alternating the load between the superior and inferior rim in order to isolate the compressive loads superiorly and isolate the tensile loads inferiorly to better understand the mechanisms of failure.

All 3 studies used the same fixation method to attach the LVDTs to the bone substitute or bone. Two custom made LVDT holders per LVDT were cemented directly to the specimens along the horizontal axis, as close to the glenoid rim as possible. One LVDT was attached to align the superior glenoid rim and one was aligning the inferior glenoid rim. The rim displacements were measured with respect to reference pins attached to pre-drilled holes in the glenoid implant rim (Fig. 7.1).



Figure 7.1: superiorly and inferiorly aligned LVDTs for rim displacement measures in 2D (left), cadaveric (middle) and 3D (right) studies. Note: figures are the same as Fig. 4.3, 5.2 and 6.4 respectively.

The change in the humeral head displacement was also monitored every 4000 cycles. In the final 3D study, the vertical head displacement was not increased beyond the subluxation limit in order to maintain physiologically viable mechanics of the joint.

7.3.3 CT Scans

All the samples in the cadaveric and 3D studies were CT scanned. In the cadaveric study all implants were scanned before testing, at 20,000, 40,000, 60,000 and failure. The scans were examined for any failure within the fixation, which are otherwise unseen during the mechanical test.

7.4 Results

7.4.1 Cyclic Results

All implants in the 2D study failed at the implant/cement interface inferiorly at 8429 ± 5518 cycles (table 7.1) and superior bone crushing was observed in all implants except two. In the cadaveric study, all 10 implants failed inferiorly at the implant/cement interface at $80,966 \pm 53,729$ cycles. Superior bone crushing or implant embedding was observed in all implants except two cases. Finally in the 3D study, only 5 implants failed completely at $33,053 \pm 15,969$ cycles and 1 partially at the implant/cement interface inferiorly. A further 7 implants from the roughened implants showed mid-failure at the cement/bone interface superiorly. Of the 20 implants tested in the 3D study, 15 showed signs of superior bone crushing and excessive implant movement. Only 7 implants in the 3D study did not show any signs of failure.

Table 7.1: Summary of results for the 3 fatigue studies, showing cycles to failure and displacements at failure. See Appendix H for displacement raw data and chapters 4, 5 and 6 for cyclic data.

Study	Cycles to failure	Superior rim displacement mm	Inferior rim displacement mm	Vertical displacement mm
2D (n=32)	8429 ± 5518	-0.411 ± 0.156	1.25 ± 0.603	3.65 ± 0.88
Cadaver (n=10)	$80,966 \pm 53,729$	-0.652 ± 0.267	0.585 ± 0.396	3.54 ± 1.48
3D (n=20)	$33,053 \pm 15,969$ (n=5)	-0.491 ± 0.133	0.343 ± 0.075	5.20 ± 0.00

7.4.2 Rim & Vertical Displacements

An increase in superior rim (more negative), inferior rim and vertical head displacements were observed in all implants across 2D, cadaveric and 3D studies (Fig 7.2). A one-way ANOVA test was carried out on each study group and two-way ANOVA test was carried out of the 3 study groups. In all measurements, a significant difference was found before and after failure ($p < 0.01$).

In the superior rim displacements, the differences before failure and at mid-failure were not significant (Appendix H). The inferior rim displacement showed no significant difference before and at mid-failure, except in the 2D studies ($p < 0.01$), this was also the case in the vertical displacement measures ($p < 0.05$). Only the 2D study showed significance between the inferior and vertical displacements before failure, at mid-failure and after failure (Appendix H).

In the 7 implants that did not fail in the 3D study, the average superior rim displacement did not increase and showed no significant changes before and after testing ($p = 0.81$) (Fig. 7.3). The average inferior rim and vertical head displacements increased before and after testing, however, this increase was not significant ($p = 0.07$ and $p = 0.81$ respectively).

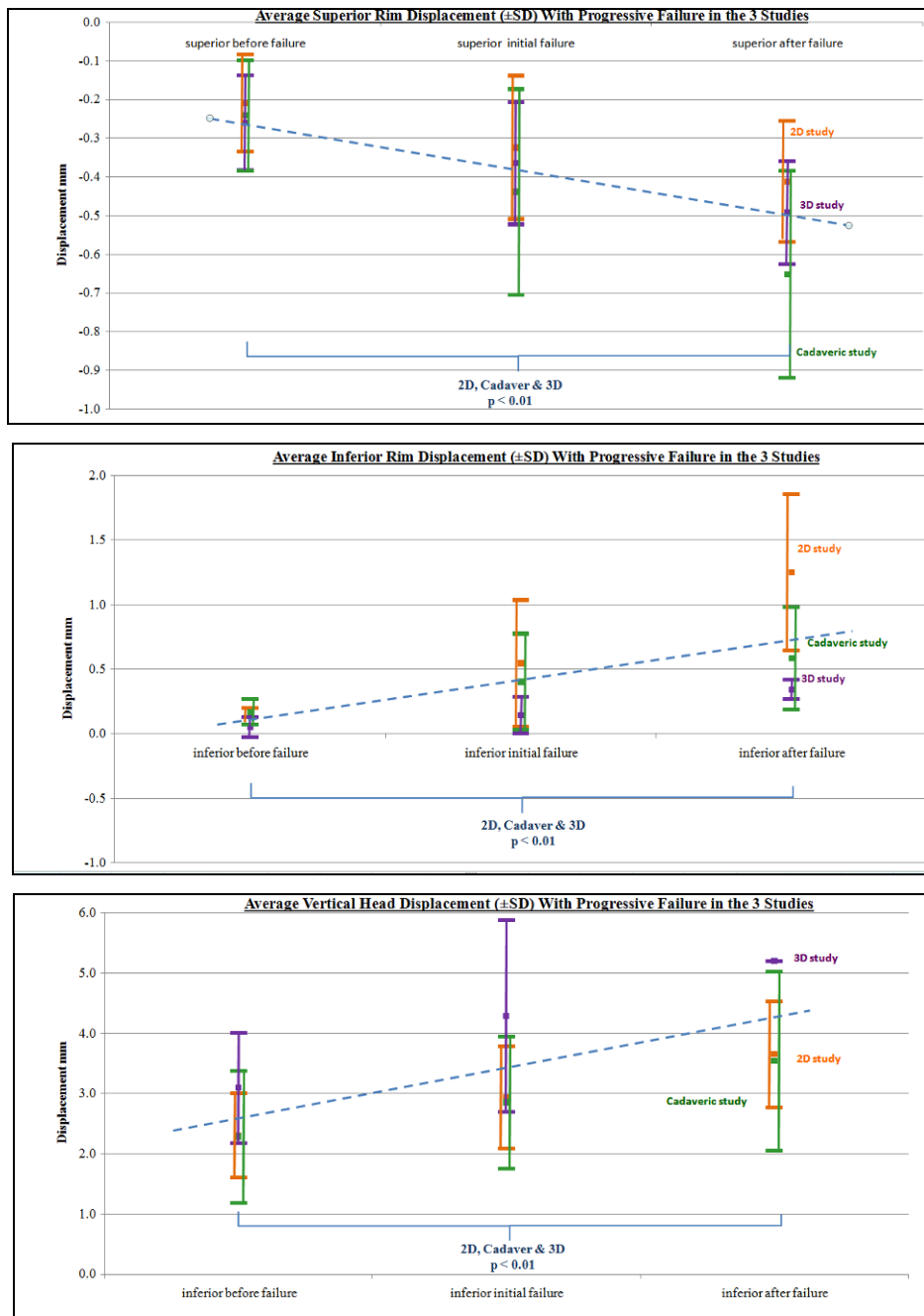


Figure 7.2: Superior rim (top), inferior rim (middle) and vertical head (bottom) displacements against failure progression in the 3 studies. Note: significant differences were found between before failure and after failure in all 3 measures and studies ($p < 0.01$).

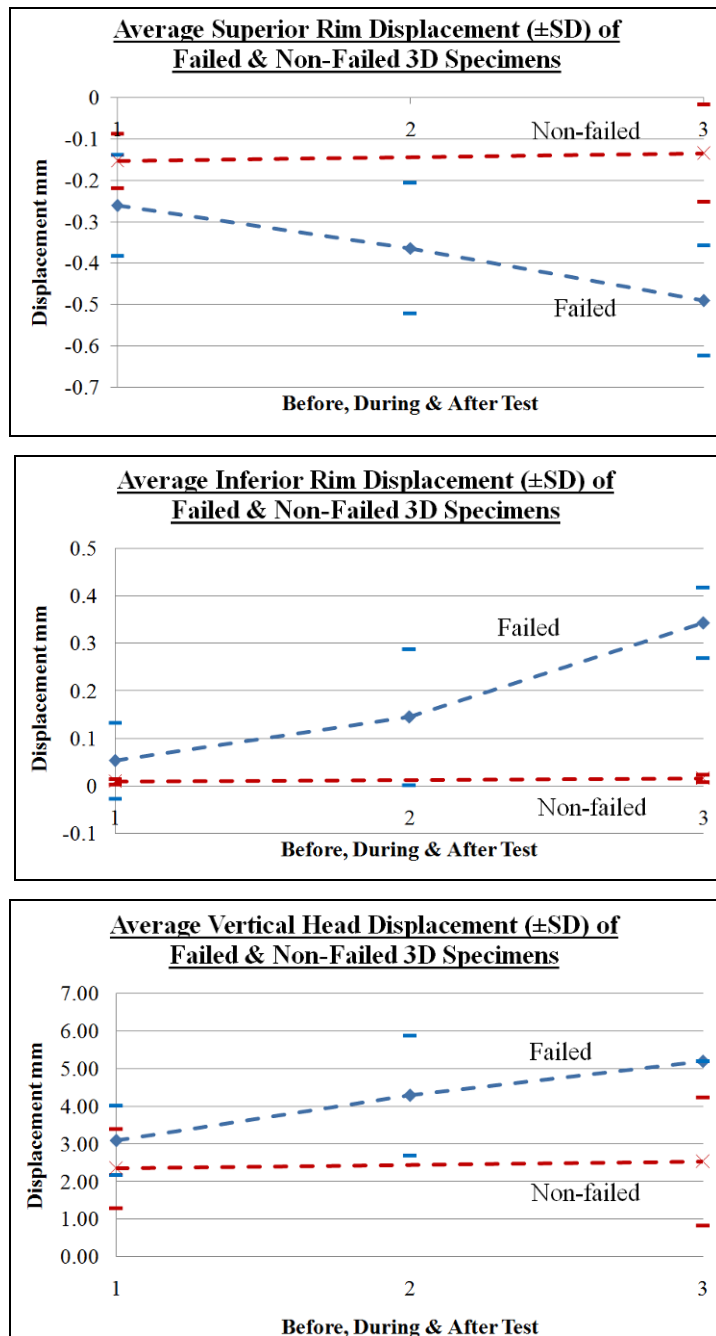


Figure 7.3: Superior, inferior and vertical displacements before, during and after testing in the implants that did not fail in the 3D study (n = 7), compared to the implants that failed (n = 5). Note: no significance was found before and after testing in the non-failed implants, whereas significance was found in the failed (p < 0.05).

7.4.3 CT Results

The cadaveric specimens showed inferior implant failure in all CT scans, which were also observed visually, however, 3 of these cases do not clearly show which interface has failed. Superior failure due to bone crushing was also observed both visually and on the CT scans.

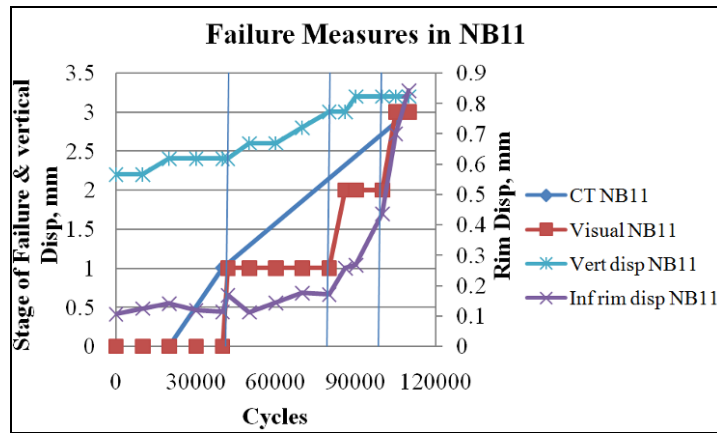


Figure 7.4: Plot showing vertical head and inferior rim displacements correlating to both CT and visual failure. Note: same figure as Fig. 5.16.

The specimens were CT scanned less frequently than the number of displacement measurements, therefore it was not possible to accurately identify whether CT failure matches a sudden increase in displacements, therefore, failure could fail anywhere between the CT scans. However, for initial failure, an increase in vertical head displacement was noted before or with CT and visual failure in 7 specimens (NB1, NB2, NB4, NB6, NB8, NB9, NB11, and NB12). For inferior rim displacement, this was also noted in 7 specimens (NB1, NB2, NB4, NB5, NB8, NB11, and NB12) (Fig. 7.4).

For mid-failure, vertical head displacement correlates in 8 specimens (NB1, NB4 (correlates to visual only), NB5 (correlates to visual only), NB6 (correlates to visual only), NB8, NB9, NB10, NB11). The inferior rim displacement correlates in 7 specimens (NB1, NB2, NB5 (correlates to visual only), NB8, NB10, NB11, NB12) (Appendix F).

7.5 Discussion

Observing glenoid fixation failure has allowed a more comprehensive discussion on the usefulness of rim displacements in monitoring implant fixation. The 2D and cadaveric studies tested the implants to failure and found rim displacements demonstrate a correlation to failure. The 3D study, showing some implants which did not fail, has allowed the study of changes in rim displacement when no failure is observed to compare to rim displacement Failure Characteristics of All Polyethylene Cemented Glenoid Implants in TSA

changes with failure, showing a clear distinguishable difference. The displacements in the 3D study compared to two other published studies demonstrate comparable results (table 7.2). The displacements at the end of the test or at failure in this chapter were understandably greater than data published, since failure was observed and the superior and inferior glenoid rims moved further into the bone and away from the bone respectively. It is also questionable from the published studies whether failure was being monitored or was the displacement changes monitoring other changes in the fixation, such as viscoelasticity, bone crushing or implant deformation. Using slightly lower density bone substitute with lower mechanical properties to normal bone to better model arthritic bone was used in the 2D and 3D study whereas Anglin (1999) used bone substitute with properties more comparable to normal healthy bone. This may also have contributed to the higher displacements observed.

7.5.1 Superior Rim Displacement & Failure

Despite the off-loaded rim displacement being used to monitor implant fixation (the inferior rim displacement in the case of this study), the loaded (or superior) rim displacements have also been reported to increase with fatigue (Table 7.2). This study demonstrates significant changes in superior rim displacements at the start of the test and after failure. This may be more of an indication of bone crushing and therefore superior failure rather than loosening of the inferior rim. However, this phenomenon contributes to the loosening of the implant since the embedding of the implant superiorly could cause the inferior rim to move away from the bone (table 7.2).

Table 7.2: Superior and inferior rim displacements before and after failure compared with published data. Note: this is the same table as table 6.2 in chapter 6.

Rim displacement mm (± SD)	Anglin (1999) Implant C, 33 mm CB keel, n = 3	Oosterom et al. (2004a) 29 mm CB keel, n = 5	This 3D study 32 mm CB keel, n = 5
Superior before testing	0.29 (± 0.317)	0.27 (± 0.07)	0.261 (± 0.122)
Superior after testing	0.383 (± 0.433)	0.37 (± 0.06)	0.491 (± 0.133)
Inferior before testing	0.107 (± 0.167)	0.01 (± 0.05)	0.053 (± 0.080)
Inferior after testing	0.125 (± 0.125)	0.05 (± 0.05)	0.343 (± 0.0747)

7.5.2 Inferior Rim Displacement & Failure

This study confirms that fatigue testing implanted glenoids increases the inferior rim displacement as shown previously (Anglin et al. 2001; Oosterom et al. 2004a, b). Furthermore, this increase is significant in failed implants ($p = 0.01$) compared to non-failed implants ($p = 0.07$). This is the first study showing rim displacement correlation to failure and therefore clears the ambiguity behind rim displacement measures.

7.5.3 2D Versus 3D

Using a 2D model to monitor failure does open the results to criticism, since the 2D scenario cannot directly extrapolate the 3D situation. The 2D study demonstrated progressive failure and allowed, for the first time, the measure of rim displacements and vertical head displacement with observed failure. The 3D study demonstrated similar modes of failure except for the roughened implants. The differences in the number of cycles to failure also differed, particularly with the smooth implants where the 2D implants (containing no macro-features) failed almost immediately. However, the results from Anglin et al. (2001), showing almost immediate failure of a completely ‘smooth’ implant, supports the 2D results and further found smooth implants with macrostructure did not fail. Thus the difference in cycles to failure between the 2D and 3D study does not indicate a discrepancy between the studies since macro-features were not used in the 2D study. Differences in geometries and loads are also expected to affect the outcomes of the two studies. Furthermore, the FE tests carried out in parallel to the in-vitro tests indicate similar stress patterns between the 2D and 3D scenario (Appendix G).

7.5.4 Cadaver Versus Bone substitute

The cadaveric study highlighted 3 main points; firstly, the mode of failure for the implant used (TOPEL) was the same as the 3D study of the same implant, secondly, failure in the implant/cement interface further supports the importance of roughness concluded in the 2D and 3D study. Finally, the number of cycles to failure, if converted to time, is comparable to the expected life of the implant in terms of short, mid and long term survivability of the implant fixation (chapter 5).

However, despite similar displacement patterns, the displacements in the cadaveric study were greater than the 3D study (table 7.3). In fact, the displacements from the cadaveric specimen in the work by Anglin (1999) were also greater compared to the bone substitute study. This is most likely due to the variability in scapula bone structure (Appendix E) and properties. It may also be that bone movement within the cement block contributed to the rim displacement measures. Despite this, the results in this study strongly suggest the use of bone substitute ($\rho = 0.20 \text{ g/cm}^2$, $E = 47.5 \text{ MPa}$) as a useful and viable alternative to model normal cadaveric scapula bone for glenoid fixation studies.

Table 7.3: Superior and inferior rim displacements in cadaveric study before and after failure compared to published data.

Rim displacement mm (\pm SD)	Anglin (1999) Cadaver, FB peg, n = 1	Anglin (1999) bone substitute, E = 193 MPa n = 3	This study Cadaver, 32 mm CB keel, n = 10	This study bone substitute, E = 47.5 MPa n = 5
Superior before testing	0.62	0.29 (\pm 0.317)	0.242 (\pm 0.143)	0.261 (\pm 0.122)
Superior after testing	1.93	0.383 (\pm 0.433)	0.708 (\pm 0.241)	0.491 (\pm 0.133)
Inferior before testing	0.32	0.107 (\pm 0.167)	0.171 (\pm 0.0987)	0.053 (\pm 0.080)
Inferior after testing	loose	0.125 (\pm 0.125)	0.585 (\pm 0.396)	0.343 (\pm 0.0747)

7.5.5 Vertical Head Displacement & Failure

The non-significant differences within the inferior rim and within the vertical head displacements in the non-failed implants in the 3D study validate the use of these measures for monitoring fixation in the glenoid. Although the changes in the non-failed group were not significant, the p-value in the inferior rim displacement ($p = 0.07$) is small enough to consider it a noticeable difference compared to the vertical head displacement ($p = 0.81$). This seems to indicate the vertical head displacement is a more robust measure for fatigue failure. Furthermore, measuring movement of the rim requires devices measuring displacement (for example, LVDTs, gauges, laser devices) and the need to design a specimen holder to incorporate the devices. Lastly, using a water bath when measuring rim displacements can be difficult and impractical. Alternatively, using the vertical head displacement requires no additional costly devices, allows the specimens to be tested in a water bath and would therefore be a less labour intensive and more time effective measure to use.

However there are a few limitations with the vertical head measure, which need to be raised. Firstly, maintaining the testing load by increasing the vertical head displacement intermittently is fundamentally important to use this measure to monitor the fatigue behaviour of the fixation. This method of maintaining the load and not the displacement has also been used by Oosterom et al. (2004a). Secondly, this measure is only useful if the subluxation displacement limit has not been reached. Since the 3D study did not test beyond the implant limit to maintain physiologically realistic conditions, this will make it impossible to measure changes in implant fixation after the maximum displacement is reached. Despite this, out of the 7 non-failed implants, none reached their subluxation limit except in 1 case. Furthermore, the vertical displacements of the 10 implants that reached the subluxation limit, all but 1 of these implants failed or partially failed.

Although the 2D study was extensive, investigating the major design parameters in chapter 4, each design was repeated three times, similarly each design in the 3D study was repeated 5 times. Therefore the sizes of the studies were by no means large. However, the displacement patterns have allowed some important conclusions to be made, which are unlikely to change if the sample size is increased. Another limitation is that the 3D and cadaveric study only investigate the fixation behaviour of one and two designs respectively. Although the aim was not to compare different commercial implants, investigating further the significance of the design features and whether they affect the displacement measures would be useful.

7.6 Conclusion

Rim displacement has been used previously to assess and measure glenoid seating (Bicknell et al. 2003; Collins et al. 1992). Glenoid loosening has been shown to continually be a major problem in TSA and in-vitro fatigue studies addressing this problem are not exhaustive.

The results in the 2D, cadaver and 3D study have shown both superior and inferior rim displacements increase with progressive failure and are therefore viable measures to monitor glenoid implant fixations in-vitro. The vertical head displacement has also been shown to be a method of measuring failure and is a more robust and superior method to rim displacement

due to improving the practicality, cost effectiveness and time efficiency of the fatigue test. The cadaveric and 3D studies validate the use of bone substitute in fatigue testing of the glenoid fixation, which until now, has not been done.

Thus suggestions to improve the testing Standard are:

- Changing the protocol to maintain the testing load by monitoring and changing the vertical head displacement.
- Using the vertical displacement as another measure to monitor the fatigue behaviour of glenoid fixations.
- Eliminating the use of the water bath unless the use relates to the objectives of the test.

7.7 References

- Anglin, C. (1999) Shoulder Prosthesis Testing. PhD Thesis, Queen's University Press, Ontario.
- Anglin, C, et al. (2001), Loosening Performance of Cemented Glenoid Prosthesis Design Pairs. *Clinical Biomechanics*, 16: 144-150.
- ASTM F 2028-02, 2004. Standard Test Methods for the Dynamic Evaluation of Glenoid Loosening or Disassociation. Book of ASTM Standards: 1083-88.
- Bicknell, R T, et al. (2003). Does Keel Size, The Use of Screws, and The Use of Bone Cement Affect Fixation of a Metal Glenoid Implant? *Journal of Shoulder and Elbow Surgery*, 12, (3): 268-275.
- Collins, D, et al. (1992), Edge Displacement and Deformation of Glenoid Components in Response to Eccentric Loading. The Effect of Preparation of the Glenoid Bone. *Journal of Bone and Joint Surgery, American Volume*, 74A, (4): 501-507.
- Gregory, T, et al. (2009). Glenoid Loosening after Total Shoulder Arthroplasty: An In Vitro CT-Scan Study, *Journal of Orthopaedic Research*, Accepted.
- Hasan, S S, et al. (2002). Characteristics of Unsatisfactory Shoulder Arthroplasties. *Journal of Shoulder and Elbow Surgery*, 11, (5): 431-441.
- Havig, M T, et al. (1997). Assessment of Radiolucent Lines about the Glenoid: An In Vitro Radiographic Study, *Journal of Bone and Joint Surgery, American Volume*, 79A, (3): 428-432.
- Matsen. III, F A, et al. (2005). Glenoid Component Failure in Total Shoulder Arthroplasty. *Journal of Bone and Joint Surgery*, 90A, (4): 885-896.
- Nuttall, D, et al. (2007). A Study of the Micromovement of Pegged and Keeled Glenoid Components Compared Using Radiostereometric Analysis. *Journal of Shoulder and Elbow Surgery*, 16, (3): 65S-70S.
- Oosterom, R, et al. (2004a). Effect of Joint Conformity on Glenoid Component Fixation in Total Shoulder Arthroplasty. *Proceedings of the Institution of Mechanical Engineers*, 218, Part H: Journal Engineering in Medicine, 339-347.
- Oosterom, R, et al. (2004b). Effect of Glenoid Component Inclination on Its Fixation and Humeral Head Subluxation in Total Shoulder Arthroplasty. *Clinical Biomechanics*, 19: 1000-1008.

Szabo, I, et al. (2005). Radiographic Comparison of Flat-back and Convex-back Glenoid Components in Total Shoulder Arthroplasty, *Journal of Shoulder and Elbow Surgery*, 14, (6): 636-642.

Chapter 8: Discussion

This thesis aimed to fatigue test glenoid implants to failure in-vitro in order to investigate the loosening behaviour of cemented glenoids in TSA and monitor failure using four methods; visual observation, rim displacement, vertical head displacement and CT. The studies have shown a number of fixation problems that have also been found clinically.

8.1 Glenoid Implant Mechanical Failure

Failure at the implant/cement interface due to low interface strength was clear in the 2D studies in all but 3 implants out of a total of 80 (chapter 3 and 4), in all the smooth glenoid implants in the cadaveric (chapter 5) and 6/10 smooth implants in the 3D study (chapter 6). Anglin (1999) similarly found almost immediate failure in two completely smooth implants compared to two roughened implants, which both tested to 250,000 without failure, and as a direct result of her work, one company has opted to roughen the back surface of their glenoids. However, the majority of glenoids on the market have not roughened their implants (table 2.1). Furthermore, failure at the implant/cement interface has been shown clinically (Nyffeler et al. 2003). The FE studies in 2D, cadaveric and 3D, have shown tensile stresses within the interface strength range inferiorly and bone crushing/implant embedding superiorly, as observed in-vitro (chapter 4, 5 & 6).

The 2D work in chapter 4 furthers the roughness study by investigating the effect of various roughnesses on the failure rate, finding a positive correlation between roughness and number of cycles to failure (Fig. 4.8). The 3D study in chapter 6 also investigates the effect of three roughnesses on the failure rate. Six out of the ten smooth glenoids failed at the implant/cement interface (5 out of the 6 were keeled), whereas the remaining ten roughened implants did not show any interfacial failure. Although there is not enough evidence to conclude that roughness is the reason for this difference and not the keel design, the implant/cement failure of one smooth pegged glenoid in the study and the results in chapter 5

showing implant/cement failure in all the smooth pegged glenoids in the cadaveric study, strongly indicates that roughening the glenoid back-surface will increase the interfacial strength and could delay failure.

Some of the limitations in investigating the effect of roughness include the compounding problem of the keel design in the 3D study. Ideally testing a roughened keel design would give a clearer picture of the effects of roughness. Secondly, the rough n-S glenoid designs (3D study) were identical to the n-R very rough implants and were smoothed down to achieve a lower roughness. Although the implant back was manually smoothed to a consistent roughness (using wet and dry fine sandpaper), there may be a more variable range of roughnesses due to the small crevices between the pegs which were difficult to smooth. This may have given a better fixation to the rough n-S group.

Finally, comparing the number of cycles to failure in the 2D and cadaveric/3D implants shows the 2D smooth implants to fail much earlier at 0-4048 cycles, compared to the smooth implants in the cadaveric and 3D study at 20,405-122,500 and 20,127-50,727 cycles respectively. Using a 2D model does open the results to criticism, since the 2D scenario cannot directly extrapolate the 3D situation. Although this appears to be a discrepancy in the results, Anglin et al. (2001), showed almost immediate failure of two completely 'smooth' implants, which supports the 2D results and furthermore, found smooth implants with macrostructures did not fail. Thus the difference in cycles to failure between the 2D and cadaveric/3D study does not indicate a discrepancy between the studies since macro-features were not used in the 2D study. Furthermore, the FE tests carried out in parallel to the in-vitro tests indicate similar stress patterns between the 2D and 3D scenario (Appendix G).

8.2 Clinical Findings & Biological Factors

One of the limitations of this thesis is the absence of biological factors that will influence the glenoid fixation and its behaviour to mechanical stimuli. It seems the failure results found in this investigation contradicts reported clinical findings. Clinical studies heavily rely on analysing radiolucent lines, although most studies do not discuss what a radiolucent line

could mean or highlight the ambiguity and inaccuracy of a radiograph (Havig et al. 1997; Lazarus et al. 2002; Nagels et al. 2002), some studies assume failure in the cement/bone interface based on r. lines found in postoperative radiographs (Bohsali et al. 2006; Matsen III et al. 2008). The few published retrieval studies do not focus on the condition of the glenoid fixation on removal of the implant and do not mention which interface has primarily loosened (Hertel & Ballmer 2003; Scarlat & Matsen III 2001; Weldon III et al. 2001). However, Hertel & Ballmer (2003) mention the indication for glenoid loosening was increasing thickness of r. lines around the peg or keel and Scarlat & Matsen III (2001) also mention the problem of polyethylene wear may lead to periprosthetic osteolysis at the cement/bone interface, causing implant loosening. Only Yian et al. (2005) reported 2 revised glenoids in the clinical study of 47 total shoulder replacements (19-55 month follow up) had failed wholly at the cement/bone interface, as indicated by cement found intact on the pegs (Fig. 2.1), however, the authors did not mention the condition of the implant back and whether the cement was intact. Furthermore, Nyffeler et al. (2003) mention that clinically, failure is usually found at the cement/bone interface, although failure at the implant/cement interface has been document in the study.

The clinical and retrieval studies do not show glenoid failure is, without a doubt, primarily due to loss of cement/bone fixation, although the radiographic data and comments on the few retrieved implants certainly indicates that this hypothesis may be true. However, even if the scenario suggested in these papers are true, in most cases, there are at least some examples where the failure mode observed in this work was also observed clinically. Although defining what r. lines mean with respect to fixation failure is ambiguous, r. lines developed after the initial postoperative radiograph are attributed to connective fibrous tissue (Matsen III et al. 2008) or resorption of the bone (Nyffeler et al. 2003) as a direct result of variable and often dramatic changes in stresses along the fixation interfaces, which produces a biological response. If this is the case, it may be that a distraction due to failure of the inert interface in the fixation, the implant/cement, may be small and indistinguishable in radiographs. Comparatively, the changes in bone morphology due to bone resorption or formation of fibrous connective tissue are progressive and more apparent. Secondly, the failures of the 2D pegged implants consistently show failure progressing from the implant/cement interface at the inferior rim to the bone and cement/bone interface around the central peg, much like the findings from the retrieved glenoids reported by Yian et al. (2005) (Fig. 2.1).

However, it is prudent to consider the biological effects on the glenoid fixation and would be a natural step to further this work. The findings in this thesis highlight the short-term mechanical problems with the fixation and therefore are relevant in analysing the glenoid implant design. The 2D and 3D studies shows early failure of the rim at the implant/cement interface alters the mechanics of the joint by the humeral head's ability to translate further across the glenoid surface, increasing the "rocking horse" effect. This has a knock on effect on the fixation interfaces and likewise, the underlying trabecular bone. Thus whether failure is observed in the implant/cement or cement/bone interface, the change in joint mechanics will alter the load distribution of the underlying bone, which in turn will alter the morphology of the bone as described by Wolff's law.

8.3 Design Recommendations

The work in the 2D studies also aimed to investigate how fatigue failure is affected by key design features currently found in glenoid implants; the peg/keel, curved-back/flat-back, surface-back roughnesses and conforming/non-conforming features. Only a small sample size for each design was used ($n = 3$) and no significant differences were found in any of the design features except the smooth versus roughened designs, which showed roughening the back surface to $\geq 3.4 \mu\text{m}$ improves resistance to failure ($p < 0.0001$) compared to 'smooth' implants of $\leq 2 \mu\text{m}$. Although the trend of average values show keel to perform worse than peg, non-conforming to perform worse than conforming and almost no difference in flat-back and curved-back, the differences were not statistically significant (Fig. 4.6).

Although the keel/peg differences are not significant, the 3D study in chapter 6 shows a poor outcome of the smooth keel compared to the smooth peg implants. However, as highlighted in chapter 6, the smooth pegged implants showed higher subluxation loads and lower displacements (Fig. 6.5), this could not be explained as the subluxation curve is dependent on the surface geometry, which is identical to the keeled implants. The FE analysis also demonstrates no differences in subluxation curves between the two implants. As a result, the pegged implants (TOPEL) were tested at the same load but experienced much lower

displacements throughout the tests of 1.4-1.6 mm compared to 2.2-5.2 mm for the identical keel group (TOKL), possibly delaying loosening. However, other studies have also suggested the keel provides less rotation stability than pegs (Nuttall et al. 2007), provides poorer seating in bone compared to pegs and shows more r. lines post-operatively (Gartsman et al. 2005; Klepps et al. 2005; Lazarus et al. 2002) and is generally worse with respect to resistance to loosening (Nuttall et al. 2007). Finally, assuming the keeled implants will have more bulk cement, this may lead to higher risks of bone necrosis compared to the pegged implants where cement surface area is greater and therefore provides better heat dissipation (Lazarus et al. 2002), although bone necrosis in TSA has not been proven to be a problem. There are several reasons why such a difference in the peg/keel was not seen in the 2D study. Clinically, the condition of the shoulder joint can govern the choice of using a keel, which can directly impact on the outcome of the implant; the keeled implant is often reserved for poorly exposed glenoids (affecting implant seating) and when the surgeon is faced with poor quality bone (Lazarus et al. 2002). Therefore, TSA surgeries where the joint is implanted with a keeled glenoid can often be more technically-challenging (Lazarus et al. 2002). Thus the work in the 2D and 3D study suggest keel is mechanically inferior to peg, however, other surgical and biological factors should be appreciated when making such a comparison.

The flat-back and curved-back implants showed the least difference in chapter 4, although the pegged implants showed better outcomes in the curved-back specimens, the keel showed the opposite is true (Fig. 4.6). Current glenoids on the market wholly advertise curved-back designs, however, flat-back glenoids are still in use and comparative studies are limited. Szabo et al. (2005), in a clinical study of flat-back and curved-back keels, reported significantly more r. lines in the flat-back immediately post-operatively, although no significance was found in 2 year radiographs, confirming the findings in chapter 4. However, it may be important to consider the flat-back implants require more resection of the glenoid rim, whereas curved-back implants possibly help preserve the cortical subchondral layer, which is thought to improve glenoid seating. This difference has not been modelled here. However, the FE analysis shows the curved-back feature lowers the erratic changes and peak normal stresses across the interfaces (Appendix E). It would have been interesting to compare a flat-back design to the curved-back implant in the cadaveric study (chapter 5), which will include these considerations, however, the aim for the cadaveric study was not to compare designs.

8.4 Indirect Measures of Failure

Measuring glenoid failure has been motivated by the need to quantify failure in-vitro. Until now the measures of inferior rim displacement have been correlated to fatigue (number of cycles), not failure (Anglin 1999; Oosterom et al. 2004a & b). Therefore there is no way of knowing what these values are measuring exactly. The 2D model was primarily designed for this purpose. Using the cross-section of a typical glenoid implant in the 2D model has enabled failure to be observed visually, allowing a direct correlation to quantitative data. Furthermore, the 2D study in chapter 4 aimed to investigate other quantitative measures, following an FE study that showed the superior rim displacement and vertical head displacement may possibly be useful measures, these were considered in the study along with the inferior rim displacement.

The qualitative observation of progressive failure positively correlates to increase inferior rim displacement and vertical head displacement. Anglin (1999) found a positive correlation between inferior rim displacement at the start and end of 100,000 cycles. Similarly Oosterom et al. (2004a & b) found an increase in inferior rim displacement after 200,000 cycles. Both reported no loosening in any specimen although Oosterom et al. (2004b) found implants were easily removed from the cement after bisecting. Both works indicate the use of rim displacement may indicate changes in the implant fixation, however, the 2D work together with the cadaveric and 3D study proves this hypothesis is true.

Furthermore, vertical head displacement has been shown throughout the 2D, cadaveric and 3D studies to correlate to visual failure. Both inferior rim displacement and vertical head displacement have shown no or little change in displacements when failure is not observed during testing, thus confirming the use of both measures of assessing fixation failure quantitatively.

8.4.1 Rim Displacement Versus Vertical Displacement Measure

The use of vertical head displacement to monitor fixation failure has shown to be as good as inferior rim displacement. However, due to ease and accuracy of measuring head displacement and no need for extra transducers or designing holders to accommodate displacement devices, the vertical head displacement has shown to be a superior measure to inferior rim displacement.

8.5 Human Bone & Bone Substitute

The outcomes of the cadaveric study (chapter 5) showed similar failure modes to the 2D and 3D studies with failure at the implant/cement interface inferiorly and superior implant embedding. The study, however, is not aimed to model biological factors into the in-vitro test but rather assess the behaviour of human bone, with its variability in quality and its anisotropic properties compared to isotropic, homogeneous bone substitute foam.

The cadaveric work intends to answer whether PU foam can represent how real glenoid bone behaves under mechanical loading. Although the outcomes of both materials are similar, perhaps using roughened implants would help to further understand the cement/bone interface behaviour in glenoid bone by strengthening the implant/cement interface. These findings are further supported by a cement/glenoid bone interface study of 7 glenoids showing a tensile interface strength of 1.60-3.76 MPa (Sanghavi et al. 2007), which is comparable to the cement/bone substitute strength of 2.32+ MPa used in this thesis. A greater range in interface strength of cement/real bone compared to cement/bone substitute is expected, however, both interfaces show similar strength margins.

8.6 Testing Recommendations

The work presented in this thesis utilised the ASTM testing standard F2028-02 throughout and often focussed on its effectiveness in measuring failure. As such some comments and suggestions to the test are useful to further develop the test:

- The observation of failure and correlation to rim displacement confirms the hypothesis that glenoid loosening can be monitored through rim displacement measures.
- Furthermore, it is suggested that the standard should include the option of measuring vertical head displacement via load controlled testing. Currently the standard suggests displacement control, whereas monitoring vertical head displacement must be load controlled, where the humeral head displacement is incrementally increased every 5000 cycles to maintain testing load until the subluxation displacement is reached. The economical advantage and efficiency of using vertical head displacement compared to rim displacement makes it a useful method to adopt and should at least be mentioned in the standard.
- The standard specifies taking 90% of the subluxation displacement as the testing parameter, the work presented here suggests using 90% of the subluxation load. Taking 90% of the subluxation displacement is affected by the shoulder plateau in the subluxation curve (Fig. 3.4) and may possibly test implants very close to subluxation. Secondly, the subluxation displacement shows greater variation within implants of the same surface geometry compared to the subluxation force. Thirdly, taking 90% of the subluxation force will fall in the common linearity region in the curves (Fig. 3.4), testing the implants at the same level.
- Using the water bath at 37°C is useful to simulate surface friction conditions and allow the implant and cement to be tested within in-vivo temperatures. Although Anglin (1999) found a small but significant decrease of 5% in the subluxation load in water bath conditions compared to air, the 2D study in chapter 3 (air) compared to the 2D study in chapter 4 (water bath) showed no change in failure modes. The possible small change in subluxation loads may have an impact on the number of cycles to failure as the range of cycles to failure in chapter 3 and 4 were 9764-13,969 and 3102-

11,729 respectively. However, comparing number of cycles to failure between implants is more useful as a relative measure, since testing conditions and loads varies from one study or research group to another. Thus, this small difference is not expected to change the outcome of these studies whether a water bath was used or not. Since the absence of a water bath will allow rim displacements to be measured throughout testing (should the research study require it) and provide a better view of the implant fixation, it would be better for the standard not to necessitate the use of a water bath unless the nature of the research requires its use.

8.7 References

- Anglin, C, (1999). *Shoulder Prosthesis Testing*, PhD Thesis, Mechanical Engineering, Queen's University, Canada.
- Anglin, C, et al. (2001), Loosening Performance of Cemented Glenoid Prosthesis Design Pairs. *Clinical Biomechanics*, 16: 144-150.
- ASTM F 2028-02, (2004). Standard Test Methods for the Dynamic Evaluation of Glenoid Loosening or Disassociation. *Book of ASTM Standards*: 1083-88.
- Bohsali, K I, et al. (2006). Complications of Total Shoulder Arthroplasty. *Journal of Bone and Joint Surgery, American Volume*, 88A, (10): 2279-2292.
- Gartsman, G M, et al. (2005). Radiographic Comparison of Pegged and Keeled Glenoid Components. *Journal of Shoulder and Elbow Surgery*, 14, (3): 252-257.
- Havig, M T, et al. (1997). Assessment of Radiolucent Lines about the Glenoid: An In Vitro Radiographic Study, *Journal of Bone and Joint Surgery, American Volume*, 79A, (3): 428-432.
- Hertel, R, and Ballmer, F T (2003). Observations on Retrieved Glenoid Components, *The Journal of Arthroplasty*, 18: 361-366.
- Klepps, S, et al. (2005). Incidence of Early Radiolucent Glenoid Lines in Patients Having Total Shoulder Replacements, *Clinical Orthopaedics and Related Research*, (435): 118-125.
- Lazarus, M D, et al. (2002). The Radiographic Evaluation of Keeled and Pegged Glenoid Component Insertion, *Journal of Bone and Joint Surgery, American Volume*, 84A, (7): 1174-1182.
- Matsen III, F A, et al. (2008). Glenoid Component Failure in Total Shoulder Arthroplasty, *Journal of Bone and Joint Surgery, American Volume*, 90A, (4): 885-896.
- Nagels, J, et al. (2002). Patterns of Loosening of the Glenoid Component, *Journal of Bone and Joint Surgery, British Volume*, 84B, (1): 83-87.
- Nuttall, D, et al. (2007). A Study of the Micromovement of Pegged and Keeled Glenoid Components Compared Using Radiostereometric Analysis, *Journal of Shoulder and Elbow Surgery*, 16, (3S): 65S-70S.
- Nyffeler, R W, et al. (2003). Influence of Peg Design and Cement Mantle Thickness on Pull-Out Strength of Glenoid Component Pegs, *Journal of Shoulder and Elbow Surgery*, 85B, (5): 748-752.

- Oosterom, R, et al. (2004a). Effect of Joint Conformity on Glenoid Component Fixation in Total Shoulder Arthroplasty. *Proceedings of the Institution of Mechanical Engineers*, 218, Part H: Journal Engineering in Medicine, 339-347.
- Oosterom, R, et al. (2004b). Effect of Glenoid Component Inclination on Its Fixation and Humeral Head Subluxation in Total Shoulder Arthroplasty, *Clinical Biomechanics*, 19: 1000-1008.
- Sanghavi, S, et al. (2007). Glenoid Bone-PMMA Interface Tensile Strength. Pending submission.
- Scarlat, M M & Matsen III, F A (2001). Observations of Retrieved Polyethylene Glenoid Components, *The Journal of Arthroplasty*, 16, (6): 795-801.
- Szabo, I, et al. (2005). Radiographic Comparison of Flat-back and Convex-back Glenoid Components in Total Shoulder Arthroplasty, *Journal of Shoulder and Elbow Surgery*, 14, (6): 636-642.
- Weldon III, E J, et al. (2001). Intrinsic Stability of Unused & Retrieved Polyethylene Glenoid Components, *Journal of Shoulder and Elbow Surgery*, 10, (5): 474-481.
- Yian, E H, et al. (2005). Radiographic and Computed Tomography Analysis of Cemented Pegged Polyethylene Glenoid Components in Total Shoulder Replacement, *Journal of Bone and Joint Surgery, American Volume*, 87A, (9): 1928-1936.

Chapter 9: Future Work

9.1 Future Work

The discussion in chapter 8 raises some limitations and improvements for the studies carried out. Some improvements in the cadaveric and 3D studies have been suggested below. A project grant proposal to expand on cementless glenoid fixations, one area of TSA which has not been discussed is presented here.

9.1.1 Improvements in In-Vitro Fatigue Test

Expanding the 3D study to monitor and analyse fatigue failure of various implants, would be useful to compare: keel/peg, curve/flat, conforming/non-conforming, smooth-back/rough-back, macro-features on back/macro-features on peg, without confounding factors, as done in the 2D study.

One of the areas where this work can be explored is the aspects of glenoid bone in the glenoid fixation, which could not be modelled in bone-substitute and which will aid the study of design parameters. For example, no differences were found in flat/curved-back designs in bone substitute, however, it would be useful to investigate whether more resection of the subchondral bone at the glenoid rim in flat-back implants will adversely affect the fixation and result in a significantly different failure rate to the curved-back implant. Another example is to test roughened implants in cadaveric glenoid bone, in order to investigate the behaviour of cement/bone failure in glenoid bone compared to bone substitute.

9.1.2 New Glenoid Implant Design Project Proposal

Testing in non-pathological bone raises questions as to whether pathological bone, particularly RA bone will behave in the same way. Thus there is a current need to pursue the study of RA bone and investigating new designs particularly in TSA.

In rheumatoid cases, the rate of complications found in TSA are more frequent and functional outcomes are poorer (Kelly et al. 1987). This is mainly attributed to poor bone quality that is insufficient to establish or maintain the cemented fixation. Often soft tissue damage and muscle tears adversely impact on the implant outcome (Stewart & Kelly 1997).

In the cadaveric study (chapter 5), 11 scapulae were intended for the study but one was excluded due to poor quality bone and excessive wear of the glenoid articular surface (Fig. 9.1). Of the 10 scapulae, one described as poor quality and sclerotic was included in the study (Fig. 9.2). Implant seating was incomplete (Fig. 9.2) and the implant was the first to fail at both the implant/cement and cement/bone interface due to tensile/shear failure. A keeled design would probably not have improved the outcome.

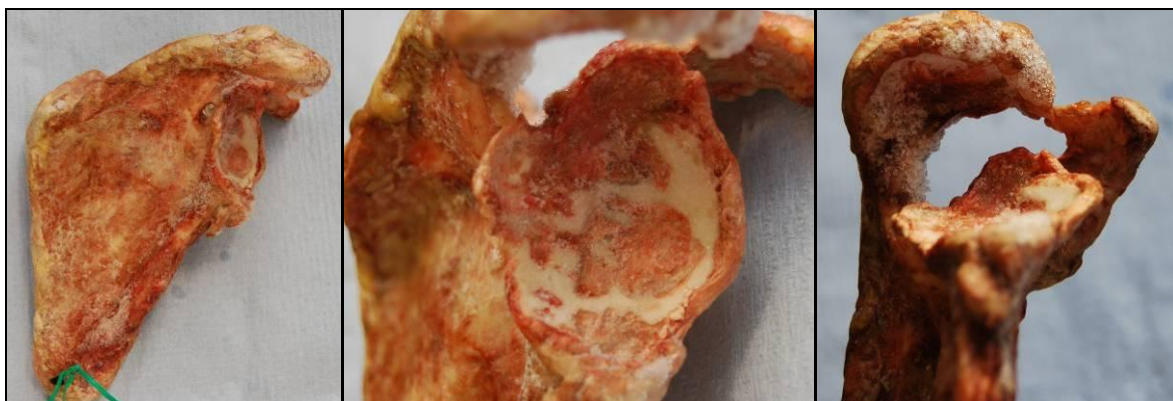


Figure 9.1: Poor quality scapula bone. Note: excessive posterior wear of the glenoid surface (right).

The number one cause for shoulder arthroplasty after trauma is rheumatoid arthritis according to the Norwegian joint registry with 32 % of 1820 cases over a 12 year period, followed by osteoarthritis (26%). Similarly statistics from the Swedish and Scottish joint registries have shown the majority of shoulder replacement surgeries are RA cases (30% of 359 cases and 41% of 451 cases respectively). However, the vast majority of shoulder arthroplasties are in fact hemiarthroplasty (84%, 87% and 88% respectively). One of the main reasons for the choice of using a hemi rather than TSA is the knowledge that glenoid implant loosening is a real mid-term concern, which is avoided by having a hemi, despite the fact that TSA has been shown to be better for pain relief (Burrough et al. 2003; Rahme et al. 2001; Sanchez-Sotelo 1997) and function (Gartsman et al. 2000; Walch et al, 1999). Furthermore, in problematic hemi cases, the shoulder is usually replaced with a TSA, which usually becomes a

complicated difficult procedure, it is therefore better to have a total shoulder replacement than having a hemi and revising to a TSA (Carroll et al. 2004). TSA in RA cases have shown to have a lower improvement of range of motion compared to OA and fracture cases (Pfahler et al. 2006). It is clear that although TSA may be preferred, due to the recurrent fixation problems of the glenoid, most shoulder arthroplasty cases are treated with a hemi, particularly RA shoulders where fixation is notoriously poor.

Thus the literature and the cadaveric study (chapter 5) indicate that the current conventional shoulder joint replacement is insufficient for a long-term fixation. Cementless designs employing a metal back and polymer articular lining have not been able to improve TSA outcomes and are further complicated by osteolysis due to articular wear of the polymer surface or detachment of the polymer lining (Tammachote et al. 1999; Wallace et al. 1999). Screw fixations employed in the glenoid have often fractured. Thus a re-design of the fixation and materials is needed to address the problems of TSA in general as well as specifically for RA cases.



Figure 9.2: Sclerotic, poor quality bone. Note: poor implant seating and excessive posterior wear (middle) and failure at the implant/cement and cement/bone interface (right).

Although there are studies on the material properties and structure of glenoid bone (Frich et al. 1997; Anglin et al. 1999; Mimar et al. 2008). There are no studies to date describing the material properties of rheumatoid shoulder bone. Current implant designs assume good bone stock at the implantation site and an intact, albeit asymmetrically worn, glenoid surface and subchondral bone present. These assumptions are often compromised in advanced rheumatoid arthritic shoulders. Therefore the authors propose a study on the material properties of rheumatoid glenoid bone, investigating the Young's modulus, yield strength,

compressive strength, viscoelasticity and density. Furthermore, a clinical study on the outcome of conventional implants in RA cases using CT data to develop finite element models and monitor changes in bone density and bone modelling using DEXA or CT scans will yield important results to better understand TSA in RA cases.

Thus this project proposal aims to:

1. Identify the material properties of glenoid bone, considering orientation, position and depth, using cadaveric RA shoulders or shoulders where RA has been diagnosed in other joints.
2. Analyse the material properties, density and outcome of rheumatoid TSA cases clinically, using CT images and FE modelling.
3. Follow the progression of conventional implants using DEXA or CT scans from clinical cases to observe changes in bone density and remodelling.
4. Propose a new design considering the material properties of rheumatoid shoulder, patient data, FE stress and bone modelling analysis.
5. Predict the outcome of the new design versus a conventional design using patient CT data and follow the progression of the conventional implant using DEXA or CT to validate the model.

9.2 References

- Anglin, C, et al. (1999). Glenoid Cancellous Bone Strength and Modulus. *Journal of Biomechanics*, 32, (10): 1091-1097.
- Burroughs, P L, et al. (2003). Shoulder Arthroplasty in the Young Patient. *The Journal of Arthroplasty*, 18, (6): 792-798.
- Carroll, R M, et al. (2004). Conversion of Painful Hemiarthroplasty to Total shoulder Arthroplasty: Long-Term Results, *Journal of Shoulder and Elbow Surgery*, 13, (6): 599-603.
- Frich, L H, et al. (1997). Bone Strength and Material Properties of the Glenoid, *Journal of Shoulder and Elbow Surgery*, 6, (2): 97-104.
- Gartsman, G M, et al. (2000). Shoulder Arthroplasty with or without Resurfacing of the Glenoid in Patients Who Have Osteoarthritis. *Journal of Bone and Joint Surgery, American Volume*, 82A, (1): 26-34.
- Kelly, I G, et al. (1987). Neer Total Shoulder Replacement in Rheumatoid-Arthritis, *Journal of Bone and Joint Surgery. British Volume*, 69B, (5): 723-726.
- Mimar, R, et al. (2008). Evaluation of the Mechanical and Architectural Properties of Glenoid Bone, *Journal of Shoulder and Elbow Surgery*, 17, (2): 336-341.
- Pfahler, M, et al. (2006). Hemiarthroplasty Versus Total Shoulder Prosthesis: Results of Cemented Glenoid Components, *Journal of Shoulder and Elbow Surgery*, 15, (2): 154-163.
- Rahme, H, et al. (2001). The Swedish Elbow Arthroplasty Register and The Swedish Shoulder Arthroplasty Register. *Acta Orthopædica Scandinandania*, 72, (2): 107–112.
- Sanchez-Sotelo, J (1997). Shoulder Arthroplasty For Osteoarthritis and Rheumatoid Arthritis. *Current Orthopaedics*, 21: 405–414.
- Stewart, M P M & Kelly, I G (1997). Total Shoulder Replacement in Rheumatoid Disease, *Journal of Bone and Joint Surgery. British Volume*, 79B, (1): 68-72.
- Tammachote, N, et al. (1999). Long-Term Results of Cemented Metal-Backed Glenoid Components for Osteoarthritis of the Shoulder, *The Journal of Bone and Joint Surgery, American Volume*, 91A, (1): 160-166.
- Wallace, A L, et al. (1999). Dissociation of the Glenoid Component in Cementless Total Shoulder Arthroplasty, *Journal of Shoulder and Elbow Surgery*, 8, (1): 81-84.

Walch, G, et al. (1999). *Glenoid Resurfacing in Shoulder Arthroplasty: Pro's and Con's*.

Walch, G & Boileau, P (1999). *Shoulder Arthroplasty*, Springer, Berlin: 177-181.

Appendix A: Table Summary of TSA Clinical Studies

1 st Author	Clinical Tests			Subjective Tests					Radiographic Tests			
	ASES	UCLA	Other	Simple Test	OSS	WOOS	SF36	Other	Ant.	Pos. Obl.	Aux.	Flour. Or CT
Aliabadi et al. '88									✓	✓	✓ some	
Barrett et al. '87	✓							✓	✓		✓	
Boileau et al. '02			✓ CS						✓	✓		
Boyd et al. '90			✓						✓			
Bryant et al. '05		✓										
Cofield '84			✓ Neer					✓		✓	✓	
Collins et al. '04			✓ Neer	✓					✓	✓	✓	
Fehringer et al. '02				✓								
Friedman '92	✓								✓		✓	
Gartsman et al. '00	✓	✓							✓		✓	
Gartsman et al. '05			✓						✓			
Gill et al. '99			✓ NC							✓	✓	
Hill & Norris '01	✓		✓ Neer								✓	✓
Kelly et al. '87			✓ Neer						✓		✓	
Kirk &			✓						✓	✓	✓	

Sorger '97												
Klepps et al. '05			✓					✓		✓		
Lazarus et al. '02								✓		✓		
Lo et al. '05	✓	✓	✓ CS			✓	✓		✓	✓	✓	
Martin et al. '05	✓							✓	✓	✓		
Mileti et al. '05			✓ Neer							✓	✓	
Nagels et al. '02			✓					✓				
Neer II & Morrison '95			✓					✓	✓	✓		
Nuttall et al. '07	✓		✓ CS									
Orflay et al. '03	✓		✓				✓	✓	✓	✓		
Rahme et al. '04												
Smith et al. '06			✓				✓					
Sperling et al. '00								✓	✓	✓	✓	
Sperling et al. '04			✓ NC							✓	✓	
Stewart & Kelly '97			✓ NC					✓		✓		
Szabo et al. '05								✓				✓
Tammac hote et al. '05			✓ NC					✓	✓	✓		
Taunton et al. '08			✓ NC					✓	✓	✓		

Torchia et al. '97			✓ NC							✓	✓	
Trail & Nuttall 2002	✓		✓ CS						✓		✓	
Walch et al. '02			✓ CS						✓		✓	
Wallace et al. '99			✓	✓			✓					✓
Yian et al. '05			✓ CS						✓		✓	✓

Note: NC = Neer & Cofield method, CS = Constant Score method.

Appendix B: Comparison of Radiographic and Clinical Results in TSA Studies

Abbreviation	Full name
RA	Rheumatoid arthritis
OA	Osteoarthritis
AN	Avascular necrosis
ON	Osteonecrosis
TA	Traumatic arthritis
Polymy R	Polymyalgia rheumatica
Chron disloc	Chronic dislocation
Cap arth	Capsulorrhaphy arthropathy
Cuff arthrop	Rotator cuff arthropathy
SepticA	Septic arthritis
InstabA	Instability arthritis
Ankyl spond	Ankylosing spondylitis
Psoriatic polyarthr	Psoriatic polyarthritis
MB	Metal-back
Post-op	Post-operative

1 st Author	% (no./total no.)			Notes
	Clinical/ pain relief	r. lines	Radiographical ly loose	
Alibadi et al. '88	?	?	15% (15/98)	68 RA, 25 OA, 5 AN, r. loose-12 RA Neer PE cemented, 0-8yrs post-op.
Barrett et al. '87	88% 44/50	74% 37/50	10% 5/50	33 OA, 11 RA, 6 frac, (24-81 ave. 59 yrs). Neer PE cemented, 2-7.5yrs post-op, 4 definitely loose
Boileau et al. '02	?	43% 17/40 85% 17/20	10% 4/40 0% 0/20	40 OA, (55-84 ave 68.5yrs). Tornier 20 PE, 20 MB cementless, 3 yrs post-op. MB: 25% 5/20, 20% 4/20
Boyd et al. '90	93% (195/210) 96%	?	12% (16/131)	95 RA, 34 OA, 4 AN, 1-ankyl spond (29-85 ave 58 yrs) PE Neer, 2-10yrs post-op. Of 16 r. loose,

	(136/146)			13 RA. 1 glenoid revision
Bryant et al. '05	(/62)	?	?	112 OA only (ave 68 yrs) 50 hemi, 62 TSA
Cofield 1984	92% (67/73)	82% (60/73)	11% (8/73)	31 OA, 29 RA, 13 TA (22-75, ave 56yrs) PE Neer, 1-6.1 yrs post-op. 37.5% (3/8) r. loose & needed surgery.
Collins et al. '04	100% (25/25)	?	?	25 RA only, hemi vs TSA Global Depuy PE-6 mm mismatch
Fehringer et al. '02	70% (71/102)	?	?	102 OA (20-89 ave 64 yrs) Only subjective. PE global peg, all bone graft, 3-5 yrs post-op.
Friedman '92	100% (13/13)	?	?	9 OA, 4 RA (50-77 ave 67 yrs) Cemented: Neer & MB Cofield, 0.5-5yrs post-op.
Gartman et al. '00	? (/51)	? (/27)	15% (4/27)	51 OA (39-82 ave 65 yrs) 24 Hemi PE keel, 2-11yrs post-op. 2/27 def loose no revision, 3/24 hemi to TSA done.
Gartsman et al. '05	?	61% (14/23) 30% (6/20)	K 4% (1/23) P 5% (1/20)	43 OA only (52-84 ave 69 yrs) PE Cofield, 6 weeks post-op.
Gill et al. '99	88% (15/18)	94% (17/18)	47% (8/18)	17 RA only (32-71 ave 54yrs) PE Neer, 0.5-14yrs post-op.
Hill & Norris '01	71% (12/17)	?	?	5 OA, 5 chron disloc, 3 cap arth, 2 RA, 2 other (30-84 ave 56yrs) PE Neer II, 5-13yrs post-op.
Kelly et al. '87	88% (36/42)	80% (33/42)	2% (1/42)	41 RA, 1 psoriatic A (21-79 ave 57 yrs). 34 weak cuff/tears, 26 osteoporotic. PE Neer, 1-5.5 yrs post-op.
Kirk & Sorger '97	100% 1/1	100% 1/1	100% 1/1	1 OA, (68yrs). Lining detachment MB cementless, 3 months post-op.
Klepps et al. '05	?	? -<< in new tech & peg	?	39 OA, 1 psoriatic A, 5 RA, 1 AN (48-82 ave 68 yrs). 28 old tech, 40 new PE Neer K & Zimmer big/flatow K/P, 1yr post-op.
Lazarus et al. '02	?	94% (308/328)	0 (0/328)	328 OA only, 39 keel, 289 peg PE global Depuy, 0 yrs post-op.
Lo et al. '05	?	? TSA better	?	41 OA only (52-98 ave 70 yrs) 21 hemi, 20 TSA PE Neer, 2 yrs post-op. TSA better

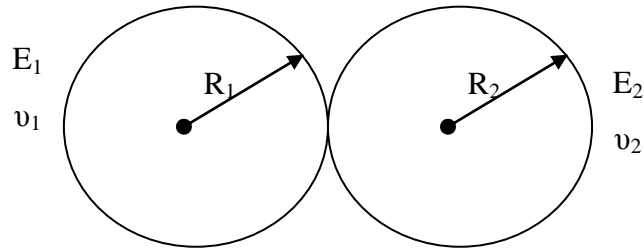
				results-not significant
Martin et al. '05	61% (85/140)	38% (53/140)	15% (21/140)	72 OA, 55 RA, 12 ON, 1 fracture (22-92 ave 63.3 yrs) 7% (10/140) glenoid revision
Mileti et al. '05	88% (60/68)	37.5% (21/56)	14% (8/56)	68 OA only (55-78 ave 67.5 yrs) PE keel Cofield, 2-10 yrs post-op.
Nagels et al. '02	?	83% (40/48)	27% (13/48)	36 RA, 12 OA (30-92 ave 71 yrs) PE keel Biomet, 2-10.5 yrs post-op.
Neer II & Morrison '95	89% (17/19)	31.5% (6/19)	0	6 RA, 2 OA, 2 chron disloc, 1 cuff arthrop (26-68 ave 53 yrs), bone grafted (19/463) PE & MB Neer, 2.4-3.5 yrs post-op.
Nuttall et al. '07	?	?	?	20 OA only, 10 peg, 10 keel (35-92 ave 67 yrs). PE global, 2 yrs post-op.
Orfaly et al. 2003	100% (37/37)	16% (6/37)	8% (3/37)	37 OA only (ave 63yrs) Study on intact cuffs 37 TSA, 28 hemi PE global, 2-8 yrs post-op.
Rahme et al. '04	100% (16/16)	81% (13/16)	0% (0/16)	8 OA, 7 RA (44-78 ave 64 yrs) PE keel 3M, 2 yrs post-op.
Smith et al. '06	?	?	?	48 OA, 10 RA, 5 ON, 3 trauma, 1 polymy R (38-81 ave 61 yrs) 0.5-22 yrs post-op.
Sperling et al. '00	72.5% (45/62)	35% (22/62)	6.5% (4/62)	46 OA, 9 RA, 4 TramA, 2 AN, 1 septicA (28-80 ave 63 yrs) 1 (1.6%) loosening revision Cofield MB cementless, 2-10 yrs post-op.
Sperling et al. '04	52% (15/29)	76% (19/25)	24% (6/25)	25 RA, 7 traumA, 2 OA, 1 AN, 1 fusion (19-50 ave 41 yrs) 78 Hemi. Only for <50yrs, hemi vs. TSA, survival better in TSA. PE Neer, 3 (10%) loosening revision, 1, 10, 14 yrs post-op.
Stewart & Kelly '97	78% (29/37)	62% (23/37)	27% (9/37)	58 RA (22-71 ave 55 yrs). All loose: female, weak/torn cuffs, poor bone, 3 revisions. Rocking Horse PE Neer, 7-13 yrs post-op.
Szabo et al. '05	?	86% (57/66) 83%FB,	?	66 OA only, (43-83 ave 67 yrs) PE Aequalis Tornier 35 FB & 31 CB, 2 yrs post-op.

		90%CB		
Tammachote et al. '05	77% 74/95	72.5% (69/95)	30.5% (29/95)	95 OA only (52-84 ave 68 yrs) Implant survival: 98% 5 yrs, 97% 10 yrs, 93% 15 yrs. 2 loose revisions 2&13yrs. MB Neer keel cemented, 1-19.5 yrs post-op.
Taunton et al. '08	60% (50/83)	60% (50/83)	40% (33/83)	74 OA, 5 traumA, 4 AN, (41-87 ave 68 yrs) Implant survival: 80% 5 yrs, 52% 10 yrs. 9 loose revision, 27 PE & tray wear revision. MB Cofield cementless, 2-15 yrs post-op.
Torchia et al. '97	81% (72/89)	84% (75/89)	44% (39/89)	44 RA, 39 OA, 17 TA, (21-83, ave 58 yrs). 5.6% (5/89) glenoid revision. PE Neer, 5-17yrs post-op.
Trail & Nuttall 2002	? (/32)	53% (17/32) P36%,K90%	3% (1/32) P0%,K10%	105 RA (33.5-84.5 ave 61 yrs), 65 hemi Hemi vs TSA, implant survival: 95% 5 yrs, 92% 8 yrs. PE Depuy global peg (22) keel (10), 2-9 yrs post-op.
Walch et al. '02	65% (276/319)	100% (319/319)	24% (76/319)	319 OA (66.5 ave 54-90) Mismatch study (min 2.5 mm tested). 5.5-10 mm ideal. PE Tornier FB, 2-10 yrs post-op.
Wallace et al. '99	84% (62/86)	33% (19/58) 41% (13/32)	21% (12/58) 19% (6/32)	36 RA, 16 OA, 1 ON (25-87 ave 64 yrs) R. lines & r. loosening cementless: 23% (6/26) & 23% (6/26) respectively PE (20), MB (5) Neer, PE Cofield (4), PE global (3), 4-7.5yrs post-op.
Yian et al. 2006	?	45% (21/47)	6% (3/47)	19 OA, 12 RA, 9 posttraumatic, 7 instabA, (26-81 ave 57 yrs) CT data: 77% (36/47), 13% (6/47). 2 loose rev (both 0 mm mismatch) PE Zimmer peg 0-4 mm mismatch, 1.5-4.5yrs post-op.

Note: most papers use both cementless and cemented implants in their study. The choice of implant is dependent on what the surgeon assesses is best for the patient.

Appendix C: 3D Versus 2D Contact Pressure Calculations

Hertzian Contact Equations



Note: Positive radius for convex, negative for concave.

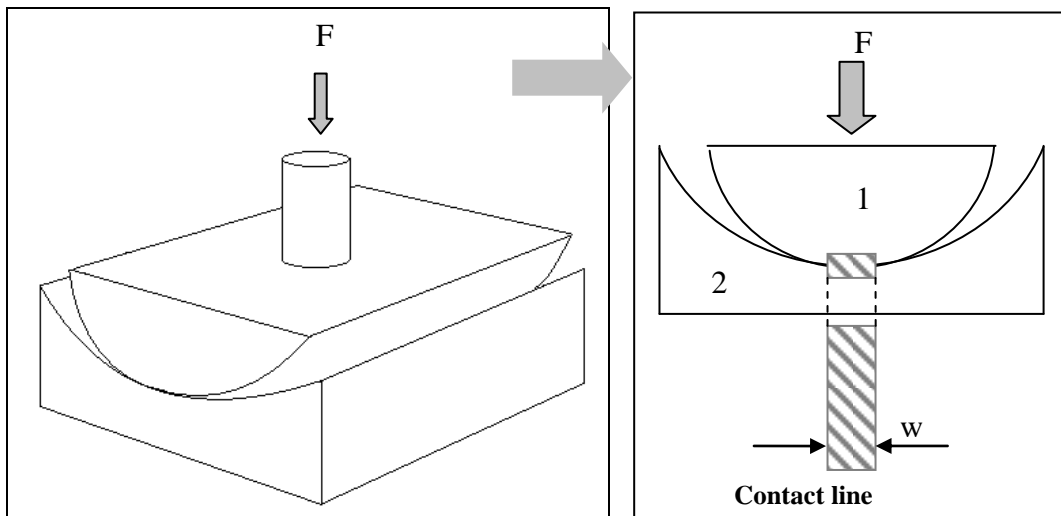
Glenoid implants 25 mm

Effective curvature: $\frac{1}{R} = \frac{1}{R_1} + \frac{1}{R_2} \rightarrow R = 600 \text{ mm}$

Contact modulus: $\frac{1}{E^*} = \frac{1-\nu_1^2}{E_1} + \frac{1-\nu_2^2}{E_2} \rightarrow E^* = 711.97 \text{ MPa}$

Material properties	Humeral head stainless steel	Glenoid UHMWPE
Young's Modulus	$E_1 = 200,000 \text{ MPa}$	$E_2 = 600 \text{ MPa}$
Poisson's Ratio	$\nu_1 = 0.3$	$\nu_2 = 0.4$
Radius	$R_1 = 24 \text{ mm}$	$R_2 = -25 \text{ mm}$

Line Contact:



Semi contact width: $\frac{w}{2} = 2 \left(\frac{F' R}{\pi E^*} \right)^{\frac{1}{2}}$

Note: Load $F' = \text{load/unit length}$, $F' = 1800/40 = 45\text{N/mm}$.

$$w = 4 \left(\frac{45 \times 600}{\pi \times 711.97} \right)^{\frac{1}{2}} = \underline{\underline{13.90\text{mm}}}$$

Contact area: $\text{Area} = w \times l = 13.9 \times 40 = \underline{\underline{555.90\text{mm}^2}}$

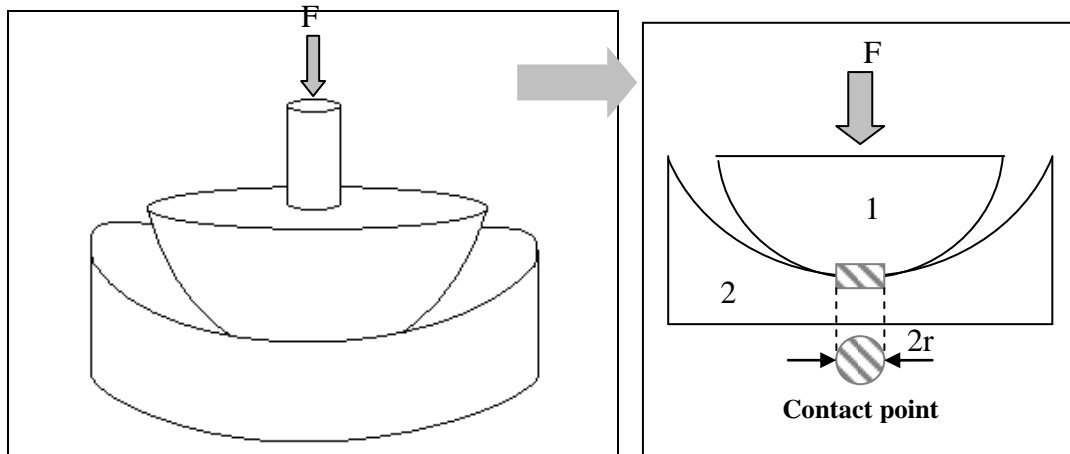
Mean contact pressure: $\bar{P} = \frac{F'}{w} \left(= \frac{\pi}{4} P_{\max} \right)$

$$\bar{P} = \frac{45}{13.9} = \underline{\underline{3.237\text{MPa}}}$$

Maximum contact pressure: $P_{\max} = \left(\frac{F' E^*}{\pi R} \right)^{\frac{1}{2}}$

$$P_{\max} = \left(\frac{45 \times 711.97}{\pi \times 600} \right)^{\frac{1}{2}} = \underline{\underline{4.123\text{MPa}}}$$

Point Contact:



Contact radius: $r = \left(\frac{3FR}{4E^*} \right)^{\frac{1}{3}}$

$$r = \left(\frac{3 \times 750 \times 600}{4 \times 711.97} \right)^{\frac{1}{3}} = \underline{\underline{7.797mm}}$$

Contact area: $Area = \pi r^2 = \pi \times 7.797^2 = \underline{\underline{190.99mm^2}}$

Mean contact pressure: $\bar{P} = \frac{F}{\pi r^2} \left(= \frac{2}{3} P_{max} \right)$

$$\bar{P} = \frac{750}{\pi \times 7.797^2} = \underline{\underline{3.927MPa}}$$

Maximum contact pressure: $P_{maz} = \frac{1}{\pi} \left(\frac{6FE^*}{R^2} \right)^{\frac{1}{3}}$

$$P_{maz} = \frac{1}{\pi} \left(\frac{6 \times 750 \times 711.97^2}{600^2} \right)^{\frac{1}{3}} = \underline{\underline{5.89MPa}}$$

Glenoid implants 29 mm

Effective curvature: $\frac{1}{R} = \frac{1}{R_1} + \frac{1}{R_2} \rightarrow R = 139.2 \text{ mm}$

Contact modulus: $\frac{1}{E^*} = \frac{1-\nu_1^2}{E_1} + \frac{1-\nu_2^2}{E_2} \rightarrow E^* = 711.97 \text{ MPa}$

Material properties	Humeral head stainless steel	Glenoid UHMWPE
Young's Modulus	$E_1 = 200,000 \text{ MPa}$	$E_2 = 600 \text{ MPa}$
Poisson's Ratio	$\nu_1 = 0.3$	$\nu_2 = 0.4$
Radius	$R_1 = 24 \text{ mm}$	$R_2 = -29 \text{ mm}$

Line Contact:

Semi contact width: $\frac{w}{2} = 2 \left(\frac{F' R}{\pi E^*} \right)^{\frac{1}{2}}$

Note: Load F' = load/unit length, $F' = 1800/40 = 45\text{N/mm}$.

$$w = 4 \left(\frac{45 \times 139.2}{\pi \times 711.97} \right)^{\frac{1}{2}} = \underline{\underline{6.694\text{mm}}}$$

Contact area: $Area = w \times l = 6.694 \times 40 = \underline{\underline{267.76\text{mm}^2}}$

Mean contact pressure: $\bar{P} = \frac{F'}{w} \left(= \frac{\pi}{4} P_{\max} \right)$

$$\bar{P} = \frac{45}{6.694} = \underline{\underline{6.722\text{MPa}}}$$

Maximum contact pressure: $P_{\max} = \left(\frac{F' E^*}{\pi R} \right)^{\frac{1}{2}}$

$$P_{\max} = \left(\frac{45 \times 711.97}{\pi \times 139.2} \right)^{\frac{1}{2}} = \underline{\underline{8.559\text{MPa}}}$$

Point Contact:

$$\text{Contact radius: } r = \left(\frac{3FR}{4E^*} \right)^{\frac{1}{3}}$$

$$r = \left(\frac{3 \times 750 \times 139.2}{4 \times 711.97} \right)^{\frac{1}{3}} = \underline{\underline{4.791mm}}$$

$$\text{Contact area: } Area = \pi r^2 = \pi \times 4.791^2 = \underline{\underline{72.11mm^2}}$$

$$\text{Mean contact pressure: } \bar{P} = \frac{F}{\pi r^2} \left(= \frac{2}{3} P_{\max} \right)$$

$$\bar{P} = \frac{750}{\pi \times 4.791^2} = \underline{\underline{10.40MPa}}$$

$$\text{Maximum contact pressure: } P_{\max} = \frac{1}{\pi} \left(\frac{6FE^{*2}}{R^2} \right)^{\frac{1}{3}}$$

$$P_{\max} = \frac{1}{\pi} \left(\frac{6 \times 750 \times 711.97^2}{139.2^2} \right)^{\frac{1}{3}} = \underline{\underline{15.60MPa}}$$

25 mm Conforming Glenoid Summary Table

	Point Contact	Line Contact	% difference
Compressive Force, N	750	1800	240%
Contact Area, mm ²	190.99	555.90	291%
Ave. Contact Pressure, MPa	3.93	3.24	82%
Max. Contact Pressure	5.89	4.12	70%

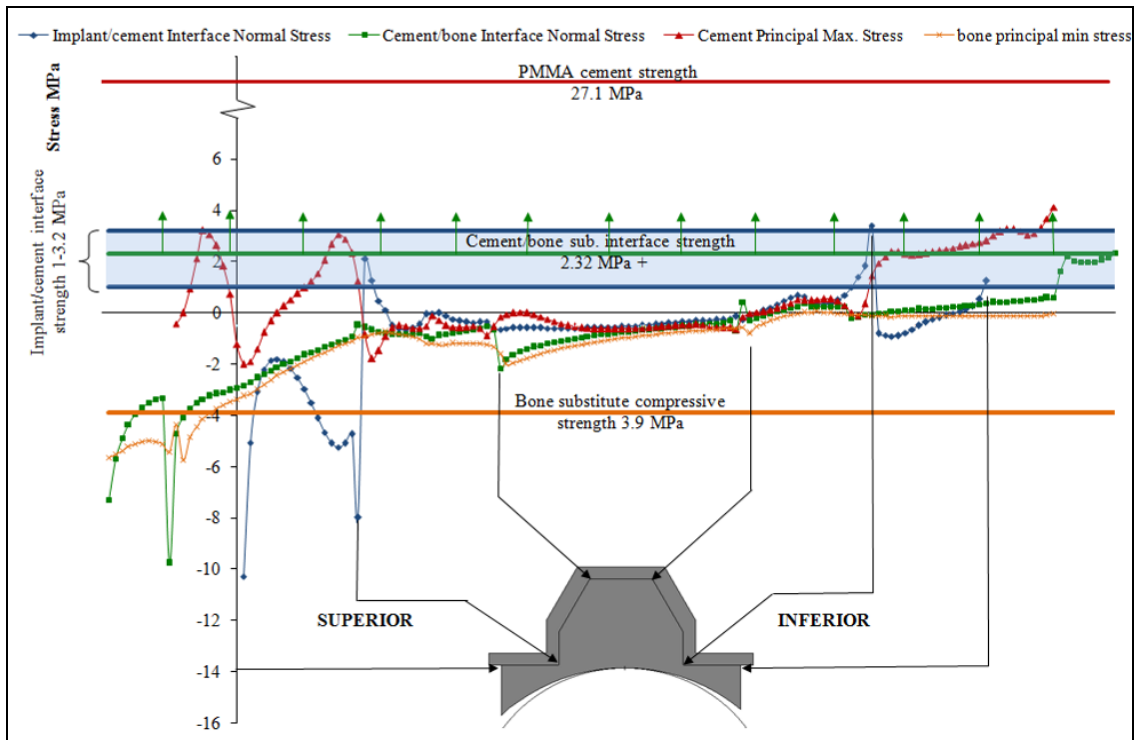
NOTE: FE contact pressure of 25 mm flat-back keel shows average and maximum contact of 3.26 MPa and 4.46 MPa, 99% and 92% of analytical values respectively.

29 mm Non-Conforming Glenoid Summary Table

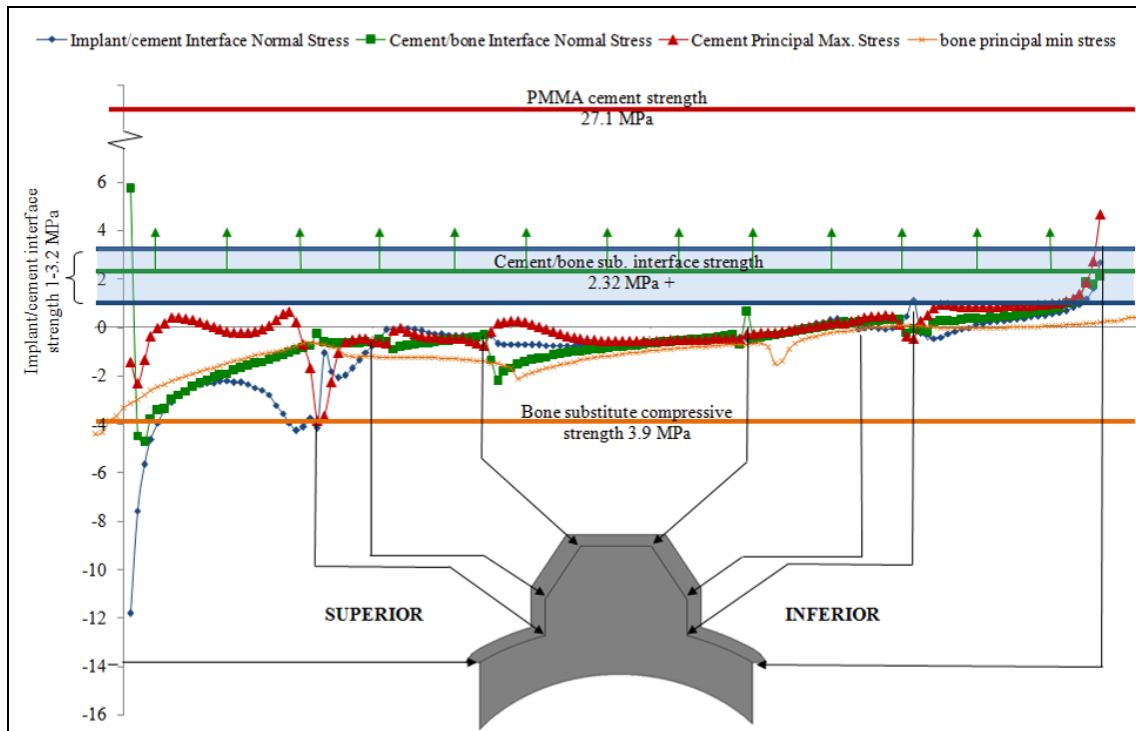
	Point Contact	Line Contact	% difference
Compressive Force, N	750	1800	240%
Contact Area, mm ²	72.11	276.76	384%
Ave. Contact Pressure, MPa	10.40	6.72	65%
Max. Contact Pressure	15.60	8.56	55%

NOTE: FE contact pressure of 29 mm flat-back keel shows average and maximum contact of 6.80 MPa and 8.68 MPa, 99% and 99% of analytical values respectively.

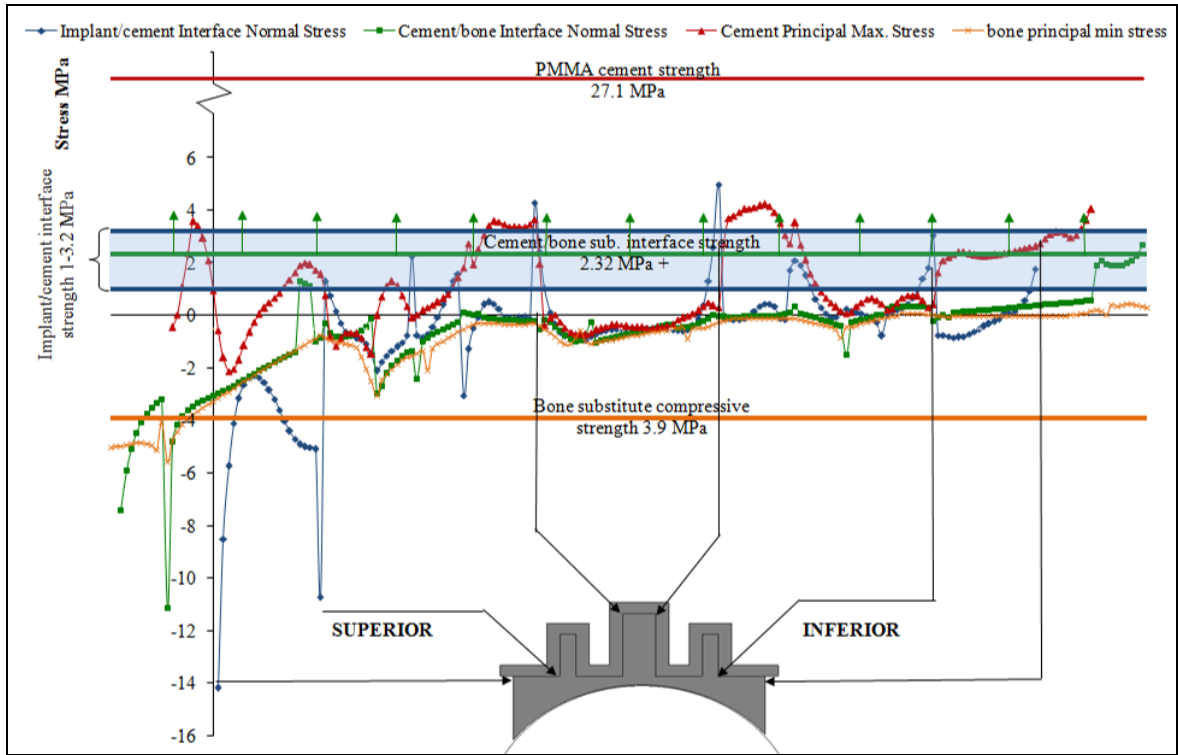
Appendix D: FE predicted interfacial and material stress plots of each 2D design



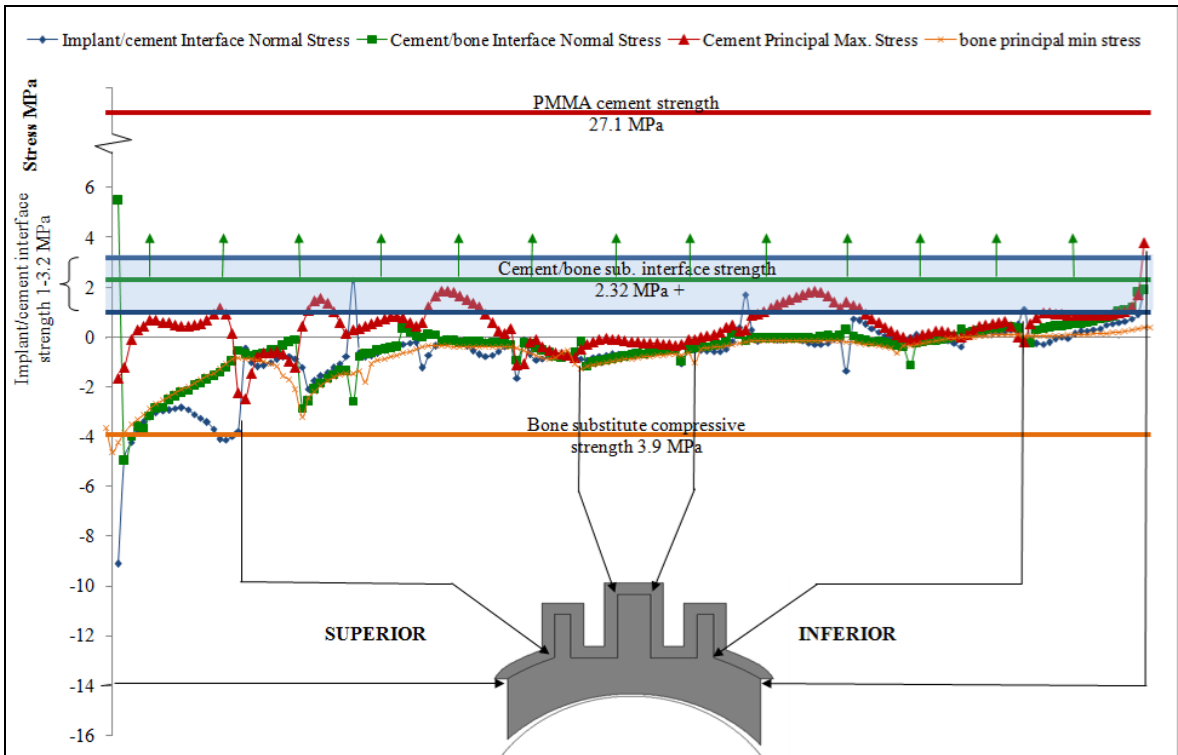
25 mm flat-back keel stress plot



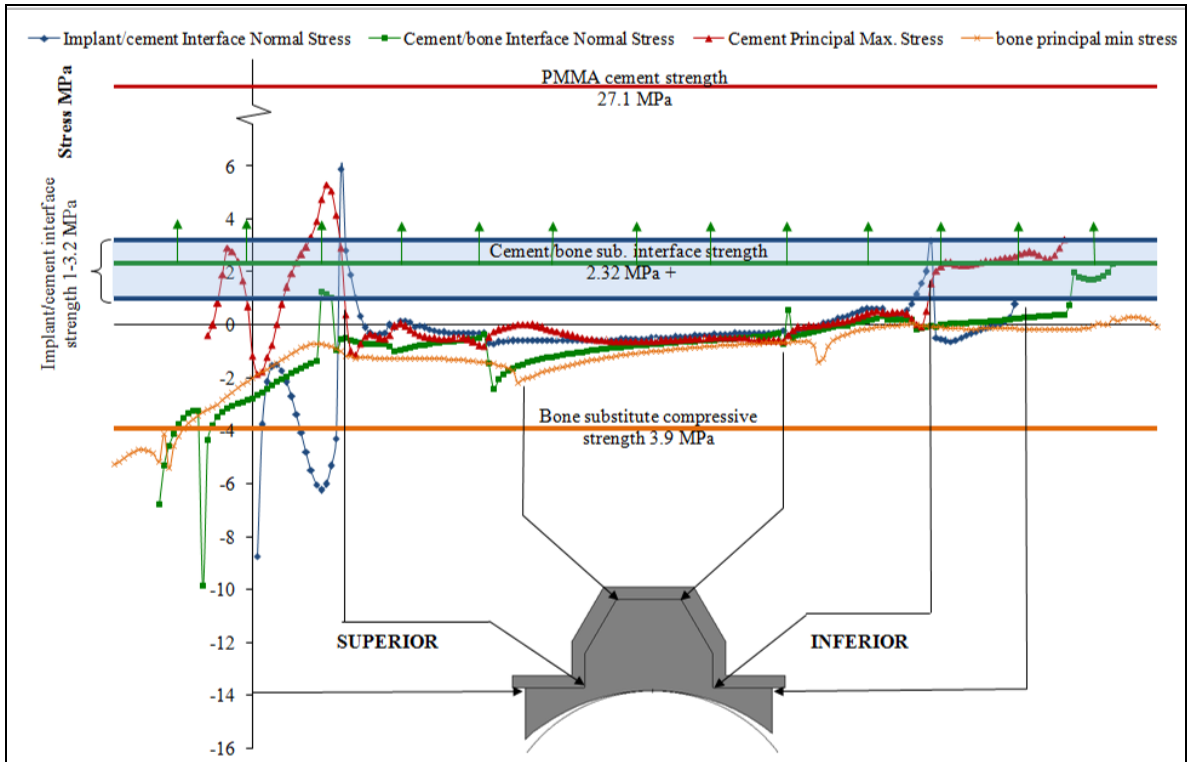
25 mm curved-back keel stress plot



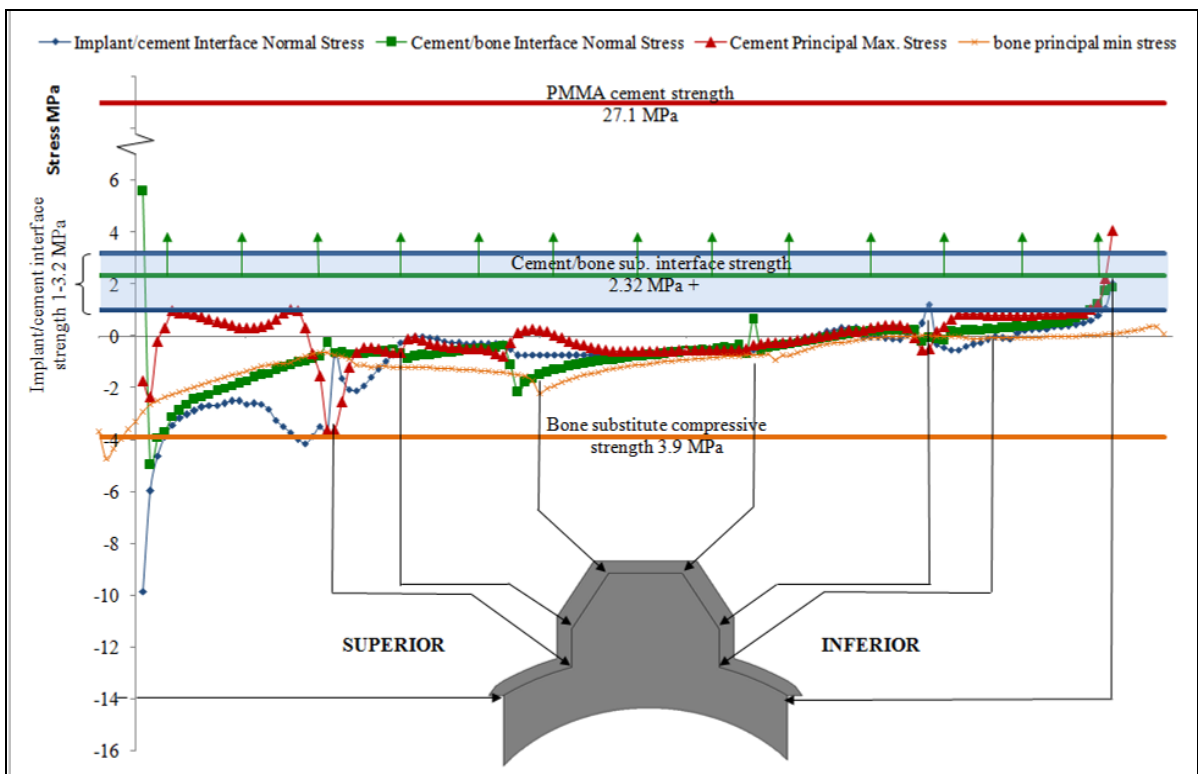
25 mm flat-back keel stress plot



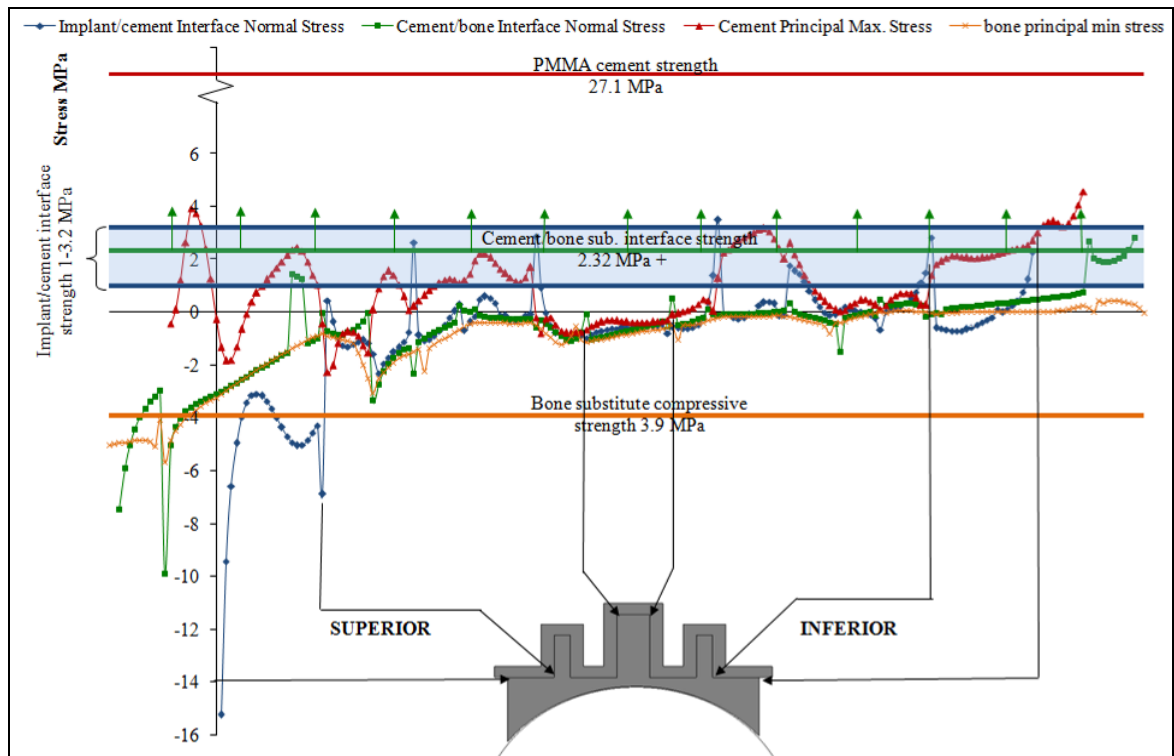
25 mm curved-back peg stress plot



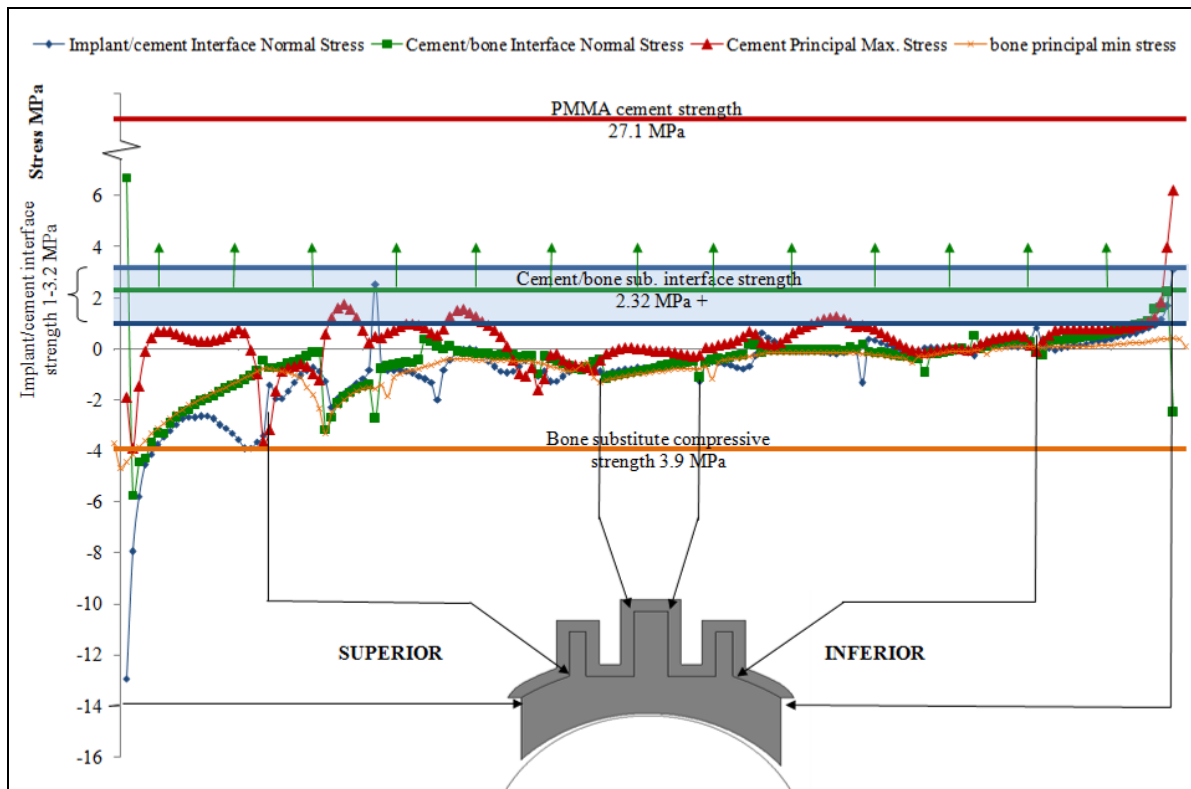
29 mm flat-back keel stress plot



29 mm curved-back keel stress plot



29 mm flat-back keel stress plot



29 mm curved-back peg stress plot

Appendix E: Cross-sectional photos of the cadaveric specimens after fatigue testing

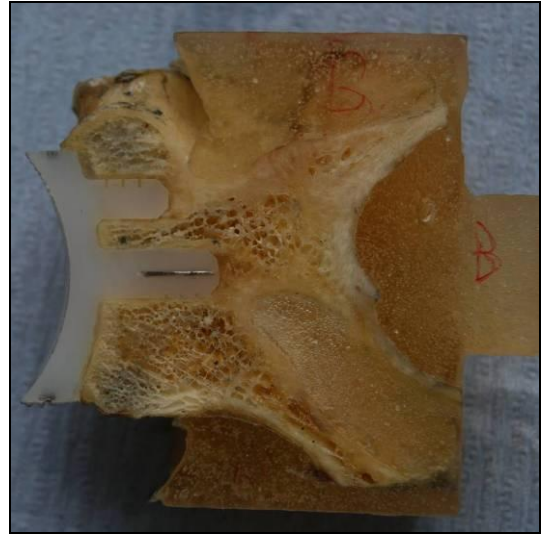
NB1 & NB2



NB4 & NB5



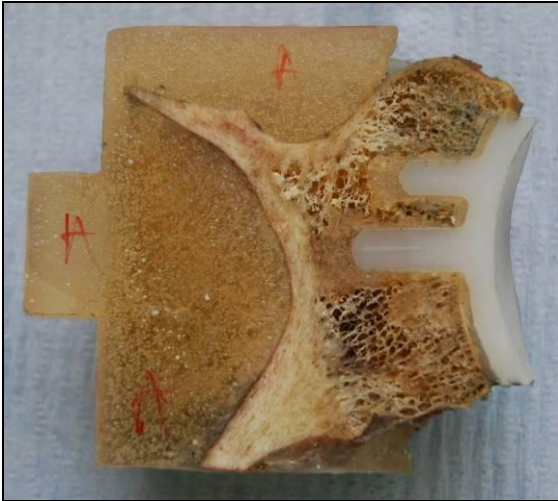
NB6 & NB8



NB9 & NB10



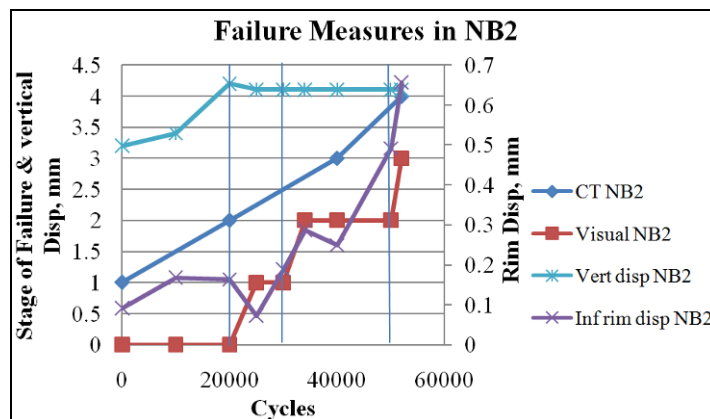
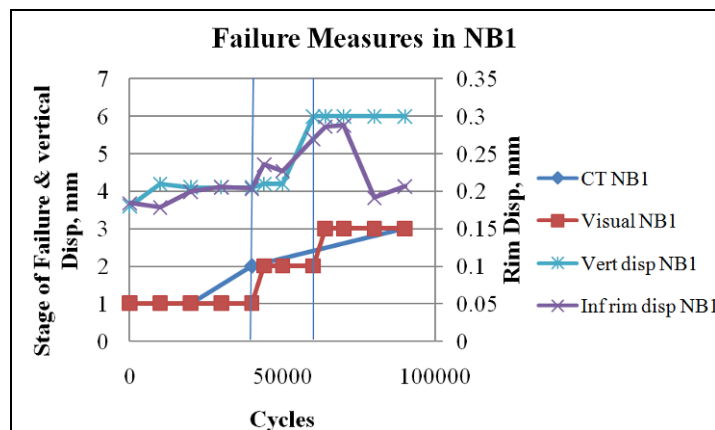
NB11 & NB12

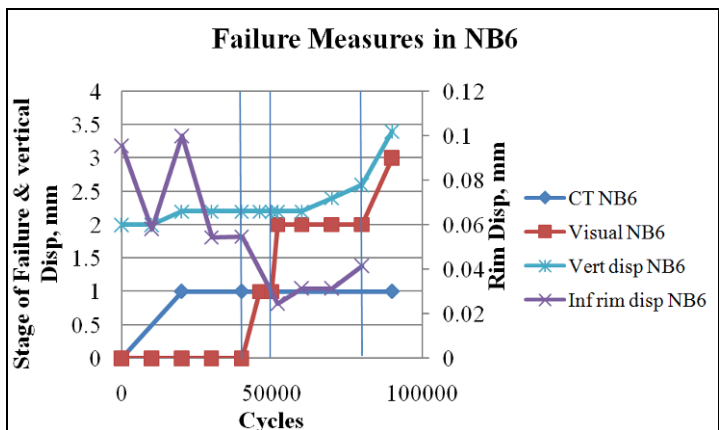
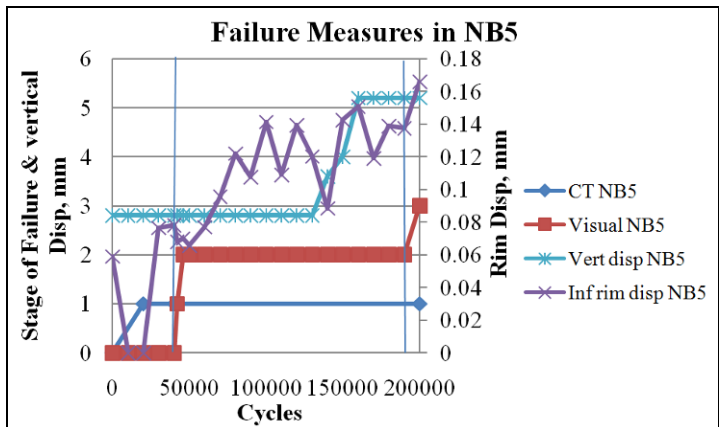
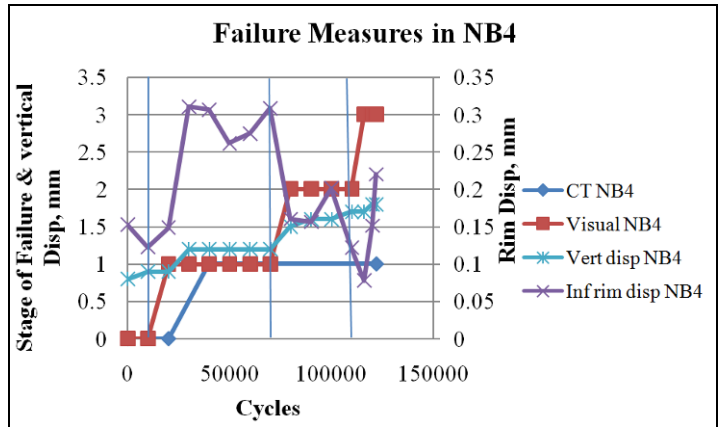


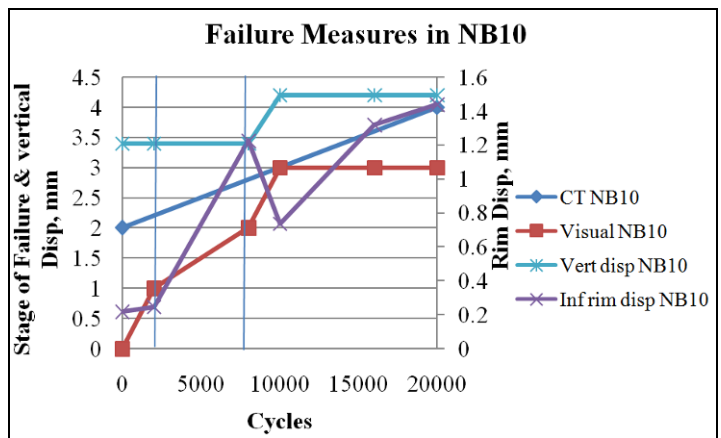
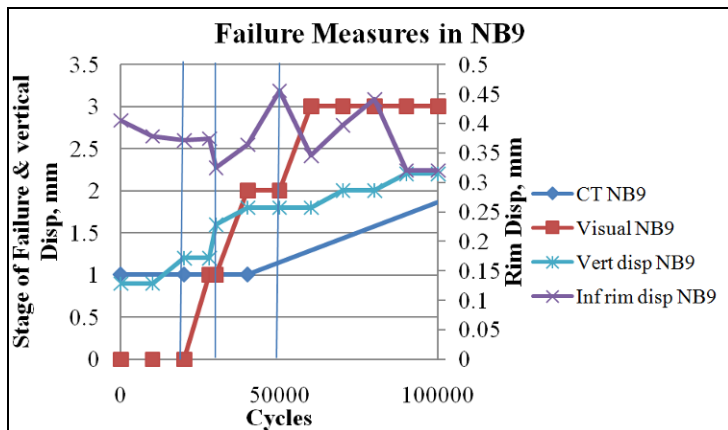
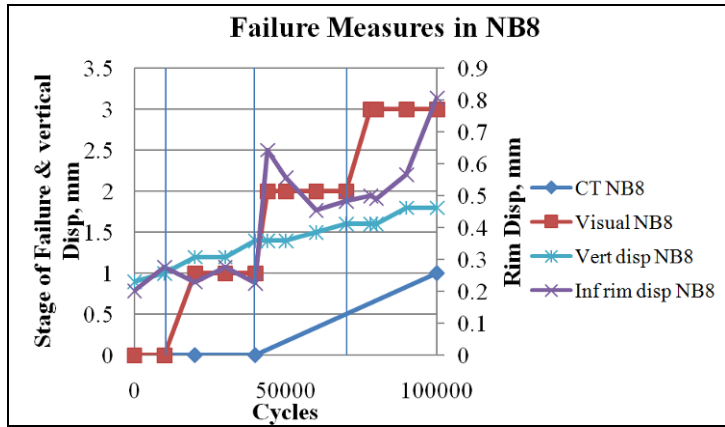
Appendix F: Failure graphs of each specimen plotting visual & CT failure with vertical head & inferior rim displacement

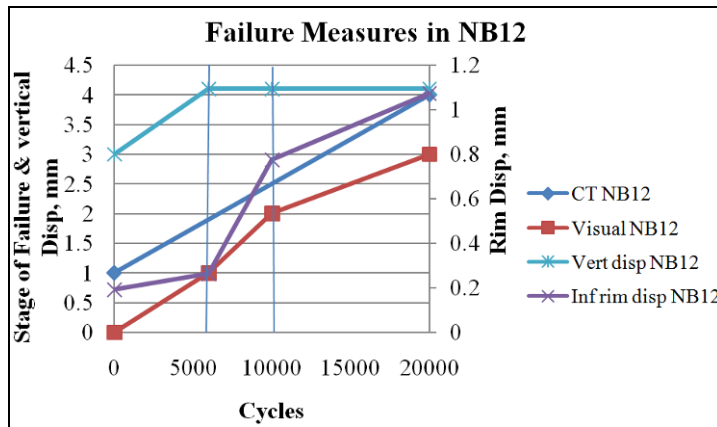
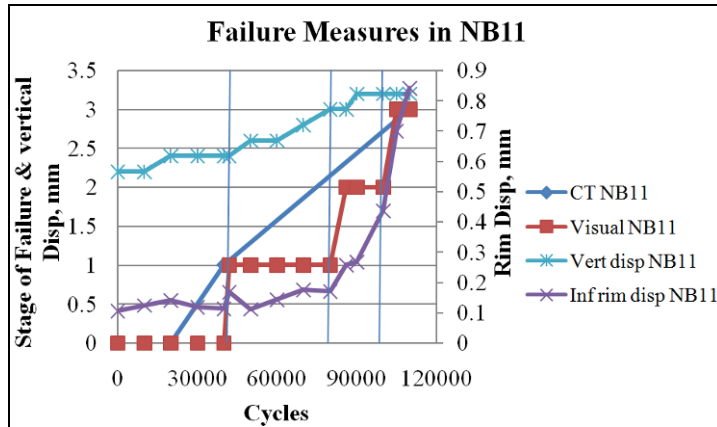
Failure key:

CT	Visual
0 = no radiolucent lines	0 = no failure
1 = inferior rim	1 = possible inferior failure
2 = inferior pegs	2 = inferior rim
3 = between inferior pegs	3 = inferior pegs visible
4 = middle peg	
5 = superior rim	5 = superior rim or bone crushing



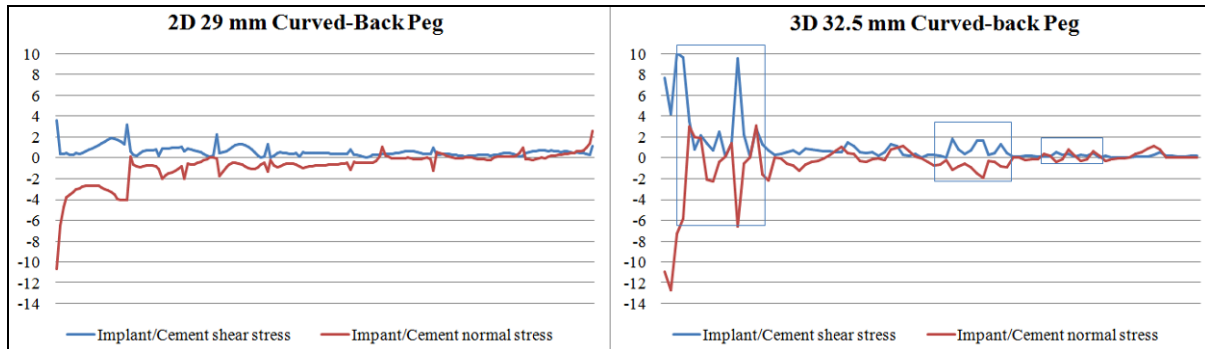




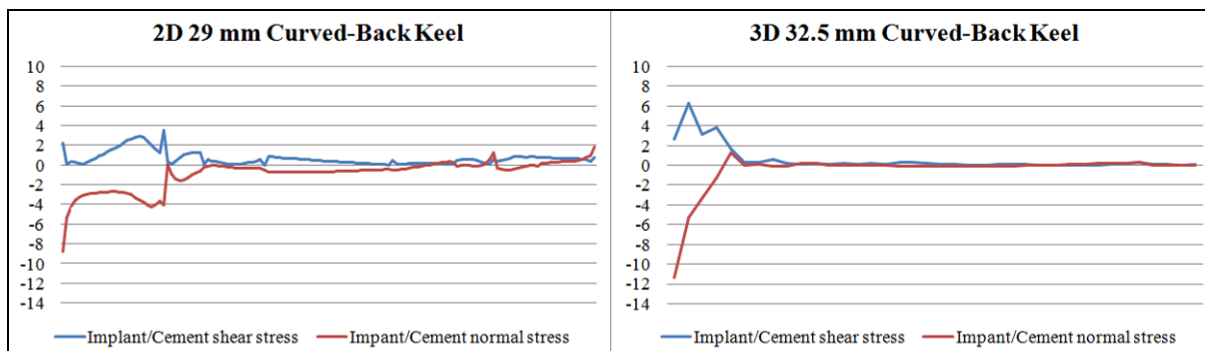


Appendix G: Comparison of implant/cement shear and normal contact stresses in the 2D and 3D cases

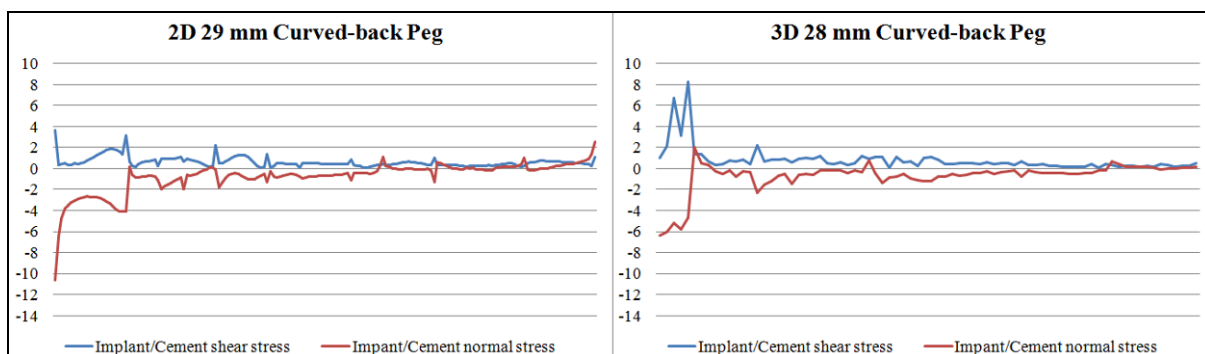
2D Versus TOPEL Implant



2D Versus TOKL Implant



2D Versus n-S/n-R Implant



Appendix H: Table of Displacements for Each Specimen in 2D, Cadaver and 3D Study & Summary Table

	Vertical Head Disp, mm			Superior Rim Disp, mm			Inferior Rim Disp, mm		
	initial	mid-failure	failure	initial	mid-failure	failure	initial	mid-failure	failure
2D	2.2	3.5	4.5	-0.231	-0.199	-0.700	0.166	1.251	2.175
	1.8	2.2	3.6	-0.154	-0.246	-0.410	0.180	0.331	1.852
	1.2	2.2	3	-0.155			0.109		
	1.7	1.7	3.5	-0.240	-0.238		0.236	0.376	
	1.6	1.7	5	-0.167	-0.185		0.154	0.130	
	1.7	2.2	2.2	-0.131	-0.259	-0.259	0.044	0.720	0.720
	1.4	1.7	2.6	-0.129	-0.258	-0.468	0.198	0.338	1.655
	2	2.6	3	-0.388	-0.569	-0.462	0.143	0.343	0.902
	2.6	4	4	-0.387	-0.664	-0.664	0.205	0.984	0.984
	1.8	2.5	3.8	-0.169	-0.105	-0.402	0.235	0.535	0.973
	1.5	3.5	4	-0.113	-0.817		0.218	1.182	2.157
	1.5	4.5	4.5	-0.061	-0.274	-0.274	0.065	1.870	1.870
	4	4	4.3	-0.651	-0.709	-0.478	0.020	0.034	1.538
	2.5	2.8	2.8	-0.067	-0.173	-0.173	0.058	0.143	0.143
	2.2	2.5	2.5	-0.139	-0.284	-0.284	0.017	0.026	0.026
	2.8	2.8	3.2	-0.206	-0.293	-0.448	0.127	0.298	0.990
	2.6	2.8	2.6	-0.174	-0.205		0.109	0.385	
	2.6	2.8	3.1	-0.164	-0.236	-0.337	0.127	0.292	0.840
	2.8	2.8	4	-0.284	-0.284	-0.596	0.096	0.096	1.842
	2.8	3.4	3.4	-0.265	-0.424	-0.506	0.173	0.412	1.149
2.8	3	3	-0.260	-0.288	-0.288	0.221	0.950	0.950	
3	3	5	-0.193	-0.205	-0.183	0.128	0.202	1.117	
3	5	5	-0.135	-0.286	-0.286	0.120	1.365	1.365	
3.2	3.2	5	-0.165	-0.246	-0.599	0.160	0.287	1.751	
cadaver	3.6	4.2	6	-0.225	-0.427	-0.350	0.184	0.235	0.286
	3.2	4.11	4.1	-0.211	-0.568	-1.012	0.092	0.287	0.656
	0.8	1.5	1.8	-0.140	-0.293	-0.483	0.153	0.160	0.220
	2.8	2.8	5.2	-0.185	-0.187	-0.681	0.059	0.070	0.166
	2	2.2	3.4	-0.590	-0.204	-0.746	0.096	0.024	
	0.9	1.4	1.6	-0.263	-0.427	-0.688	0.202	0.644	0.500
	0.9	1.8	1.8	-0.293	-0.755	-1.044	0.405	0.364	0.345
	3.4	3.4	4.2	-0.162	-0.438	-0.882	0.218	1.225	1.317
	2.2	3	3.2	-0.105	-0.121	-0.489	0.106	0.257	0.699
	3	4.1	4.1		-0.970		0.190	0.773	1.072

3D	4.4	5.2	5.2	-0.515	-0.502	-0.363	0.236	0.496	0.443
	2.6	2.4	5.2	-0.243	-0.309	-0.493	0.204	0.217	0.294
	2.4	5.2	5.2	-0.241	-0.594	-0.420	0.060	0.180	0.249
	2.2	2.6	5.2	-0.237	-0.360	-0.712	0.035	0.267	0.354
	2.2	2.6	5.2	-0.091	-0.556	-0.469	0.006	0.224	0.375
	1.4	1.6		-0.201	-0.119		0.015	0.120	
	4	4.4		-0.287	-0.441		0.005	0.021	
	3.8	5.2		-0.448	-0.267		0.014	0.018	
	4	6		-0.332	-0.484		0.019	0.093	
	3.5	6		-0.166	-0.235		0.020	0.017	
	3.2	4.2		-0.141	-0.130		0.019	0.060	
	3.4	6		-0.224	-0.377		0.000	0.020	

Superior displacement average and statistical summary

	superior initial (1)	superior mid-failure (2)	superior at failure (3)	ANOVA
2D	-0.209 0.125	-0.324 0.185	-0.411 0.156	p < 0.0001 1-2 ns 1-3 p < 0.01 2-3 ns
Cadaver	-0.242 0.143	-0.439 0.267	-0.652 0.267	p > 0.001 1-2 ns 1-3 p < 0.01 2-3 p < 0.05
3D	-0.261 0.122	-0.364 0.157	-0.491 0.133	p = 0.01 1-2 ns 1-3 p < 0.01 2-3 ns
3D - No failure	-0.154 0.066		-0.135 0.118	p = 0.71 -

Inferior displacement average and statistical summary

	inferior initial (1)	inferior mid-failure (2)	inferior at failure (3)	ANOVA
2D	0.138 0.065	0.546 0.491	1.250 0.603	p < 0.0001 1-2 p < 0.01 1-3 p < 0.01 2-3 p < 0.01
Cadaver	0.170 0.099	0.404 0.372	0.585 0.396	p = 0.03 1-2 ns 1-3 p < 0.05 2-3 ns
3D	0.053 0.080	0.144 0.143	0.343 0.075	p = 0.0002 1-2 ns 1-3 p < 0.01 2-3 p < 0.01
3D - No failure	0.008 0.005		0.015 0.008	p = 0.07 -

Vertical displacement average and statistical summary

	vertical initial (1)	vertical mid-failure (2)	vertical at failure (3)	ANOVA
2D	2.30 0.70	2.93 0.85	3.65 0.88	p < 0.0001 1-2 p < 0.05 1-3 p < 0.01 1-3 p < 0.01
Cadaver	2.28 1.09	2.85 1.09	3.54 1.48	p = 0.09 1-2 ns 1-3 p = 0.04 2-3 ns
3D	3.09 0.92	4.28 1.59	5.20 0.00	p = 0.006 1-2 ns 1-3 p < 0.01 2-3 ns
3D - No failure	2.34 1.06		2.53 1.71	p = 0.81 -

Displacement averages before and after testing in non-failed specimens in the 3D study (n = 7) and statistical summary

3D	Displacement before testing	Displacement after testing	
Superior	-0.154 0.066	-0.145 0.118	p = 0.81 -
Inferior	0.008 0.005	0.015 0.008	p = 0.07 -
Vertical	2.34 1.06	2.53 1.71	p = 0.81 -